Journal of Ophthalmology

Genetics in Ophthalmology

Lead Guest Editor: Lev Prasov
Guest Editors: Stephen T. Armenti, Robert B. Hufnagel, Virginia M. Utz, and Julia E. Richards

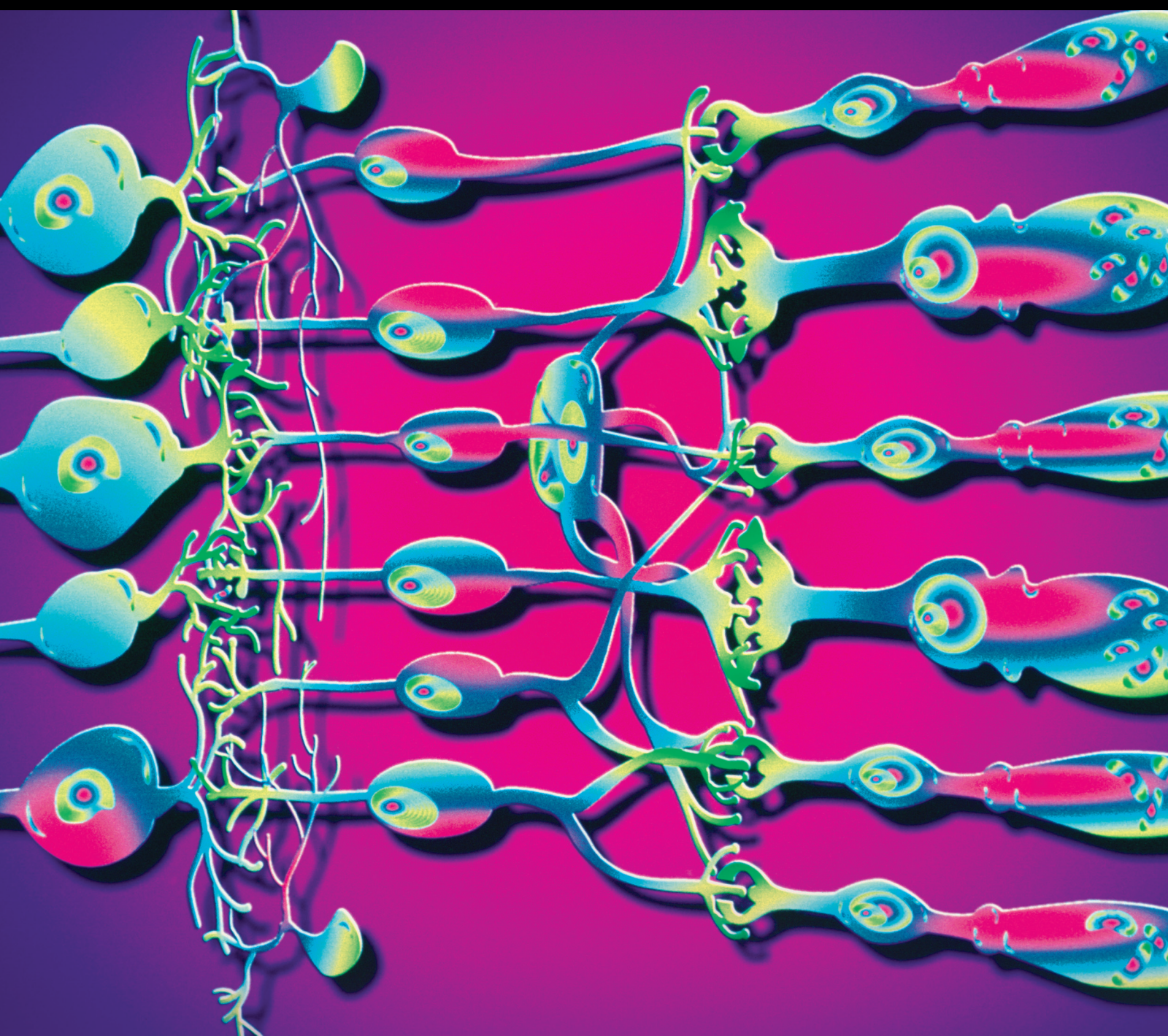

Genetics in Ophthalmology

Journal of Ophthalmology

Genetics in Ophthalmology

Lead Guest Editor: Lev Prasov
Guest Editors: Stephen T. Armenti, Robert B. Hufnagel, Virginia M. Utz, and Julia E. Richards

Editorial Board

Contents

Genetics in Ophthalmology
Lev Prasov, Stephen T. Armenti, Virginia Miraldi Utz, Julia E. Richards, and Robert B. Hufnagel
Editorial (3 pages), Article ID 4608946, Volume 2018 (2018)

Peripheral Cone Dystrophy: Expanded Clinical Spectrum, Multimodal and Ultrawide-Field Imaging, and Genomic Analysis
Robert A. Sisk, Robert B. Hufnagel, Ailee Laham, Elizabeth S. Wohler, Nara Sobreira, and Zubair M. Ahmed
Research Article (13 pages), Article ID 2984934, Volume 2018 (2018)

Association of Genes in the High-Density Lipoprotein Metabolic Pathway with Polypoidal Choroidal Vasculopathy in Asian Population: A Systematic Review and Meta-Analysis
Ming-zhen Yuan, Ruo-an Han, Chen-xi Zhang, and You-xin Chen
Review Article (14 pages), Article ID 9538671, Volume 2018 (2018)

Comparison of SNP Genotypes Related to Proliferative Vitreoretinopathy (PVR) across Slovenian and European Subpopulations
Xhevat Lumi, Mateja M. Jelen, Daša Jevšinek Skok, Emanuela Boštjančič, Metka Ravnik-Glavač, Marko Hawlina, and Damjan Glavač
Research Article (7 pages), Article ID 8761625, Volume 2018 (2018)

Nanophthalmos: A Review of the Clinical Spectrum and Genetics
Pedro C. Carricondo, Thais Andrade, Lev Prasov, Bernadete M. Ayres, and Sayoko E. Moroi
Review Article (9 pages), Article ID 2735465, Volume 2018 (2018)

Mutation Spectrum of the *ABCA4* Gene in a Greek Cohort with Stargardt Disease: Identification of Novel Mutations and Evidence of Three Prevalent Mutated Alleles
Kamakari Smaragda, Kokkinou Vassiliki, Koutsodontis George, Stamatiou Polixeni, Giatzakis Christoforos, Anastasakis Anastasios, Aslanides Ioannis Minas, Koukoula Stavrenia, Panagiotoglou Theoni, Datseris Ioannis, and Tsilimbaris K. Miltiadis
Research Article (10 pages), Article ID 5706142, Volume 2018 (2018)

Evaluation of TGF-Beta 2 and VEGFα Gene Expression Levels in Epiretinal Membranes and Internal Limiting Membranes in the Course of Retinal Detachments, Proliferative Diabetic Retinopathy, Macular Holes, and Idiopathic Epiretinal Membranes
Joanna Stafiej, Karolina Kaźmierczak, Katarzyna Linkowska, Paweł Żuchowski, Tomasz Grzybowski, and Grażyna Malukiewicz
Research Article (6 pages), Article ID 8293452, Volume 2018 (2018)

Phenotypic Variation in a Four-Generation Family with Aniridia Carrying a Novel *PAX6* Mutation
Grace M. Wang, Lev Prasov, Hayder Al-Hasani, Colin E. R. Marrs, Sahil Tolia, Laurel Wiinikka-Buesser, Julia E. Richards, and Brenda L. Bohnsack
Research Article (10 pages), Article ID 5978293, Volume 2018 (2018)

Molecular Genetics of Pigment Dispersion Syndrome and Pigmentary Glaucoma: New Insights into Mechanisms
Adrian A. Lahola-Chomiak and Michael A. Walter
Review Article (11 pages), Article ID 5926906, Volume 2018 (2018)

Association of Optic Neuritis with *CYP4F2* Gene Single Nucleotide Polymorphism and IL-17A Concentration
Mantas Banevicius, Alvita Vilkeviciute, Brigita Glebauskiene, Loresa Kriauciuniene, and Rasa Liutkeviciene
Research Article (8 pages), Article ID 1686297, Volume 2018 (2018)

Phenotypic Progression of Stargardt Disease in a Large Consanguineous Tunisian Family Harboring New *ABCA4* Mutations
Yousra Falfoul, Imen Habibi, Ahmed Turki, Ahmed Chebil, Asma Hassairi, Daniel F. Schorderet, and Leila El Matri
Research Article (7 pages), Article ID 1030184, Volume 2018 (2018)

DNA Methylation Status of the Interspersed Repetitive Sequences for LINE-1, Alu, HERV-E, and HERV-K in Trabeculectomy Specimens from Glaucoma Eyes
Sunee Chansangpetch, Sasiprapa Prombhul, Visanee Tantisevi, Pimpayao Sodsai, Anita Manassakorn, Nattiya Hirankarn, and Shan C. Lin
Research Article (10 pages), Article ID 9171536, Volume 2018 (2018)

Hindawi
Journal of Ophthalmology
Volume 2018, Article ID 4608946, 3 pages
https://doi.org/10.1155/2018/4608946

Editorial
Genetics in Ophthalmology

Lev Prasov,[1,2] Stephen T. Armenti,[2] Virginia Miraldi Utz,[3] Julia E. Richards,[2,4] and Robert B. Hufnagel[1]

[1]*Ophthalmic Genetics and Visual Function Branch, National Eye Institute, National Institutes of Health, 10 Center Drive, Bethesda, MD 20892, USA*
[2]*Department of Ophthalmology and Visual Sciences, W. K. Kellogg Eye Center, University of Michigan, 1000 Wall St., Ann Arbor, MI 48105, USA*
[3]*Department of Ophthalmology, Abrahamson Eye Institute, Cincinnati Children's Hospital Medical Center, 3333 Burnet Ave., No. 4008, Cincinnati, OH 45229, USA*
[4]*Department of Epidemiology, University of Michigan, 1415 Washington Heights, Ann Arbor, MI 48109, USA*

Correspondence should be addressed to Lev Prasov; lprasov@umich.edu

Received 28 May 2018; Accepted 28 May 2018; Published 29 August 2018

The clinical and molecular diagnostic evaluation of patients with heritable ocular disorders has evolved immensely since the first retinal dystrophy genes were cloned and sequenced in 1988 [1]. In addition, the modalities for studying the pathogenesis and future therapeutics for genetic eye disorders are constantly advancing. Through thoughtful consideration and detailed examination, imaging, electrophysiology, and family history, ophthalmologists and geneticists can select cytogenetic testing that confirms the clinical diagnosis in more than 50% of patients with retinal dystophies [2]. However, our understanding of disorders with complex inheritance as well as some Mendelian eye conditions is still in need of further investigation. For these unsolved traits, whole-exome and whole-genome sequencing provides a route for further investigation to identify a causative gene. This special issue of the *Journal of Ophthalmology* highlights the range of clinical and genetic testing modalities both for common and rare disorders, as well as complex and Mendelian traits.

Classic familial studies are highlighted in several studies presented in this issue. Wang and colleagues present a 4-generation family with a novel loss-of-function frameshift mutation in *PAX6*. The seven affected family members highlight significant intrafamilial ocular phenotypic variability. The authors propose mechanisms for phenotypic variability including interaction with and expression of other transcriptional factors involved in embryonic development, as well as variations in transcription and other epigenetic factors involved in *PAX6* expression. Falfoul et al. described two branches of a consanguineous Tunisian family harboring two *ABCA4* alleles, where different allelic combinations all led to cone-rod degeneration. They describe a novel complex structural *ABCA4* variant that has not been previously reported. In the paper by Smaragda et al., nearly 60 Greek patients with Stargardt disease were genotyped for *ABCA4* single-nucleotide and copy-number variant alleles, and almost 90% were detected to have pathogenic alleles. Surprisingly, the two most prevalent alleles were alleles with mild phenotypic expression. Beyond characterizing variant-level prevalence in specific populations, these studies may provide insight into predicting disease burden and progression in individuals based on their geographical origin.

Genetic and phenotypic heterogeneity are two important ideas that are continually discussed in this volume. A review paper by Carricondo et al. presents the clinical features of nanophthalmos and discusses the genetic factors implicated in this disease. Both autosomal dominant inheritance and autosomal recessive inheritance of nanophthalmos have been reported, and a fair amount of genetic heterogeneity is suggested by the finding so far of five nanophthalmos genes and two nanophthalmos loci. Phenotypic heterogeneity is reflected in the fact that four of the five known nanophthalmos genes

(MFRP, PRSS56, CRB1, and BEST1/VMD1) can cause phenotypes other than nanophthalmos, although that level of heterogeneity has not yet been reported for nanophthalmos gene TMEM98. Sisk and colleagues present three patients who share a common phenotype of peripheral cone dystrophy (PCD), a condition in which the fovea and central visual acuity are preserved, but parafoveal photoreceptors undergo atrophy-accompanied macular vascular attenuation. The authors have redefined the clinical features to also include a nonprogressive course, normal choroidal thickness in areas of atrophy, and large affected regions giving a "bifocal" atrophic experience in 2 of 3 patients. The authors propose that genotypic heterogeneity and/or environmental influences may contribute to a common phenotype, as whole-exome sequencing failed to identify a common gene.

Association and gene expression studies have significantly advanced our understanding of complex traits. In the paper by Mingzen et al., the association of genes in the high-density lipopoprotein metabolic pathway with polypoidal choroidal vasculopathy (PCV) is explored. The authors found that 7 polymorphisms in genes in this pathway increase susceptibility to PCV, suggesting that the misregulation of this lipoprotein metabolism may be involved in the pathogenesis of this condition. Banevicius and colleagues evaluated the risk for optic neuritis in patients suspected to have impaired arachadonic acid (AA) metabolism and increased Th17 cell regulation. The authors show that single-nucleotide polymorphisms (SNPs) in CYPF2, a cytochrome P450 enzyme suspected to impair AA metabolism, were more frequent in men with optic neuritis (ON) and multiple sclerosis (MS) and that serum inflammatory cytokines (IL-17a) are elevated in patients with ON and MS. These results suggest that these factors may be associated with predisposition to ON and MS. In the paper by Stafiej et al., the authors explore the levels of TGF-beta2 and VEGF-a expression in epiretinal membranes (ERM) and internal limiting membranes (ILM) from vitrectomy specimens. They identify that TGF-beta2 and VEGF-a, factors associated with angiogenesis and wound healing, are upregulated in ERM as compared to ILM in all vitrectomy groups. Lumi and colleagues evaluate the frequency of SNPs in patients with and without proliferative vitreoretinopathy (PVR) to further validate whether polymorphisms in specific growth factors or cytokines may help stratify patients at risk for subsequent PVR after vitrectomy. Here, the authors suggest that although the variability in the distribution of SNPs across European subpopulations is significant, there are specific SNPs that occur with higher frequency in patients with PVR after vitrectomy compared to healthy controls in both interleukins and tumor necrosis factor genes. Drs. Lahola-Chomiak and Walter review the molecular genetics of pigment dispersion syndrome and pigmentary glaucoma, highlighting the clear genetic components of these disorders but the absence of clear single-gene mutations. Animal studies have demonstrated a role of melanosome function in the disease mechanism, but the precise pathogenic role of these genes in humans remains to be determined.

Epigenetic mechanisms also play a substantial role in gene regulation and the pathogenesis of ocular disease. In the paper by Chansangpetch et al., the authors explore the DNA methylation status of trabeculectomy specimens from primary open-angle glaucoma, primary angle-closure glaucoma, and secondary glaucoma patients, as compared to control specimens. They identified differences in the methylation status of Alu elements among glaucoma specimens as compared to controls, suggesting that methylation patterns may be associated with glaucoma pathogenesis.

The mixture of clinical ophthalmology and ophthalmic genetics found in these papers reflects the dawning role of precision medicine in ophthalmology. Diagnosis and medical management in a successful ophthalmic genetics practice requires expertise found in ophthalmology, medical genetics, genetic counseling, clinical molecular genetics, and often pediatrics. The team must apply rapidly changing molecular advances in the recent literature to patient care. Because so few individuals are trained and board-certified in all or most of these specialties, a multidisciplinary clinic is a viable alternative to have a single destination for families with inherited ocular disease. Another benefit to the combined clinic model is added power to interpret next-generation sequencing results and added education between specialties. As clinical molecular genetic testing options expand, we expect to see an increase in patients with disorders that cannot be diagnosed by gene panels or chromosomal technologies alone. As the range of molecular diagnoses delineate the list of clinical diagnoses into gene-specific diseases, involving medical and molecular geneticists for interpretation and second opinion of variants of uncertain or unknown significance may be crucial. It will help families and providers guide reproductive planning, medical and surgical interventions, and testing and surveillance of other family members where appropriate.

Optimally, the scope of testing will include known disease genes related to phenotypes. However, as the cost of whole-exome and whole-genome sequencing becomes more affordable, these technologies will be more frequently adopted. While analyzing with the intention to determine the primary cause of a condition, these methods will also yield additional information about variants of known or unknown significance (VOUS) without relation to the phenotype or desired diagnosis. So far, the American College of Medical Genetics has released a recommendation to counsel about unrelated results found in 59 genes that are medically actionable [3]. Perhaps more importantly, seeing the patient in a multidisciplinary clinic prior to ordering exome sequencing will aid in fully comprehending the family's intention and desire either to learn these unrelated risks or to blind themselves from knowledge of conditions for which no treatment exists.

In summary, this issue highlights the importance of genetics in every clinical specialty in ophthalmology. In this era of rapid genomics advancements, we face the challenge of interpreting and explaining complex testing options and results to patients. Thus, a collaborative, multidisciplinary approach is needed to provide comprehensive and informed care to patients. With recent advances in testing modalities, it will become increasingly important and complicated to

obtain, distill, and present results of large datasets to our patients. Genetic testing has become more prevalent for identifying disease risk and for prognosis and is increasingly becoming used for understanding disease mechanism and developing new treatments. This in turn is creating important new opportunities that will call for every specialty in ophthalmology to join in this multidisciplinary clinical/genomic perspective on diagnostic and treatment choices. As our knowledge and experience expands, the role of genetics in ophthalmology will continue to grow in the years to come.

Lev Prasov
Stephen T. Armenti
Virginia Miraldi Utz
Julia E. Richards
Robert B. Hufnagel

References

[1] G. A. Mitchell, L. C. Brody, J. Looney et al., "An initiator codon mutation in ornithine-delta-aminotransferase causing gyrate atrophy of the choroid and retina," *Journal of Clinical Investigation*, vol. 81, no. 2, pp. 630–633, 1988.

[2] J. M. Ellingford, S. Barton, S. Bhaskar et al., "Molecular findings from 537 individuals with inherited retinal disease," *Journal of Medical Genetics*, vol. 53, no. 11, pp. 761–767, 2016.

[3] S. S. Kalia, K. Adelman, S. J. Bale et al., "Recommendations for reporting of secondary findings in clinical exome and genome sequencing, 2016 update (ACMG SF v2.0): a policy statement of the American College of Medical Genetics and Genomics," *Genetics in Medicine*, vol. 19, no. 2, pp. 249–255, 2017.

Hindawi
Journal of Ophthalmology
Volume 2018, Article ID 2984934, 13 pages
https://doi.org/10.1155/2018/2984934

Research Article

Peripheral Cone Dystrophy: Expanded Clinical Spectrum, Multimodal and Ultrawide-Field Imaging, and Genomic Analysis

Robert A. Sisk,[1,2,3] **Robert B. Hufnagel**,[4] **Ailee Laham**,[1] **Elizabeth S. Wohler**,[5] **Nara Sobreira**,[5] **and Zubair M. Ahmed**[6]

[1]*Department of Ophthalmology, University of Cincinnati College of Medicine, Cincinnati, OH, USA*
[2]*Cincinnati Eye Institute, Cincinnati, OH, USA*
[3]*Division of Pediatric Ophthalmology, Cincinnati Children's Hospital Medical Center, Cincinnati, OH, USA*
[4]*Division of Human Genetics, Cincinnati Children's Hospital Medical Center, Cincinnati, OH, USA*
[5]*McKusick-Nathans Institute of Genetic Medicine, Johns Hopkins University School of Medicine, Baltimore, MD, USA*
[6]*Department of Otorhinolaryngology, School of Medicine, University of Maryland, Baltimore, MD, USA*

Correspondence should be addressed to Robert A. Sisk; rsisk@cincinnatieye.com

Robert A. Sisk and Robert B. Hufnagel contributed equally to this work.

Received 4 January 2018; Revised 19 April 2018; Accepted 2 May 2018; Published 11 July 2018

Academic Editor: Hyeong Gon Yu

Purpose. To present new clinical features, multimodal and ultrawide-field imaging characteristics of peripheral cone dystrophy (PCD), and results of laboratory and genetic investigation to decipher the etiology. *Methods*. Retrospective observational case-series. *Results*. Three patients with PCD presented with bilateral paracentral scotomas and a mean visual acuity of 20/25. All exhibited confluent macular hyperautofluorescence with a central bull's eye lesion. Spectral-domain optical coherence tomography revealed loss of outer retinal elements, particularly the inner segment ellipsoid band and external limiting membrane, within the area of macular hyperautofluorescence. This area corresponded with a lightened fundus appearance and variable retinal pigment epithelium (RPE) abnormalities. Full field and multifocal electroretinography distinguished PCD from other photoreceptor dystrophies. Ultrawide-field imaging revealed irregular peripheral retinal lesions in a distribution greater nasally than temporally and not contiguous with the macular lesion. Functional and anatomic testing remained stable over a mean follow-up of 3 years. Laboratory investigation for causes of uveitis was negative. Whole exome sequencing identified rare variants in genes associated with macular or cone dystrophy or degeneration. *Conclusions*. In contrast to the original description, the funduscopic and fluorescein angiographic appearance of PCD is abnormal, although the defects are subtle. Peripheral lesions may be observed in some patients. Bilateral, symmetric, macular hyperautofluorescence associated with outer retinal atrophy that spares the fovea is a characteristic of PCD. Pathogenic variants in the same gene were not shared across the cohort, suggesting genetic heterogeneity. Further evaluation is warranted.

1. Introduction

Cone dystrophy is a slowly progressive, diffuse photoreceptor dystrophy that presents as hemeralopia, reduced visual acuity, and nystagmus associated with macular cone photoreceptor and retinal pigment epithelium (RPE) atrophy [1–6]. Two forms of localized cone dysfunction syndromes have been described: occult macular dystrophy (OCMD; MIM 613587) and peripheral cone dystrophy (PCD; MIM 609021) [7–16]. OCMD and PCD can be segregated by electrophysiologic responses to full field electroretinography (ffERG) and multifocal electroretinography (mfERG). OCMD displays normal photopic waveforms on ffERG and reduced mfERG responses only at the fovea, which correlates clinically with reduced visual acuities and foveal cone photoreceptor atrophy seen on spectral-domain optical coherence tomography (SDOCT). OCMD is inherited in a dominant fashion and is usually associated with mutations in *RP1L1* [17].

PCD is a very rare retinal disease originally characterized by normal fundoscopic appearance, normal fluorescein

angiographic imaging, mildly reduced photopic potentials with preserved scotopic potentials on ffERG, and relative preservation of foveal cone function by mfERG. The name "peripheral cone dystrophy" is unfortunately a misnomer, as central rather than peripheral cone involvement is a prominent feature, but the name was selected to contrast "central" cone dystrophy, or OCMD, because the foveola is preserved. Kondo and Miyake, who also first described OCMD, first reported three cases of PCD, who presented with bilateral ring scotomas and near-normal visual acuity [7, 12]. These seminal cases included a pair of affected siblings, suggesting autosomal recessive inheritance or autosomal dominant inheritance with parental germline mosaicism. However, no genetic cause has been associated with this disorder.

PCD is a diagnosis of exclusion. The differential diagnosis includes Stargardt disease, cone dystrophy, enhanced S-cone syndrome, pericentral retinitis pigmentosa, syphilitic placoid chorioretinitis, acute zonal occult outer retinopathy (AZOOR), posterior scleritis, traumatic retinopathy (commotio retinae), posterior uveitis, hydroxychloroquine toxicity, and autoimmune retinopathy [18–22]. Here, we report previously undescribed funduscopic, fundus autofluorescence (FAF), infrared imaging, fluorescein angiography (FA), and SDOCT abnormalities in three probands with PCD. We also describe results of our investigation using whole exome sequencing (WES) to identify a causative gene among our three unrelated probands.

2. Methods

2.1. Human Subjects Research. Institutional Review Board (IRB) approval was obtained for retrospective and prospective evaluation of all cases of PCD diagnosed at the Cincinnati Eye Institute between September 1, 2009, and May 1, 2013. Records were reviewed for patient age, sex, demographics, family history, medical history, toxic and infectious exposures, and ocular examination findings. Patients underwent extensive ophthalmic testing including fundus imaging with standard (TRC-50DX®, Topcon Medical Systems, Oakland, NJ) and ultrawide-field cameras (Optos 200Tx®, Optos, Marlborough, MA). Multimodal imaging (Spectralis® HRA-OCT, Heidelberg Engineering, Dossenheim, Germany) was utilized including red-free imaging, infrared imaging (IR), FAF, FA, and SDOCT. Full field and multifocal electroretinography (Diagnosys D218, Software V6.0.47 with 61 hexagon array, Lowell, MA) was performed to meet ISCEV standards. B-scan ultrasonography (Eye Cubed I^3® unit, Ellex, Minneapolis, MN) was performed to exclude posterior scleritis or infiltrative choroidal disease. Laboratory testing was performed for infectious and noninfectious causes of uveitis, including syphilis, tuberculosis, cat-scratch disease, Lyme disease, toxoplasmosis, ANCA-associated uveitides, systemic lupus erythematosus, and sarcoidosis. HLA testing was performed to evaluate for HLA-B27-associated uveitis and birdshot chorioretinopathy.

2.2. Molecular Genetic Investigation. After informed consent was obtained to participate in genetic research, whole blood samples were obtained from all patients. Genetic analysis was performed through the BHCMG and the National Eye Institute (eyeGENE®, National Ophthalmic Genotyping and Phenotyping Network, Stage 1—Creation of DNA Repository for Inherited Ophthalmic Diseases). Sanger sequencing for *ABCA4*, *PRPH2*, and *ELOVL4* was performed on one proband (case 1), and *PRPH2*/RDS-peripherin was sequenced in all cases. The Baylor-Hopkins Center for Mendelian Genomics (BHCMG) performed WES and analysis on all three probands. The aforementioned testing, clinical histories, and family histories were provided to these organizations with the patients' permission using PhenoDB [23].

We used WES to investigate both for variations in retinal dystrophy genes in each proband and for genes commonly mutated in the 3 affected individuals. The Agilent SureSelect HumanAllExonV4_51MbKit_S03723314 was used for exome capture. Libraries were sequenced on the HiSeq2500 platform with onboard clustering using 100 bp paired end runs and sequencing chemistry kits TruSeq Rapid PE Cluster Kit-HS and TruSeq Rapid SBS-HS. FASTQ files were aligned with BWA [24] version 0.5.10-tpx to the 1000 genomes phase 2 (GRCh37) human genome reference. Duplicate reads were flagged with Picard version 1.74. Local realignment around indels and base call quality score recalibration were performed using the Genome Analysis Toolkit (GATK) 2.3–9 multisample calling with a Unified Genotyper [25]. Variant filtering was done using the variant quality score recalibration (VQSR) method [26]. The variant prioritization strategy was designed using the Variant Analysis Tool of PhenoDB [27] and Ingenuity Variant Analysis (Qiagen, Redwood City, CA). Rare functional variants (missense, nonsense, splice site variants, and indels) with a MAF ≤ 0.01 in the Exome Variant Server (release ESP6500SI-V2) or 1000 Genomes Project were prioritized [28]. We also excluded all variants found in in-house controls for PhenoDB (CIDRVar 51 Mb) and Cincinnati Children's Hospital Medical Center (CCHMC). Post-analysis, PCR primers were designed to amplify exons and flanking intronic splice sites followed by direct Sanger sequencing to validate the candidate causative variants.

3. Results

3.1. Case Descriptions. Three patients (two female and one male) were identified at a median age of 51 years (range 42 to 57 years) with visual symptoms that began at a mean of 9 years prior. Mean best-corrected visual acuity was 20/25, and it remained stable throughout the mean follow-up of 3 years. All complained of paracentral visual field loss and mildly reduced best-corrected visual acuities, and no patient described progression beyond their initial presentation. No patient could attribute a precipitating event, injury, or illness to the onset of symptoms, yet none described their vision loss as acute. Only case 2 had any family history of retinal dystrophy or blindness or exposure to any medication known to be toxic to the retina or RPE. Laboratory investigation for causes of infectious and noninfectious uveitis was negative in all patients.

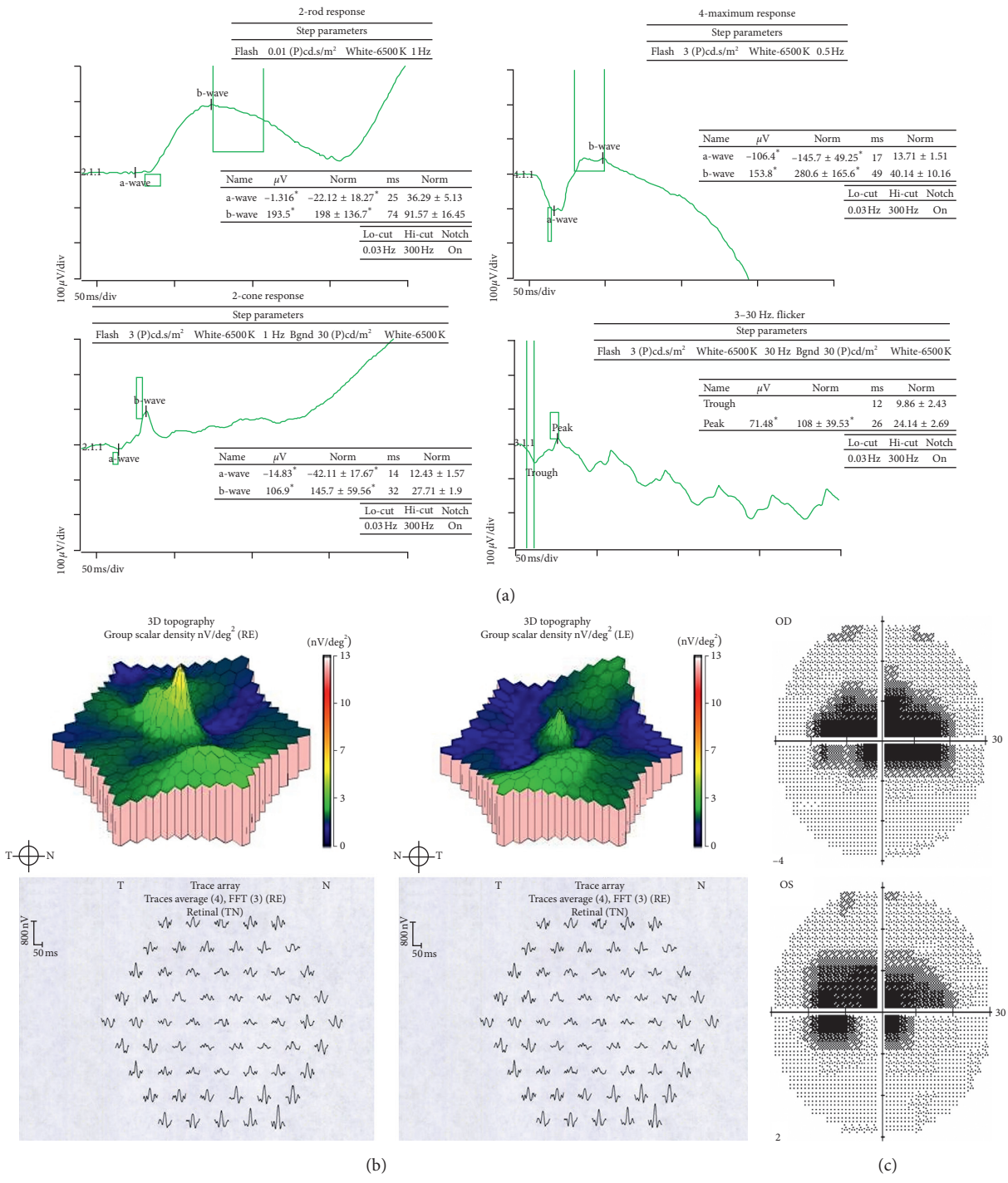

Figure 1: Full field electroretinography (ffERG), multifocal electroretinography (mfERG), and visual field testing of case 1. (a) Full field electroretinography demonstrated low normal a- and b-wave amplitudes and implicit times on scotopic testing. Photopic testing showed moderately reduced a- and b-wave amplitudes with mildly delayed implicit times. See Supplementary Figure 1 for normal reference and ffERG for cases 2 and 3. (b) Central amplitudes were reduced in the central and paracentral 15° with relative sparing of the fovea on multifocal electroretinography. See Supplementary Figure 2 for normal reference and mfERG testing for cases 2 and 3. (c) Humphrey Sita-Standard protocol with size III stimulus revealed bilateral dense paracentral scotomas that spared foveal sensitivities. See Supplementary Figure 3 for visual field testing of cases 2 and 3.

3.1.1. Case 1. A 57-year-old Caucasian male presented with a ten-year history of nonprogressive ring scotomas OU (Figure 1). He denied other ocular- or nonocular-associated symptoms or any prior ocular trauma. Family history was negative for any retinal disease, uncorrectable vision loss, hemeralopia, or nystagmus. Best-corrected visual acuities on presentation were 20/25-2 OU. Ishihara color vision testing was diminished to four out of eleven plates in each eye.

Anterior segment examination was unremarkable except for mild nuclear sclerotic cataracts in both eyes. He exhibited typical funduscopic findings for pathologic myopia including staphylomatous changes, parapapillary atrophy, and inferotemporal lacquer cracks in the left eye and areas of chorioretinal atrophy in both the posterior pole and periphery OU.

3.1.2. Case 2. A 52-year-old African American female was referred for evaluation after three years of hydroxychloroquine treatment for rheumatoid arthritis. The medication dosage was never supratherapeutic, and she denied visual changes on the medication. Interestingly, her visual complaints predated the use of the medication by two years, but no baseline visual field testing had been performed. She described her mother as having "macular degeneration and retinitis pigmentosa" that began as central vision loss in her forties and progressed to nyctalopia and peripheral vision loss. Visual acuities were 20/20 OU, and anterior segment examination was unremarkable. Ishihara color vision testing was diminished to ten out of fifteen plates in the right eye and eleven out of fifteen plates in the left eye. The right eye had received laser retinopexy after posterior vitreous detachment for symptomatic retinal holes associated with lattice degeneration.

3.1.3. Case 3. A 42-year-old Caucasian female who originally presented 22 years prior with perimacular pigmentary changes had been diagnosed with bilateral choroidal osteomas, although neither eye had an orange choroidal lesion nor hyperreflective plaque by B-scan ultrasonography on any prior testing. She denied progression of vision loss, although visual acuities at original presentation were 20/20 OD and 20/30 OS and declined to 20/30 OU when diagnosed with PCD. Ishihara color vision testing was diminished to three out of fifteen plates in each eye. Her family history was negative for eye-related phenotypes. Anterior segment examination was normal, but fundus examination showed perimacular arcuate and circumferential nasal retinal lightening with central pigmentary clumping OU.

3.2. Electroretinography. Full field electroretinography (ffERG) showed a pattern consistent with cone dystrophy for cases 1 and 3 (Supplementary Figure 1). There were relatively preserved (at the lower limit of our normal reference range) a- and b-wave amplitudes with normal implicit times on scotopic testing and moderately reduced amplitudes with mildly increased implicit times on photopic testing. ffERG resembled cone-rod dystrophy for case 2 with moderate reductions in a- and b-wave amplitudes and delayed implicit times on scotopic and photopic testing (Supplementary Figure 2). Responses were symmetrical between OD and OS in most recorded waveforms in all patients. Waveforms had otherwise typical architecture and specifically did not have a sinusoidal appearance. Multifocal electroretinography demonstrated diffusely reduced amplitudes and increased implicit times with relative sparing of the foveal spike OU (Supplementary Figure 2).

3.3. Visual Fields. Humphrey 30-2 Sita Standard and Goldmann threshold visual field testing confirmed bilateral paracentral scotomas in all patients that remained stable throughout follow-up (Supplementary Figure 3). The macular appearance was unremarkable funduscopically in all cases except for the myopic fundus changes in case 1. Peripheral RPE alterations were observed in the nasal peripheral retina in all patients. These were unilateral in case 2 and attributable to a history of laser retinopexy for retinal breaks associated with posterior vitreous detachment. Scotomas were not observed corresponding to these peripheral lesions.

3.4. Blue-Light Fundus Autofluorescence. All probands had bilateral, relatively symmetric, central, geographic areas of confluent macular hyperautofluorescence with rounded or scalloped borders that extended nasally past the optic disc (Figure 2). In cases 1 and 3, this area was sharply delineated from the surrounding isoautofluorescence by a narrow border of hyperautofluorescence of greater intensity than the central confluence. This transition could be observed funduscopically by a subtle color change best appreciated on the laser-generated ultrawide-field images (Figure 3). Case 2 had a gradual transition in FAF and no funduscopically visible transition. The caliber of retinal vessels was reduced with the areas of central FAF alterations in all patients. Focal curvilinear hypoautofluorescent interruptions were present in two probands with funduscopically visible RPE alterations (lacquer cracks of high myopia in case 1 and a superior, symmetrical, serpiginous band of RPE thinning and clumping extending away from the disc in case 3). Centrally, a bull's eye lesion of alternating rings centripetally of hypoautofluorescence and hyperautofluorescence surrounding normal foveal hypoautofluorescence was observed in all patients, although the bull's eye lesion was least distinct in case 2.

Peripheral autofluorescence abnormalities were appreciated on ultrawide-field imaging in cases 1 and 3 (Figure 4). These ranged from clustered patches of arcuate, amoeboid hyperautofluorescence with variable central hypoautofluorescence to discrete, isolated ovoid areas of hyperautofluorescence of variable size. The location of peripheral lesions was variable but tended to involve the nasal hemiretina, producing a bifocal appearance when viewed against the macula on the ultrawide-field images. Funduscopically, this corresponded to lightened areas of the nasal fundus (cases 1 and 3) with central RPE pigment clumping and intraretinal migration (case 3).

3.5. Fluorescein Angiography. FA demonstrated a subtle hyperfluorescence at the area of confluent macular hyperautofluorescence. Areas of funduscopically visible RPE thinning and atrophy demonstrated anticipated window defects. Areas of RPE clumping exhibited blockage. No patient had

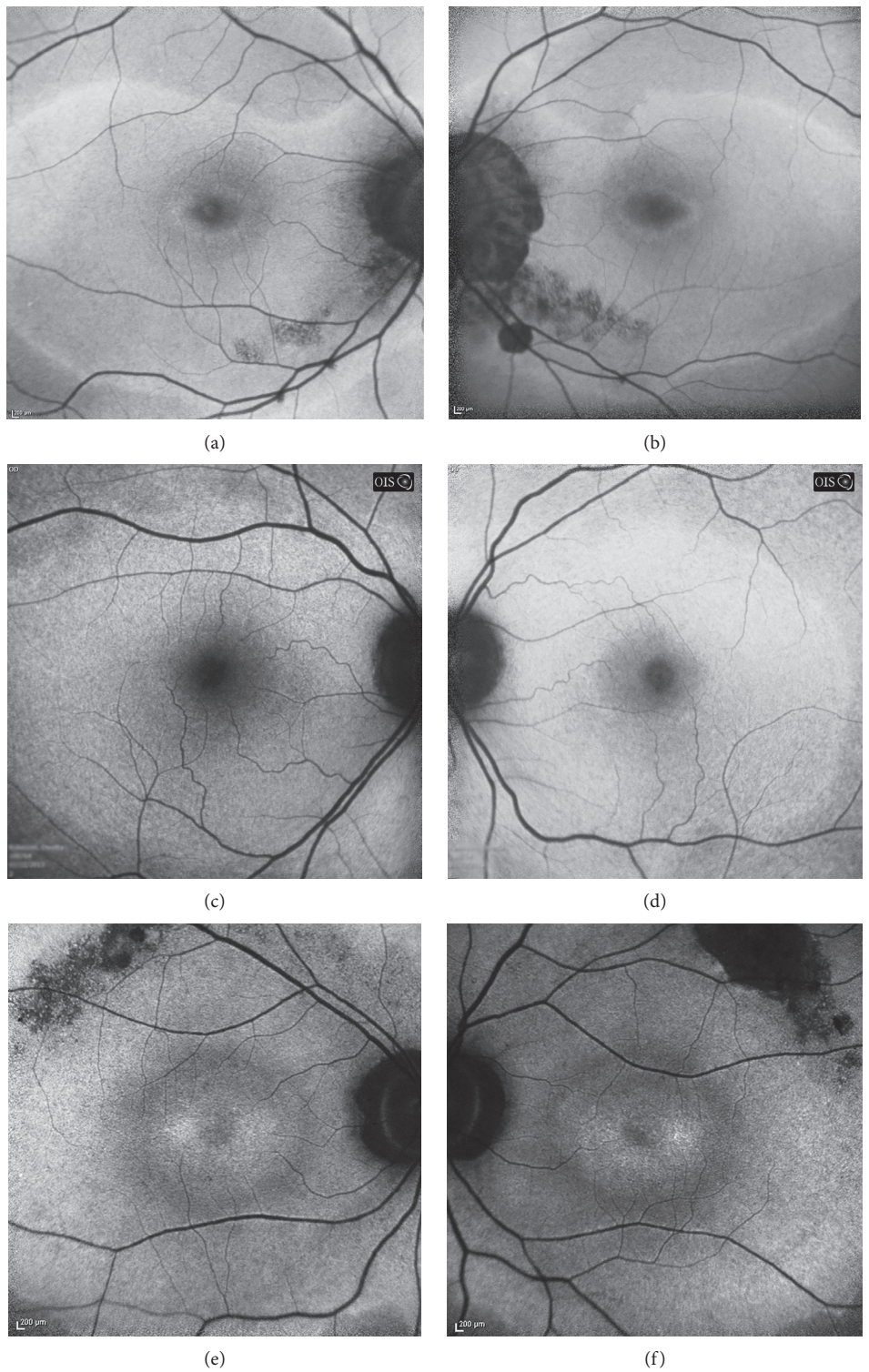

(a) (b) (c) (d) (e) (f)

Figure 2: Thirty degree confocal scanning laser ophthalmoscope-based fundus autofluorescence by 488 nm argon blue laser excitation and emission filtered less than 500 nm. (a, b) Right and left maculas of case 1 had a geographic area of hyperautofluorescence with uniform hyperautofluorescent scalloped border that encompassed the majority of the macula and parapapillary retina outside alpha zone atrophy (seen as intensely hypoautofluorescent). A central ovoid bull's eye lesion of alternating hyper- and hypoautofluorescence was centered on the fovea. Linear granular hypoautofluorescence from lacquer cracks was observed in this patient with high myopia. (c, d) Right and left maculas of case 2 showed similar features, except the outer hyperautofluorescent border and bull's eye lesions were not as prominent. (e, f) Right and left maculas of case 3 also exhibited coarse, densely hypoautofluorescent arcs along the superotemporal arcades and a larger central bull's eye lesion in each eye.

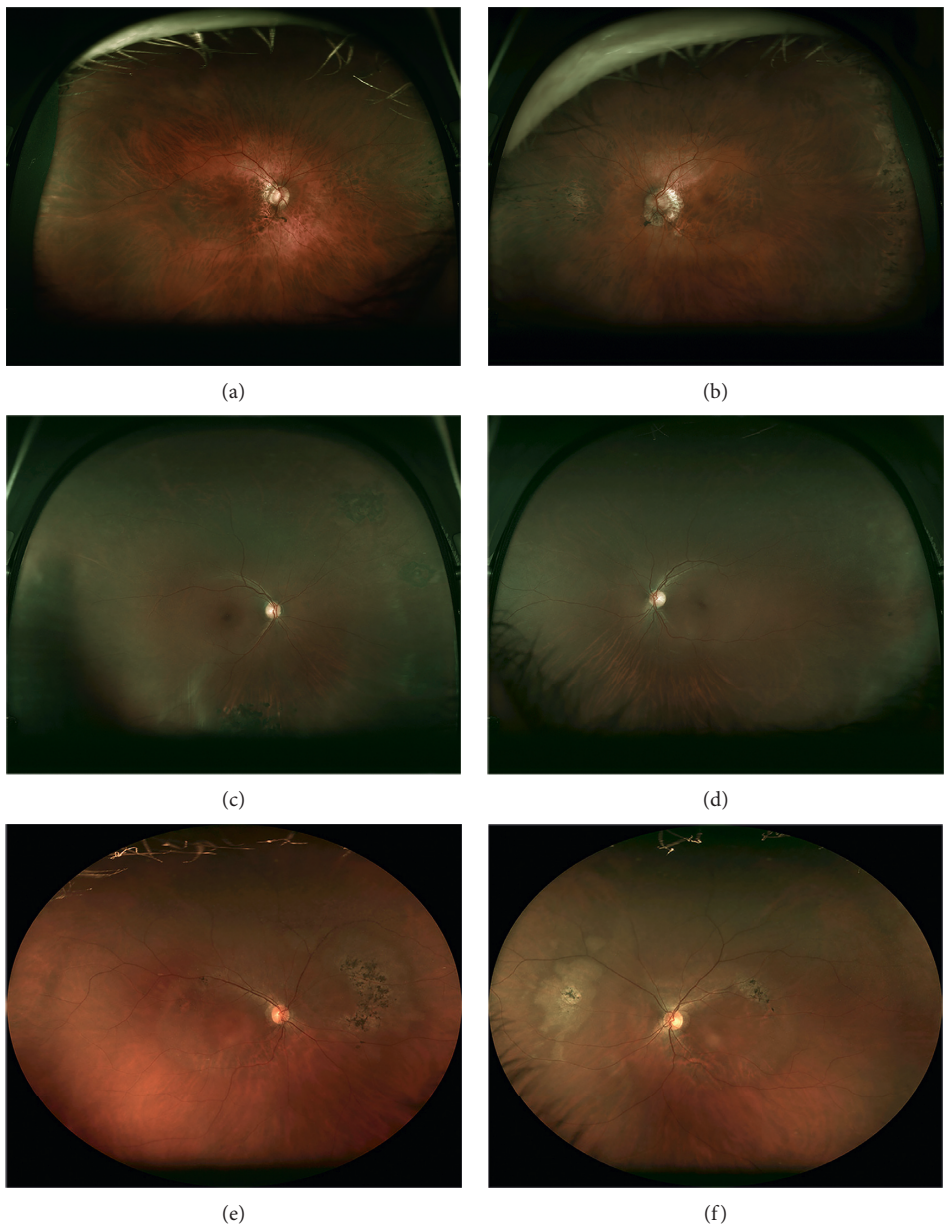

Figure 3: Two hundred degree ultrawide-field color retinal imaging using 633 nm, 532 nm, and 488 nm lasers demonstrate subtle retinal whitening in all patients corresponding to the geographic areas of hyperautofluorescence observed in Figure 2. Peripheral retinal pigment epithelial abnormalities were seen in the nasal periphery in all patients, although these were attributable to prior laser retinopexy in case 2. (a, b) Right and left fundi of case 1 exhibited alpha zone parapapillary atrophy and surrounding fundus lightening associated with high myopia. A nasal tongue of pigmentary changes extended from the peripheral retina posteriorly along the horizontal midline in each eye. (c, d) Right and left fundi of case 2 showed areas of lattice degeneration in both eyes surrounded by chorioretinal scarring from laser treatment. (e, f) Right and left fundi of case 3 had prominent posterior rings of retinal whitening and pigmentary alterations centered around the maculas. Irregular circumferential lesions with central reticular intraretinal pigment migration were observed nasally in both eyes.

vascular filling defects or leakage. Case 2 had blocked choroidal fluorescence. Interestingly, case 1, who had a single pathologic *ABCA4* mutation, did not have blocked choroidal fluorescence.

3.6. Infrared Imaging. Infrared imaging was less useful for discerning the transition from abnormal to intact outer retinal architecture, although there was a subtle intensity change that mirrored the transition zone on FAF imaging.

3.7. Ultrasonography. B-scan ultrasonography excluded posterior scleritis, choroidal thickening or infiltration, or retrobulbar disease (data not shown).

3.8. Spectral-Domain Optical Coherence Tomography. SDOCT demonstrated reduced macular thickness and volume measurements in all probands due to loss of outer retinal elements (Figure 5). Inner retinal thickness and architecture were undisturbed. The inner segment ellipsoid

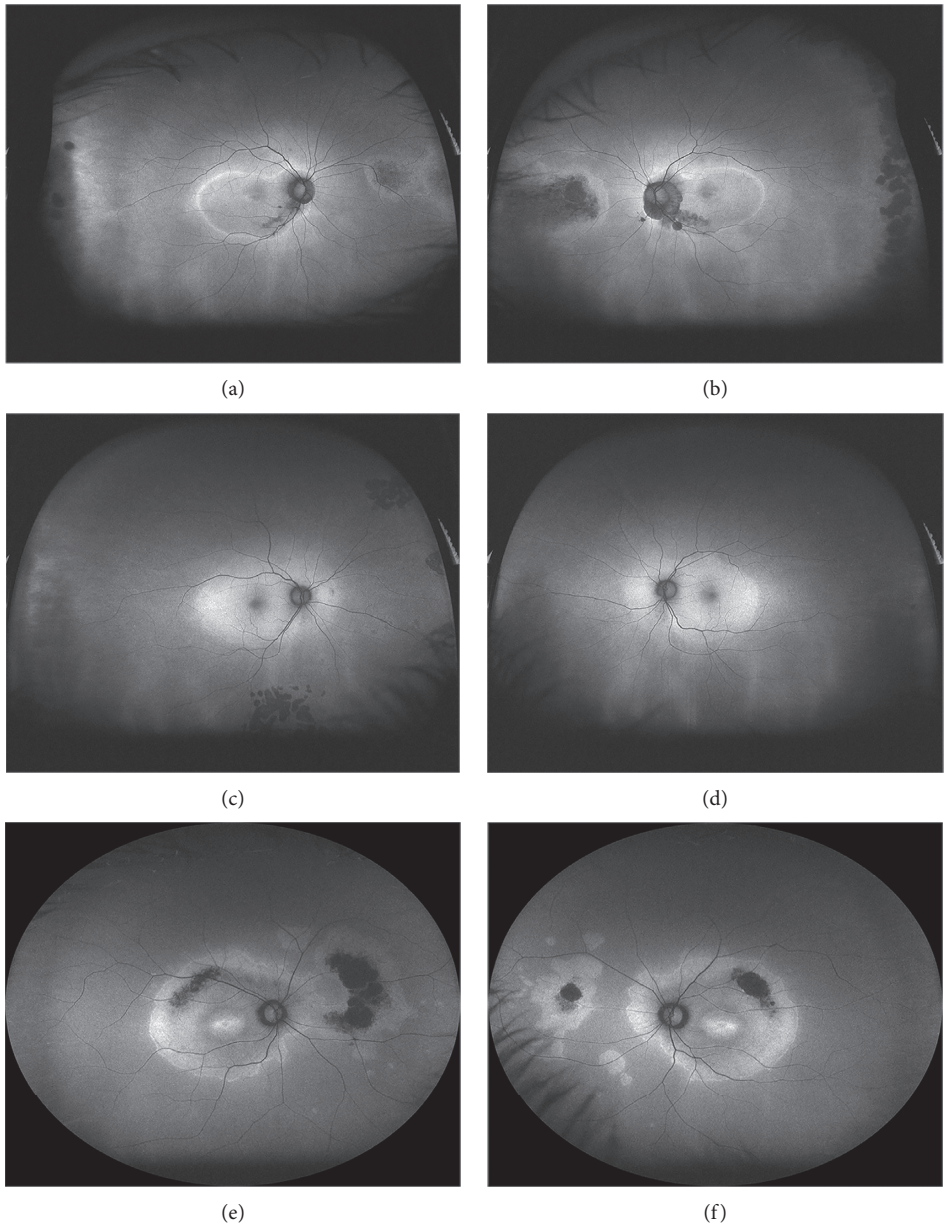

Figure 4: Two hundred degree ultrawide-field fundus autofluorescence with 488 nm laser excitation demonstrates macular changes as described in Figure 2 but reveals additional peripheral autofluorescence abnormalities in all patients. (a, b) Right and left fundi of case 1 had grouped nummular hypoautofluorescent areas anterior to the equator from cobblestone degeneration. A hypoautofluorescent tongue with hyperautofluorescent borders extended posteriorly towards the optic nerve in both eyes. Areas of funduscopically visible black pigment clumping appeared densely hypoautofluorescent. (c, d) Hypoautofluorescence from prior laser treatment of lattice degeneration in the right eye was the only evident peripheral autofluorescence abnormality seen in case 2. (e, f) A bifocal area of hyperautofluorescence with central hypoautofluorescence to the nasal portion was observed in the right and left fundi of case 3. In the right eye, the lesions were contiguous and the area of hypoautofluorescence was larger.

(iSE) band, external limiting membrane (ELM), and even photoreceptor cell bodies were diminished or absent within the well-defined area of confluent macular hyperautofluorescence. The external border between hyperautofluorescence and iso-autofluorescence marked the transition from abnormal to intact outer retinal architecture and lamination. The central bull's eye lesion on FAF imaging represented a transition from diminished to intact iSE and ELM bands, a pattern previously observed with other photoreceptor dystrophies. Within the macula, retinal architecture was most intact at the fovea, consistent with the sparing of central visual acuities relative to the surrounding paracentral scotomas. The choroid was normal in thickness, except for an anticipated amount of thinning in case 1 related to high myopia.

3.9. Genetic Analysis. Genetic testing for genes associated with cone dysfunction, retinitis pigmentosa, or lipofuscin

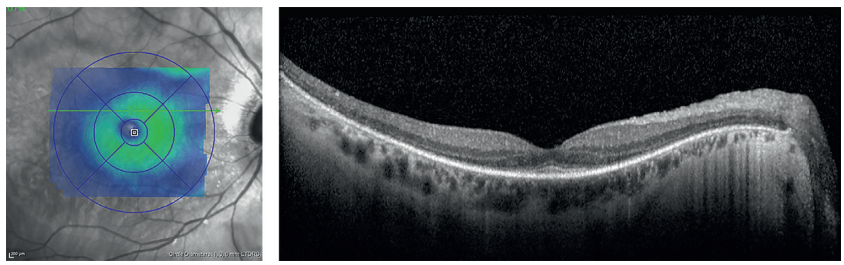

(a)

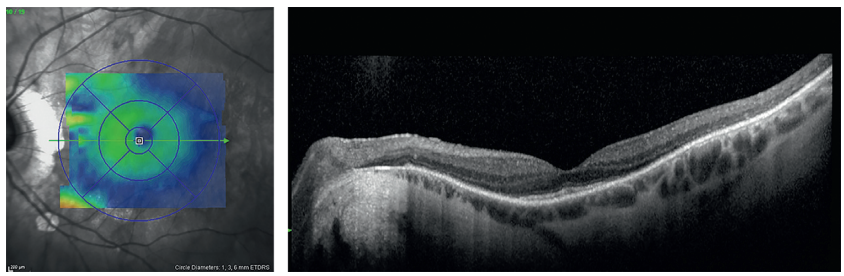

(b)

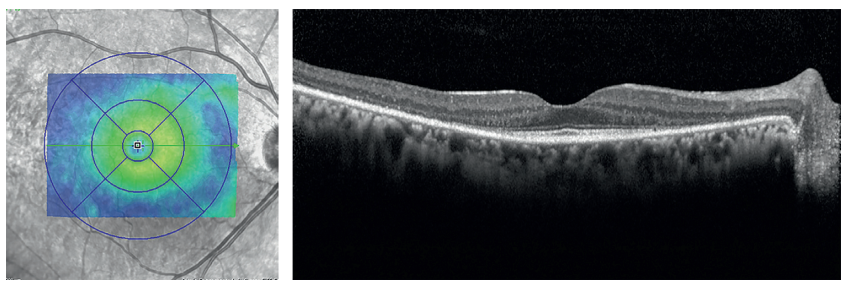

(c)

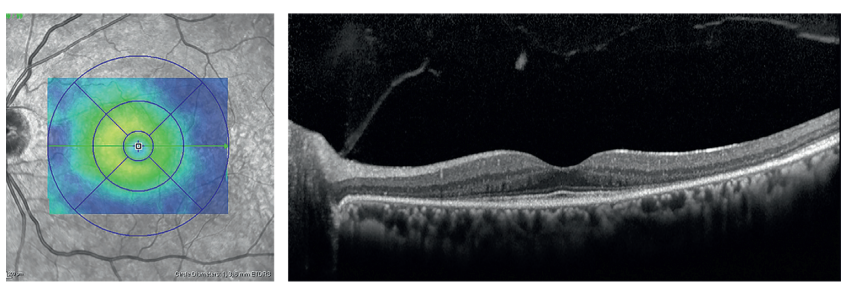

(d)

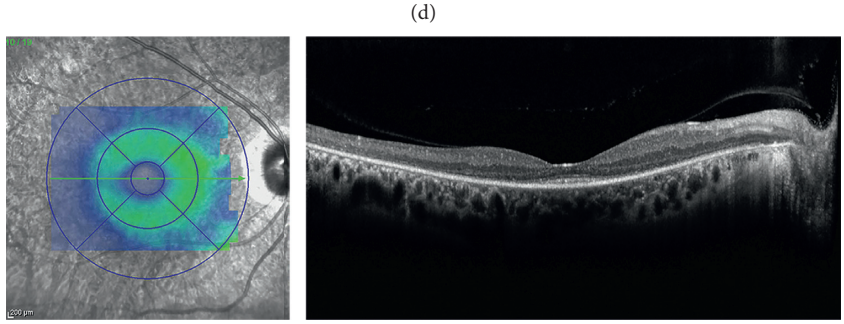

(e)

Figure 5: Continued.

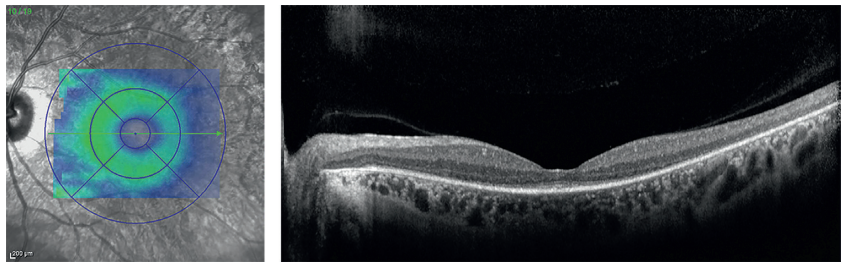

(f)

Figure 5: Spectral-domain optical coherence tomography registration thickness maps (left column) exhibited severe retinal thinning in all eyes. Accompanying foveal horizontal raster scans (right column) demonstrated outer retinal loss sparing the foveola in both eyes of all patients. The external limiting membrane, inner segment ellipsoid band, and photoreceptor outer segments were lost centrifugally until the hyperautofluorescent border of the macular lesions in Figure 2, where there was transition to normal retinal architecture. All cases had normal choroidal thickness, except case 1, who had pathologic myopia. (a, b) Right and left maculas of case 1 had staphylomatous posterior pole curvature, alpha zone parapapillary RPE atrophy, and choroidal thinning associated with pathologic myopia. (c, d) Right and left maculas of case 2 had the greatest preservation of outer retinal layers at the fovea and the nerve fiber layer throughout the macula compared to the other two cases. (e, f) Right and left maculas of case 3 had reduced inner retinal thickness with preservation of inner retinal lamination, similar to case 1.

accumulation revealed no pathogenic variants in a pattern consistent with a monogenic cause for disease. Specifically, Sanger sequencing of *ABCA4*, *PRPH2*/RDS-peripherin, and *ELOVL4* was negative except for Proband 1, who had a heterozygous *ABCA4* missense variant (c.2588G>C; p.Gly863Ala) and no family history of Stargardt disease or cone-rod dystrophy. This substitution has been previously reported as disease-causing (rs76157638; HGMD ID CS024003), but not associated with pericentral retinal degeneration (PRD) [29–32].

WES was then performed on the three probands. Details of bioinformatics analysis are available in Methods. Briefly, we prioritized rare functional variants (missense, nonsense, splice site variants, and indels) that were heterozygous, homozygous, or compound heterozygous in each of the 3 probands and excluded variants with a MAF >0.01 in the Exome Variant Server (release ESP6500SI-V2), 1000 Genomes Project, or Exome Aggregation Consortium (ExAC) [28, 33]. We also excluded all variants with a frequency of >0.01 found in in-house controls for BHCMG (CIDRVar 51 Mb) and CCHMC. This allele frequency cutoff was used to account for variants causing autosomal recessive disease. Parent and sibling samples were not available for segregation analysis.

Variant lists generated for each proband were first screened for rare variants (<1% minor allele frequency) in 52 genes related to pattern dystrophy, macular dystrophy, cone dystrophy, cone-rod dystrophy, rod-cone dystrophy, and cone photoreceptor development and function, including cone opsin genes (Supplementary Table 1). Supplementary Table 2 lists the 7 variants that were validated by Sanger sequencing. The *ABCA4* variant in case 1 was also detected by the WES. In cases 1 and 2, missense variants were identified in *IMPG2*, p.Leu842Met, and p.Ser11Tyr, respectively. *IMPG2* is associated with autosomal dominant vitelliform macular dystrophy 5 [MIM #616152] [34]. Both variants were predicted pathogenic by SIFT and Polyphen-2 [35, 36]. In case 2, a rare, predicted-pathogenic variant was noted in the protein kinase domain of *GUCY2D* (p.Glu779Lys), associated with autosomal dominant cone-rod dystrophy 6 [MIM #601777] [37, 38]. Additionally in case 2, we identified two variants in *RP1L1*, p.Ala624Thr, and p.Trp2306Arg. However, neither were predicted pathogenic by Polyphen-2, and only p.Trp2306Arg was predicted pathogenic by SIFT. In case 3, we identified one predicted-pathogenic variant in *ADAM9* (p.Gln800His), associated with cone-rod dystrophy 9 [MIM #612775] [39]. We then searched for genes with rare variants in other retinal dystrophy genes (Supplementary Table 3) and rare variants in all 3 probands (not shown), though no common candidate gene was identified with rare variants. These variants are all considered variants of uncertain significance (VOUSs).

4. Discussion

At the time of its initial description a decade ago, PCD was an electrophysiologic diagnosis in individuals with normal fundus appearance and fluorescein angiography [12]. OCT and FAF had limited clinical applications and lacked the resolution available with conventional scanning laser ophthalmoscope-based platforms. Yet review of the fundus photography and fluorescein angiography images from the report by Kondo and coauthors demonstrates the same features we describe in our cohort: (a) a lightened macular color funduscopically that transitions at the temporal arcades, (b) narrowing of retinal vessels within the affected macular region, (c) macular hyperfluorescence on FA that transitions at the same location as the funduscopic color change, and (d) variable blocked choroidal fluorescence outside the macular lesion. In our cohort, two of the three probands also had nasal RPE and retinal changes that were not described in the original report. From the findings presented, we assert that PCD has features on ophthalmoscopy and multimodal imaging that distinguishes this diagnosis from other rare diseases.

SDOCT and FAF clarify the functional deficits observed by visual field and electroretinographic testing. The total macular volume is reduced, and the photoreceptor layer

within the macular lesion, except of the fovea, is thinned and disorganized. The iSE and ELM bands particularly are diminished or absent with greater involvement of cone photoreceptor cell bodies centrifugally until the border of the hyperautofluorescent lesion. This unveiling of outer retinal elements was associated with the observed window defect of confluent macular hyperautofluorescence [40]. The transition between affected and unaffected outer retina correlated well with the transition from hyperautofluorescence to isoautofluorescence. Unlike SDOCT changes observed in retinitis pigmentosa and typical cone-rod dystrophies, choroidal thickness was not reduced, and the RPE remained largely intact except focal disruptions which were also evident funduscopically [41–49]. These findings corroborate that the photoreceptor layer is primarily affected, and the RPE may be secondarily affected. Ultrawide-field FAF imaging revealed large affected regions nasally that produced a bifocal appearance and helped explain the greater reduction in cone amplitudes than would be expected for a purely macular disease. Despite no reduction in inner retinal thickness by SDOCT, retinal arterioles within the central hyperautofluorescent region with photoreceptor disease were thinned. There was no evidence from SDOCT or FA imaging of a primary vascular disease. Without photoreceptor-generated impulses from affected areas, presumably, there is a reduced activity of inner retinal layers, reduced oxygen demand, and a resultant reduction in vessel caliber by autoregulation. This has been observed commonly in other photoreceptor dystrophies [50]. We observed greater variation in full field electroretinographic findings than the original series presented by Kondo et al., with cases 1 and 3 displaying the typical pattern reported for PCD and case 2 having a cone-rod dystrophy pattern.

PCD can be distinguished from pericentral retinal degeneration (PRD), which shares many clinical features, and has heterogeneous genetic causes, particularly genes causing retinitis pigmentosa and Stargardt disease. Foremost, the electrophysiologic profile for PRD resembles rod-cone dystrophy rather than cone or cone-rod dystrophy. Annular visual field loss is complete in PRD and may be incomplete in PCD. Peripheral retinal pigmentary changes are not observed in PRD, so annular or curvilinear visual field deficits are not observed beyond forty degrees, as are seen in our cases of PCD. Cases of *ABCA4*-related PRD involve mutations that prevent production of a protein product and produce photoreceptor dysfunction. Heterozygous mutations in ABCA4 can produce bull's eye lesions or occult macular dystrophy, but photoreceptor loss does not extend past the arcades and is accompanied by progressive RPE atrophy.

PCD may be a nonspecific rare presentation of cone dystrophy, and this is supported by pathogenic variants associated with macular dystrophy in all patients without a consensus candidate gene among them. Although WES did not reveal the leading candidate gene(s) among the probands, all probands harbored VOUSs in known photoreceptor dystrophy genes. We observed rare and predicted pathogenic variants in *IMPG2* in cases 1 and 2, which is associated with autosomal dominant vitelliform macular dystrophy, and variants in *RP1L1* in case 2, which is associated with autosomal dominant occult macular dystrophy [17, 34]. Both genes cause a variable macular phenotype overlapping with peripheral cone dystrophy. The manifestations of *RP1L1* pathogenic variants are complex and include both limited and diffuse forms of cone dystrophy [17, 51, 52]. We speculate that *RP1L1* may modulate the effects of another cone dystrophy gene or autoimmune retinopathy contributing to allow sparing of the foveolar cones in the PCD phenotype. In case 2, the previously unreported variant in *GUCY2D*, associated with autosomal dominant cone-rod dystrophy, was considered as potentially contributing to this phenotype given the cone-rod pattern on ffERG and her mother's end stage cone-rod dystrophy phenotype. Given foveal sparing in both case 2 and her mother, the phenotype may be modulated by the *RP1L1* variant. No prior report of *GUCY2D* or *ADAM9*-related cone dystrophy involves broad macular involvement sparing the foveola [39, 53–55]. Rather, those diseases typically involve the fovea early and have prominent macular RPE changes, and those with bull's eye lesions sparing the umbo do not extend beyond the parafovea.

Several features of PCD could also be consistent with postinflammatory changes of a retinal white dot syndrome [19, 56–65]. The geographic and racial backgrounds were variable, and two cases were sporadic. The regional clustering of both cohorts in the peer-reviewed literature against time and geography favors an autoimmune disease incited by a local pathogen or toxin. The lack of progression observed by anatomical and electrophysiological testing is atypical for retinal dystrophy, although follow-up with high-resolution anatomic testing was performed after three years and may represent the end stage of disease progression. Case 3 was noted to have nonprogressive symptoms and stable fundus appearance when compared with her original retinal drawings from twenty years prior. The Japanese cohort has exhibited similar stability after the publication (Kondo, *personal communication* 2013). The variable involvement of the peripheral retina resembles the random pattern observed in inflammation more than the predictable patterns observed in retinal dystrophies. The peripheral hyperautofluorescent lesions with central hypofluorescent RPE disruption are similar to those observed in other retinal white dot syndromes (MEWDS, AZOOR, and PIC). On the contrary, specific sparing of the fovea while the surrounding outer retina is decimated would be unexpected for an inflammatory disease. With the exception of MEWDS, severe RPE alterations and persistent scotomas usually accompany preceding chorioretinal inflammation, and these were not observed with the peripheral lesions. The presence of tapetal sheen, seen intermittently in case 2 and not previously described with PCD, is a characteristic for a retinal dystrophy rather than inflammation or drug toxicity.

A third explanation is that both genetic and environmental factors play a role in the development and manifestations of PCD. An environmental agent or pathogen may create an autoimmune response against short wavelength (S-cone) photoreceptors modulated by a pathogenic variant in cone dystrophy genes like *RP1L1*. In case 2, we cannot rule

out the contribution of hydroxychloroquine toxicity to her phenotype, although photoreceptor damage to the arcades would be unusual without prominent RPE changes.

In summary, PCD is a distinct clinical entity with ring scotomas, outer retinal attenuation relatively sparing the foveola, macular hyperautofluorescence with bull's eye lesions, and variable peripheral lesions. However, the etiology remains unknown. Studies of human and primate retinas demonstrate absence of S-cone photoreceptors within the foveola, greater S-cone concentrations within the macula than peripheral retina, and greater concentrations in the retinal periphery nasally than temporally [66–68]. This pattern highly correlates with the location of disease observed in our cohort. Given the limitation of patient numbers for this rare disease, further investigation is warranted, including whole exome sequencing of other probands, investigation of trios, animal models, and serum analysis from more recently affected individuals, and a search for an infectious homologue or compound with selective toxicity to S-cone proteins.

Data Availability

The data used to support the findings of this study are available from the corresponding author upon request.

Disclosure

One case was presented as an unknown at the 45th Annual Retina Society Conference in Washington, DC, October 4, 2012. The full cohort was presented at the 32nd annual meeting of the American Society of Retina Specialists in San Diego, CA, August 9–13, 2014.

Conflicts of Interest

The authors declare that they have no conflicts of interest.

Acknowledgments

The Baylor-Hopkins Center for Mendelian Genomics (BHCMG) and the National Ophthalmic Disease Genotyping and Phenotyping Network (eyeGENE) performed genetic analysis at no cost to the patients or the authors. Grants from the National Human Genome Research Institute, (1U54HG006542) and National Institute for Deafness and Communication Disorders (R01DC016295) provided support for this work.

Supplementary Materials

This article contains additional online-only material. The following should appear online only: Supplementary Tables 1–3. Supplementary Figure 1: results of full field electroretinography of the right eye for the 3 probands and a normal age-matched control. Waveforms were symmetrical between the two eyes of each patient and the control. Supplementary Figure 2: multifocal electroretinography of the right eye for the 3 probands and a normal age-matched control. Waveforms and 3D topography plots were symmetrical between the two eyes of each patient and the control. Supplementary Figure 3: visual field testing for the 3 probands. Humphrey visual field testing using a 30-2 Sita-Standard protocol with a size III stimulus was used for case 1. Cases 2 and 3 were tested using Goldmann threshold perimetry. Paracentral scotomas were identified by the smallest isopter. Case 2 could not discern I2E targets and had constricted I3E within 30°. Case 3 could not discern I3E targets. Supplementary Table 1: candidate photoreceptor and macular dystrophy genes. Supplementary Table 2: variants detected in candidate photoreceptor or macular dystrophy genes. Supplementary Table 3: variants detected in 2 of 3 probands in genes with known retinal expression. (*Supplementary Materials*)

References

[1] S. Roosing, A. A. Thiadens, C. B. Hoyng et al., "Causes and consequences of inherited cone disorders," *Progress in Retinal and Eye Research*, vol. 42, pp. 1–26, 2014.

[2] G. A. Fishman, "Electrophysiology and inherited retinal disorders," *Documenta Ophthalmologica*, vol. 60, no. 2, pp. 107–119, 1985.

[3] M. P. Simunovic and A. T. Moore, "The cone dystrophies," *Eye*, vol. 12, no. 3, pp. 553–565, 1998.

[4] M. Michaelides, D. M. Hunt, and A. T. Moore, "The cone dysfunction syndromes," *British Journal of Ophthalmology*, vol. 88, no. 2, pp. 291–297, 2004.

[5] M. Michaelides, A. J. Hardcastle, D. M. Hunt, and A. T. Moore, "Progressive cone and cone-rod dystrophies: phenotypes and underlying molecular genetic basis," *Survey of Ophthalmology*, vol. 51, no. 3, pp. 232–258, 2006.

[6] C. P. Hamel, "Cone rod dystrophies," *Orphanet Journal of Rare Diseases*, vol. 2, p. 7, 2007.

[7] Y. Miyake, M. Horiguchi, N. Tomita et al., "Occult macular dystrophy," *American Journal of Ophthalmology*, vol. 122, no. 5, pp. 644–653, 1996.

[8] Y. Miyake, K. Ichikawa, Y. Shiose, and Y. Kawase, "Hereditary macular dystrophy without visible fundus abnormality," *American Journal of Ophthalmology*, vol. 108, no. 3, pp. 292–299, 1989.

[9] R. A. Sisk, A. M. Berrocal, and B. L. Lam, "Loss of foveal cone photoreceptor outer segments in occult macular dystrophy," *Ophthalmic Surgery, Lasers and Imaging*, vol. 9, pp. 1–3, 2010.

[10] S. J. Park, S. J. Woo, K. H. Park et al., "Morphologic photoreceptor abnormality in occult macular dystrophy on spectral-domain optical coherence tomography," *Investigative Ophthalmology & Visual Science*, vol. 51, no. 7, pp. 3673–3679, 2010.

[11] K. Fujinami, K. Tsunoda, G. Hanazono et al., "Fundus autofluorescence in autosomal dominant occult macular dystrophy," *Archives of Ophthalmology*, vol. 129, no. 5, pp. 597–602, 2011.

[12] M. Kondo, Y. Miyake, N. Kondo et al., "Peripheral cone dystrophy: a variant of cone dystrophy with predominant dysfunction in the peripheral cone system," *Ophthalmology*, vol. 111, no. 4, pp. 732–739, 2004.

[13] T. Okuno, H. Oku, T. Kurimoto, S. Oono, and T. Ikeda, "Peripheral cone dystrophy in an elderly man," *Clinical and Experimental Ophthalmology*, vol. 36, no. 9, pp. 897–899, 2008.

[14] M. S. Vaphiades and J. I. Doyle, "Peripheral cone dystrophy: a diagnostic improbability?," *Journal of Neuro-Ophthalmology*, vol. 34, no. 4, pp. 366–368, 2014.

[15] Y. Mochizuki, K. Shinoda, C. S. Matsumoto et al., "Case of unilateral peripheral cone dysfunction," *Case Reports in Ophthalmology*, vol. 3, no. 2, pp. 162–168, 2012.

[16] J. Baek, H. K. Lee, and U. S. Kim, "Spectral domain optical coherence tomography findings in bilateral peripheral cone dystrophy," *Documenta Ophthalmologica*, vol. 126, no. 3, pp. 247–251, 2013.

[17] M. Akahori, K. Tsunoda, Y. Miyake et al., "Dominant mutations in *RP1L1* are responsible for occult macular dystrophy," *American Journal of Human Genetics*, vol. 87, no. 3, pp. 424–429, 2010.

[18] I. Cima, J. Brecelj, M. Sustar et al., "Enhanced S-cone syndrome with preserved macular structure and severely depressed retinal function," *Documenta Ophthalmologica*, vol. 125, no. 2, pp. 161–168, 2012.

[19] T. Fujiwara, Y. Imamura, V. J. Giovinazzo, and R. F. Spaide, "Fundus autofluorescence and optical coherence tomographic findings in acute zonal occult outer retinopathy," *Retina*, vol. 30, no. 8, pp. 1206–1216, 2010.

[20] R. F. Spaide, "Collateral damage in acute zonal occult outer retinopathy," *American Journal of Ophthalmology*, vol. 138, no. 5, pp. 887–889, 2004.

[21] J. T. Pearlman, J. Saxton, and G. Hoffman, "Unilateral retinitis pigmentosa sine pigmento," *British Journal of Ophthalmology*, vol. 60, no. 5, pp. 354–360, 1976.

[22] M. Mititelu, B. J. Wong, M. Brenner et al., "Progression of hydroxychloroquine toxic effects after drug therapy cessation: new evidence from multimodal imaging," *JAMA Ophthalmology*, vol. 131, no. 9, pp. 1187–1197, 2013.

[23] A. Hamosh, N. Sobreira, J. Hoover-Fong et al., "PhenoDB: a new web-based tool for the collection, storage, and analysis of phenotypic features," *Human Mutation*, vol. 34, no. 4, pp. 566–571, 2013.

[24] H. Li and R. Durbin, "Fast and accurate long-read alignment with Burrows-Wheeler transform," *Bioinformatics*, vol. 26, no. 5, pp. 589–595, 2010.

[25] A. McKenna, M. Hanna, E. Banks et al., "The Genome Analysis Toolkit: a MapReduce framework for analyzing next-generation DNA sequencing data," *Genome Research*, vol. 20, no. 9, pp. 1297–1303, 2010.

[26] M. A. DePristo, E. Banks, R. Poplin et al., "A framework for variation discovery and genotyping using next-generation DNA sequencing data," *Nature Genetics*, vol. 43, no. 5, pp. 491–498, 2011.

[27] N. Sobreira, F. Schiettecatte, C. Boehm et al., "New tools for Mendelian disease gene identification: PhenoDB variant analysis module; and GeneMatcher, a web-based tool for linking investigators with an interest in the same gene," *Human Mutation*, vol. 36, no. 4, pp. 425–431, 2015.

[28] G. R. Abecasis, A. Auton, L. D. Brooks et al., "An integrated map of genetic variation from 1,092 human genomes," *Nature*, vol. 491, no. 7422, pp. 56–65, 2012.

[29] C. E. Briggs, D. Rucinski, P. J. Rosenfeld, T. Hirose, E. L. Berson, and T. P. Dryja, "Mutations in ABCR (ABCA4) in patients with Stargardt macular degeneration or cone-rod degeneration," *Investigative Ophthalmology & Visual Science*, vol. 42, no. 10, pp. 2229–2236, 2001.

[30] A. Maugeri, M. A. van Driel, D. J. van de Pol et al., "The 2588G-->C mutation in the ABCR gene is a mild frequent founder mutation in the Western European population and allows the classification of ABCR mutations in patients with Stargardt disease," *American Journal of Human Genetics*, vol. 64, no. 4, pp. 1024–1035, 1999.

[31] J. Comander, C. Weigel-DiFranco, M. Maher et al., "The genetic basis of pericentral retinitis pigmentosa-a form of mild retinitis pigmentosa," *Genes*, vol. 8, no. 10, 2017.

[32] R. Matsui, A. V. Cideciyan, S. B. Schwartz et al., "Molecular heterogeneity within the clinical diagnosis of pericentral retinal degeneration," *Investigative Ophthalmology & Visual Science*, vol. 56, no. 10, pp. 6007–6018, 2015.

[33] M. Lek, K. J. Karczewski, E. V. Minikel et al., "Analysis of protein-coding genetic variation in 60,706 humans," *Nature*, vol. 536, no. 7616, pp. 285–291, 2016.

[34] I. Meunier, G. Manes, B. Bocquet et al., "Frequency and clinical pattern of vitelliform macular dystrophy caused by mutations of interphotoreceptor matrix IMPG1 and IMPG2 genes," *Ophthalmology*, vol. 121, no. 12, pp. 2406–2414, 2014.

[35] P. C. Ng and S. Henikoff, "Predicting deleterious amino acid substitutions," *Genome Research*, vol. 11, no. 5, pp. 863–874, 2001.

[36] I. A. Adzhubei, S. Schmidt, L. Peshkin et al., "A method and server for predicting damaging missense mutations," *Nature Methods*, vol. 7, no. 4, pp. 248-249, 2010.

[37] R. E. Kelsell, K. Gregory-Evans, A. M. Payne et al., "Mutations in the retinal guanylate cyclase (RETGC-1) gene in dominant cone-rod dystrophy," *Human Molecular Genetics*, vol. 7, no. 7, pp. 1179–1184, 1998.

[38] I. Perrault, J. M. Rozet, S. Gerber et al., "A retGC-1 mutation in autosomal dominant cone-rod dystrophy," *American Journal of Human Genetics*, vol. 63, no. 2, pp. 651–654, 1998.

[39] D. A. Parry, C. Toomes, L. Bida et al., "Loss of the metalloprotease ADAM9 leads to cone-rod dystrophy in humans and retinal degeneration in mice," *American Journal of Human Genetics*, vol. 84, no. 5, pp. 683–691, 2009.

[40] K. B. Freund, S. Mrejen, J. Jung et al., "Increased fundus autofluorescence related to outer retinal disruption," *JAMA Ophthalmology*, vol. 131, no. 12, pp. 1645–1649, 2013.

[41] Y. Makiyama, S. Ooto, M. Hangai et al., "Macular cone abnormalities in retinitis pigmentosa with preserved central vision using adaptive optics scanning laser ophthalmoscopy," *PLoS One*, vol. 8, no. 11, Article ID e79447, 2013.

[42] A. Oishi, K. Ogino, Y. Makiyama et al., "Wide-field fundus autofluorescence imaging of retinitis pigmentosa," *Ophthalmology*, vol. 120, no. 9, pp. 1827–1834, 2013.

[43] M. Oishi, A. Oishi, K. Ogino et al., "Wide-field fundus autofluorescence abnormalities and visual function in patients with cone and cone-rod dystrophies," *Investigative Ophthalmology and Visual Science*, vol. 55, no. 6, pp. 3572–3577, 2014.

[44] A. G. Robson, Z. Saihan, S. A. Jenkins et al., "Functional characterisation and serial imaging of abnormal fundus autofluorescence in patients with retinitis pigmentosa and normal visual acuity," *British Journal of Ophthalmology*, vol. 90, no. 4, pp. 472–479, 2006.

[45] A. G. Robson, M. Michaelides, V. A. Luong et al., "Functional correlates of fundus autofluorescence abnormalities in patients with *RPGR* or *RIMS1* mutations causing cone or cone rod dystrophy," *British Journal of Ophthalmology*, vol. 92, no. 1, pp. 95–102, 2008.

[46] N. Tojo, T. Nakamura, C. Fuchizawa et al., "Adaptive optics fundus images of cone photoreceptors in the macula of patients with retinitis pigmentosa," *Clinical Ophthalmology*, vol. 7, pp. 203–210, 2013.

[47] A. G. Robson, E. Lenassi, Z. Saihan et al., "Comparison of fundus autofluorescence with photopic and scotopic fine

matrix mapping in patients with retinitis pigmentosa: 4- to 8-year follow-up," *Investigative Ophthalmology & Visual Science*, vol. 53, no. 10, pp. 6187–6195, 2012.

[48] L. H. Lima, J. M. Sallum, and R. F. Spaide, "Outer retina analysis by optical coherence tomography in cone-rod dystrophy patients," *Retina*, vol. 33, no. 9, pp. 1877–1880, 2013.

[49] S. C. Cho, S. J. Woo, K. H. Park, and J. M. Hwang, "Morphologic characteristics of the outer retina in cone dystrophy on spectral-domain optical coherence tomography," *Korean Journal of Ophthalmology*, vol. 27, no. 1, pp. 19–27, 2013.

[50] D. Y. Yu and S. J. Cringle, "Retinal degeneration and local oxygen metabolism," *Experimental Eye Research*, vol. 80, no. 6, pp. 745–751, 2005.

[51] S. Kikuchi, S. Kameya, K. Gocho et al., "Cone dystrophy in patient with homozygous RP1L1 mutation," *Biomed Research International*, vol. 2015, Article ID 545243, 13 pages, 2015.

[52] Y. Miyake and K. Tsunoda, "Occult macular dystrophy," *Japanese Journal of Ophthalmology*, vol. 59, no. 2, pp. 71–80, 2015.

[53] S. Hull, G. Arno, V. Plagnol, A. Robson, A. R. Webster, and A. T. Moore, "Exome sequencing reveals ADAM9 mutations in a child with cone-rod dystrophy," *Acta Ophthalmologica*, vol. 93, no. 5, pp. e392–e393, 2014.

[54] O. Goldstein, J. G. Mezey, A. R. Boyko et al., "An ADAM9 mutation in canine cone-rod dystrophy 3 establishes homology with human cone-rod dystrophy 9," *Molecular Vision*, vol. 16, pp. 1549–1569, 2010.

[55] D. Zobor, E. Zrenner, B. Wissinger et al., "GUCY2D- or GUCA1A-related autosomal dominant cone-rod dystrophy: is there a phenotypic difference?," *Retina*, vol. 34, no. 8, pp. 1576–1587, 2014.

[56] A. Joseph, E. Rahimy, K. B. Freund et al., "Fundus autofluorescence and photoreceptor bleaching in multiple evanescent white dot syndrome," *Ophthalmic Surgery, Lasers and Imaging Retina*, vol. 44, no. 6, pp. 588–592, 2013.

[57] B. J. Thomas, T. A. Albini, and H. W. Flynn, "Multiple evanescent white dot syndrome: multimodal imaging and correlation with proposed pathophysiology," *Ophthalmic Surgery, Lasers and Imaging Retina*, vol. 44, no. 6, pp. 584–587, 2013.

[58] D. Li and S. Kishi, "Restored photoreceptor outer segment damage in multiple evanescent white dot syndrome," *Ophthalmology*, vol. 116, no. 4, pp. 762–770, 2009.

[59] R. Aoyagi, T. Hayashi, A. Masai et al., "Subfoveal choroidal thickness in multiple evanescent white dot syndrome," *Clinical and Experimental Optometry*, vol. 95, no. 2, pp. 212–217, 2012.

[60] R. Dell'Omo, A. Mantovani, R. Wong et al., "Natural evolution of fundus autofluorescence findings in multiple evanescent white dot syndrome: a long-term follow-up," *Retina*, vol. 30, no. 9, pp. 1479–1487, 2010.

[61] J. D. Gass, A. Agarwal, and I. U. Scott, "Acute zonal occult outer retinopathy: a long-term follow-up study," *American Journal of Ophthalmology*, vol. 134, no. 3, pp. 329–339, 2002.

[62] Q. V. Hoang, R. Gallego-Pinazo, and L. A. Yannuzzi, "Long-term follow-up of acute zonal occult outer retinopathy," *Retina*, vol. 33, no. 7, pp. 1325–1327, 2013.

[63] T. Wakazono, S. Ooto, M. Hangai, and N. Yoshimura, "Photoreceptor outer segment abnormalities and retinal sensitivity in acute zonal occult outer retinopathy," *Retina*, vol. 33, no. 3, pp. 642–648, 2013.

[64] R. F. Spaide and C. A. Curcio, "Anatomical correlates to the bands seen in the outer retina by optical coherence tomography: literature review and model," *Retina*, vol. 31, no. 8, pp. 1609–1619, 2011.

[65] M. Mkrtchyan, B. J. Lujan, D. Merino et al., "Outer retinal structure in patients with acute zonal occult outer retinopathy," *American Journal of Ophthalmology*, vol. 153, no. 4, pp. 757–68.e1, 2012.

[66] K. Bumsted and A. Hendrickson, "Distribution and development of short-wavelength cones differ between Macaca monkey and human fovea," *Journal of Comparative Neurology*, vol. 403, no. 4, pp. 502–516, 1999.

[67] P. R. Martin and U. Grünert, "Analysis of the short wavelength-sensitive ("blue") cone mosaic in the primate retina: comparison of New World and Old World monkeys," *Journal of Comparative Neurology*, vol. 406, no. 1, pp. 1–14, 1999.

[68] C. A. Curcio, K. A. Allen, K. R. Sloan et al., "Distribution and morphology of human cone photoreceptors stained with anti-blue opsin," *Journal of Comparative Neurology*, vol. 312, no. 4, pp. 610–624, 1991.

Hindawi
Journal of Ophthalmology
Volume 2018, Article ID 9538671, 14 pages
https://doi.org/10.1155/2018/9538671

Review Article

Association of Genes in the High-Density Lipoprotein Metabolic Pathway with Polypoidal Choroidal Vasculopathy in Asian Population: A Systematic Review and Meta-Analysis

Ming-zhen Yuan, Ruo-an Han, Chen-xi Zhang, and You-xin Chen

Department of Ophthalmology, Peking Union Medical College Hospital, Chinese Academy of Medical Sciences and Peking Union Medical College, Beijing, China

Correspondence should be addressed to You-xin Chen; chenyouxinpumch@163.com

Received 18 November 2017; Accepted 29 March 2018; Published 6 June 2018

Academic Editor: Lev Prasov

Purpose. To assess the association of genes in the high-density lipoprotein metabolic pathway (HDLMP) with polypoidal choroidal vasculopathy (PCV) and the genetic difference in the HDLMP between PCV and age-related macular degeneration (AMD). *Methods*. We performed a literature search in EMBASE, PubMed, and Web of Science for genetic studies on 7 single nucleotide polymorphisms (SNPs) from 5 genes in the HDLMP including cholesteryl ester transfer protein (CETP), hepatic lipase (LIPC), lipoprotein lipase (LPL), ATP-binding cassette transporter A1 (ABCA1), and ATP-binding cassette transporter G1 (ABCG1) in PCV. All studies were published before September 30, 2017, without language restriction. Pooled odds ratios (ORs) and 95% confidence intervals (CIs) of each polymorphism were estimated. We also compared the association profiles between PCV and AMD and performed a sensitivity analysis. *Results*. Our result is based on 43 articles. After excluding duplicates and articles without complete information, 7 studies were applicable to meta-analysis. 7 polymorphisms were meta-analyzed: CETP rs2303790/rs3764261, LIPC rs10468017/rs493258, LPL rs12678919, ABCA1 rs1883025, and ABCG1 rs57137919. We found that in Asian population, CETP rs3764261 (T allele; OR = 1.46; 95% CI: 1.28–1.665, $P < 0.01$), CETP rs2303790 (G allele; OR = 1.57; 95% CI: 1.258–1.96, $P < 0.01$), and ABCG1 rs57137919 (A allele; OR = 1.168; 95% CI: 1.016–1.343, $P < 0.01$) were significantly associated with PCV, and ABCG1 rs57137919 (A allele; OR = 1.208, 95% CI: 1.035–1.411, $P < 0.01$) has different effects in PCV and AMD. The other 4 polymorphisms in LIPC/LPL/ABCA1 had no significant association with PCV ($P > 0.05$). The sensitivity analysis validated the significance of our analysis. *Conclusions*. Our study revealed 7 polymorphisms in 5 genes. Among them, CETP (rs3764261/rs2303790) and ABCG1 (rs57137919) were the major susceptibility genes for PCV in Asian population and ABCG1 (rs57137919) showed allelic diversity between PCV and AMD. Since the size for PCV and AMD was small, we need to study these genes genotyping in larger samples.

1. Introduction

Polypoidal choroidal vasculopathy (PCV) is a choroidal vascular disease of first described in the early 1980s as polypoidal subretinal vascular lesions associated with serous or hemorrhagic detachment of the retinal pigment epithelium (RPE) [1]. Later, PCV is regarded as a particular type of choroidal neovascularization (CNV) characterized by the distinct presence of polypoidal vascular lesions and a branching vascular network. PCV can be clearly demonstrated and diagnosed by indocyanine green angiography [2]. From a clinical perspective, PVC is considered as a subtype of AMD because of some similarities like neovascularization, subretinal hemorrhage and fluid, pigment epithelial detachment (PED), vision loss owing to bleeding, leakage, scar formation, and other similarities in phenotypic features [3–6]. Genetically, PCV and AMD also have the common susceptible genes, such as high temperature required factor A1 gene (HTRA1) and the complementary factor H gene (CFH) [7]. However, many controversial studies demonstrate that PCV should be classified as a distinct disease entity of AMD for their different epidemiological, clinical characteristics, natural history, and treatment outcomes [8–11]. Moreover, recent researches in the field of genetics suggest that

PCV may not be as closely related to AMD, such as its differential risk to a mutation in FGD6, viralicidic activity 2-like (SKIV2L), complement component 3 (C3), elastin (ELN), and apolipoprotein E (APOE) [12–16]. These literatures make for a question whether PCV is a subtype of AMD or a distant disease from AMD.

Many studies have indicated lipid deposition in Bruch's membrane and soft drusen, and the amount of lipid was lower in the peripheral area than in the macula of human eyes [17]. A number of population-based studies revealed the association between drusen and the AMD, and drusen are regarded as one of the determinant factors of both early and late AMD [18, 19]. In addition, some studies indicated that the prevalence of drusen under RPE was lower in PCV than in AMD [20, 21], which pointed out that absence of drusen may be one of the important criteria to diagnose PCV. However, some clinical studies insisted that drusen were frequently seen in PCV [22, 23], and several studies reported that drusen were observed in 20% to 27% of unaffected [21, 24]. Therefore, whether drusen plays a functional role in the occurrence and development is still up for debate. As we know, lipids stand for over 40% of the drusen volume [25]; therefore, many academics studied the vital function of lipids in the pathogenesis of PCV and AMD. Due to the different ethnic groups and lifestyles of individuals, the strength of such relevances is widely variable [26–28]; therefore, many studies investigated the effect between gene variations in the HDLMP and risk factors on PCV and AMD. Genetic studies in the HDLMP with PCV and AMD have identified susceptibility single nucleotide polymorphisms (SNPs) in multiple genes, including rs3764261/rs2303790 in CETP, rs493258/rs10468017 in LIPC, rs12678919 in LPL, rs1883025 in ABCA1, and rs57137919 in ABCG1.

Thus far, some studies have studied the impact of lipid metabolism-related and systemic lipoprotein genes in PCV. Here, in order to give the comprehensive analysis of effects and solve the controversies, we conduct meta-analysis and report a systematic review by summing up all published articles of genetic associations in the HDLMP of PCV. This study (1) conducted an investigation of which genetic variants of the HDLMP are meaningfully associated with PCV and their effect sizes and (2) analyzed whether there were differences between genetic risks of the HDLMP in PCV and AMD.

2. Methods

2.1. Search Strategy. We searched EMBASE, PubMed, and Web of Science using the following MeSH terms and free words: (polypoidal choroidal vasculopathy or polypoidal choroidal vascular disease or polypoidal choroidal vascular diseases or PCV) and (cholesteryl ester transfer protein or CETP or hepatic lipase or LIPC or lipoprotein lipase or LPL or ATP-binding cassette transporter A1 or ABCA1 or ATP-binding cassette transporter G1 or ABCG1). All searched articles were published before September 30, 2017, without language restriction. We also screened the reference lists of all eligible studies, reviews, and meta-analyses to ensure that any relevant studies were not omitted. We also searched all reported genome-wide association studies of PCV including the supplementary materials to maximize the usable data. The detail of search strategy is revealed in Table S1.

2.2. Inclusion and Exclusion Criteria. We included those studies that satisfied the following criteria in the meta-analysis: (1) case-control studies, cohort studies, or population-based studies that evaluated the association of gene variants of CETP/LIPC/LPL/ABCA1/ABCG1 with PCV or its subtypes and (2) allele or genotype counts and/or frequencies being presented or able to be calculated from the data in the study. Case reports, conference reports, reviews, animal studies, and reports with insufficient information were excluded (Table S2).

2.3. Data Extraction and Quality Assessment. Two reviewers (Y. M. z. and Y. J. y.) independently reviewed and extracted data from studies on the association between CETP/LIPC/LPL/ABCA1/ABCG1 SNPs and PCV. If there were any differences between them, another two reviewers would help to resolve it (Z. C. x. and H. R. a.) after thorough discussion. The following information was extracted from each article: the name of first author, publication year, ethnicity of the study population, study design, genotyping method, sample size, demographics, allele and genotype distribution (Table 1), and the results of the Hardy–Weinberg equilibrium (HWE) test in controls (Table S3). We assessed the quality of individual studies using the Newcastle–Ottawa Scale [29]. Briefly, 9 quality indicators were used; if a study fulfilled 1 indicator, we assigned a "yes" under this item or a "no." Thus, the quality score for each study might be between 0 and 9 (Table S4).

2.4. Statistical Analysis. We conducted meta-analysis for each polymorphism which had been reported in ≥2 studies or cohorts. The association was evaluated by different genetic models, including allelic, heterozygous, and homozygous models. For each study, the odds ratio (OR) with 95% confidence interval (95% CI) was calculated to evaluate the strength of association between the each SNP and PCV risk. Moreover, we used the I^2 value to quantify the proportion of the variability in effect estimates, which is due to heterogeneity rather than sampling error. The I^2 value was shown as of no (0–25%), low (25–50%), moderate (50–75%), or high heterogeneity (75–100%) [30]. The I^2 test was to assess heterogeneity among studies. The potential publication bias was assessed visually in a funnel plot of log (OR) against its standard error, and the degree of asymmetry was evaluated using Begg's test and Egger's test ($P < 0.05$ was considered to be statistically significant). We undertook the sensitivity analysis to examine the influence by removing the unreliable study [31]. The software STATA (version 12.0, StataCorp LP, College Station, TX) was used for the meta-regression analysis. A pooled P value of less than 0.05 was considered statistically significant.

3. Results

3.1. Eligibility and Characteristics of Included Studies. Figure 1 illustrates the study inclusion of this meta-analysis. A total of 43 articles published before September 30, 2017,

Table 1: Characteristics of the included studies in the meta-analysis.

First author and reference	Year	Ethnicity	Study design	Genotyping method	HWE reported	PCV			AMD			Control			Gene/loci investigated
						N	Male ratio	Mean age ± SD (yrs)	*N*	Male ratio	Mean age ± SD (yrs)	*N*	Male ratio	Mean age ± SD (yrs)	
Nakata et al. [32]	2013	Japanese	1	TaqMan and Beadchip	Yes	581	0.73	72.59 ± 8.13	—	—	—	793	0.41	65.99 ± 4.33	CETP, LIPC, LPL
Zhang et al. [33]	2013	Chinese	1	PCR	Yes	250	0.66	65 ± 8.6	157	0.64	67 ± 9.21	204	0.61	69 ± 9	LIPC, ABCA1, CETP, LPL,
Li et al. [34]	2014	Chinese	1	PCR	Yes	298	0.62	66.8 ± 9.7	300	0.63	69.4 ± 8.9	296	0.48	65.1 ± 9.5	ABCA1
Liu et al. [13]	2014	Chinese	1	PCR	Yes	233	0.7	68.5 ± 5.9	200	0.55	75.3 ± 7.7	275	0.44	74.3 ± 7.6	ABCA1, LIPC, CETP, ABCG1
Meng et al. [36]	2015	Chinese	1	PCR	Yes	291	0.79	66.6 ± 9.6	230	0.63	69.3 ± 8.8	221	0.48	67.2 ± 9.6	CETP, LIPC, LPL
	2016	Chinese (Hong Kong)	1	TaqMan and PCR	Yes	236	0.69	68.5 ± 9	235	0.55	75.3 ± 7.6	365	0.42	74.4 ± 7.7	ABCG1
Li et al. [37]	2016	Chinese (Shantou)	1	TaqMan and PCR	Yes	187	0.72	63.1 ± 10.5	189	0.69	67.3 ± 10.1	670	0.43	73.8 ± 6.8	ABCG1
	2016	Japanese (Osaka)	1	TaqMan and PCR	Yes	204	0.77	72.2 ± 8.0	192	0.67	74.3 ± 7.3	157	0.33	47.9 ± 15.1	ABCG1
Qiao et al. [38]	2017	Chinese (Hong Kong)	1	Beadchip	Yes	156	—	—	310	—	—	1006	—	—	CETP

The characteristics of the eligible studies are shown. PCV: polypoidal choroidal vasculopathy; AMD: age-related macular degeneration; HWE: Hardy–Weinberg equilibrium.

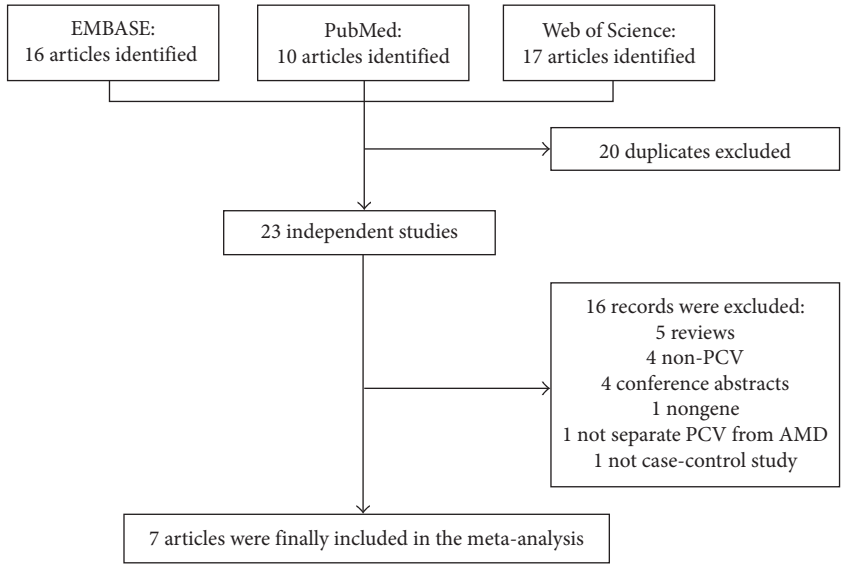

Figure 1: Flow diagram and results of literature review. The flow diagram describes the filtering process of related articles, including the number and reason of exclusion. PCV: polypoidal choroidal vasculopathy; AMD: age-related macular degeneration.

were identified in the EMBASE, PubMed, and Web of Science databases. Of these, we excluded 20 articles because they were duplicates. For the remaining 23 studies, the full texts were retrieved. After reviewing the full texts, we excluded another 16 reports, among which 5 studies were reviews, 4 were not related to PCV, 4 were conference abstracts, 1 was not about the genetic studies, 1 did not separate PCV from AMD, and 1 was not the case-control study. Finally, 7 articles were eligible for the meta-analysis [32–38], involving 3342 PCV cases versus 8256 controls and 2761 PCV cases versus 2660 AMD cases. The main traits of the included studies are summed up in Table 1. Patients from each study received complete ophthalmic examinations, including fluorescein angiography and ICGA. Polypoidal choroidal vasculopathy was diagnosed on the basis of choroidal polypoidal lesions shown by ICGA. All studies adopted a case-control design. These studies were performed in various populations, including Chinese (6 studies), Japanese (3 studies), and Korean (1 study). In all studies, valid genotyping approaches were used, including polymerase chain reaction, TaqMan genotyping assay, and BeadChip.

3.2. Risk of Bias Assessment in Eligible Studies. As shown in Table S4, all eligible studies clearly described the diagnostic criteria for PCV and AMD. Patients with other macular diseases like central serous chorioretinopathy, myopic choroidal neovascularization, angioid streaks, presumed ocular histoplasmosis, or with CNV and PCV in the same or fellow eye were excluded. In all studies, comprehensive ophthalmic examinations were performed on the control subjects. One study used control subjects recruited from the community [32], and the others used hospital-recruited controls. Two studies were diverse-ethnic population study [37, 38]. One study did not provide the sex and age of cohorts. There was no ethnic difference between cases and controls. Confounding factors were matched between cases and controls in 7 studies. The scores for the quality assessment ranged from 5 to 7. All the studies informed HWE in controls.

3.3. Meta-Analysis of CETP/LIPC/LPL/ABCA1/ABCG1 Polymorphisms in PCV. Totally 17 SNPs had been studied in PCV in the literature (Figure 2). However, only 7 SNPs (CETP rs2303790/rs3764261, LIPC rs10468017/rs493258, LPL rs12678919, ABCA1 rs1883025, and ABCG1 rs57137919) in PCV were reported in more than one study and thus eligible for meta-analysis (details can be seen in Table S5). Summary of the allelic associations of these polymorphisms is shown in Table 2. The other 10 SNPs reported in only one report but performed no association with PCV [33, 36].

CETP rs3764261 is the most widely investigated SNP in PCV, with a number of 1355 cases and 1493 controls studied for the meta-analysis [32, 33, 35, 36]. The results showed statistically significant association between CETP rs3764261 and PCV in Asian population (Table 2). As for the allelic model, the odds ratio (OR) for the risk allele T was 1.46 (95% confidence interval (CI): 1.28–1.665, $P < 0.01$, $I^2 = 0\%$). In the subgroup analysis by ethnicity, still significant association was detected in Chinese (OR = 1.528, 95% CI: 1.268–1.841, $P < 0.01$, $I^2 = 0\%$). Also, CETP rs2303790 [33, 38] and ABCG1 rs57137919 [35, 37] showed significant associations with PCV in the allelic model. As for CETP rs2303790, the frequency of the G allele was significantly higher in PCV patients than in controls, conferring a 1.57-fold increased risk toward PCV (95% CI: 1.258–1.96, $P < 0.01$, $I^2 = 0$). As for ABCG1 rs57137919, the frequency of the A allele was significantly higher in PCV patients than in controls, conferring a 1.168-fold increased risk (95% CI: 1.016–1.343, $P = 0.029$, $I^2 = 61.5\%$). Through quality assessment and sensitivity analysis, we found the heterogeneity derived from the data of Shantou population [37]. After excluding the data of Shantou population, the result showed that the pooled allelic OR was significantly elevated (A allele; OR = 1.313,

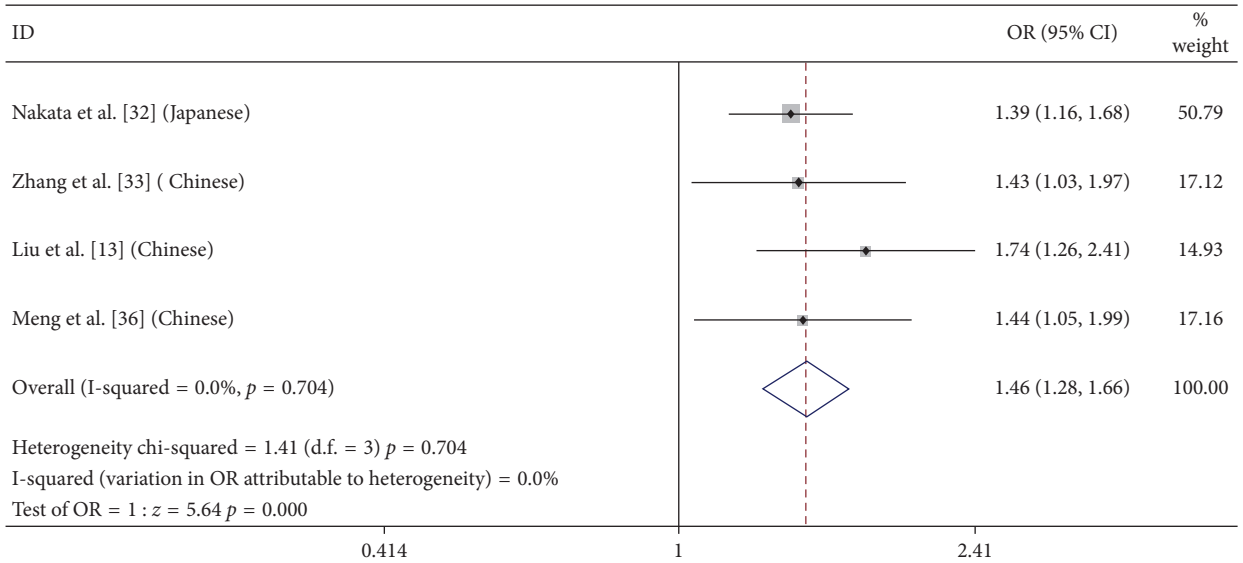

(a)

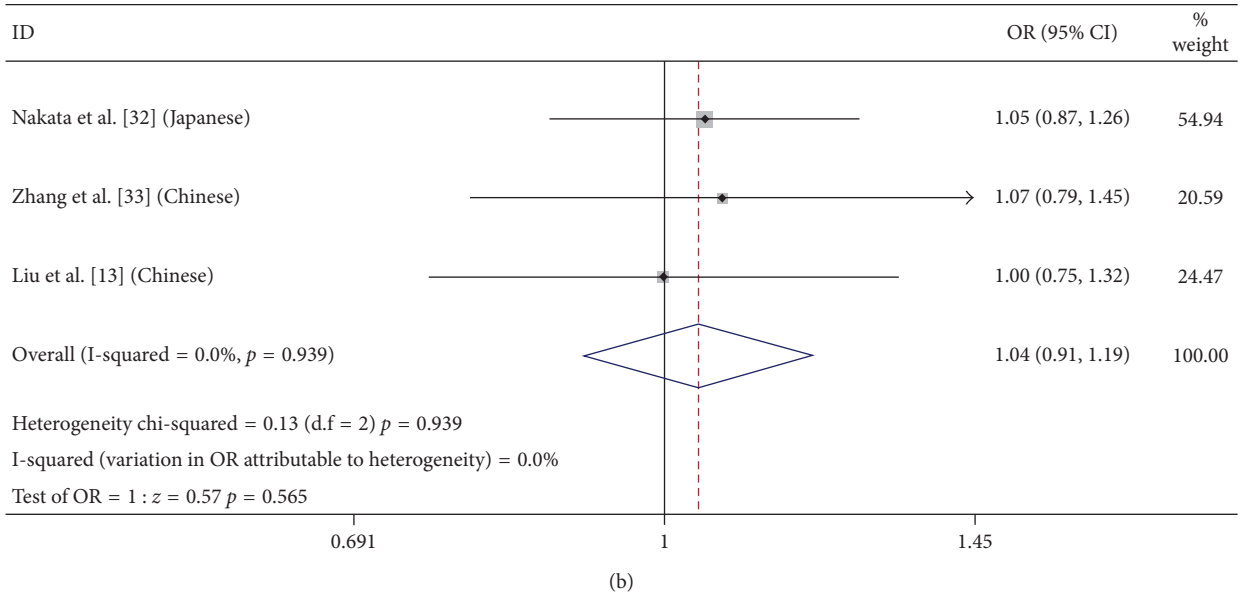

(b)

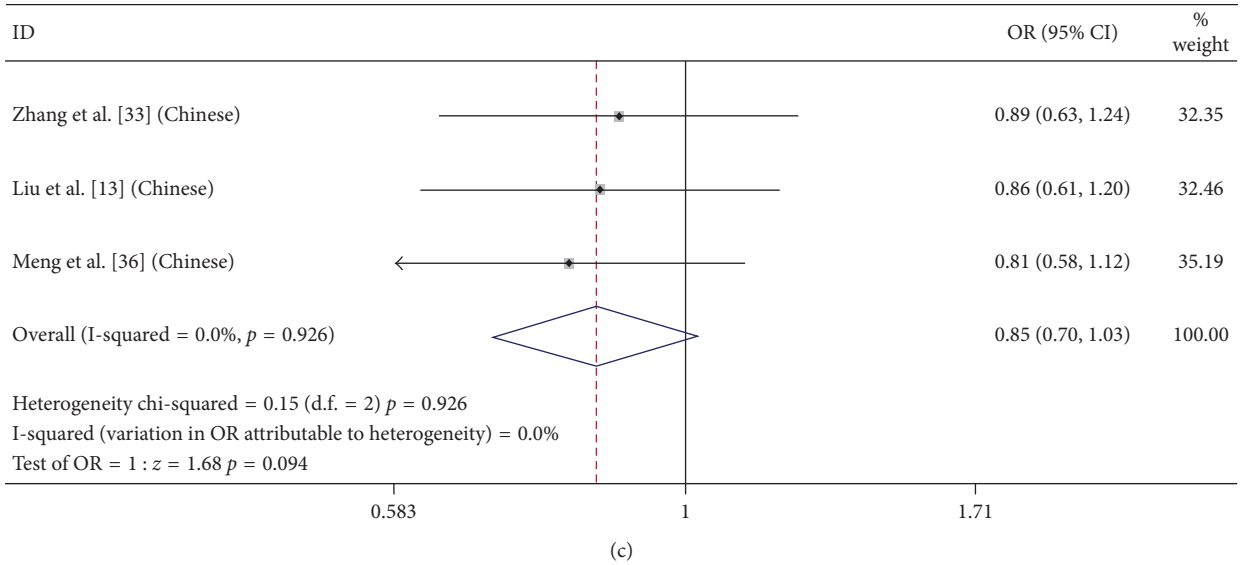

(c)

Figure 2: Continued.

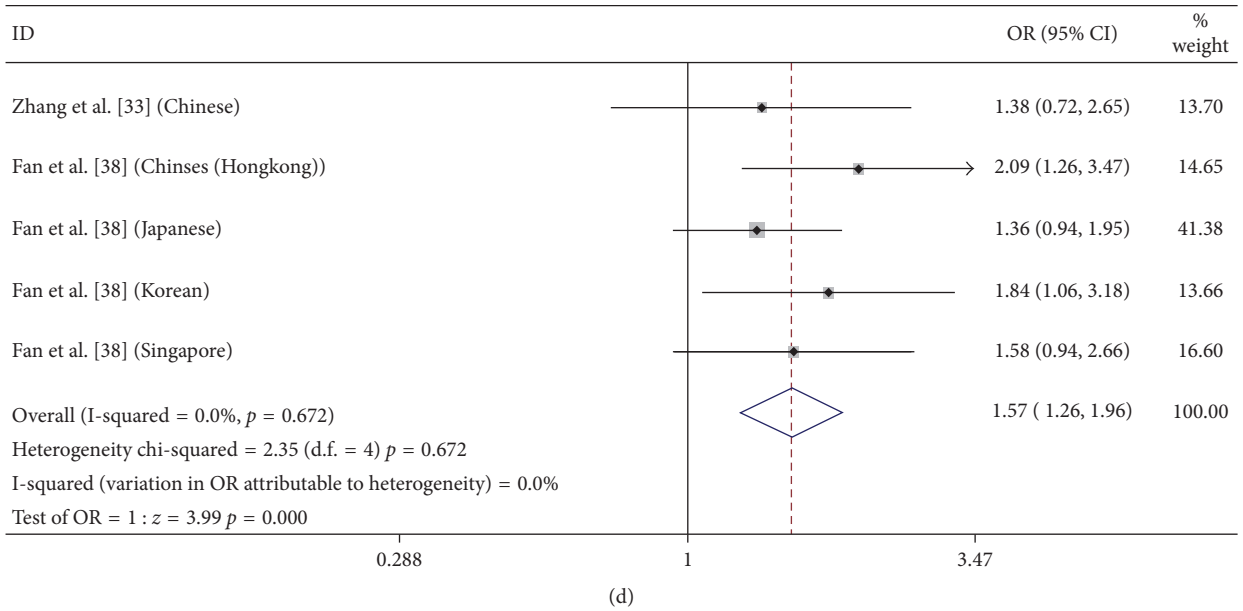

(d)

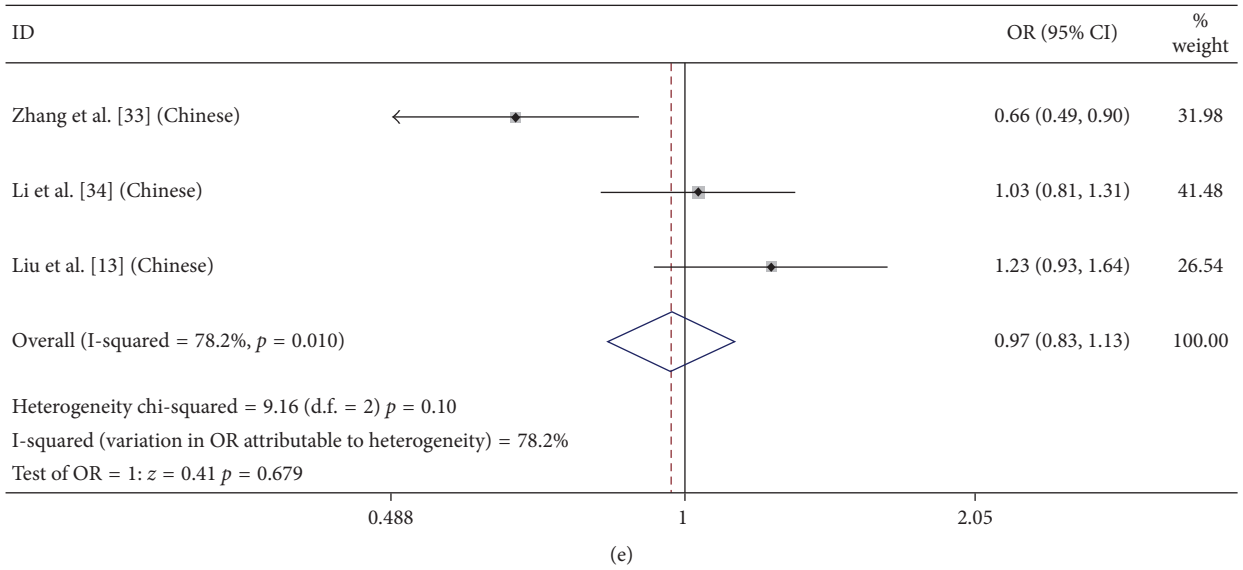

(e)

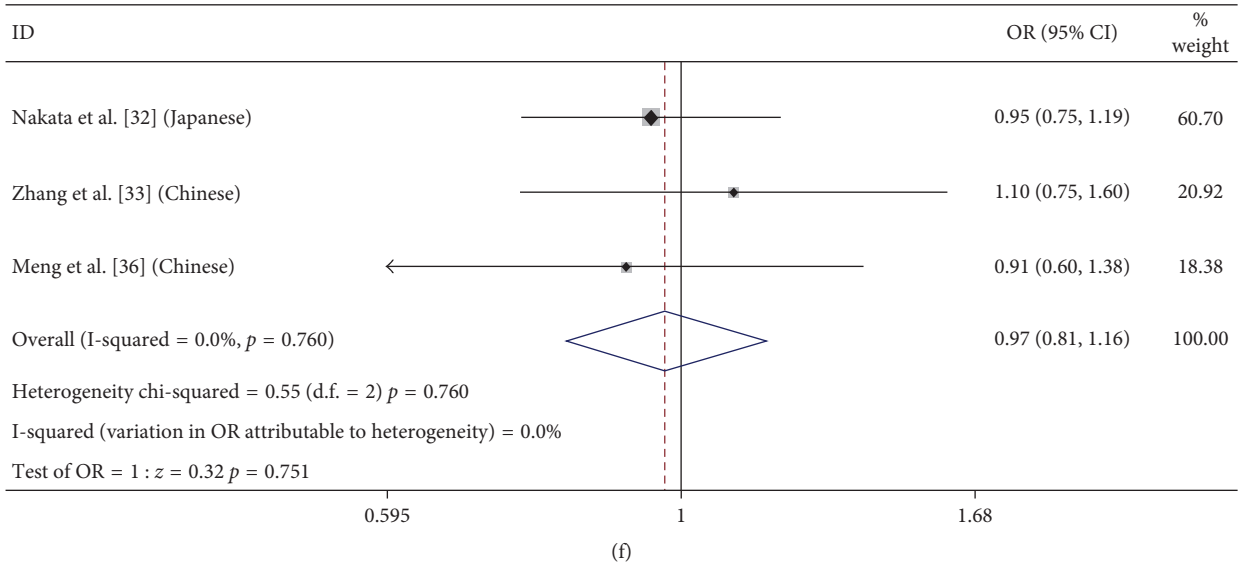

(f)

Figure 2: Continued.

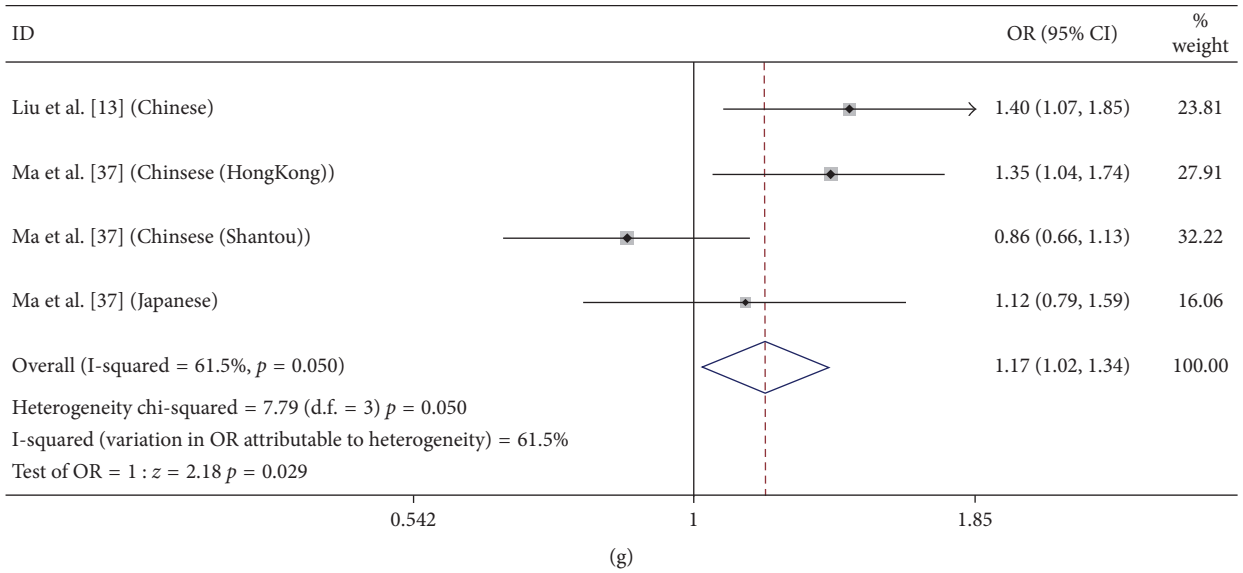

Figure 2: Forest plot of 7 SNPs in PCV in allelic model. The figure shows specific odds ratios (ORs) for study. The size of the box is proportional to the weight of the study. Horizontal lines represent 95% confidence intervals (CIs). A diamond is on behalf of the summary OR with its corresponding 95% CI. (a) CETP rs3764261 (T); (b) LIPC rs493258 (G); (c) LIPC rs10468017 (T); (d) CETP rs2303790 (G); (e) ABVA1 rs1883025 (T); (f) LPL rs12678919 (G); (g) ABCG1 rs57137919 (A).

Table 2: Meta-analysis of CETP/LIPC/LPL/ABCA1/ABCG1 polymorphisms in PCV.

Region	Gene	Polymorphism	Ethnicity	Associated versus reference allele	Number of cohorts	Sample size (case/control)	OR (95% CI)	Z score	P value	I^2 (%)	P value of Begg's test	P value of Egger's test
16q21	*CETP*	rs3764261	Asia	T versus G	4	1355/1493	1.46 (1.28–1.665)	5.64	0	0	0.308	0.415
			Chinese	T versus G	3	774/700	1.528 (1.268–1.841)	4.46	0	0	>0.999	0.071
9q31	*ABCA1*	rs1883025	Chinese	T versus C	3	781/775	0.968 (0.828–1.131)	0.41	0.679	78.2	>0.999	0.745
9q31	*LIPC*	rs493258	Asia	G versus A	3	1064/1272	1.041 (0.907–1.195)	0.57	0.565	0	>0.999	0.867
15q22	*LIPC*	rs10468017	Chinese	T versus C	3	774/700	0.849 (0.7–1.028)	1.68	0.094	0	>0.999	0.465
15q22	*LPL*	rs12678919	Asia	G versus A	3	1122/1218	0.972 (0.814–1.161)	0.32	0.751	0	>0.999	0.799
21q22	*ABCG1*	rs57137919	Asia	A versus G	4	860/1467	1.168 (1.016–1.343)	2.18	0.029	61.5	>0.999	0.808
16q21	CETP	rs2303790	Asia	G versus A	5	1312/5479	1.57 (1.258–1.96)	3.99	0	0	>0.999	0.527

Summary of the allelic associations of CETP/LIPC/LPL/ABCA1/ABCG1 polymorphisms in PCV. PCV: polypoidal choroidal vasculopathy; AMD: age-related macular degeneration; OR: odds ratio; CI: confidence intervals.

95% CI: 1.113–1.548, $P < 0.01$, $I^2 = 0\%$). Regarding the other 4 SNPs, LIPC rs10468017/rs493258, LPL rs12678919, and ABCA1 rs1883025, the pooled ORs were not statistically significant in PCV in the allelic ($P > 0.05$). As for ABCA1 rs1883025 (T allele; OR = 0.968, 95% CI: 0.828–1.131, $P = 0.679$, $I^2 = 78.2\%$), quality assessment and sensitivity analysis showed that the study of Zhang et al. was of higher risk of causing bias than the other cohorts [33]. Therefore, we excluded the study and also found that the pooled allelic OR was not significant (T allele; OR = 1.1, 95% CI: 0.926–1.335, $P = 0.257$, $I^2 = 0\%$).

3.4. Meta-Analysis of CETP/LIPC/LPL/ABCA1/ABCG1 Polymorphisms Compared between PCV and AMD. We identified 6 studies in which both PCV and AMD were assessed for associations with a total of 7 SNPs in 5 genes (i.e., CETP rs2303790/rs3764261, LIPC rs10468017/rs493258, LPL rs12678919, ABCA1 rs1883025, and ABCG1 rs57137919) (Table 3 and Figure 3). Only 1 SNP (ABCG1 rs57137919) showed significant difference between PCV and AMD (A allele; OR = 1.208, 95% CI: 1.035–1.411, $P = 0.017$, $I^2 = 0\%$) [35, 37]. The other 6 SNPs, namely, CETP rs2303790/rs3764261, LIPC rs10468017/rs493258, LPL rs12678919, and ABCA1 rs1883025,

Table 3: Meta-analysis of CETP/LIPC/LPL/ABCA1/ABCG1 polymorphisms compared between PCV and AMD.

Region	Gene	Polymorphism	Ethnicity	Associated versus reference allele	Number of cohorts	Sample size (PCV/AMD)	OR (95% CI)	Z score	P value	I^2 (%)	P value of Begg's test	P value of Egger's test
16q21	*CETP*	rs3764261	Chinese	T versus G	3	774/587	1.17 (0.971–1.409)	1.65	0.178	33.6	>0.999	0.572
9q31	*ABCA1*	rs1883025	Chinese	T versus C	3	781/775	1.025 (0.869–1.208)	0.29	0.77	0	>0.999	0.832
9q31	*LIPC*	rs493258	Chinese	G versus A	2	483/357	1.123 (0.897–1.407)	1.01	0.312	0	>0.999	—
15q22	*LIPC*	rs10468017	Chinese	T versus C	3	774/587	1.101 (0.892–1.359)	0.89	0.371	0	0.296	0.483
15q22	*LPL*	rs12678919	Asia	G versus A	2	541/387	1.163 (0.861–1.572)	0.98	0.325	0	>0.999	—
21q22	*ABCG1*	rs57137919	Asia	A versus G	4	860/816	1.208 (1.035–1.411)	2.39	0.017	0	0.734	0.156
16q21	CETP	rs2303790	Asia	G versus A	5	1312/1314	1.067 (0.825–1.378)	0.49	0.622	0	0.462	0.299

Summary of the genetic difference in CETP/LIPC/LPL/ABCA1/ABCG1 polymorphisms between PCV and AMD is shown. PCV: polypoidal choroidal vasculopathy; AMD: age-related macular degeneration; OR: odds ratio; CI: confidence interval.

were evaluated in 2 to 3 cohorts and showed no significant differences between PCV and AMD ($P > 0.05$). As for CETP rs3764261 (T allele; OR = 1.17, 95% CI: 0.971–1.409, $P = 0.178$, $I^2 = 33.6\%$), quality assessment and sensitivity analysis showed that the study of Liu et al. was of higher risk of causing bias than the other cohorts [35]. Therefore, we ruled out the cohort, and then the pooled allelic OR of the result was significant (T allele; OR = 1.301, 95% CI: 1.033–1.638, $P = 0.025$, $I^2 = 0\%$) [33, 36].

3.5. Publication Bias Analysis. In theory, due to the limited number of available studies, it is not suitable for publication bias analysis. But in order to make this meta-analysis more powerful and more creditable, we used funnel plots and Begg's/Egger's test to detect publication bias. Begg's test and Egger's test suggested an absence of publication bias in the all SNPs ($P > 0.05$) (Tables 2 and 3). The shape of the funnel plots did not reveal any evidence of obvious asymmetry (Figures S1 and S2).

4. Discussion

In the systematic review and meta-analysis, we have summarized the association profiles of genes in the HDLMP in PCV and assessed the genetic difference in the HDLMP between PCV and AMD for the first time (i.e., CETP, LIPC, LPL, ABCA1, and ABCG1). We found significant association between reported CETP rs2303790/rs3764261, ABCG1 rs57137919, and PCV. Also, we identified ABCG1 rs57137919 showing significant differences between PCV and AMD. In contrast, LIPC rs10468017/rs493258, LPL rs12678919, and ABCA1 rs1883025 were not statistically significant in PCV and reported SNPs in 4 genes in the HDLMP (i.e., CETP, LIPC, LPL, and ABCA1) showed no significant differences between PCV and AMD.

CETP can make oxidized lipids transfer from the outer segments of the photoreceptors or other membranes to HDL-like lipoprotein particles. The particles are internalized by RPE and excreted back into the circulation via ABCG1 transporters through Bruch's membrane [39]. ABCG1 was relevant to an increased macrophage apoptosis, which may be due to the accumulation of oxysterol in macrophages caused by decreased ABCG1-mediated cholesterol efflux [40]. ABCA1 was expressed in the retina and retinal pigment epithelium [41], and ABCA1 can form nascent HDL by mediating the efflux of cholesterol and phospholipids to lipid-poor apolipoproteins [42, 43]. Also, several studies have demonstrated ABCA1 was significantly related to the progression of drusen, but the association between large drusen and geographic atrophy/neovascular was not significant [44]. Besides, LIPC gene is a critical enzyme in HDL metabolism which has the function of encoding hepatic triglyceride lipase and catalyzing the hydrolysis of phospholipids, monoglycerides, diglycerides, triglycerides, and acylCoA thioesters [45, 46]. LPL gene encodes LPL which can play an important role in HDL metabolism. LPL can not only facilitate triglyceride hydrolysis but also serve as a ligand/bridging factor for receptor-mediated lipoprotein uptake [47]. Besides, lipoproteins derived from plasma have been proved to be the crucial upstream source of fatty acids within Bruch's membrane and supply an energy source to the retina [48–50] as well as perform significant roles in the transportation of vitamin C, vitamin E, lutein, and zeaxanthin for use by photoreceptors [51, 52]. Therefore, dysfunction of CETP, LIPC, LPL, ABCA1, and ABCG1 may cause accumulation of oxidized lipids in the retina, and the unreasonable products could induce inflammation and vascular anomaly, which play a crucial role in the development of PCV and AMD via lipid metabolism [53, 54].

In the studies (including 3 in Chinese [33, 35, 36] and 1 in Japanese [32]), we found that CETP rs3764261 was to be associated with PCV in Asian population with an odds ratio of 1.46 (95% CI: 1.28–1.665, $P = 0$, $I^2 = 0\%$) for the T allele. Apart from CETP rs3764261, we also found that CETP

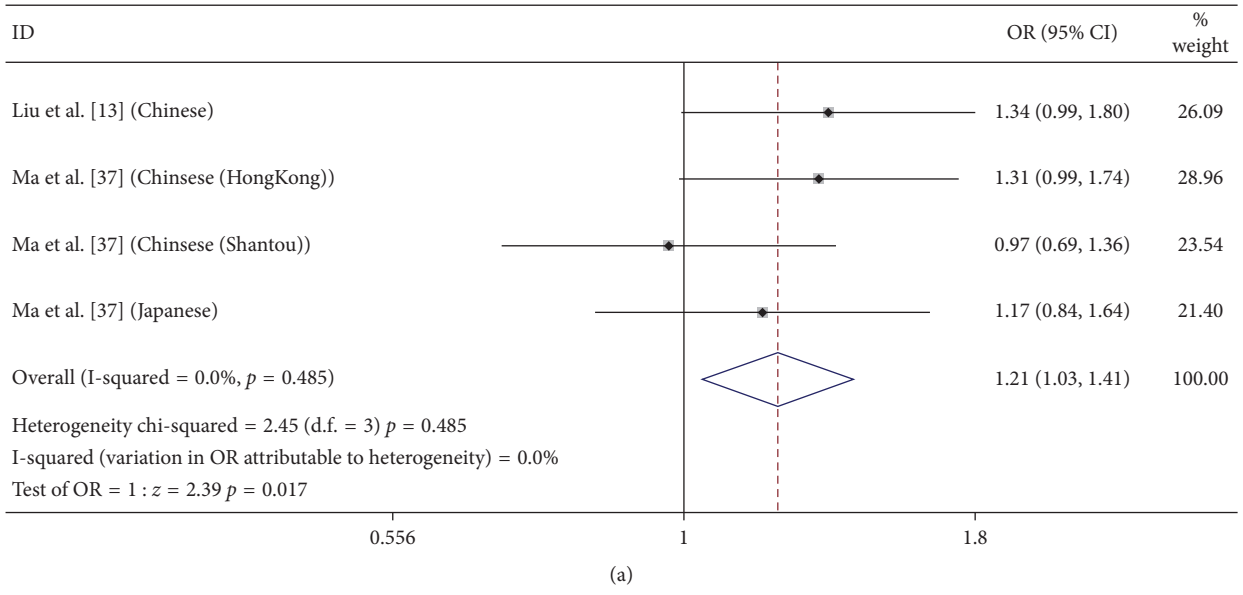

(a)

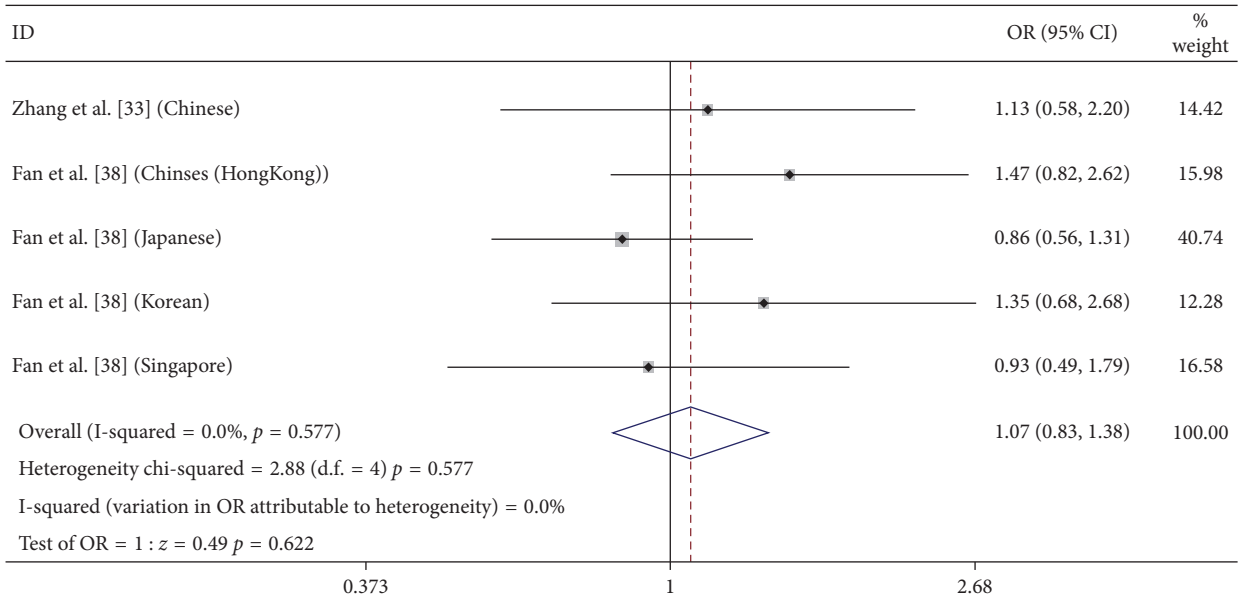

(b)

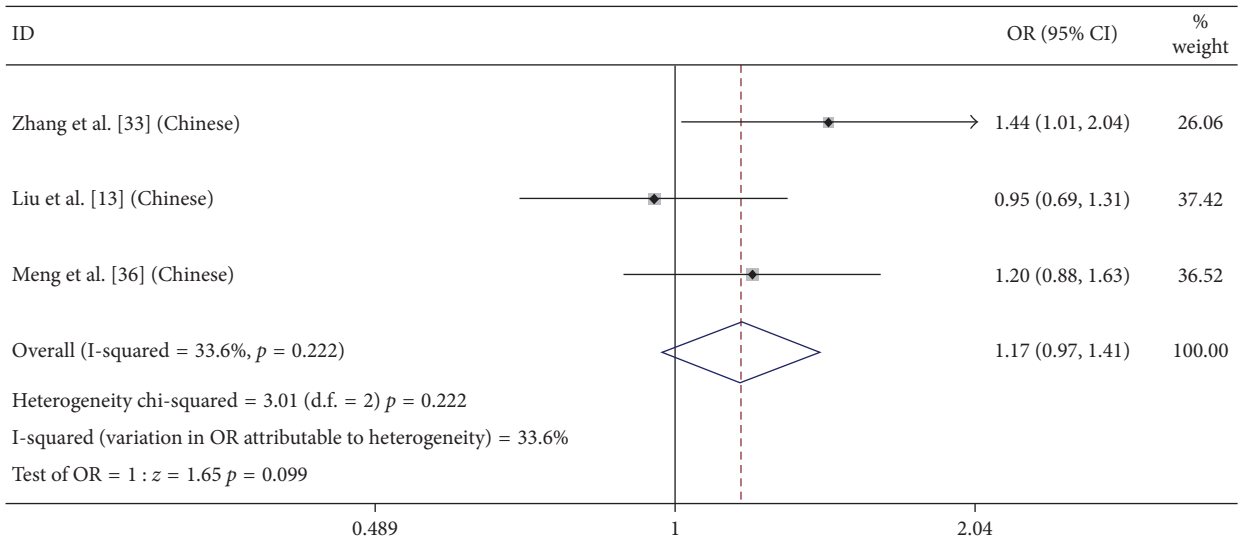

(c)

Figure 3: Continued.

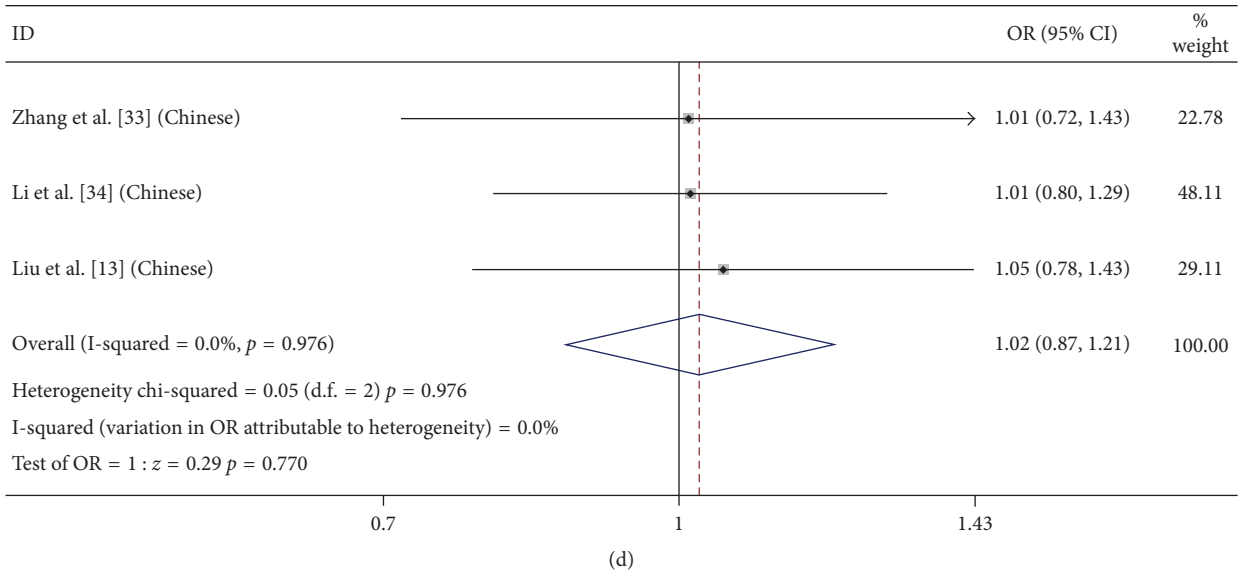

(d)

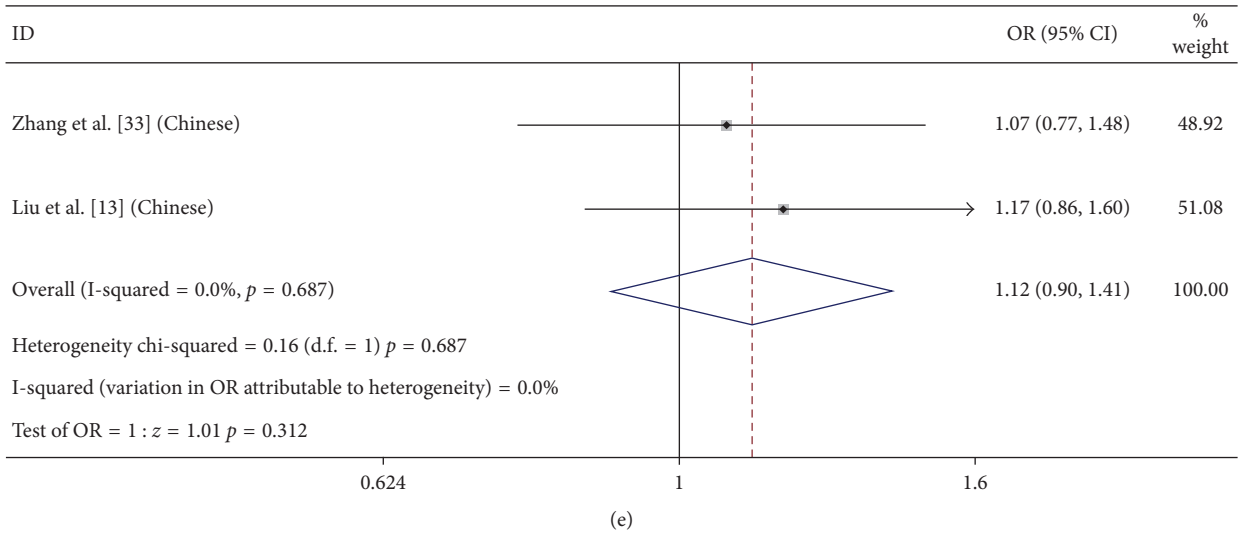

(e)

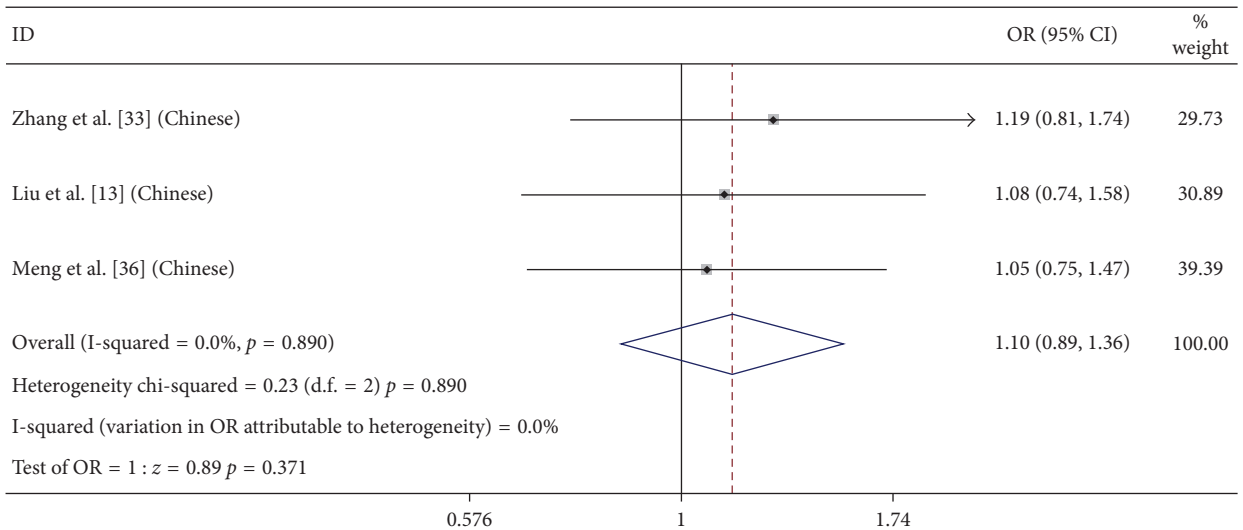

(f)

Figure 3: Continued.

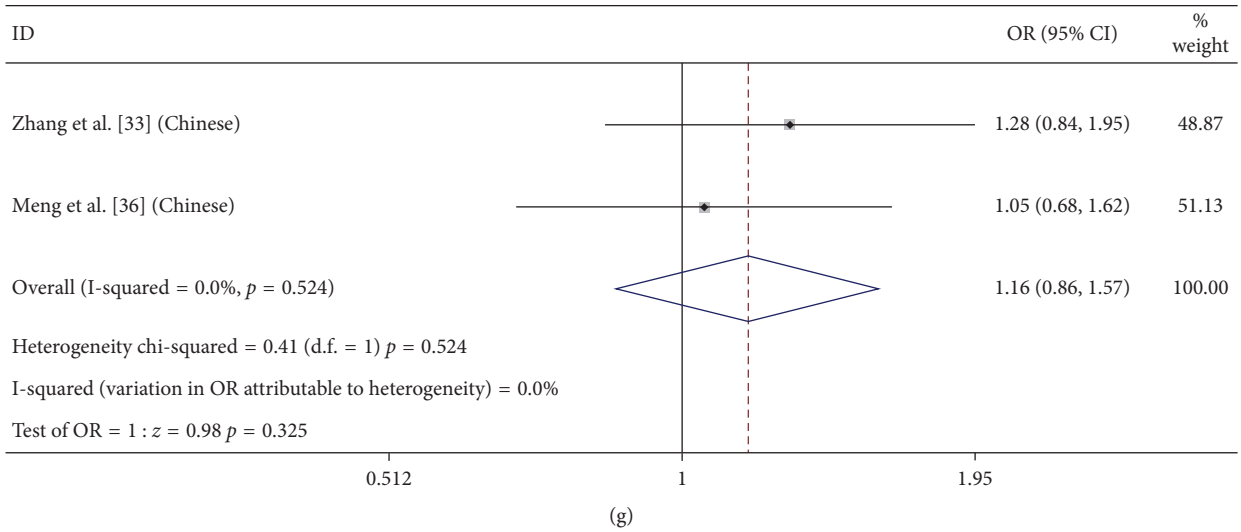

(g)

Figure 3: Forest plot of SNPs compared between PCV and AMD in allelic model. The figure shows specific odds ratios (ORs) for study. The size of the box is proportional to the weight of the study. Horizontal lines represent 95% confidence intervals (CIs). A diamond is on behalf of the summary OR with its corresponding 95% CI. (a) ABCG1 rs57137919 (A); (b) CETP rs2303790 (G); (c) CETP rs3764261 (T); (d) ABCA1 rs1883025 (T); (e) LIPC rs493258 (G); (f) LIPC rs10468017 (T); (g) LPL rs12678919 (G).

rs2303790 was associated with PCV in Asian population [33, 38] (G allele; OR = 1.57, 95% CI: 1.258–1.96, $P < 0.01$, $I^2 = 0$). Therefore, CETP rs3764261/rs2303790 provided an increased risk for PCV in Asian population. Through the analysis of the studies in which both PCV and AMD were assessed for associations with CETP, we found CETP rs2303790 showed no significant difference between PCV and AMD. However, as for CETP rs3764261, two studies dedicated that CETP rs3764261 was significantly associated with an increased risk for PCV, but no association was found with AMD(T allele; OR = 1.301, 95% CI: 1.033–1.638, $P = 0.025$, $I^2 = 0\%$) [33, 40], but one study showed that CETP rs3764261 is a susceptibility gene for PCV and AMD [35]. According to the article of GWAS and meta-analysis published by Cheng et al., the minor allele at CETP rs3764261 variant was proved to be a risk factor to the development of AMD in Asian population [55]. However, several recent studies indicated that CETP rs3764261 was related to a decreased risk of AMD in Chinese population and Lithuanian population [56, 57]. Therefore, it is still disputed whether CETP rs3764261 has different effects in PCV and AMD, and we need further studies in which both PCV and AMD are assessed for associations with CETP to confirm it.

From the studies [35, 37], for ABCG1 rs57137919, the frequency of the A allele in PCV patients was significantly higher than in controls (OR = 1.168, 95% CI: 1.016–1.343, $P = 0.029$, $I^2 = 61.5\%$). Interestingly, we found the result had the heterogeneity. Through quality assessment and sensitivity analysis, we found the heterogeneity derived from the data of Shantou population. After reading the related articles, we found all the studies used TaqMan genotyping assays, as well as the same inclusion criteria and exclusion criteria. Therefore, we speculate that there may be racial differences between Shantou population and others, but we need further studies to prove the view and find the causes of heterogeneity. Also, we found the significant difference between PCV and AMD in ABCG1 rs57137919 (G allele; OR = 1.208, 95% CI: 1.035–1.411, $P = 0.017$, $I^2 = 0\%$). In one of the studies, Li et al. studied the relevance of ABCG1 rs57137919 to PCV and AMD in Hong Kong, Shantou, and Osaka study subjects, and the results showed that the association of ABCG1 rs57137919 with PCV was significant in the Hong Kong cohort, but not in the Shantou or the Osaka cohort. Also, they indicated that the association of ABCG1 rs57137919 with AMD was not significant in the Hong Kong, Shantou, and Osaka cohorts. In another study, Liu et al. provided putative evidence of a role of ABCG1 rs57137919 in the vascularized complication of PCV. Because there were only two studies about relevance of ABCG1 rs57137919 to PCV and AMD, we need further replication studies in other ethnic populations to confirm the role of ABCG1 in PCV and AMD.

From our meta-analysis, we found other 4 SNPs (LIPC rs10468017/rs493258, LPL rs12678919, and ABCA1 rs1883025) were not statistically significant in PCV and AMD. Besides, the associations of eleven SNPs in CETP/LIPC/ABCA1/ABCG1 were reported in only 1 study [33, 36–38] (details can be seen in Table S5). Among these SNPs, Zhang et al. discovered that the rs5882 variant in CETP was significantly associated with PCV (G allele; $P = 0.73E-04$), but not with AMD (G allele; $P = 0.297$), and suggested the need to find biological clues about the different underlying HDL pathways by separating PCV from AMD so as to explore the pathogenesis of PCV and AMD [33].

Another recent study reported that LIPC rs1532085 conferred an increased risk for PCV (A allele; $P = 0.0094$), but not AMD (A allele; $P = 0.0938$). Also, this study found hyperlipidemia is a risk factor for PCV [36]. Recently, Li et al. have newly identified ABCG1 rs225396 to be associated with

PCV (T allele; $P = 0.026$) and AMD (T allele; $P = 0.048$) in Chinese and Japanese subjects, which pointed out ABCG1 as a new susceptibility gene for PCV and AMD [37]. In 2017, Qiao et al. reported that the strongest PCV-associated SNP, CETP rs183130 (T allele; $P = 3.07E-07$), was in high LD with the currently studied SNP rs3764261 in Europeans, and similar association patterns were shown in AMD at CETP rs183130 (T allele; $P = 4.31E-05$). Also, they found that the most significant association signals recognized in Europeans were at rs5817082, rs1864163, and rs17231506 in CETP, but only rs17232506 showed significant association with PCV and AMD [38]. However, all the results above were reported in only 1 study, and they were challenged by pretty small sample sizes, so we need more researches with independent cohorts to verify these association findings.

In conclusion, our systematic review and meta-analysis has provided an overview of the association profiles of genes in the HDLMP in PCV for the first time and assessed the genetic difference in the HDLMP between PCV and AMD. The results suggest that CETP (rs3764261/rs2303790) and ABCG1 (rs57137919) are the major susceptibility genes for PCV in the Asian population, and ABCG1 (rs57137919) has different effects in PCV and AMD in the Asian population. However, due to the small pooled sample size for PCV and AMD, further studies of these genes in larger samples are warranted to confirm the association of gene variations in the HDLMP with PCV in other populations such as Caucasian and Australian. Moreover, further studies should focus on the genotype-phenotype correlations and the relevance of genotype to therapy in PCV, which may provide us the clues about the pathogenesis of PCV.

Conflicts of Interest

The authors declare that there are no conflicts of interest regarding the publication of this paper.

Supplementary Materials

Table S1: the search strategy applied in all databases. Table S2: lists of included/excluded studies with reasons. Table S3: Hardy–Weinberg equilibrium of polymorphisms in control subjects. Table S4: quality assessment of each study based on the Newcastle–Ottawa Scale. Table S5: the number of studies for CETP/LIPC/LPL/ABCA1/ABCG1 polymorphisms in PCV. Figure S1: funnel plot of 7 SNPs in PCV in the allelic model. Figure S2: funnel plot of 7 SNPs compared between PCV and AMD in the allelic model. (*Supplementary Materials*)

References

[1] L. A. Yannuzzi, J. Sorenson, R. F. Spaide et al., "Idiopathic polypoidal choroidal vasculopathy (IPCV)," *Retina*, vol. 10, no. 1, pp. 1–8, 1990.

[2] C. S. Tan, W. K. Ngo, L. W. Lim et al., "A novel classification of the vascular patterns of polypoidal choroidal vasculopathy and its relation to clinical outcomes," *British Journal of Ophthalmology*, vol. 98, no. 11, pp. 1528–1533, 2014.

[3] S. Honda, W. Matsumiya, and A. Negi, "Polypoidal choroidal vasculopathy: clinical features and genetic predisposition," *Ophthalmologica*, vol. 231, no. 2, pp. 59–74, 2014.

[4] A. Laude, P. D. Cackett, E. N. Vithana et al., "Polypoidal choroidal vasculopathy and neovascular age-related macular degeneration: same or different disease?," *Progress in Retinal and Eye Research*, vol. 29, no. 1, pp. 19–29, 2010.

[5] L. A. Yannuzzi, D. W. Wong, B. S. Sforzolini et al., "Polypoidal choroidal vasculopathy and neovascularized age-related macular degeneration," *Archives of Ophthalmology*, vol. 117, no. 11, pp. 1503–1510, 1999.

[6] J. Z. Kuo, T. Y. Wong, and F. S. Ong, "Genetic risk, ethnic variations and pharmacogenetic biomarkers in age-related macular degeneration and polypoidal choroidal vasculopathy," *Expert Review of Ophthalmology*, vol. 8, no. 2, pp. 127–140, 2013.

[7] X. Y. Liang, T. Y. Lai, D. T. Liu et al., "Differentiation of exudative age-related macular degeneration and polypoidal choroidal vasculopathy in the ARMS2/HTRA1 locus," *Investigative Opthalmology and Visual Science*, vol. 53, no. 6, pp. 3175–3182, 2012.

[8] D. R. Goldman, K. B. Freund, C. A. McCannel et al., "Peripheral polypoidal choroidal vasculopathy as a cause of peripheral exudative hemorrhagic chorioretinopathy: a report of 10 eyes," *Retina*, vol. 33, no. 1, pp. 48–55, 2013.

[9] I. Mantel, A. Schalenbourg, and L. Zografos, "Peripheral exudative hemorrhagic chorioretinopathy: polypoidal choroidal vasculopathy and hemodynamic modifications," *American Journal of Ophthalmology*, vol. 153, no. 5, pp. 910–922, 2012.

[10] S. Honda, H. Imai, K. Yamashiro et al., "Comparative assessment of photodynamic therapy for typical age-related macular degeneration and polypoidal choroidal vasculopathy: a multicenter study in Hyogo prefecture, Japan," *Ophthalmologica*, vol. 223, no. 5, pp. 333–338, 2009.

[11] W. Matsumiya, S. Honda, S. Kusuhara et al., "Effectiveness of intravitreal ranibizumab in exudative age-related macular degeneration (AMD): comparison between typical neovascular AMD and polypoidal choroidal vasculopathy over a 1 year follow-up," *BMC Ophthalmology*, vol. 13, no. 1, p. 10, 2013.

[12] L. Huang, H. Zhang, C. Y. Cheng et al., "A missense variant in FGD6 confers increased risk of polypoidal choroidal vasculopathy," *Nature Genetics*, vol. 48, no. 6, pp. 640–647, 2016.

[13] K. Liu, T. Y. Lai, S. W. Chiang et al., "Gender specific association of a complement component 3 polymorphism with polypoidal choroidal vasculopathy," *Scientific Reports*, vol. 4, no. 1, p. 7018, 2014.

[14] K. Liu, L. J. Chen, P. O. Tam et al., "Associations of the C2-CFB-RDBP-SKIV2L locus with age-related macular degeneration and polypoidal choroidal vasculopathy," *Ophthalmology*, vol. 120, no. 4, pp. 837–843, 2013.

[15] N. Gotoh, S. Kuroiwa, T. Kikuchi et al., "Apolipoprotein E polymorphisms in Japanese patients with polypoidal choroidal vasculopathy and exudative age-related macular degeneration," *American Journal of Ophthalmology*, vol. 138, no. 4, pp. 567–573, 2004.

[16] N. Kondo, S. Honda, K. Ishibashi et al., "Elastin gene polymorphisms in neovascular age-related macular degeneration and polypoidal choroidal vasculopathy," *Investigative Opthalmology and Visual Science*, vol. 49, no. 3, pp. 1101–1105, 2008.

[17] F. G. Holz, G. Sheraidah, D. Pauleikhoff et al., "Analysis of lipid deposits extracted from human macular and peripheral Bruch's membrane," *Archives of Ophthalmology*, vol. 112, no. 3, pp. 402–406, 1994.

[18] R. Reynolds, B. Rosner, and J. M. Seddon, "Serum lipid biomarkers and hepatic lipase gene associations with age-related macular degeneration," *Ophthalmology*, vol. 117, no. 10, pp. 1989–1995, 2010.

[19] L. Hyman, A. P. Schachat, Q. He et al., "Hypertension, cardiovascular disease, and age-related macular degeneration. Age-related macular degeneration risk factors study group," *Archives of Ophthalmology*, vol. 118, no. 3, pp. 351–358, 2000.

[20] Y. Hirami, M. Mandai, M. Takahashi et al., "Association of clinical characteristics with disease subtypes, initial visual acuity, and visual prognosis in neovascular age-related macular degeneration," *Japanese Journal of Ophthalmology*, vol. 53, no. 4, pp. 396–407, 2009.

[21] I. Maruko, T. Iida, M. Saito et al., "Clinical characteristics of exudative age-related macular degeneration in Japanese patients," *American Journal of Ophthalmology*, vol. 144, no. 1, pp. 15–22, 2007.

[22] T. Mathis, L. Kodjikian, M. Mauget-Faysse et al., "Polypoidal choroidal vasculopathy occurring in the context of large colloid drusen," *Ophthalmic Surgery, Lasers and Imaging Retina*, vol. 47, no. 12, pp. 1154–1156, 2016.

[23] D. Iwama, A. Tsujikawa, M. Sasahara et al., "Polypoidal choroidal vasculopathy with drusen," *Japanese Journal of Ophthalmology*, vol. 52, no. 2, pp. 116–121, 2008.

[24] I. D. Ladas, A. A. Rouvas, M. M. Moschos et al., "Polypoidal choroidal vasculopathy and exudative age-related macular degeneration in Greek population," *Eye*, vol. 18, no. 5, pp. 455–459, 2004.

[25] L. Wang, M. E. Clark, D. K. Crossman et al., "Abundant lipid and protein components of drusen," *PLoS One*, vol. 5, no. 4, article e10329, 2010.

[26] R. Klein, T. Peto, A. Bird et al., "The epidemiology of age-related macular degeneration," *American Journal of Ophthalmology*, vol. 137, no. 3, pp. 486–495, 2004.

[27] U. Chakravarthy, T. Y. Wong, A. Fletcher et al., "Clinical risk factors for age-related macular degeneration: a systematic review and meta-analysis," *BMC Ophthalmology*, vol. 10, no. 1, p. 31, 2010.

[28] B. J. Cho, J. W. Heo, T. W. Kim et al., "Prevalence and risk factors of age-related macular degeneration in Korea: the Korea National Health and Nutrition Examination Survey 2010-2011," *Investigative Opthalmology and Visual Science*, vol. 55, no. 2, pp. 1101–1108, 2014.

[29] D. Yuan, D. Yuan, S. Yuan et al., "The age-related maculopathy susceptibility 2 polymorphism and polypoidal choroidal vasculopathy in Asian populations: a meta-analysis," *Ophthalmology*, vol. 120, no. 10, pp. 2051–2057, 2013.

[30] J. P. Higgins, S. G. Thompson, J. J. Deeks et al., "Measuring inconsistency in meta-analyses," *BMJ*, vol. 327, no. 7414, pp. 557–560, 2003.

[31] A. Thakkinstian, G. J. McKay, M. McEvoy et al., "Systematic review and meta-analysis of the association between complement component 3 and age-related macular degeneration: a HuGE review and meta-analysis," *American Journal of Epidemiology*, vol. 173, no. 12, pp. 1365–1379, 2011.

[32] I. Nakata, K. Yamashiro, T. Kawaguchi et al., "Association between the cholesteryl ester transfer protein gene and polypoidal choroidal vasculopathy," *Investigative Opthalmology and Visual Science*, vol. 54, no. 9, pp. 6068–6073, 2013.

[33] X. Zhang, M. Li, F. Wen et al., "Different impact of high-density lipoprotein-related genetic variants on polypoidal choroidal vasculopathy and neovascular age-related macular degeneration in a Chinese Han population," *Experimental Eye Research*, vol. 108, pp. 16–22, 2013.

[34] F. Li, Y. Li, M. Li et al., "ABCA1 rs1883025 polymorphism shows no association with neovascular age-related macular degeneration or polypoidal choroidal vasculopathy in a Northern Chinese population," *Ophthalmic Research*, vol. 51, no. 4, pp. 210–215, 2014.

[35] K. Liu, L. J. Chen, T. Y. Lai et al., "Genes in the high-density lipoprotein metabolic pathway in age-related macular degeneration and polypoidal choroidal vasculopathy," *Ophthalmology*, vol. 121, no. 4, pp. 911–916, 2014.

[36] Q. Meng, L. Huang, Y. Sun et al., "Effect of high-density lipoprotein metabolic pathway gene variations and risk factors on neovascular age-related macular degeneration and polypoidal choroidal vasculopathy in China," *PLoS One*, vol. 10, no. 12, article e143924, 2015.

[37] L. Ma, K. Liu, M. Tsujikawa et al., "Association of ABCG1 with neovascular age-related macular degeneration and polypoidal choroidal vasculopathy in Chinese and Japanese," *Investigative Opthalmology and Visual Science*, vol. 57, no. 13, pp. 5758–5763, 2016.

[38] Q. Fan, C. Cheung, L. J. Chen et al., "Shared genetic variants for polypoidal choroidal vasculopathy and typical neovascular age-related macular degeneration in East Asians," *Journal of Human Genetics*, vol. 62, no. 12, pp. 1049–1055, 2017.

[39] I. R. Rodriguez and I. M. Larrayoz, "Cholesterol oxidation in the retina: implications of 7KCh formation in chronic inflammation and age-related macular degeneration," *Journal of Lipid Research*, vol. 51, no. 10, pp. 2847–2862, 2010.

[40] F. Liu, W. Wang, Y. Xu et al., "ABCG1 rs57137919G>a polymorphism is functionally associated with varying gene expression and apoptosis of macrophages," *PLoS One*, vol. 9, no. 6, article e97044, 2014.

[41] K. G. Duncan, K. Hosseini, K. R. Bailey et al., "Expression of reverse cholesterol transport proteins ATP-binding cassette A1 (ABCA1) and scavenger receptor BI (SR-BI) in the retina and retinal pigment epithelium," *British Journal of Ophthalmology*, vol. 93, no. 8, pp. 1116–1120, 2009.

[42] G. Schmitz and T. Langmann, "Structure, function and regulation of the ABC1 gene product," *Current Opinion in Lipidology*, vol. 12, no. 2, pp. 129–140, 2001.

[43] S. Yokoyama, "ABCA1 and biogenesis of HDL," *Journal of Atherosclerosis and Thrombosis*, vol. 13, no. 1, pp. 1–15, 2006.

[44] Y. Yu, R. Reynolds, B. Rosner et al., "Prospective assessment of genetic effects on progression to different stages of age-related macular degeneration using multistate Markov models," *Investigative Opthalmology and Visual Science*, vol. 53, no. 3, pp. 1548–1556, 2012.

[45] B. M. Neale, J. Fagerness, R. Reynolds et al., "Genome-wide association study of advanced age-related macular degeneration identifies a role of the hepatic lipase gene (LIPC)," *Proceedings of the National Academy of Sciences*, vol. 107, no. 16, pp. 7395–7400, 2010.

[46] J. Lee, J. Zeng, G. Hughes et al., "Association of LIPC and advanced age-related macular degeneration," *Eye*, vol. 27, no. 2, pp. 265–270, 2013.

[47] W. Chen, D. Stambolian, A. O. Edwards et al., "Genetic variants near TIMP3 and high-density lipoprotein-associated loci influence susceptibility to age-related macular degeneration," *Proceedings of the National Academy of Sciences*, vol. 107, no. 16, pp. 7401–7406, 2010.

[48] I. A. Pikuleva and C. A. Curcio, "Cholesterol in the retina: the best is yet to come," *Progress in Retinal and Eye Research*, vol. 41, pp. 64–89, 2014.

[49] L. Bretillon, G. Thuret, S. Gregoire et al., "Lipid and fatty acid profile of the retina, retinal pigment epithelium/choroid, and

the lacrimal gland, and associations with adipose tissue fatty acids in human subjects," *Experimental Eye Research*, vol. 87, no. 6, pp. 521–528, 2008.

[50] L. Wang, C. M. Li, M. Rudolf et al., "Lipoprotein particles of intraocular origin in human Bruch membrane: an unusual lipid profile," *Investigative Opthalmology and Visual Science*, vol. 50, no. 2, pp. 870–877, 2009.

[51] E. Loane, J. M. Nolan, and S. Beatty, "The respective relationships between lipoprotein profile, macular pigment optical density, and serum concentrations of lutein and zeaxanthin," *Investigative Opthalmology and Visual Science*, vol. 51, no. 11, pp. 5897–5905, 2010.

[52] C. A. Curcio, M. Johnson, J. D. Huang et al., "Aging, age-related macular degeneration, and the response-to-retention of apolipoprotein B-containing lipoproteins," *Progress in Retinal and Eye Research*, vol. 28, no. 6, pp. 393–422, 2009.

[53] J. G. Hollyfield, V. L. Bonilha, M. E. Rayborn et al., "Oxidative damage-induced inflammation initiates age-related macular degeneration," *Nature Medicine*, vol. 14, no. 2, pp. 194–198, 2008.

[54] P. X. Shaw, L. Zhang, M. Zhang et al., "Complement factor H genotypes impact risk of age-related macular degeneration by interaction with oxidized phospholipids," *Proceedings of the National Academy of Sciences*, vol. 109, no. 34, pp. 13757–13762, 2012.

[55] C. Y. Cheng, K. Yamashiro, L. J. Chen et al., "New loci and coding variants confer risk for age-related macular degeneration in East Asians," *Nature Communications*, vol. 6, p. 6063, 2015.

[56] D. Wang, J. Zhou, X. Hou et al., "CETP gene may be associated with advanced age-related macular degeneration in the Chinese population," *Ophthalmic Genetics*, vol. 36, no. 4, pp. 303–308, 2015.

[57] R. Liutkeviciene, A. Vilkeviciute, G. Streleckiene et al., "Associations of cholesteryl ester transfer protein (CETP) gene variants with predisposition to age-related macular degeneration," *Gene*, vol. 636, pp. 30–35, 2017.

Hindawi
Journal of Ophthalmology
Volume 2018, Article ID 8761625, 7 pages
https://doi.org/10.1155/2018/8761625

Research Article

Comparison of SNP Genotypes Related to Proliferative Vitreoretinopathy (PVR) across Slovenian and European Subpopulations

Xhevat Lumi,[1] **Mateja M. Jelen**,[2] **Daša Jevšinek Skok**,[2] **Emanuela Boštjančič**,[2] **Metka Ravnik-Glavač**,[2] **Marko Hawlina**,[1] **and Damjan Glavač**[2]

[1]*Eye Hospital, University Medical Centre Ljubljana, Ljubljana, Slovenia*
[2]*Department of Molecular Genetics, Institute of Pathology, Faculty of Medicine, University of Ljubljana, Ljubljana, Slovenia*

Correspondence should be addressed to Damjan Glavač; damjan.glavac@mf.uni-lj.si

Received 20 September 2017; Accepted 21 January 2018; Published 15 May 2018

Academic Editor: Stephen T. Armenti

The present study investigated the distribution of genotypes within single nucleotide polymorphisms (SNPs) in genes, related to PVR pathogenesis across European subpopulations. Genotype distributions of 42 SNPs among 96 Slovenian healthy controls were investigated and compared to genotype frequencies in 503 European individuals (Ensembl database) and their subpopulations. Furthermore, a case-control status was simulated to evaluate effects of allele frequency changes on statistically significant results in gene-association studies investigating functional polymorphisms. In addition, 96 healthy controls were investigated within 4 SNPs: rs17561 (*IL1A*), rs2069763 (*IL2*), rs2229094 (*LTA*), and rs1800629 (*TNF*) in comparison to PVR patients. Significant differences ($P < 0.05$) in distribution of genotypes among 96 Slovenian participants and a European population were found in 10 SNPs: rs3024498 (*IL10*), rs315952 (*IL1RN*), rs2256965 (*LST1*), rs2256974 (*LST1*), rs909253 (*LTA*), rs2857602 (*LTA*), rs3138045 (*NFKB1A*), rs3138056 (*NFKB1A*), rs7656613 (*PDGFRA*), and rs1891467 (*TGFB2*), which additionally showed significant differences in genotype distribution among European subpopulations. This analysis also showed statistically significant differences in genotype distributions between healthy controls and PVR patients in rs17561 of the *IL1A* gene (OR, 3.00; 95% CI, 0.77–11.75; $P = 0.036$) and in rs1800629 of the *TNF* gene (OR, 0.48; 95% CI, 0.27–0.87; $P = 0.014$). Furthermore, we have shown that a small change (0.02) in minor allele frequency (MAF) significantly affects the statistical p value in case-control studies. In conclusion, the study showed differences in genotype distributions in healthy populations across different European countries. Differences in distribution of genotypes may have had influenced failed replication results in previous PVR-related SNP-association studies.

1. Introduction

The impact of genome-wide association studies and genetic-association studies has become enormous in the past ten years, providing researchers with extensive data repositories [1]. As genetic factors affect susceptibility to certain diseases, identifying the relevant genes and/or their polymorphisms contribute greatly to the development of novel prevention programs and treatments of disease. Numerous evaluations of genetic association have also led to the remarkable potential for the discovery of novel genetic biomarkers. However, the execution of such analysis in many cases is cumbersome with considerable statistical and computational challenges and also requires reproducibility [2]. The potential for the discovery of false positive findings when results are not properly corrected is high and represents the most conspicuous problem in gene-disease-association studies [3–5].

Proliferative vitreoretinopathy (PVR) represents the growth and contraction of cellular membranes on both retinal surfaces and within the vitreous cavity in patients with rhegmatogenous retinal detachment (RRD) [6–8]. It is the major complication following retinal detachment surgery

and a leading cause of failure in the management of RRD [6, 9]. It is estimated to occur in 5–10% of patients with RRD [6]. Technological advances in high-throughput screening have been introduced in gene-association studies, including PVR. These studies revealed numerous inflammatory molecules to be implicated in the PVR development, such as growth factors (PDGF, HGF, VEGF, and EGF), transforming growth factors (TGFA, TGFB), molecules from the SMAD family and interleukins (IL1, IL6, IL8, and IL10), tumor necrosis factors (TNF), and tumor suppressor protein (p53) [10–15]. Studies, published in the past ten years, by the "Retina 4 Project" consortium, have demonstrated that specific single nucleotide polymorphisms (SNPs), located in genes involved in PVR pathways, may represent potential predictive factors for the PVR development [10, 11, 14, 16–20]. Among 200 studied SNPs in more than 30 candidate genes, the "Retina 4 Project" identified 8 SNPs in 7 genes, encoding CCL2, FGF2, IL1RN, LTA, NFKBIA, SMAD7, and TGFB2, as significant individual predictors for PVR [11] and demonstrated associations between PVR and SNPs in *BAX*, *p53*, *PIK3CG*, *MDM2*, *SMAD7*, and *TNFB2* in the TNF locus [10, 16–19]. A more recent genetic-association study, on a Slovenian PVR patient population, demonstrated significant differences in genotype distributions between RRD patients with and without PVR in SNPs within *IL6*, in the vicinity of *IL10*, and the *TGFB1* gene. Interestingly, several associations between SNP genotypes and the PVR phenotype could not be replicated throughout a series of "Retina 4 Project" studies and by a recent study on a Slovenian population. To establish the credibility of an association between a SNP and disease, a replication of SNP effect among different study populations is essential. It is possible that fluctuations between genotype frequencies across studied countries reflect the difference in population ancestry, which could influence the variability in allele frequencies even in unrelated conditions of interest [21]. As success of replication of a genetic-association study depends on many factors, including enrollment of independent population datasets, information on the effect of different allele frequencies in genetic-association studies remains scarce.

The present study is a part of an ongoing gene-association study in Slovenian RRD patients who developed PVR after vitrectomy. In order to expand the current perspective on differences between PVR patients and healthy controls and SNP effects in patients with different geographical background, we further investigated our previously established in-house genomic databases. Firstly, we aimed to assess basic differences in SNP genotype distributions among European subpopulations. For this purpose, we compared distributions of 42 SNP genotypes between a Slovenian healthy population and European subpopulations and among European subpopulations. Additionally, this study designed a simulation of a case-control gene-association study in order to demonstrate that even a minor allele frequency (MAF) change could result in a considerable increase in the power to replicate the previously established SNP effect. In the second part of the study, we examined differences in distribution of SNP genotypes between Slovenian healthy controls and PVR patients.

2. Methods

2.1. Study Population. The genetic-association study conducted on 191 Slovenian patients with primary RRD, who underwent vitrectomy at the Eye Hospital, University Medical Centre Ljubljana, Slovenia. In the study we recruited 153 patients who developed PVR grade C1 or higher within 3 months after the surgery. We also enrolled 96 healthy controls without retinal detachment. The study was approved by the National Medical Ethics Committee of the Republic of Slovenia and followed the tenets of the Helsinki Declaration. All patients provided written informed consent.

Ninety-six healthy Slovenian blood donors (52 men and 44 women), aged between 20 and 55 years, originating from 11 geographic areas, representative for the country of Slovenia, were statistically analyzed in 4 SNPs.

2.2. Blood Collection and DNA Extraction. Six milliliters of peripheral blood were collected from each participant and stored until DNA extraction at −20°C. DNA was extracted using QIAamp DNA Blood Midi Kit (100) (QIAGEN, Hilden, Germany), according to the manufacturer's instructions. Extracted DNA was stored until used for amplification at −20°C.

2.3. Genotype Distribution in Slovenian and European Populations. Genotype distributions of 42 SNPs of 96 Slovenian healthy controls, genotyped using HumanOmniExpress-14 platform (Illumina, San Diego, CA, USA), were compared across 503 European residents, using data on specific SNP genotypes obtained from the Ensembl database (release 83) (Supplemental Table 1). In case a difference among SNP genotype distribution was observed among Slovenian and European populations, the differences between the populations were further examined, as follows: the frequencies of genotypes were subsequently compared between the Slovenian and three European subpopulations, namely, 99 Utah residents with northern and western European ancestry (CEU), 91 residents from Britain in England and Scotland (GBR), and 107 Iberian residents from Spain (IBS).

2.4. Evaluation of Genetic Effects in a Simulated Population Dataset. We hypothesized that some statistically significant differences in SNP genotype distributions could not be replicated due to even small changes in allele frequencies. To test this hypothesis, we designed a simulated case-control status. The genotype frequency of the original case dataset was AA = 1, AG = 39, and GG = 73, and the minor allele frequency (MAF) was 0.18 ($P = 0.13$). The control dataset remained unchanged. Genotypes were added one by one in each homozygote or heterozygote category to evaluate effects of minor allele frequency (MAF) changes on statistically significant results (Table 1).

2.5. Genotyping of 96 Healthy Participants. Ninety-six Slovenian healthy controls were genotyped for 713,014 markers, using HumanOmniExpress-14 platform (Illumina, San Diego, CA, USA). Genotypes were assigned according to the standard Illumina protocol in GenomeStudio Software,

Table 1: Simulation of genotype distribution in a potential population dataset.

Number of simulations	Genotype case dataset (n)			Number of genotypes added to the case dataset (n)			Allele frequency		MAF	P value
	AA	AG	GG	AA	AG	GG	A	G		
1	1	39	73	0	0	0	0.18	0.82	0.18	0.130
2	1	40	73	0	1	0	0.18	0.82	0.18	0.110
3	1	41	73	0	2	0	0.19	0.81	0.19	0.092
4	1	42	73	0	3	0	0.19	0.81	0.19	0.078
5	1	43	73	0	4	0	0.19	0.81	0.19	0.066
6	1	44	73	0	5	0	0.19	0.81	0.19	0.056
7	1	45	73	0	6	0	0.20	0.80	0.20	0.047
8	2	39	73	1	0	0	0.19	0.81	0.19	0.091
9	2	40	73	1	1	0	0.19	0.81	0.19	0.077
10	2	41	73	1	2	0	0.19	0.81	0.19	0.065
11	2	42	73	1	3	0	0.20	0.80	0.20	0.055
12	2	43	73	1	4	0	0.20	0.80	0.20	0.047
13	3	39	73	2	0	0	0.20	0.80	0.20	0.065
14	3	40	73	2	1	0	0.20	0.80	0.20	0.055
15	3	41	73	2	2	0	0.20	0.80	0.20	0.046
16	4	39	73	3	0	0	0.20	0.80	0.20	0.041

Note: original case dataset is shown in the second column. The control dataset is not shown. Added genotypes to the original dataset are represented in the third column. Genotypes were added one by one in each homozygote or heterozygote category. Allele frequency, MAF, and P values changed according to the performed simulation.

version V2011.1. Only individuals with a genotyping success rate of >95% were considered as positive for a respective genotype. The HumanOmniExpress-14 platform included only 4 SNPs, investigated previously in RRD and PVR patients. Therefore, our subsequent analysis included comparison of 96 control PVR patients for 4 SNPs: rs17561 (*IL1A*), rs2069763 (*IL2*), rs229094 (*LTA*) and rs1800629 (*TNF*).

2.6. TaqMan Genotyping of PVR Patients. Genotypes of 4 SNPs, located within or in the vicinity of the 4 genes rs17561 (*IL1A*), rs2069763 (*IL2*), rs2229094 (*LTA*), and rs1800629 (*TNF*), were determined using TaqMan assay (Applied Biosystems, Foster City, CA, USA) according to the manufacturer's instructions.

2.7. Statistical Analysis. Differences in genotype distributions among Slovenian healthy controls and European subpopulations were evaluated with the chi-square test, calculated using SAS software version 9.2 (JMP®, SAS Institute Inc., 2010, Cary, North Carolina, USA) and presented as pie charts (Figures 1 and 2).

To assess the differences in SNP genotype distribution among healthy population and PVR patients, odds ratios (ORs) with 95% confidence intervals (95% CIs) were calculated in SNPStats software [22], using the unconditional logistic regression. For inheritance model identification, the Akaike information criteria (AIC) were used, according to the authors' instructions. An α value was set to 0.05 in all calculations.

3. Results

The genotype distribution comparison of 42 SNPs among 96 Slovenian healthy controls (SLO) and a European population (data for 503 individuals were obtained from the Ensembl database) revealed significant differences ($P < 0.05$) in distribution of genotypes in 10 SNPs: rs3024498 (*IL10*), rs315952 (*IL1RN*), rs2256965 (*LST1*), rs2256974 (*LST1*), rs909253 (*LTA*), rs2857602 (*LTA*), rs3138045 (*NFKB1A*), rs3138056 (*NFKB1A*), rs7656613 (*PDGFRA*), and rs1891467 (*TGFB2*) (see Figures 1 and 2).

The frequencies of genotypes rs315952 (*IL1RN*), rs2256965 (*LST1*), and rs2256974 (*LST1*) varied significantly between SLO and CEU, SLO and GBR, and SLO and IBS, while the differences between GBR and IBS were not observed. Similar differences were observed for SNP rs1891467 (*TGFB2*), where we noticed the differences between all comparisons with the Slovenian population, as well as between GBR and IBS. Differences in the frequency of genotypes for the SNP rs3024498 (*IL10*) were observed between SLO and GRB, SLO and IBS, and between GBR and IBS. For the SNP rs3138056 (*NFKB1A*), differences between SLO and CEU and between SLO and IBS were observed. The differences in the frequencies of genotypes for the SNP rs3138045 (*NFKB1A*) were observed between SLO and IBS and GBR and IBS, while the frequencies of genotypes rs7656613 (*PDGFRA*), rs909253 (*LTA*), and rs2857602 (*LTA*) differ between populations of SLO and CEU and SLO and GBR.

Simulation of the potential population dataset of SNP genotypes revealed that adding six heterozygotes (AG) to the

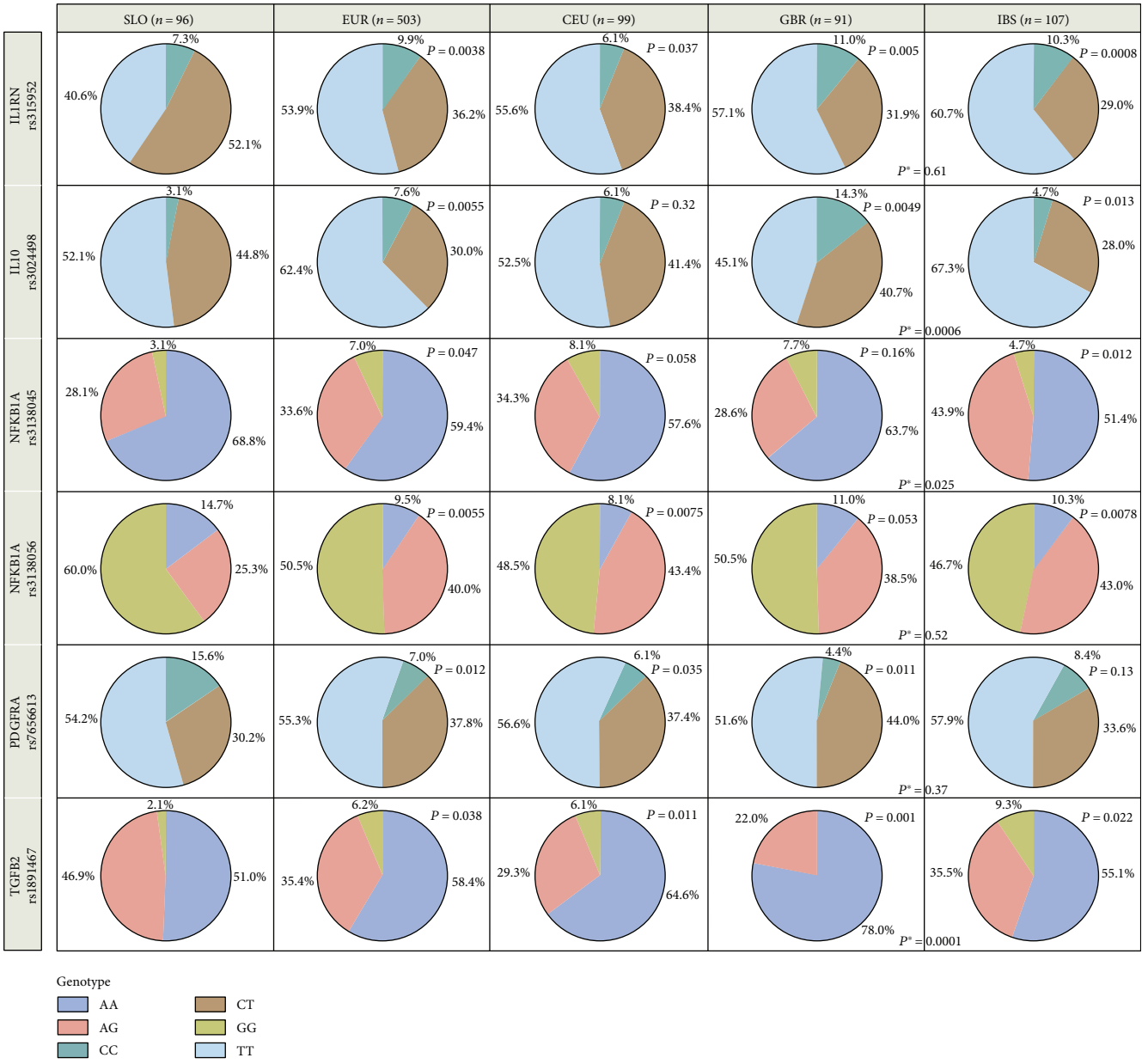

Figure 1: The genotype frequencies for 6 SNPs across European subpopulations. *P* value means difference in genotype distribution between Slovenian population (SLO) and other populations (EUR, CEU, GBR and IBS). *P** value means difference in genotype distribution between Great Britain population (GBR) and Iberian population (IBS) only.

original case dataset showed a statistically significant difference between the two populations ($P = 0.047$) (Table 1). Similarly, statistically significant differences were shown when one homozygote (AA) and four heterozygotes (AG), or two homozygotes (AA) and two heterozygotes (AG), or three homozygotes (AA), were added to the original case dataset. Despite the fact that MAF increased from 0.18 to 0.20 in all described cases of events, the small change (0.02) in MAF showed an important decrease of the *P* value below 0.05.

In addition, the analysis showed two statistically significant differences in genotype distributions between 96 healthy controls and PVR patients (Table 2). In *IL1A* (rs17561), a statistically significant difference in distribution of genotypes was found between PVR patients and healthy controls (OR, 3.00; 95% CI, 0.77 to 11.75; $P = 0.036$). A significantly different distribution of genotypes was found also in rs1800629 of the *TNF* gene (OR, 0.48; 95% CI, 0.27 to 0.87; $P = 0.014$).

4. Discussion

Numerous inflammatory mediators, growth factors, and cytokines have been implicated in PVR pathogenesis. Statistical results of several genetic-association studies within the "Retina 4 Project" have emphasized the possible potential of those inflammatory mediators as novel biomarkers in the diagnostics and treatment of PVR [7, 8, 20, 23]. Replication

FIGURE 2: The genotype frequencies for 4 SNPs across European subpopulations. *P* value means difference in genotype distribution between Slovenian population (SLO) and other populations (EUR, CEU, GBR and IBS). P^* value means difference in genotype distribution between Great Britain population (GBR) and Iberian population (IBS) only.

of statistical results in gene-association studies has become the golden standard for assessing the independent effect of SNP and/or its genomic location to a certain disease [3]. Unfortunately, reproducibility is frequently challenging to achieve due to genetic heterogeneity, inadequate population size, or variability in phenotype definitions, environmental interactions, inadequate statistical power, and age-dependent effects [1, 2, 24–26].

Previous gene-association studies investigating SNPs in PVR have demonstrated significant differences between PVR cases, RRD controls, and healthy controls and predicted several genetic associations for PVR development [10, 16–19]. Fundamental studies in PVR research were based on international investigation of SNP genotype associations and included patients from Spain, Portugal, UK, and Netherlands [18, 19]. However, these studies did not include the comparison of genotype distributions in healthy populations across European subpopulations. For this reason, it is possible that failed replications of SNP effects in studies that followed were a consequence of different genetic structures across studied populations *per se*.

The present study compared the distribution of 42 SNP genotypes between Slovenian and European healthy populations and revealed significant differences in 10 SNPs, suggesting a somewhat similar distribution of genotypes among residents of common European ancestry. Our results firstly suggest that genotype polymorphisms more frequently identified in individuals from one European country could probably share a similar genotype pattern in individuals from other European countries as well. Our observations also indicate that different allele frequencies across independent datasets indeed influence the final SNP effect, frequently leading to spurious results in replication studies. The mentioned bias has been confirmed in our study by manipulating a simulated case-control dataset, which revealed that already a small change of 0.02 in MAF indeed causes important differences in statistical significance in genetic-association studies. Similar results were obtained in a simulation study of two interacting SNPs by Greene et al. which showed that the power to replicate the statistically significant independent effect of one SNP can drop dramatically with a change in allele frequency of less than 0.1 at the second interacting polymorphism [3]. On the other hand, it has been proposed that population structure has so far caused less inaccurate associations in genetic-association studies than it was initially predicted. When systematic ethnicity

Table 2: Genotype distributions of 4 SNPs in Slovenian patients with PVR and 96 healthy controls. Inheritance models and odds ratios (ORs) were determined.

Gene	SNP	Genotype	Genotype frequency in healthy controls (%)	Genotype frequency in cases (%)	Inheritance model*	OR (95% CI)	*P* value
IL1A	rs17561 C/A	CC	49 (51)	49 (43.39)	Codominant (CC-CA/AA)	3.00 (0.77–11.75)	**0.036**
		CA	38 (40)	59 (52.29)			
		AA	9 (9)	3 (2.7)			
		ND	0 (0)	2 (1.8)			
Total number of participants			96 (100)	113 (100)			
IL2	rs2069763 C/A	CC	39 (41)	52 (46.0)	Recessive** (CC/CA-AA)	1.51 (0.71–3.18)	0.28
		CA	39 (41)	46 (40.7)			
		AA	18 (19)	15 (13.3)			
Total number of participants			96 (100)	113 (100)			
LTA	rs2229094 T/C	CC	8 (8.3)	15 (9.8)	Additive	1.15 (0.78–1.70)	0.49
		TC	33 (34.4)	55 (36.0)			
		TT	55 (57.3)	79 (51.6)			
		ND	0 (0)	4 (2.6)			
Total number of participants			96 (100)	153 (100)			
TNF	rs1800629 G/A	GG	74 (77)	96 (62.7)	Overdominant (GG-AA/AG)	0.48	**0.014**
		AG	20 (21)	54 (35.3)		0.27–0.87	
		AA	2 (2)	3 (2.0)			
Total number of participants			96 (100)	153 (100)			

Abbreviations: OR: odds ratio; 95% CI: 95% confidence interval; ND: patients, in which genotype could not be identified. *Inheritance models: additive: each copy of the rare variant modifies the risk; dominant: a single copy of the frequent variant is enough to modify the risk; recessive: two copies of the variant allele are necessary to change the risk; overdominant: heterozygosity modifies the risk. **In case of IL2, the inheritance model could be also additive (OR, 1.23; 95% CI, 0.84–1.80; $P = 0.28$).

matching and application of standard quality control measures are not provided by research executors, population effect can still represent a major bias in these studies [5]. In the second part of our study, we have found a statistically significant difference in distribution of genotypes between healthy controls and PVR patients in rs17561 within the *IL1A* gene and rs1800629 (*TNF*). Similar significance was observed in a previously published study by Sanabria Ruiz-Colmenares et al. for *TGFB1* (rs1800471), when no significant difference in genotype distribution was observed between patients with and without PVR; instead, a statistically significant difference was observed between PVR patients and healthy controls [14].

The impact of different distributions of genotypes in SNPs in TNF locus, which encodes also TNF-α, has been investigated in three subsequent studies by a Spanish group of the Retina 4 Project [10, 11, 16]. Various SNPs in *TNF* have been shown to be associated with increased risk of PVR development, including the rs1800629. However, we have found a statistically significant difference in distributions of genotypes between healthy controls and PVR patients. In conclusion, the ultimate goal in PVR research as well as in other human diseases is to detect genetic associations, which replicate in studies without a significant bias. Our study showed that differences in genotype distributions exist between healthy populations across different European countries and may have had influenced the failed replication results in PVR SNP-association studies. This study confirmed the importance of baseline screening of the healthy population before investigating patients originating from the same dataset. Considering the fact that genotype distributions in patients with PVR and RRD patients without PVR have been compared within a limited number of European countries (Netherlands, Portugal, Slovenia, Spain, and United Kingdom), and that results of different previous PVR studies failed to be replicated, it is crucial to conduct larger multicentric population-based study.

Conflicts of Interest

None of the authors has any conflicting interests to disclose.

Acknowledgments

The authors thank Borut Jerman, PhD, for technical support with PLINK software. This work is a part of the PhD thesis of candidate Xhevat Lumi, MD. This work was supported by the Slovenian Research Agency (ARRS) (Programs P3-054 and P3-0333).

Supplementary Materials

Supplemental Table 1: genotype distributions of 42 SNPs in a Slovenian population ($n = 96$) versus a European population ($n = 503$). *(Supplementary Materials)*

References

[1] T. A. Pearson and T. A. Manolio, "How to interpret a genome-wide association study," *JAMA*, vol. 299, no. 11, pp. 1335–1344, 2008.

[2] J. N. Hirschhorn and M. J. Daly, "Genome-wide association studies for common diseases and complex traits," *Nature Reviews Genetics*, vol. 6, no. 2, pp. 95–108, 2005.

[3] C. S. Greene, N. M. Penrod, S. M. Williams, and J. H. Moore, "Failure to replicate a genetic association may provide important clues about genetic architecture," *PLoS One*, vol. 4, no. 6, article e5639, 2009.

[4] P. Gorroochurn, S. E. Hodge, G. A. Heiman, M. Durner, and D. A. Greenberg, "Non-replication of association studies: "pseudo-failures" to replicate?," *Genetics in Medicine*, vol. 9, no. 6, pp. 325–331, 2007.

[5] J. Nsengimana and D. T. Bishop, "Design considerations for genetic linkage and association studies," *Methods in Molecular Biology*, vol. 850, pp. 237–262, 2012.

[6] J. C. Pastor, "Proliferative vitreoretinopathy: an overview," *Survey of Ophthalmology*, vol. 43, no. 1, pp. 3–18, 1998.

[7] J. C. Pastor, J. Rojas, S. Pastor-Idoate, S. di Lauro, L. Gonzalez-Buendia, and S. Delgado-Tirado, "Proliferative vitreoretinopathy: a new concept of disease pathogenesis and practical consequences," *Progress in Retinal and Eye Research*, vol. 51, pp. 125–155, 2016.

[8] S. Yang, H. Li, M. Li, and F. Wang, "Mechanisms of epithelial-mesenchymal transition in proliferative vitreoretinopathy," *Discovery Medicine*, vol. 20, no. 110, pp. 207–217, 2015.

[9] A. Sadaka and G. P. Giuliari, "Proliferative vitreoretinopathy: current and emerging treatments," *Clinical Ophthalmology*, vol. 6, pp. 1325–1333, 2012.

[10] J. Rojas, I. Fernandez, J. C. Pastor et al., "A genetic case-control study confirms the implication of *SMAD7* and *TNF locus* in the development of proliferative vitreoretinopathy," *Investigative Ophthalmology & Visual Science*, vol. 54, no. 3, pp. 1665–1678, 2013.

[11] J. Rojas, I. Fernandez, J. C. Pastor et al., "Development of predictive models of proliferative vitreoretinopathy based on genetic variables: the Retina 4 Project," *Investigative Ophthalmology & Visual Science*, vol. 50, no. 5, pp. 2384–2390, 2009.

[12] S. Pennock, L. J. Haddock, D. Eliott, S. Mukai, and A. Kazlauskas, "Is neutralizing vitreal growth factors a viable strategy to prevent proliferative vitreoretinopathy?," *Progress in Retinal and Eye Research*, vol. 40, pp. 16–34, 2014.

[13] F. Rouberol and C. Chiquet, "Proliferative vitreoretinopathy: pathophysiology and clinical diagnosis," *Journal Français d'Ophtalmologie*, vol. 37, no. 7, pp. 557–565, 2014.

[14] M. R. Sanabria Ruiz-Colmenares, J. C. Pastor Jimeno, J. A. Garrote Adrados, J. J. Telleria Orriols, and M. I. Yugueros Fernández, "Cytokine gene polymorphisms in retinal detachment patients with and without proliferative vitreoretinopathy: a preliminary study," *Acta Ophthalmologica Scandinavica*, vol. 84, no. 3, pp. 309–313, 2006.

[15] S. Saika, O. Yamanaka, I. Nishikawa-Ishida et al., "Effect of Smad7 gene overexpression on transforming growth factor β-induced retinal pigment fibrosis in a proliferative vitreoretinopathy mouse model," *Archives of Ophthalmology*, vol. 125, no. 5, pp. 647–654, 2007.

[16] J. Rojas, I. Fernandez, J. C. Pastor et al., "A strong genetic association between the tumor necrosis factor locus and proliferative vitreoretinopathy: the Retina 4 Project," *Ophthalmology*, vol. 117, no. 12, pp. 2417–2423.e2, 2010.

[17] S. Pastor-Idoate, I. Rodríguez-Hernández, J. Rojas et al., "BAX and BCL-2 polymorphisms, as predictors of proliferative vitreoretinopathy development in patients suffering retinal detachment: the Retina 4 Project," *Acta Ophthalmologica*, vol. 93, no. 7, pp. e541–e549, 2015.

[18] S. Pastor-Idoate, I. Rodríguez-Hernández, J. Rojas et al., "The T309G MDM2 gene polymorphism is a novel risk factor for proliferative vitreoretinopathy," *PLoS One*, vol. 8, no. 12, article e82283, 2013.

[19] S. Pastor-Idoate, I. Rodriguez-Hernández, J. Rojas et al., "The *p53* codon 72 polymorphism (rs1042522) is associated with proliferative vitreoretinopathy: the Retina 4 Project," *Ophthalmology*, vol. 120, no. 3, pp. 623–628, 2013.

[20] J. Rojas, I. Fernandez, J. C. Pastor et al., "Predicting proliferative vitreoretinopathy: temporal and external validation of models based on genetic and clinical variables," *The British Journal of Ophthalmology*, vol. 99, no. 1, pp. 41–48, 2015.

[21] J. Attia, J. P. A. Ioannidis, A. Thakkinstian et al., "How to use an article about genetic association: B: are the results of the study valid?," *JAMA*, vol. 301, no. 2, pp. 191–197, 2009.

[22] X. Sole, E. Guino, J. Valls, R. Iniesta, and V. Moreno, "SNPStats: a web tool for the analysis of association studies," *Bioinformatics*, vol. 22, no. 15, pp. 1928-1929, 2006.

[23] K. Nassar, S. Grisanti, A. Tura et al., "A TGF-β receptor 1 inhibitor for prevention of proliferative vitreoretinopathy," *Experimental Eye Research*, vol. 123, pp. 72–86, 2014.

[24] J. Ott, "Association of genetic loci: replication or not, that is the question," *Neurology*, vol. 63, no. 6, pp. 955–958, 2004.

[25] J. P. A. Ioannidis, "Non-replication and inconsistency in the genome-wide association setting," *Human Heredity*, vol. 64, no. 4, pp. 203–213, 2007.

[26] J. Lasky-Su, H. N. Lyon, V. Emilsson et al., "On the replication of genetic associations: timing can be everything!," *The American Journal of Human Genetics*, vol. 82, no. 4, pp. 849–858, 2008.

Hindawi
Journal of Ophthalmology
Volume 2018, Article ID 2735465, 9 pages
https://doi.org/10.1155/2018/2735465

Review Article

Nanophthalmos: A Review of the Clinical Spectrum and Genetics

Pedro C. Carricondo,[1] **Thais Andrade**,[1] **Lev Prasov**,[2] **Bernadete M. Ayres**,[2] **and Sayoko E. Moroi**[2]

[1]*Department of Ophthalmology, Hospital das Clínicas HCFMUSP, Faculdade de Medicina, Universidade de São Paulo, São Paulo, SP, Brazil*
[2]*Department of Ophthalmology and Visual Sciences, Kellogg Eye Center, University of Michigan, 1000 Wall St., Ann Arbor, MI 48105, USA*

Correspondence should be addressed to Pedro C. Carricondo; pedro.carricondo@gmail.com

Received 11 December 2017; Revised 20 February 2018; Accepted 8 April 2018; Published 9 May 2018

Academic Editor: Lisa Toto

Nanophthalmos is a clinical spectrum of disorders with a phenotypically small but structurally normal eye. These disorders present significant clinical challenges to ophthalmologists due to a high rate of secondary angle-closure glaucoma, spontaneous choroidal effusions, and perioperative complications with cataract and retinal surgeries. Nanophthalmos may present as a sporadic or familial disorder, with autosomal-dominant or recessive inheritance. To date, five genes (i.e., *MFRP*, *TMEM98*, *PRSS56*, *BEST1*, and *CRB1*) and two loci have been implicated in familial forms of nanophthalmos. Here, we review the definition of nanophthalmos, the clinical and pathogenic features of the condition, and the genetics of this disorder.

1. Introduction

The clinical spectrum of the small eye phenotype comprises conditions in which there is a global ocular reduction in size (e.g., microphthalmos and nanophthalmos) or shortening of either the anterior or posterior segments of the eye (e.g., relative anterior and posterior microphthalmos, resp.) (Table 1) [1–3]. The axial length and anterior chamber structures present a continuum of sizes (Table 2), where microphthalmos and nanophthalmos comprise the smallest or shortest eyes. Nanophthalmos derives from Greek "dwarf eye." In this ocular condition, the anterior and posterior segments have no other congenital malformations, but are both reduced in size, with secondary thickening of choroid and sclera.

The management of the small eye phenotype represents a major challenge for all ophthalmologists, from cataract surgeons to glaucoma and retina specialists. Small eyes may be associated with ophthalmic or systemic comorbidities. These eyes represent significant surgical challenges with a very high rate of intraoperative complications [4] and require a surgical approach that involves precision and care. Recognizing and correctly diagnosing the diverse presentations of this condition is of great importance for appropriate clinical and surgical management. Understanding the genetic mechanisms involved in the pathogenesis of nanophthalmos will ultimately help us to provide potential markers for genetic diagnosis and development of innovative therapies for this condition. The goal of this review is to define nanophthalmos and provide a brief summary of the advances in the clinical characterization and genetic basis for nanophthalmos.

2. Methods

A Medline/PubMed search was performed using the terms "nanophthalmos," "ocular development," and "genetics" and their combinations. All studies published in English, Portuguese, or Spanish up to December 2017 were reviewed, and relevant publications were included in this review. The pertinent references of the selected articles were also included. All patient images were obtained with the permission of participating individuals or from parents of minor patients, as part of a study on nanophthalmos. This study

Table 1: The clinical spectrum of the small eye phenotype.

Anophthalmia	Absence of the eye
Simple microphthalmos	Short axial length due to global eye reduction with no other findings
Complex microphthalmos	Short axial length due to global eye reduction and associated ocular malformations (e.g., colobomas, persistent fetal vasculature, retinal dysplasia)
Relative anterior microphthalmos	Short axial length due to reduced anterior chamber dimension only, with normal posterior segment dimension and normal scleral thickness
Posterior microphthalmos	Short axial length due to reduced posterior segment dimension with normal anterior chamber dimensions
Nanophthalmos	Short axial length due to small anterior and posterior segments with thickened choroid and sclera and normal lens volume

was approved by the University of Michigan Institutional Review Board and complied with the US Health Insurance Portability and Accountability Act of 1996 and the Declaration of Helsinki.

3. Nanophthalmos: Definition and Clinical Features

Microphthalmos is a developmental disorder of the eye characterized by an axial length of at least 2 standard deviations below the mean for age [1]. This condition is classified as simple, when presented as an isolated finding, or complex, when accompanied by other malformations such as colobomas, anterior segment dysgenesis, lens abnormalities, and posterior segment anomalies [1]. It may also appear as a syndrome with other systemic features. These malformations result from a variety of genetic defects that induce abnormalities in early ocular embryogenesis [9–13].

Nanophthalmos is a special subtype of microphthalmia, in which the eye, although small, has preserved functionality and organization (Figure 1) [13, 14]. It usually presents as a small hyperopic eye set into a deep orbit, with narrow palpebral fissures [15, 16]. A high hypermetropic refractive error is an invariable feature, ranging from +8.00 D sphere to +25.00 or higher [2, 17]. However, the diagnostic criteria vary widely across the literature and considering only one parameter is simplistic. Wu et al. considered shallow anterior chamber, high hyperopia, axial length up to 21 mm, and posterior wall thickness greater than 1.7 mm as conditions to define nanophthalmic eyes [18]. Similarly, Yalvac et al. considered the same characteristics (with axial length defined as less than 20.5 mm) as diagnostic criteria but also added the high lens/eye volume ratio [19].

Another diagnostic issue that has been debated in the literature is the distinction between nanophthalmos and posterior microphthalmos. Posterior microphthalmos is described as a subtype of microphthalmia, in which the axial length is shortened in the posterior segment only. In this condition, the anterior segment of the eye has normal depth and angle configuration. Some investigators consider that nanophthalmos and posterior microphthalmos are synonymous [20]. The report that the reduction of the corneal diameter in high hyperopia is proportional to the axial shortening of the eye supports the hypothesis that these entities represent manifestations of the spectrum of hyperopia, rather than two completely different conditions. In addition, the fact that mutations in the same genes may cause both posterior microphthalmos and nanophthalmos reinforces this idea [20, 21].

However, other groups point to the clinical and structural differences between these conditions, such as the cornea size and curvature, anterior chamber depth, lens thickness, angle characteristics, and propensity for complications [2, 3, 20]. Relhan et al. [2] biometrically analyzed eyes of 38 patients with high hyperopia (defined in the study as greater than +7.00 D spherical equivalent on refraction), all of them with an axial length equal or less than 20.5 mm. In this study, they defined the patients with corneal diameters below 11.0 mm as nanophthalmic and those with corneal diameters greater than or equal to 11.0 mm as posterior microphthalmos. They found that nanophthalmic eyes have shallow anterior chamber depth, thicker lens, and steeper cornea, in comparison with posterior microphthalmic eyes [2]. They also reported different tendencies to complications: the incidence of angle-closure glaucoma was 69.23% in the nanophthalmos group versus 0% in the posterior microphthalmos group, while the incidence of macular folds was 0% versus 24%, respectively [2].

In addition to these clinical features, nanophthalmic eyes have abnormal collagen fibrils in each of the three layers of the sclera [22]. These abnormal fibers are thought to be the cause for the increase scleral thickness as mentioned above (Figure 1). In addition, the combination of increased scleral thickness and abnormal collagen also contributes to its inelasticity, which impairs vortex venous drainage and reduces transcleral flow of proteins [22]. These histopathologic features and anatomy described above are thought to be the mechanism by which nanophthalmic eyes develop complications of angle-closure glaucoma, uveal effusion syndrome, and retinal detachment [19, 22–28]. However, it is unclear whether the abnormal scleral structure is a primary or secondary effect of the genetic changes that induce nanophthalmos as many of the genes implicated in this condition are expressed in retina and retinal pigment epithelium [14, 29–32].

Other ocular findings include topographic corneal steepening and irregular astigmatism [33], absent or rudimentary foveal avascular zone [34], optic disc drusen, retinoschisis and foveoschisis and retinitis pigmentosa (RP) [35, 36], crowded optic disk, chorioretinal folds, and retinal cysts [37], central retinal vein occlusion [38], increased subfoveal choroidal thickness [39], and abnormalities in the retinal layers' thickness and distribution [40, 41] (Figure 1).

In summary, the described anatomical features and histopathology of the nanophthalmic eye explain the severe visual consequences in individuals with nanophthalmos. If the axial hyperopia is not corrected in early childhood,

Table 2: Clinical spectrum of eye size phenotypes based on axial length [5] and anterior segment features by anterior chamber depth and white-to-white corneal diameter [6–8].

		Axial length		
		Short (<21 mm)	Average (24 mm)	Long (>27 mm)
Anterior segment	Small (WTW < 11 mm; ACD < 3.0 mm)	Microphthalmos and nanophthalmos	Relative anterior microphthalmos	Complex dysgenesis
	Average (WTW~11–12.5 mm; ACD~3.3 mm)	Hyperopia posterior microphthalmos	Normal	Myopia
	Large (WTW > 12.5 mm ACD > 3.3 mm)	Complex dysgenesis	Megalocornea	Infantile or congenital glaucoma myopia

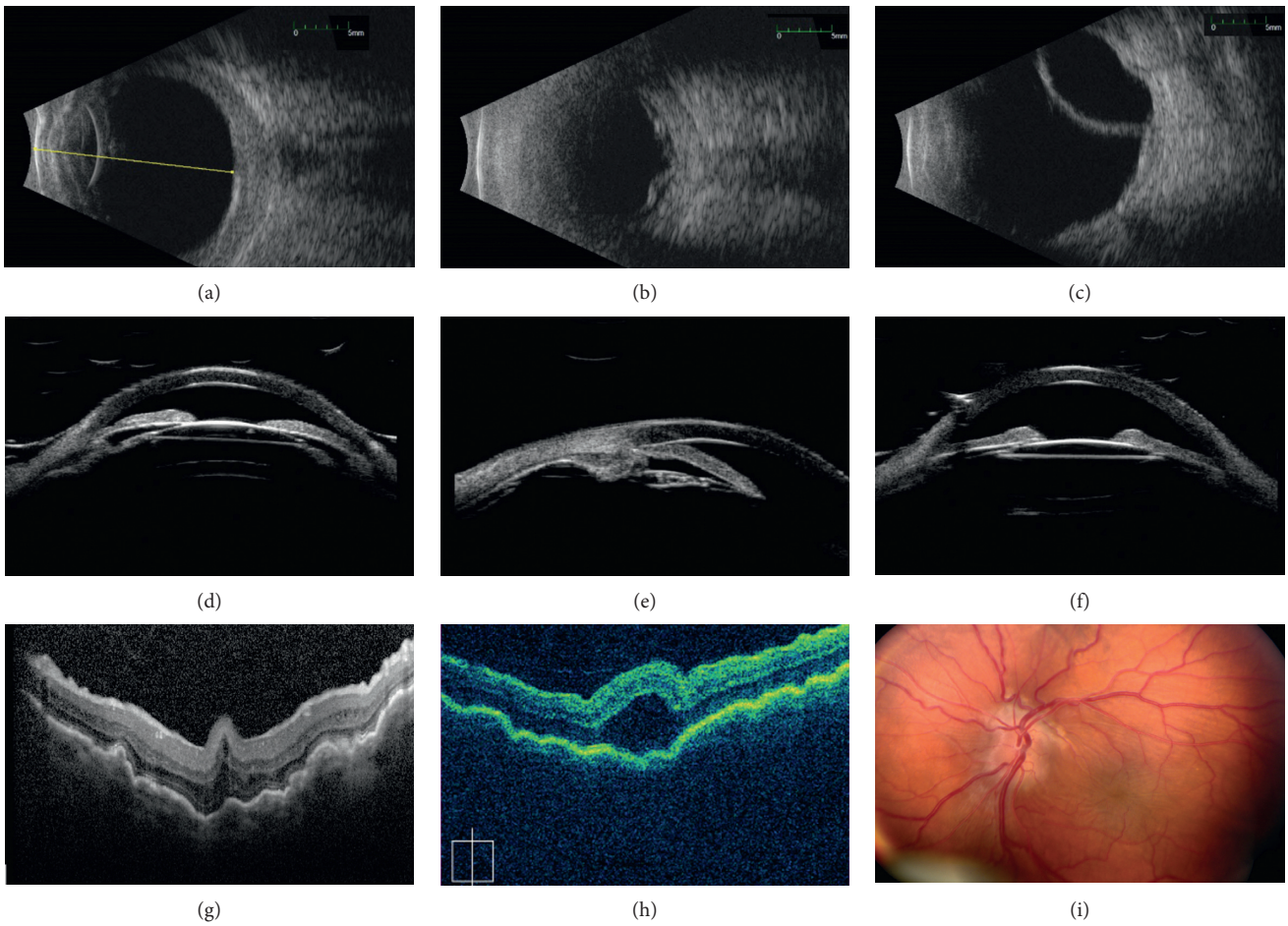

Figure 1: Typical ultrasonographic and retinal features of nanophthalmos. (a–c) B-scan ultrasounds showing features of nanophthalmos including short axial length, thickened sclera, and choroid (a), serous retinal detachment (b), and choroidal effusion (c). (d–f) Ultrasound biomicroscopy in a nanophthalmic eyes showing shallow anterior chamber (d), angle closure (e), and anterior rotation of the lens-iris diaphragm (f). (g) Heidelberg Spectralis OCT showing prominent choroidal and retinal folds in a small eye. (h) Zeiss Cirrus OCT showing foveoschisis and choroidal folds in a nanophthalmic eye. (i) Fundus photos in a patient with nanophthalmos and optic disc drusen, showing chorioretinal folds and crowded disc with mild vascular tortuousity.

then this results in irreversible amblyopia. The unrecognized and untreated angle-closure glaucoma can lead to progressive optic nerve damage and blindness [26]. Furthermore, intraocular surgeries in nanophthalmic eyes have significant risks and complications, both intraoperatively and postoperatively [3, 25, 42, 43]. Proper preoperative planning and anatomic understanding can lead to good outcomes and improved quality of life in these patients [18], despite a nearly 40–60% rate of intraoperative complications [4, 22, 44, 45].

4. Genetic Aspects of Nanophthalmos

Nanophthalmos occurs due to arrested development of the eye in the early stages of embryogenesis. It is thought to have a strong genetic basis. There are many reported familial cases

Table 3: Genes and phenotypes in nanophthalmos.

Gene (locus)	OMIM	Location	Inheritance	Gene expression (localization)	Gene function	Phenotypic characteristics of mutations
MFRP (NNO2)	606227	11q23.3	AR	RPE/CB (transmembrane)	Wnt signalling pathway effector	(i) Nanopthalmos, high hyperopia, and angle-closure glaucoma (ii) Retinitis pigmentosa, foveoschisis, and optic disc drusen syndrome
TMEM98 (NNO4)	615949	17q11.2	AD	RPE/CB/sclera (transmembrane)	Unknown	(i) High hyperopia, angle-closure glaucoma, and increased optic disc drusen
PRSS56 (MCOP6)	613858	2q37.1	AR	Retina/sclera (cytoplasmic)	Serine protease	(i) Nanophthalmos, angle-closure glaucoma, and high hyperopia (ii) Posterior microphthalmia
CRB1	604210	1q31.3	AR	Retina (transmembrane)	Controls cell polarity	(i) Nanophthalmos and retinitis pigmentosa (ii) Leber congenital amaurosis 8 (iii) Pigmented paravenous chorioretinal atrophy (iv) Retinitis pigmentosa
Best1/VMD2	607854	11q12	AD or AR	RPE/CB (transmembrane)	Chloride channel	(i) ADVIRC: autosomal-dominant vitreoretinochoroidopathy with nanophthalmos (ii) ARB: autosomal-recessive bestrophinopathy (iii) BVMD: best vitelliform macular dystrophy
Unknown (NNO3)	611897	2q11-q14	AD			(i) Microphthalmia, microcornea, and high hyperopia
Unknown (NNO1)	600165	11p12-11q13	AD			(i) High hyperopia, high lens/eye volume ratio, and angle-closure glaucoma

RPE: retinal pigment epithelium; CB: ciliary body.

with autosomal-dominant and recessive forms of inheritance [26, 30, 46, 47]. However, nanophthalmos can also occur as a sporadic condition [23, 28, 48, 49], which may represent either environmental effects or somatic or new mutations that result in arrest of ocular growth.

To date, five genetic loci (Table 3) were reported to be linked to nanophthalmos: NNOS 2 is related to mutations in membrane frizzled-related protein (*MFRP*); NNOS 4 is related to mutations in *TMEM98*; MCOP6 is related to mutations in serine protease 56 (*PRSS56*) [50, 51]; and NNOS 1 and 3 were localized to chromosomal regions only (11p12-11q13 and 2q11-q14) [26, 29, 30]. Two additional genes, *CRB1* and *BEST1* (*VMD2*), have been implicated in nanophthalmos (Table 3) and have profound roles in photoreceptor and retinal pigment epithelial (RPE) function, respectively.

4.1. Membrane-Type Frizzled-Related Protein Gene (MFRP). A significant number of cases of recessive nanophthalmos have been assigned to mutations in the membrane-type frizzled-related protein gene (*MFRP*, OMIM 606227) [29]. This gene is located in chromosome 11q23 and encodes a glycosylated transmembrane protein that has an extracellular frizzled-related cysteine-rich domain. Frizzled proteins are receptors involved in the regulation of growth, differentiation, and cell polarity during development through the Wnt signaling pathway [52, 53].

In humans, the *MFRP* gene is expressed in the retinal pigment epithelium and in the ciliary body [14, 29]. Outside of the eye, it can only be found at very low levels in the brain, likely accounting for the localized ocular phenotype in MFRP deficiency [29]. This gene seems to play an important role in both the ocular growth during childhood, functioning as a regulator of ocular size. It also has a role in maintenance of the RPE, which supports photoreceptor function [14, 54–56]. Mouse models of MFRP deficiency, such as rd6 ($Mfrp^{rd6}$) and rdx ($Mfrp^{174delG}$) mice, have flecked retina disorders and photoreceptor degeneration, supporting the importance of this gene for retinal and RPE physiology [57–60].

The link between eye size and RPE/ciliary body function has yet to be elucidated. It has been proposed that MFRP affects the physiologic mechanism of emmetropization, in which the refractive error is corrected by postnatal axial growth during the first six years of life [14]. Soundrarajan suggested that a complex regulatory network may influence the postnatal eye development and indicated the participation of another gene (*PRSS56*) in the same pathway [61]. Besides these, other proposed mechanisms for the role of the RPE/ciliary body in eye size include the mechanical stress effects and the inflammatory response observed in the retina [14, 62, 63]. Most recently, Velez et al. [64] found that introducing a normal copy of *Mfrp* gene through adenoviral-based gene therapy may reverse some of these pathogenic changes in Mfrp *rd6*/*rd6* mice. Specifically, subretinal injection of this vector resulted in rescue of photoreceptor death, normalization of retinal function, and regulation of eye length in adult mice. These findings suggest that gene therapy may be a viable option for this disease.

Mouse models of *Mfrp* loss-of-function have failed to demonstrate the full nanophthalmic phenotype observed in

humans and instead present with predominant retinal degeneration [57–60]. This may be in part due to the differences in the lens size and ocular anatomy in mice and humans. Collery et al. proposed a new model using zebrafish (*Danio rerio*) that better mimics the human phenotype and may be useful in studying and better understanding this condition [62].

To date, several cases of MFRP mutations leading to reduced eye axial length have been reported. According to Wasmann et al. [65], by the time of the publication in 2014, there were 14 different described *MFRP* mutations: two of them were single amino acid substitutions at extremely conserved sites and 12 caused severe truncation of the protein. Since that time, three new mutations have been described [55], and additional known mutations have been reported in other populations [36, 66]. All of these cases presented with high hyperopia, but the effect of the mutation on retinal rod photoreceptor function was different between individuals, and the clinical spectrum of age of onset and severity of disease was quite variable [65]. The reason for this clinical variability may be a combination of the spectrum of genetic mutations in *MFRP* and other genetic or environmental modifiers that remain to be determined [67].

Wasmann et al. reported a case of two sisters with confirmed *MFRP* mutations. They both presented low visual acuity, high hyperopia, macular retinal folds, with the older sibling also having thickened sclera, and optic nerve head drusen [65]. The mutations in the *MFRP* gene have also been linked to the autosomal-recessive syndrome of posterior microphthalmos, retinitis pigmentosa, foveoschisis, and optic disc drusen [29, 35, 66–68]. These results represent the broad clinical spectrum of *MFRP* mutations, which occurs likely due to differences in early gene expression and environmental factors that shape the development of the eye.

4.2. Transmembrane Protein 98 Gene (TMEM98). The transmembrane protein 98 (*TMEM98*, OMIM 615949) gene encodes a transmembrane protein that is universally expressed in the human body, including in the ocular tissues, such as iris, choroid, retinal pigment epithelium, and sclera. Its specific function still remains unclear, but it is hypothesized to lead to pathologic scleral pathologic thickening and secondary glaucoma development in nanophthalmic eyes or play a role in the development of the RPE [30, 31].

In a large pedigree, Awadalla and coworkers found a missense mutation in the *TMEM98* (A193P) that could be associated with autosomal-dominant nanophthalmos [30]. Although its pathogenic relationship with the disease was not clear, this association has been greatly strengthened by Khorram and colleagues' recent report of two novel *TMEM98* mutations (His196Pro and c.694_721delAG AATGAAGACTGGATCGAAGATGCCTCgtaagg) in autosomal-dominant nanophthalmic patients [31]. Additional studies are still needed to identify the specific role of this gene in the pathogenesis of nanophthalmos.

4.3. Protease Serine 56 (PRSS56). *PRSS56*, also known as LOC646960, is located in the chromosome 2q37.1 and encodes a protein of 603 amino acids, which functions as a serine protease. It is suggested that it is expressed in the embryonic tissue, brain, testis, and eye [50]. There are reports of its association with nanophthalmos and posterior microphthalmos cases [21, 50, 69] although its physiologic and pathogenic mechanisms remain to be fully determined [21].

It has been reported that *PRSS56* is highly expressed in retinal ganglion cells of adult animals [50], and its presence in this tissue and in the brain cells suggest its relevance in the regulation of ocular development [69]. Nair et al. [51] demonstrated this role in the homozygous mutant mice $Prss56^{Grm4}$, which showed shortened axial length and higher susceptibility to angle closure. Furthermore, they found that the differences in ocular size between mutant mice and wild-type controls were progressively greater after birth, with no significant difference prior to that time [51]. They found that the genetic background had a strong influence of magnitude of eye size differences between wild-type and mutant mice, suggesting the existence of genetic modifiers that influence eye growth in concert with *Prss56*. Soundararajan et al. also suggested that PRSS56 and MFRP may function through a common biological pathway that affects the emmetropization process, but nature of this interaction is still unclear [61].

4.4. Crumbs Homologue 1 Gene (CRB1). Human *CRB1* is a 1406 amino acids transmembrane protein that localizes to photoreceptor inner segments and is vital for the neuronal development of the retina [70, 71]. The *CRB1* gene is located in chromosome 1, in the interval 1q31.2-1q32.1, and its mutations are classically associated with various heritable retinal dystrophies, including Leber Congenital Amaurosis [70, 72, 73]. Furthermore, some recent reports showed association of mutation in *CRB1* with nanophthalmos and retinitis pigmentosa [74, 75].

4.5. Bestrophin 1 (BEST1/VMD2). The *BEST1 (VMD2)* gene is located on chromosome 11q12 and is primarily expressed in the RPE [32]. It encodes an integral membrane protein, bestrophin 1, localized predominantly in the basolateral plasma membrane of the RPE and most prominently near the macula [76, 77]. *BEST1* mutations are classically associated with Best vitelliform macular dystrophy (BVMD), a disease restricted to the macula. However, it has been reported to be in association with other widespread ocular abnormalities, such as autosomal-dominant vitreoretinochoroidopathy (ADVIRC) and autosomal-recessive bestrophinopathy (ARB), which are both associated with nanophthalmos [76]. Other studies also strongly suggest an association between *BEST1* mutations and angle-closure glaucoma [77, 78].

ADVIRC is a rare condition characterized by a peripheral circumferential hyperpigmented band with punctate white opacities in the retina, chorioretinal atrophy in the midperipheral or peripapillary retina, and vitreous fibrillary condensations [76, 79]. There are reports of association of this condition with nanophthalmos and a higher incidence of angle-closure glaucoma [79, 80].

ARB is also a rare condition characterized by macular and midperipheral subretinal whitish to yellowish deposits

that may become scars and lead to decrease in visual acuity [81–83]. Patients are usually hyperopic and have a shallow anterior chamber and a higher propensity to angle-closure glaucoma [81–85].

4.6. Other Loci for Nanophthalmos. The autosomal-dominant nanophthalmos NNO1 (OMIM 600165) is caused by a defect on chromosome 11, between D11S905 and D11S987. This region may also be associated with severity of angle-closure glaucoma manifestations [26]. The precise genetic change at this locus has yet to be confirmed, though coding and regulatory mutations in BEST1 have been excluded as a cause (data not shown). Another form of autosomal-dominant disease, NNO3 (OMIM 611897), was described in a family with simple microphthalmia, microcornea, and high hyperopia, and it was reported to be linked to chromosome 2q11-14 [86].

5. Conclusion

With the progress of the imaging and surgical technologies, there have been significant advances in the diagnosis and management of the nanophthalmic eye. These have improved outcomes for individuals with such challenging eyes. Furthermore, substantial new discoveries in the genetics of nanophthalmos have led to the discovery of many new genes and pathways in the pathogenesis of this condition. These advances will ultimately improve early detection of this condition and provide novel avenues for treatment, including the possibility for gene therapy. Genetic diagnoses will facilitate genetic counseling for familial forms of this condition and may help to decrease amblyopia from uncorrected hyperopia, prevent vision loss from complications, and improve monitoring to minimize glaucoma and retinal complications from nanophthalmos.

Conflicts of Interest

The authors declare that they have no conflicts of interest.

Acknowledgments

This work was supported in part by a Career Starter Award from the Knights Templar Eye Foundation to Lev Prasov. The authors thank the clinicians and the photographers who participated in the care of these patients at the Kellogg Eye Center at the University of Michigan.

References

[1] M. J. Elder, "Aetiology of severe visual impairment and blindness in microphthalmos," *British Journal of Ophthalmology*, vol. 78, no. 5, pp. 332–334, 1994.

[2] N. Relhan, S. Jalali, N. Pehre, H. L. Rao, U. Manusani, and L. Bodduluri, "High-hyperopia database, part I: clinical characterisation including morphometric (biometric) differentiation of posterior microphthalmos from nanophthalmos," *Eye*, vol. 30, no. 1, pp. 120–126, 2016.

[3] R. S. Hoffman, A. R. Vasavada, Q. B. Allen et al., "Cataract surgery in the small eye," *Journal of Cataract and Refractive Surgery*, vol. 41, no. 11, pp. 2565–2575, 2015.

[4] S. Rajendrababu, N. Babu, S. Sinha et al., "A randomized controlled trial comparing outcomes of cataract surgery in nanophthalmos with and without prophylactic sclerostomy," *American Journal of Ophthalmology*, vol. 183, pp. 125–133, 2017.

[5] M. De Bernardo, L. Zeppa, R. Forte et al., "Can we use the fellow eye biometric data to predict IOL power?," *Seminars in Ophthalmology*, vol. 32, no. 3, pp. 363–370, 2017.

[6] G. U. Auffarth, M. Blum, U. Faller, M. R. Tetz, and H. E. Volcker, "Relative anterior microphthalmos: morphometric analysis and its implications for cataract surgery," *Ophthalmology*, vol. 107, no. 8, pp. 1555–1560, 2000.

[7] M. Khairallah, R. Messaoud, S. Zaouali, S. Ben Yahia, A. Ladjimi, and S. Jenzri, "Posterior segment changes associated with posterior microphthalmos," *Ophthalmology*, vol. 109, no. 3, pp. 569–574, 2002.

[8] I. Guber, C. Bergin, S. Perritaz, and F. Majo, "Correcting interdevice bias of horizontal white-to-white and sulcus-to-sulcus measures used for implantable collamer lens sizing," *American Journal of Ophthalmology*, vol. 161, pp. 116–125 e1, 2016.

[9] A. M. Slavotinek, "Eye development genes and known syndromes," *Molecular Genetics and Metabolism*, vol. 104, no. 4, pp. 448–456, 2011.

[10] T. M. Bardakjian and A. Schneider, "The genetics of anophthalmia and microphthalmia," *Current Opinion in Ophthalmology*, vol. 22, no. 5, pp. 309–313, 2011.

[11] D. R. Fitzpatrick and V. van Heyningen, "Developmental eye disorders," *Current Opinion in Genetics and Development*, vol. 15, no. 3, pp. 348–353, 2005.

[12] M. Warburg, "Classification of microphthalmos and coloboma," *Journal of Medical Genetics*, vol. 30, no. 8, pp. 664–669, 1993.

[13] A. S. Verma and D. R. Fitzpatrick, "Anophthalmia and microphthalmia," *Orphanet Journal of Rare Diseases*, vol. 2, p. 47, 2007.

[14] O. H. Sundin, S. Dharmaraj, I. A. Bhutto et al., "Developmental basis of nanophthalmos: MFRP is required for both prenatal ocular growth and postnatal emmetropization," *Ophthalmic Genetics*, vol. 29, no. 1, pp. 1–9, 2008.

[15] O. S. Singh, R. J. Simmons, R. J. Brockhurst, and C. L. Trempe, "Nanophthalmos: a perspective on identification and therapy," *Ophthalmology*, vol. 89, no. 9, pp. 1006–1012, 1982.

[16] A. K. Altintaş, M. A. Acar, I. S. Yalvaç, I. Koçak, A. Nurözler, and S. Duman, "Autosomal recessive nanophthalmos," *Acta Ophthalmologica Scandinavica*, vol. 75, no. 3, pp. 325–328, 1997.

[17] A. O. Khan, "Posterior microphthalmos versus nanophthalmos," *Ophthalmic Genetics*, vol. 29, no. 4, p. 189, 2008.

[18] W. Wu, D. G. Dawson, A. Sugar et al., "Cataract surgery in patients with nanophthalmos: results and complications," *Journal of Cataract and Refractive Surgery*, vol. 30, no. 3, pp. 584–590, 2004.

[19] I. S. Yalvac, B. Satana, G. Ozkan, U. Eksioglu, and S. Duman, "Management of glaucoma in patients with nanophthalmos," *Eye*, vol. 22, no. 6, pp. 838–843, 2008.

[20] S. R. Nowilaty, A. O. Khan, M. A. Aldahmesh, K. F. Tabbara, A. Al-Amri, and F. S. Alkuraya, "Biometric and molecular characterization of clinically diagnosed posterior microphthalmos," *American Journal of Ophthalmology*, vol. 155, no. 2, pp. 361–372.e7, 2013.

[21] M. B. Said, E. Chouchène, S. B. Salem et al., "Posterior microphthalmia and nanophthalmia in Tunisia caused by a founder c.1059_1066insC mutation of the PRSS56 gene," *Gene*, vol. 528, no. 2, pp. 288–294, 2013.

[22] A. Yamani, I. Wood, I. Sugino, M. Wanner, and M. A. Zarbin, "Abnormal collagen fibrils in nanophthalmos: a clinical and histologic study," *American Journal of Ophthalmology*, vol. 127, no. 1, pp. 106–108, 1999.

[23] Y. M. Buys and C. J. Pavlin, "Retinitis pigmentosa, nanophthalmos, and optic disc drusen: a case report," *Ophthalmology*, vol. 106, no. 3, pp. 619–622, 1999.

[24] A. Neelakantan, P. Venkataramakrishnan, B. S. Rao et al., "Familial nanophthalmos: management and complications," *Indian Journal of Ophthalmology*, vol. 42, no. 3, pp. 139–143, 1994.

[25] E. Areiter, M. Neale, and S. M. Johnson, "Spectrum of angle closure, uveal effusion syndrome, and nanophthalmos," *Journal of Current Glaucoma Practice*, vol. 10, no. 3, pp. 113–117, 2016.

[26] M. I. Othman, S. A. Sullivan, G. L. Skuta et al., "Autosomal dominant nanophthalmos (NNO1) with high hyperopia and angle-closure glaucoma maps to chromosome 11," *American Journal of Human Genetics*, vol. 63, no. 5, pp. 1411–1418, 1998.

[27] N. Kara, O. Baz, H. Altinkaynak, C. Altan, and A. Demirok, "Assessment of the anterior chamber angle in patients with nanophthalmos: an anterior segment optical coherence tomography study," *Current Eye Research*, vol. 38, no. 5, pp. 563–568, 2013.

[28] A. K. Mandal, T. Das, and V. K. Gothwal, "Angle closure glaucoma in nanophthalmos and pigmentary retinal dystrophy: a rare syndrome," *Indian Journal of Ophthalmology*, vol. 49, no. 4, pp. 271-272, 2001.

[29] O. H. Sundin, G. S. Leppert, E. D. Silva et al., "Extreme hyperopia is the result of null mutations in MFRP, which encodes a frizzled-related protein," *Proceedings of the National Academy of Sciences of the United States of America*, vol. 102, no. 27, pp. 9553–9558, 2005.

[30] M. S. Awadalla, K. P. Burdon, E. Souzeau et al., "Mutation in TMEM98 in a large white kindred with autosomal dominant nanophthalmos linked to 17p12-q12," *JAMA Ophthalmology*, vol. 132, no. 8, pp. 970–977, 2014.

[31] D. Khorram, M. Choi, B. R. Roos et al., "Novel TMEM98 mutations in pedigrees with autosomal dominant nanophthalmos," *Molecular Vision*, vol. 21, pp. 1017–1023, 2015.

[32] K. Petrukhin, M. J. Koisti, B. Bakall et al., "Identification of the gene responsible for Best macular dystrophy," *Nature Genetics*, vol. 19, no. 3, pp. 241–247, 1998.

[33] S. Srinivasan, M. Batterbury, I. B. Marsh, A. C. Fisher, C. Willoughby, and S. B. Kaye, "Corneal topographic features in a family with nanophthalmos," *Cornea*, vol. 25, no. 6, pp. 750–756, 2006.

[34] M. K. Walsh and M. F. Goldberg, "Abnormal foveal avascular zone in nanophthalmos," *American Journal of Ophthalmology*, vol. 143, no. 6, pp. 1067-1068, 2007.

[35] J. Crespí, J. A. Buil, F. Bassaganyas et al., "A novel mutation confirms MFRP as the gene causing the syndrome of nanophthalmos–renititis pigmentosa–foveoschisis–optic disk drusen," *American Journal of Ophthalmology*, vol. 146, no. 2, pp. 323–328, 2008.

[36] L. C. Zacharias, R. Susanna, O. Sundin, S. Finzi, B. N. Susanna, and W. Y. Takahashi, "Efficacy of topical dorzolamide therapy for cystoid macular edema in a patient with MFRP-related nanophthalmos–retinitis pigmentosa–foveoschisis–optic disk drusen syndrome," *Retinal Cases and Brief Reports*, vol. 9, no. 1, pp. 61–63, 2015.

[37] C. J. MacKay, M. S. Shek, R. E. Carr, L. A. Yanuzzi, and P. Gouras, "Retinal degeneration with nanophthalmos, cystic macular degeneration, and angle closure glaucoma. A new recessive syndrome," *Archives of Ophthalmology*, vol. 105, no. 3, pp. 366–371, 1987.

[38] A. A. Albar, S. R. Nowilaty, and N. G. Ghazi, "Nanophthalmos and hemiretinal vein occlusion: a case report," *Saudi Journal of Ophthalmology*, vol. 29, no. 1, pp. 89–91, 2015.

[39] A. Demircan, C. Altan, O. A. Osmanbasoglu, U. Celik, N. Kara, and A. Demirok, "Subfoveal choroidal thickness measurements with enhanced depth imaging optical coherence tomography in patients with nanophthalmos," *British Journal of Ophthalmology*, vol. 98, no. 3, pp. 345–349, 2014.

[40] H. Xiao, X. Guo, Y. Zhong, and X. Liu, "Retinal and choroidal changes of nanophthalmic eyes with and without secondary glaucoma," *Retina*, vol. 35, no. 10, pp. 2121–2129, 2015.

[41] F. Helvacioglu, Z. Kapran, S. Sencan, M. Uyar, and O. Cam, "Optical coherence tomography of bilateral nanophthalmos with macular folds and high hyperopia," *Case Reports in Ophthalmological Medicine*, vol. 2014, Article ID 173853, 3 pages, 2014.

[42] J. S. Chang, J. C. Ng, V. K. Chan, and A. K. Law, "Cataract surgery with a new fluidics control phacoemulsification system in nanophthalmic eyes," *Case Reports in Ophthalmology*, vol. 7, no. 3, pp. 218–226, 2016.

[43] S. Srinivasan, "Small eyes-big problems," *Journal of Cataract and Refractive Surgery*, vol. 41, no. 11, pp. 2345-2346, 2015.

[44] G. Carifi, F. Safa, F. Aiello, C. Baumann, and V. Maurino, "Cataract surgery in small adult eyes," *British Journal of Ophthalmology*, vol. 98, no. 9, pp. 1261–1265, 2014.

[45] H. Singh, J. C. Wang, D. C. Desjardins, K. Baig, S. Gagné, and I. I. Ahmed, "Refractive outcomes in nanophthalmic eyes after phacoemulsification and implantation of a high-refractive-power foldable intraocular lens," *Journal of Cataract and Refractive Surgery*, vol. 41, no. 11, pp. 2394–2402, 2015.

[46] S. Moradian, A. Kanani, and H. Esfandiari, "Nanophthalmos," *Journal of Ophthalmic and Vision Research*, vol. 6, no. 2, pp. 145-146, 2011.

[47] M. Martorina, "Familial nanophthalmos," *Journal Français D'Ophtalmologie*, vol. 11, no. 4, pp. 357–361, 1988.

[48] S. Ghose, M. S. Sachdev, and H. Kumar, "Bilateral nanophthalmos, pigmentary retinal dystrophy, and angle closure glaucoma—a new syndrome?," *British Journal of Ophthalmology*, vol. 69, no. 8, pp. 624–628, 1985.

[49] H. Proença, A. Castanheira-Dinis, and M. Monteiro-Grillo, "Bilateral nanophthalmos and pigmentary retinal dystrophy–an unusual syndrome," *Graefe's Archive for Clinical and Experimental Ophthalmology*, vol. 244, no. 9, pp. 1203–1205, 2006.

[50] A. Gal, I. Rau, L. El Matri et al., "Autosomal-recessive posterior microphthalmos is caused by mutations in PRSS56, a gene encoding a trypsin-like serine protease," *American Journal of Human Genetics*, vol. 88, no. 3, pp. 382–390, 2011.

[51] K. S. Nair, M. Hmani-Aifa, Z. Ali et al., "Alteration of the serine protease PRSS56 causes angle-closure glaucoma in mice and posterior microphthalmia in humans and mice," *Nature Genetics*, vol. 43, no. 6, pp. 579–584, 2011.

[52] P. Bhanot, M. Brink, C. H. Samos et al., "A new member of the frizzled family from drosophila functions as a wingless receptor," *Nature*, vol. 382, no. 6588, pp. 225–230, 1996.

[53] M. Katoh, "Molecular cloning and characterization of MFRP, a novel gene encoding a membrane-type frizzled-related protein," *Biochemical and Biophysical Research Communications*, vol. 282, no. 1, pp. 116–123, 2001.

[54] M. Mameesh, A. Ganesh, B. Harikrishna et al., "Co-inheritance of the membrane frizzled-related protein ocular phenotype and glycogen storage disease type Ib," *Ophthalmic Genetics*, vol. 38, no. 6, pp. 1–5, 2017.

[55] R. Mukhopadhyay, P. I. Sergouniotis, D. S. Mackay et al., "A detailed phenotypic assessment of individuals affected by MFRP-related oculopathy," *Molecular Vision*, vol. 16, pp. 540–548, 2010.

[56] M. N. Mandal, V. Vasireddy, M. M. Jablonski et al., "Spatial and temporal expression of MFRP and its interaction with CTRP5," *Investigative Ophthalmology and Visual Science*, vol. 47, no. 12, pp. 5514–5521, 2006.

[57] S. Kameya, N. L. Hawes, B. Chang, J. R. Heckenlively, J. K. Naggert, and P. M. Nishina, "Mfrp, a gene encoding a frizzled related protein, is mutated in the mouse retinal degeneration 6," *Human Molecular Genetics*, vol. 11, no. 16, pp. 1879–1886, 2002.

[58] J. Fogerty and J. C. Besharse, "174delG mutation in mouse MFRP causes photoreceptor degeneration and RPE atrophy," *Investigative Ophthalmology and Visual Science*, vol. 52, no. 10, pp. 7256–7266, 2011.

[59] N. L. Hawes, B. Chang, G. S. Hageman et al., "Retinal degeneration 6 (rd6): a new mouse model for human retinitis punctata albescens," *Investigative Ophthalmology and Visual Science*, vol. 41, no. 10, pp. 3149–3157, 2000.

[60] O. H. Sundin, "The mouse's eye and Mfrp: not quite human," *Ophthalmic Genetics*, vol. 26, no. 4, pp. 153–155, 2005.

[61] R. Soundararajan, J. Won, T. M. Stearns et al., "Gene profiling of postnatal Mfrprd6 mutant eyes reveals differential accumulation of Prss56, visual cycle and phototransduction mRNAs," *PLoS One*, vol. 9, no. 10, article e110299, 2014.

[62] R. F. Collery, P. J. Volberding, J. R. Bostrom, B. A. Link, and J. C. Besharse, "Loss of zebrafish Mfrp causes nanophthalmia, hyperopia, and accumulation of subretinal macrophages," *Investigative Ophthalmology and Visual Science*, vol. 57, no. 15, pp. 6805–6814, 2016.

[63] P. Wang, Z. Yang, S. Li, X. Xiao, X. Guo, and Q. Zhang, "Evaluation of MFRP as a candidate gene for high hyperopia," *Molecular Vision*, vol. 15, pp. 181–186, 2009.

[64] G. Velez, S. H. Tsang, Y. T. Tsai et al., "Gene therapy restores Mfrp and corrects axial eye length," *Scientific Reports*, vol. 7, no. 1, p. 16151, 2017.

[65] R. A. Wasmann, J. S. Wassink-Ruiter, O. H. Sundin, E. Morales, J. B. Verheij, and J. W. Pott, "Novel membrane frizzled-related protein gene mutation as cause of posterior microphthalmia resulting in high hyperopia with macular folds," *Acta Ophthalmologica*, vol. 92, no. 3, pp. 276–281, 2014.

[66] A. Neri, R. Leaci, J. C. Zenteno, C. Casubolo, E. Delfini, and C. Macaluso, "Membrane frizzled-related protein gene-related ophthalmological syndrome: 30-month follow-up of a sporadic case and review of genotype-phenotype correlation in the literature," *Molecular Vision*, vol. 18, pp. 2623–2632, 2012.

[67] R. Ayala-Ramirez, F. Graue-Wiechers, V. Robredo, M. Amato-Almanza, I. Horta-Diez, and J. C. Zenteno, "A new autosomal recessive syndrome consisting of posterior microphthalmos, retinitis pigmentosa, foveoschisis, and optic disc drusen is caused by a MFRP gene mutation," *Molecular Vision*, vol. 12, pp. 1483–1489, 2006.

[68] J. C. Zenteno, B. Buentello-Volante, M. A. Quiroz-González, and M. A. Quiroz-Reyes, "Compound heterozygosity for a novel and a recurrent MFRP gene mutation in a family with the nanophthalmos-retinitis pigmentosa complex," *Molecular Vision*, vol. 15, pp. 1794–1798, 2009.

[69] A. Orr, M. P. Dubé, J. C. Zenteno et al., "Mutations in a novel serine protease PRSS56 in families with nanophthalmos," *Molecular Vision*, vol. 17, pp. 1850–1861, 2011.

[70] A. J. Lotery, S. G. Jacobson, G. A. Fishman et al., "Mutations in the CRB1 gene cause Leber congenital amaurosis," *Archives of Ophthalmology*, vol. 119, no. 3, pp. 415–420, 2001.

[71] S. G. Jacobson, A. V. Cideciyan, T. S. Aleman et al., "Crumbs homolog 1 (CRB1) mutations result in a thick human retina with abnormal lamination," *Human Molecular Genetics*, vol. 12, no. 9, pp. 1073–1078, 2003.

[72] A. I. den Hollander, J. R. Heckenlively, L. I. van den Born et al., "Leber congenital amaurosis and retinitis pigmentosa with Coats-like exudative vasculopathy are associated with mutations in the crumbs homologue 1 (CRB1) gene," *American Journal of Human Genetics*, vol. 69, no. 1, pp. 198–203, 2001.

[73] H. Abouzeid, Y. Li, I. H. Maumenee, S. Dharmaraj, and O. Sundin, "A G1103R mutation in CRB1 is co-inherited with high hyperopia and Leber congenital amaurosis," *Ophthalmic Genetics*, vol. 27, no. 1, pp. 15–20, 2006.

[74] C. C. Paun, B. J. Pijl, A. M. Siemiatkowska et al., "A novel crumbs homolog 1 mutation in a family with retinitis pigmentosa, nanophthalmos, and optic disc drusen," *Molecular Vision*, vol. 18, pp. 2447–2453, 2012.

[75] J. C. Zenteno, B. Buentello-Volante, R. Ayala-Ramirez, and C. Villanueva-Mendoza, "Homozygosity mapping identifies the Crumbs homologue 1 (Crb1) gene as responsible for a recessive syndrome of retinitis pigmentosa and nanophthalmos," *American Journal of Medical Genetics Part A*, vol. 155A, no. 5, pp. 1001–1006, 2011.

[76] C. J. Boon, B. J. Klevering, B. P. Leroy, C. B. Hoyng, J. E. Keunen, and A. I. den Hollander, "The spectrum of ocular phenotypes caused by mutations in the BEST1 gene," *Progress in Retinal and Eye Research*, vol. 28, no. 3, pp. 187–205, 2009.

[77] L. Toto, C. J. Boon, L. Di Antonio et al., "Bestrophinopathy: a spectrum of ocular abnormalities caused by the c.614T>C mutation in the BEST1 gene," *Retina*, vol. 36, no. 8, pp. 1586–1595, 2016.

[78] E. Wittström, V. Ponjavic, M. L. Bondeson, and S. Andréasson, "Anterior segment abnormalities and angle-closure glaucoma in a family with a mutation in the BEST1 gene and Best vitelliform macular dystrophy," *Ophthalmic Genetics*, vol. 32, no. 4, pp. 217–227, 2011.

[79] J. Yardley, B. P. Leroy, N. Hart-Holden et al., "Mutations of VMD2 splicing regulators cause nanophthalmos and autosomal dominant vitreoretinochoroidopathy (ADVIRC)," *Investigative Ophthalmology and Visual Science*, vol. 45, no. 10, pp. 3683–3689, 2004.

[80] B. A. Lafaut, B. Loeys, B. P. Leroy, W. Spileers, J. J. De Laey, and P. Kestelyn, "Clinical and electrophysiological findings in autosomal dominant vitreoretinochoroidopathy: report of a new pedigree," *Graefe's Archive for Clinical and Experimental Ophthalmology*, vol. 239, no. 8, pp. 575–582, 2001.

[81] R. Burgess, I. D. Millar, B. P. Leroy et al., "Biallelic mutation of BEST1 causes a distinct retinopathy in humans," *American Journal of Human Genetics*, vol. 82, no. 1, pp. 19–31, 2008.

[82] R. Burgess, R. E. MacLaren, A. E. Davidson et al., "ADVIRC is caused by distinct mutations in BEST1 that alter pre-mRNA splicing," *Journal of Medical Genetics*, vol. 46, no. 9, pp. 620–625, 2009.

[83] C. J. Boon, L. I. van den Born, L. Visser et al., "Autosomal recessive bestrophinopathy: differential diagnosis and treatment options," *Ophthalmology*, vol. 120, no. 4, pp. 809–820, 2013.

[84] A. E. Davidson, P. I. Sergouniotis, R. Burgess-Mullan et al., "A synonymous codon variant in two patients with autosomal recessive bestrophinopathy alters in vitro splicing of BEST1," *Molecular Vision*, vol. 16, pp. 2916–2922, 2010.

[85] C. Crowley, R. Paterson, T. Lamey et al., "Autosomal recessive bestrophinopathy associated with angle-closure glaucoma," *Documenta Ophthalmologica*, vol. 129, no. 1, pp. 57–63, 2014.

[86] H. Li, J. X. Wang, C. Y. Wang et al., "Localization of a novel gene for congenital nonsyndromic simple microphthalmia to chromosome 2q11-14," *Human Genetics*, vol. 122, no. 6, pp. 589–593, 2008.

Hindawi
Journal of Ophthalmology
Volume 2018, Article ID 5706142, 10 pages
https://doi.org/10.1155/2018/5706142

Research Article

Mutation Spectrum of the *ABCA4* Gene in a Greek Cohort with Stargardt Disease: Identification of Novel Mutations and Evidence of Three Prevalent Mutated Alleles

Kamakari Smaragda[1], **Kokkinou Vassiliki**[1], **Koutsodontis George**[1], **Stamatiou Polixeni**[1], **Giatzakis Christoforos**[2], **Anastasakis Anastasios**[3], **Aslanides Ioannis Minas**[4], **Koukoula Stavrenia**[5], **Panagiotoglou Theoni**[6], **Datseris Ioannis**[7] and **Tsilimbaris K. Miltiadis**[6]

[1]*Ophthalmic Genetics Unit, OMMA Ophthalmological Institute of Athens, Athens, Greece*
[2]*DNAbiolab, Cretan Center for Research and Development of Applications on Genetics and Molecular Biology, Heraklion, Crete, Greece*
[3]*Department of Clinical Electrophysiology of Vision, Athens Eye Hospital, Glyfada, Athens, Greece*
[4]*Department of Ophthalmology, Emmetropia Mediterranean Eye Institute, Heraklion, Crete, Greece*
[5]*Ophthalmica Institute of Ophthalmology and Microsurgery, Thessaloniki, Greece*
[6]*Department of Ophthalmology, University of Crete School of Medicine, Heraklion, Greece*
[7]*Department of Retinal Disorders, OMMA Ophthalmological Institute of Athens, Athens, Greece*

Correspondence should be addressed to Kamakari Smaragda; kamakari@hotmail.gr

Received 14 December 2017; Accepted 15 February 2018; Published 30 April 2018

Academic Editor: Robert B. Hufnagel

Aim. To evaluate the frequency and pattern of disease-associated mutations of *ABCA4* gene among Greek patients with presumed Stargardt disease (STGD1). *Materials and Methods*. A total of 59 patients were analyzed for *ABCA4* mutations using the ABCR400 microarray and PCR-based sequencing of all coding exons and flanking intronic regions. MLPA analysis as well as sequencing of two regions in introns 30 and 36 reported earlier to harbor deep intronic disease-associated variants was used in 4 selected cases. *Results*. An overall detection rate of at least one mutant allele was achieved in 52 of the 59 patients (88.1%). Direct sequencing improved significantly the complete characterization rate, that is, identification of two mutations compared to the microarray analysis (93.1% versus 50%). In total, 40 distinct potentially disease-causing variants of the *ABCA4* gene were detected, including six previously unreported potentially pathogenic variants. Among the disease-causing variants, in this cohort, the most frequent was c.5714+5G>A representing 16.1%, while p.Gly1961Glu and p.Leu541Pro represented 15.2% and 8.5%, respectively. *Conclusions*. By using a combination of methods, we completely molecularly diagnosed 48 of the 59 patients studied. In addition, we identified six previously unreported, potentially pathogenic *ABCA4* mutations.

1. Introduction

Stargardt disease (STGD1, OMIM 248200) is a juvenile-onset form of macular dystrophy (MD) [1]. It is inherited mainly in an autosomal recessive manner and is one of the most frequent causes of MD in childhood [2]. The disease is characterized by loss of photoreceptor cells in the macula and affects 1 in 10,000 individuals [3]. STGD1 is associated with the appearance of orange-yellow flecks around the macula and accumulation of lipofuscin—a combination of fluorescent by-products of the visual cycle—in the choroid. This accumulation appears to have toxic effects on the retinal pigment epithelium [4].

Mutations in the *ABCA4* (gene ID: 24; OMIM: 601691) gene have been described in *ABCA4*-associated retinopathies, including STGD1, cone-rod dystrophy (CRD), retinitis pigmentosa (RP), and retinal dystrophy [1, 5]. *ABCA4* is a large

gene that consists of 50 exons located in chromosome 1p13. It is a member of the subfamily A of the ATP-binding cassette (ABC) transporters that is expressed in the retinal photoreceptors. This gene is involved in the transport and clearance of all-transretinal aldehyde, a by-product of the retinoid cycle of vision, and other essential molecules across the disc membrane into the cytoplasm [6–8]. It is the only gene whose mutations are known to be associated with autosomal recessive STGD1 [3]. Over 800 disease-causing mutations have been identified to date in *ABCA4*-associated phenotypes. The *ABCA4* mutation spectrum ranges from single base substitutions to deletions of several exons, although the majority of reported changes are missense mutations [9–11]. Numerous genetic studies on STGD1 patients have revealed that the disease-associated *ABCA4* alleles are extraordinarily heterogeneous. While some founder mutations accounting for a significant proportion of disease alleles have been identified in specific ethnic groups, hundreds of extremely rare or private variants have also been identified [12–14].

In this study, we used a combination of the ABCR400 microarray analysis and direct sequencing of the entire coding sequence of *ABCA4* gene to investigate the frequency and pattern of disease-associated mutations and polymorphisms in a large cohort of Greek patients with presumed STGD1. Our data extend the mutational spectrum of the *ABCA4* gene and, in addition, facilitate the screening of *ABCA4* mutations in Greek patients by identifying a set of three prevalent alleles.

2. Methods

This study adhered to the tenets of the Declaration of Helsinki and the ARVO statement of human subjects and was approved by the Human Subjects Review Committee at the University Hospital of Heraklion, Crete. Informed written consent was obtained for all study participants.

All patients were referred for genotyping after a clinical diagnosis of presumed Stargardt disease was put from treating ophthalmologists. A complete medical and familial history (including consanguineous marriages) was obtained from each patient. Age of symptom onset was documented. Familial STGD1 cases had to be compatible with autosomal recessive inheritance.

2.1. Mutation Screening of the ABCA4 Gene. Total genomic DNA was extracted from whole blood samples on an iPrep purification instrument using the iPrep PureLink gDNA Blood Kit (Invitrogen, Life Technologies, Carlsbad, CA) according to the manufacturer's instructions. A group of 30 Greek STGD1 patients were analyzed for variants on the ABCR400 microarray version 11.0 including 513–558 alterations (http://www.asperbio.com), as described elsewhere [15]. A second independent group of 29 patients and 8 patients from the microarray group were analyzed by direct sequencing of all 50 exons and intron-exon junctions of the *ABCA4* gene following PCR amplification with PCR primers designed using the Web Primer program. To test for deep intronic sequence variants [16] in 4 patients, primer pairs *ABCA4*-Exon30.1 fwd (5′-CACCCGATCCC TGCTCTTTTTTAT-3′)/rev (5′-TTACATTTTGTCCAGG GACCAAGG-3′) and *ABCA4*-Exon36.1 fwd (5′-ACAGGG ATCATTATGACATCAACCCC-3′)/rev (5′-AGCTACATC TCTCTCCATAGGCTCAGA-3′) were used to amplify and sequence a 406- and 596-bp fragment within *ABCA4* intervening sequences 30 and 36, respectively. All primer sequences are shown in Supplementary Table 1. We followed the methods of Kamakari et al. [17] for PCR and Sanger sequencing conditions. Specifically, PCR reactions were performed in a 25 μl total reaction volume, containing 50–100 ng genomic DNA, 2.5 μl of 10x PCR buffer (w/o $MgCl_2$), 3 μl of 10 mM dNTPs mix, 0.75 μl of 50 mM $MgCl_2$, 1.75 μl of 10 μM forward primer, 1.75 μl of 10 μM reverse primer, and 0.25 μl of 5 U/μl Platinum Taq DNA polymerase (Invitrogen, Life Technologies). Amplification was performed with the following cycling profile: incubation at 94°C for 5 min followed by 36 cycles of 45 sec denaturation at 94°C, 45 sec annealing at 58°C, and 45 sec elongation at 72°C. The last cycle was followed by a final extension of 3 min at 72°C. Excess primers and dNTPs were removed using exonuclease I and shrimp alkaline phosphatase, and PCR products were sequenced with the BigDye Terminator v3.1 Cycle Sequencing Kit (Applied Biosystems, Foster City, CA) according to the manufacturer's instructions. All sequences were analyzed in forward and reverse directions on an ABI3500 fluorescent sequencer (Applied Biosystems). Nucleotide sequences were compared with the published DNA sequence of *ABCA4* gene (GenBank accession number NG_011605.1 or NG_009073.1) and cDNA (GenBank accession number NM_000350.2). For the *ABCA4* gene, cDNA numbering +1 corresponds to A in the ATG translation initiation codon of ABCA4 transcript.

2.2. Multiplex Ligation-Dependent Probe Amplification. Multiplex ligation-dependent probe amplification (MLPA) reagents were obtained from MRC-Holland (SALSA MLPA kit P151-P152 ABCA4, Amsterdam), and the reactions were performed according to the manufacturer's instructions (MRC-Holland).

Whenever possible, segregation analysis was performed according to whether relatives were willing to offer clinical material.

3. Results

A total of 59 Greek patients with a presumed clinical diagnosis of STGD1 were screened for *ABCA4* mutations, including 25 males and 34 females. At least two cases reported consanguinity, and notably, two other cases had affected relatives across two successive generations which represent an atypical pattern of inheritance for the disease. The patients are presented in two groups. The first group of 30 patients was screened by an early version of the ABCR400 microarray chip (version 11.0) and the second group of 29 patients by direct sequencing. Direct sequencing was also performed as a complementary method in a subset of 8 patients of the microarray group with one identified mutation leading to the identification of the second mutant allele in 6 of them (Supplementary Table 2). Finally, additional sequencing of two regions in introns 30 and 36 as well as MLPA analysis

in 4 patients with one single mutation from both subgroups did not identify the second mutant allele.

ABCR400 *Microarray Screening*. Of the 30 patients screened using the ABCR400 microarray, 15 (50%) were found to carry two disease-causing mutations whereas 8 were found to carry a single mutation in heterozygous state (26.7%) (Supplementary Table 2). No mutations were identified in 7 patients (23.3%).

Direct Sequencing and MLPA Analysis. Of the 29 patients screened by PCR-based Sanger sequencing, 27 (93.1%) were found to carry two disease-causing mutations whereas 2 carried a single mutation (6.9%) (Supplementary Table 2). In addition, direct sequencing was performed in the 8 patients of the microarray-analyzed group with one identified mutation leading to the identification of the second mutation in 6 of them. Conclusively, 4 patients from both subgroups remained with one identified mutation. These 4 patients were tested for the known pathogenic deep intronic mutations in introns 30 and 36 [16] and, in addition, screened for large deletions or duplications by MLPA analysis, but no second mutation was identified in them.

In addition, direct sequencing revealed several polymorphic variants in *ABCA4* gene summarized in Supplementary Table 3.

3.1. Frequency of Mutations. Altogether, 100 potentially disease-causing *ABCA4* alleles were identified in this cohort of 59 Greek patients presenting with presumed STGD1. Among these 100 mutant alleles, a total of 40 distinct mutations were identified (Table 1). However, three mutations (c.5714+5G>A, p.Gly1961Glu, and p.Leu541Pro (alone or as a complex allele with the p.Ala1038Val)) occurred at a significantly higher frequency, compared to other variants in this cohort (Supplementary Table 2, Table 1). The most frequent mutation c.5714+5G>A (intron 40) was detected in 19 alleles in 16 patients (13 heterozygous, 3 homozygous) accounting for 16.1% of the total number of alleles ($n = 118$). The second most frequent mutation p.Gly1961Glu was detected in 18 alleles in 18 patients (all heterozygous) accounting for 15.2% of the total number of alleles ($n = 118$). The third most frequent mutation p.Leu541Pro was detected in 15 alleles either as a single mutation (5 alleles) or as a complex allele with the p.Ala1038Val (10 alleles) in 14 patients (13 heterozygous, 1 homozygous) accounting for 12.7% ($n = 118$). p.Ala1038Val was not detected as a single allele (Supplementary Table 2, Table 1).

A few mutations were detected more than once, that is, p.Gly607Arg in 4 alleles in 4 patients (all heterozygous), accounting for 3.3% ($n = 118$), and p.Val1973* and the novel mutation c.5714+1G>C (intron 40) both found in 3 alleles in 2 patients each (1 heterozygous, 1 homozygous), each accounting for 2.45% ($n = 118$). In addition, mutations c.4352+1G>A (intron 29) first reported by us [18], p.Arg18Trp, p.Arg212Cys, and p.Arg1108Cys were detected each in 2 alleles in 4 patients (all heterozygous), each accounting for 1.6% ($n = 118$). In addition, the allelic variant p.Arg1108Leu of the latter mutation was found in 1 patient.

The remainder of 22 distinct mutations was detected once in heterozygosity each accounting for 0.8% ($n = 118$) (Supplementary Table 2, Table 1), including five of the six previously unreported potentially pathogenic mutations p.Trp12* (exon 1), p.Asn76Thr (exon 3), p.Ser673Argfs*6 (exon 14), p.Cys698Arg (exon 14), and c.4352+4A>C (intron 29). Mutations p.Asn76Thr and p.Cys698Arg and the previously reported p.Arg107*, p.Pro143Leu, p.Gly 607Arg, and p.Trp1449* were detected in compound heterozygosity with the most frequent mutation c.5714 +5G>A in intron 40. Mutations p.Arg290Trp, p.Gly607Arg, p.Ser673Argfs*6, c.4352+1G>A, p.Glu1087Lys, p.Arg1108 Cys, p.Met1115Cysfs*33, p.Glu1271Gly, p.Gln1412*, p. Cys1488Arg, p.Ser1696Asn, c.5714+1G>C, p.Val1973*, and p.Arg2038Trp were detected in compound heterozygosity with the second most frequent mutation p.Gly1961Glu. Mutations p.Gly2146Asp and p.Arg1108Leu were detected in compound heterozygosity with c.4352+1G>A (intron 29) and p.Arg212Cys, respectively. Some of these once occurring mutations were detected in the same patient, namely, p.Arg18Trp and p.His1625Gln (patient ABCA4-20A), p.Gl u1122Lys and p.Gly1591Arg (patient ABCA4-39A), and p.Arg220Cys and p.Gly607Arg (patient ABCA4-35A).

In 4 patients, only one mutant allele was identified even after the use of direct sequencing and MLPA, these mutant alleles being p.Asn380Lys, p.Arg1640Trp, and c.5714+5G>A (the latter in 2 patients).

The majority of the distinct mutations were evenly distributed along the exons of the *ABCA4* gene. Three different mutations were observed in exon 22 and two in each of exons 1, 4, 6, 13, 14, 23, 35, and 44 and introns 29 and 40; however, no accumulation in a specific exon was observed. No mutation was identified in exons 2, 5, 7, 10, 11, 15, 18–20, 24, 26, 27, 31, 32, 34, 37–41, 45, 46, and 48–50 which comprise 50% (25/50) of the exons of the *ABCA4* gene.

Twenty-six of the detected mutations were missense, 5 were splice defects, 6 were nonsense, and 3 were frameshift mutations (Table 1).

3.2. Novel Mutations. Six novel mutations, namely, p.Trp12* (exon 1), p.Asn76Thr (exon 3), p.Ser673Argfs*6 (exon 14), p.Cys698Arg (exon 14), c.4352+4A>C (intron 29) and c.5714+1G>C (intron 40), and c.4352+1G>A (intron 29) previously reported by us [18], were detected in this study. Two were missense, three were splicing mutations (two of which occur in intron 29), one nonsense, and one small deletion of 13 nucleotides leading to a frameshift mutation of the *ABCA4* gene. These seven distinct mutations were detected in 10 apparently unrelated patients, 9 in heterozygous, and 1 in homozygous state. p.Trp12* (exon 1), p.Asn76Thr (exon 3), p.Ser673Argfs*6 (exon 14), p.Cys698Arg (exon 14), and c.4352+4A>C (intron 29) were each detected once in heterozygosity in 5 respective patients, and c.5714+1G>C was detected twice in two patients (1 in homozygosity, 1 in heterozygosity) and c.4352+1G>A (in three patients in heterozygosity).

Of these, the mutations p.Asn76Thr and p.Cys698Arg were detected in compound heterozygosity with the most frequently detected mutation c.5714+5G>A (intron 40) in one male (ABCA4-47A, Supplementary Figures 1A and B) and

Table 1: Frequency of 40 distinct mutations detected in 59 Greek patients with presumed STGD1.

Mutation number	Amino acid change	Nucleotide change	Exon	Number of alleles detected	Frequency	References
1	p.Trp12*	c.36G>A	1	1	0.8%	This study
2	p.Arg18Trp	c.52C>T	1	2	1.6%	[33]
3	p.Asn76Thr	c.227A>C	3	1	0.8%	This study
4	p.Pro143Leu	c.428C>T	4	1	0.8%	[13]
5	p.Arg107*	c.319C>T	4	1	0.8%	[34]
6	NA	c.571-2A>T	Intron 5	1	0.8%	[35]
7	p.Arg212Cys	c.635C>T	6	2	1.6%	[33]
8	p.Arg220Cys	c.658C>T	6	1	0.8%	[11]
9	p.Arg290Trp	c.868C>T	8	1	0.8%	[36]
10	p.Asn380Lys	c.1140T>A	9	1	0.8%	[11]
11[a]	p.Leu541Pro	c.1622T>C	12	10	8.5%	[37]
12	p.Gly607Arg	c.1819G>A	13	4	3.3%	[10]
13	p.Asp645Asn	c.1933G>A	13	1	0.8%	[9]
14	p.Ser673Argfs*6	c.2019_2031del13	14	1	0.8%	This study
15	p.Cys698Arg	c.2092T>C	14	1	0.8%	This study
16	p.Ser795Argfs*43	c.2385_2400delCTTACTGTCTCCGGTG	16	1	0.8%	[38]
17	p.Gln876*	c.2626C>T	17	1	0.8%	[39]
18	p.Ala1038Val	c.3113C>T	21	6	5.1%	[3]
19	p.Arg1108Cys	c.3322C>T	22	2	1.6%	[37]
20	p.Arg1108Leu	c.3323G>T	22	1	0.8%	[36]
21	p.Glu1087Lys	c.3259G>A	22	1	0.8%	[3]
22	p.Met1115Cysfs*33	c.3342delC	23	1	0.8%	[36]
23	p.Glu1122Lys	c.3364G>A	23	1	0.8%	[9]
24	p.Glu1271Gly	c.3812A>G	25	1	0.8%	[40]
25	p.Gln1412*	c.4234C>T	28	1	0.8%	[12]
26	p.Trp1449*	c.4346G>A	29	1	0.8%	[9]
27	NA	c.4352+1G>A	Intron 29	3	2.5%	[18, 40, 41]
28	NA	c.4352+4A>C	Intron 29	1	0.8%	This study
29	p.Cys1488Arg	c.4462T>C	30	1	0.8%	[9]
30	p.Gly1591Arg	c.4771G>A	33	1	0.8%	[42]
31	p.Arg1640Trp	c.4918C>T	35	1	0.8%	[37]
32	p.His1625Gln	c.4875T>A	35	1	0.8%	[13]
33	p.Ser1696Asn	c.5087G>A	36	1	0.8%	[9]
34	NA	c.5714+5G>A	Intron 40	19	16.1%	[30]
35	NA	c.5714+1G>C	Intron 40	3	2.5%	This study
36	p.Gly1961Glu	c.5882G>A	42	18	15.2%	[43]
37	p.Val1973*	c.5917delG	43	3	2.5%	[10]
38	p.Leu2026Pro	c.6077T>C	44	1	0.8%	[44]
39	p.Arg2038Trp	c.6112C>T	44	1	0.8%	[3]
40	p.Gly2146Asp	c.6437G>A	47	1	0.8%	[36]

[a]4 times was detected as single and 6 times as complex with p.A1038V.

one female patient (ABCA4-27A, Supplementary Figures 2A and B), respectively. The age of onset for patient ABCA4-47A carrying the p.Asn76Thr was 52 years according to the patient who was initially erroneously diagnosed with age-related macular degeneration in 2012. He had a cataract surgery at the age of 42 and eventually diagnosed with presumed Stargardt disease of late onset.

The age of onset for patient ABCA4-27A carrying the novel potentially pathogenic missense mutation p.Cys698Arg was 13 years of age.

Mutation c.4352+4A>C (intron 29) was detected in 1 patient in compound heterozygosity with p.Arg18Trp (exon 1) (patient ABCA4-37A, Supplementary Figures 3A and 3B). The age at diagnosis for this patient was 15. Segregation analysis documented that the unaffected parents were heterozygous for each mutation with the c.4352+4A>C paternally inherited and the p. Arg18Trp maternally inherited whereas her affected sister carried both mutations (Supplementary Figure 3A).

c.4352+1G>A was detected in two unrelated patients in compound heterozygosity with p.Gly2146Asp (exon 47) in patient ABCA4-5A (Supplementary Figures 4A and 4B) and with the complex allele p.Leu541Pro/p.Ala1038Val (exons 12/21) in patient ATH44A, (Supplementary Figures 5A and B). For patient ATH44A, five additional family members including two affected siblings, their unaffected parents, and an unaffected maternal uncle were tested for the two mutations. Both affected siblings were compound heterozygous for the two mutations; the mother was a heterozygous carrier of the c.4352+1G>A and the father of the p.Leu541Pro/p.Ala1038Val (Supplementary Figure 5A) whereas the maternal uncle was free of mutation.

The c.5714+1G>C mutation was initially detected in homozygous state in one young female patient (ABCA4-31A, Supplementary Figures 6A–C). Five additional family members including her unaffected parents (ABCA4-31B, C), her two affected maternal third male cousins (ABCA4-33A, B), and their unaffected mother (ABCA4-33C) were tested for the novel mutation. All parents were found heterozygous carriers whereas the affected cousins were homozygous (Supplementary Figures 6A–6C). All three young patients were diagnosed with presumed Stargardt disease approximately at the age of 7. Furthermore, the same novel potentially pathogenic mutation was detected in a seemingly unrelated patient (ABCA4-14A, Supplementary Figures 7A and 7B) in compound heterozygosity with the p.Gly1961Glu mutation.

Genetic analysis of patient (ATH73A) revealed a novel nonsense mutation c.36G>A (p.Trp12*) and a previously reported mutation c.571-2A>T occurring in a compound heterozygous state in exon 1 and intron 5, respectively, in the ABCA4 gene (Supplementary Figures 8A and 8B). This mutation leads to premature truncation after just 12 amino acids, which is likely to render the protein to be nonfunctional or lead to nonsense-mediated mRNA decay. It is included in the SNP database (https://www.ncbi.nlm.nih.gov/snp/) (rs761209432); however, according to our knowledge, it has not been associated previously with disease.

The sixth mutation c.2019_2031delCATCGTCTTGGAG was detected in patient ATH-53A. It consists of a deletion of 13 nucleotides from c.2019 to c.2031 (Supplementary Figures 9A and 9B) which would cause a frameshift that changes codon Ser673 to Arg, leading to a premature stop codon at position 678 (p.Ser673Argfs*6). The predicted translation product from this allele would consist of 677 amino acid residues instead of the 2273 found in the mature protein. This mutation was detected in compound heterozygosity with the p.Gly1961Glu mutation. The disease onset for this patient was at the age of 17.

In silico analysis for missense variants using the predictive algorithms of "Sorting Intolerant From Tolerant" ((SIFT) in the public domain, http://sift.jcvi.org), Polymorphism Phenotyping v2 ((PolyPhen-2) in the public domain, http://genetics.bwh.harvard.edu/pph2), and Protein Variation Effect Analyzer ((PROVEAN) in the public domain, http://provean.jcvi.org/index.php) tools predicted novel changes p.Asn76Thr and p.Cys698Arg to have a deleterious effect, whereas novel changes c.4352+4A>C and c.5714+1G>C are predicted to affect normal splicing by the Human Splicing Finder ((HSF); in the public domain, http://www.umd.be/HSF3/ prediction tool (Supplementary Table 4)).

3.3. Results of Relatives. Allelic segregation analyses were performed in 11 families. A total of 37 relatives were tested (data not shown). The analysis of one family (F11) that showed atypical pattern of inheritance is presented in detail hereafter.

3.4. Family F11A: A Family with an Atypical Pattern of Inheritance. In this family, the male proband (F11A, Figure 1(a)) and one of his brothers (F11B, Figure 1(a)) were diagnosed with presumed STGD1 before school age. Their parents (F11M, F11L) were unaffected which supported an autosomal recessive pattern of inheritance. However, two paternal aunts (F11C and F11J) were also affected but the disease presented in their twenties. Genotyping using the ABCR400 microarray was performed initially in the proband (F11A) and in one of his two affected aunts (F11C). The analysis revealed the complex p.Leu541Pro/p.Ala1038Val mutation in both of them. The proband was homozygous for the detected mutation; however, his aunt was compound heterozygous with p.Gly1961Glu. Following the initial analysis, thirteen additional family members including the proband's six siblings, parents, paternal grandparents, paternal aunts, and paternal cousin were tested for the two aforementioned mutations. Their results shown in Figures 1(a)–1(f) confirmed that the proband's affected siblings presenting with an early onset severe form of the disease were homozygous for the p.Leu541Pro/p.Ala1038Val complex allele whereas his second affected aunt with the later onset milder phenotype was a compound heterozygote with the p.Gly1961Glu mutation. The proband's unaffected parents were found heterozygous carriers for the p.Leu541Pro/p.Ala1038Val mutation. In addition, the paternal grandmother was a heterozygous carrier of the p.Gly1961Glu mutation and his grandfather heterozygous for the p.Leu541Pro/p.Ala1038Val. The parents of the proband did not report consanguinity, but their

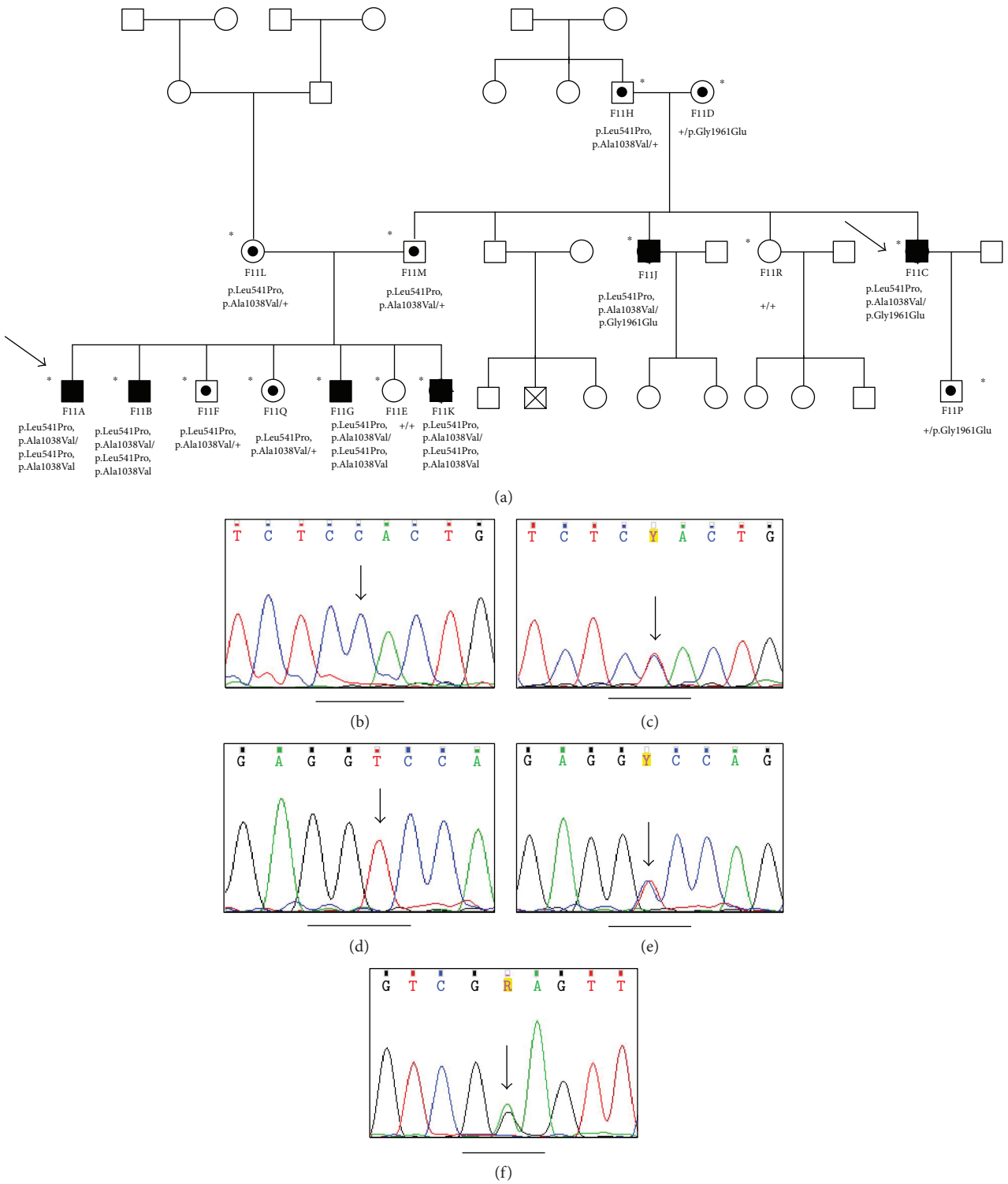

Figure 1: Family F11. (a) Pedigree of patients F11A and F11C (probands). Arrows indicate the probands. Affected and unaffected individuals are represented with black and open circles, respectively. Males are represented with a quadrant and females with a circle. The asterisk denotes the individuals genetically examined. A dot in a symbol denotes an unaffected carrier of the respective mutation. Pluses (+) denote the wild type alleles. (b, c, d, and e) Sequence chromatograms of the F11A and F11C showing the complex allele c.1622T>C/c.3113C>T (p.Leu541Pro/p.Ala1038Val) in homozygosity in proband F11A (b, d) and in heterozygosity in proband F11C (c, e). (f) Sequence chromatogram of the proband F11C showing the missense mutation c.5882G>A (p.Gly1961Glu) in heterozygosity on the second allele. The arrow indicates the position of the G to A substitution at the second nucleotide of codon 1961 encoded by GGA marked by a horizontal line.

ascendants originated from the same part of Northern Greece. Genotyping resolved the atypical pattern of inheritance of STGD1 disease in this family.

4. Discussion

Genetic analysis of 59 Greek patients with presumed STGD1 revealed 40 different mutations in the *ABCA4* gene and an overall detection rate of at least one mutant allele in 88.1% (52 patients) using a combination of the ABCR400 microarray, direct sequencing, and MLPA methods. Of these 52 patients, 48 were completely characterized (two mutant alleles detected) (81.3%) and 4 partially characterized (one mutant allele detected) (6.7%). This is well within the published range of biallelic mutation identification that ranges between 55% and 80% [19]. However, clinical heterogeneity and variable diagnostic criteria in our cohort of patients who were referred by a number of collaborating ophthalmologists may have led to uncertainties in clinical diagnosis in some of our patients.

Specifically, using the ABCR400 microarray screening method between the years 2006 and 2009 in 30 patients, two mutations were identified in 15 (50%), one mutation in 8 (26.7%), and no mutation in the remaining 7 (23.3%) cases. Valverde et al. [15] have reported similar mutation detection rates using the same microarray in a cohort of 76 patients, but Jaakson et al. [13] have reported somewhat lower detection rates (36.6% with two mutations and 24.4% with no mutations).

Using direct sequencing in 29 patients, both disease-causing mutations were identified in 27 (93.1%) whereas one mutation was identified in 2 patients (6.9%). Moreover, direct sequencing of *ABCA4*, used as a complementary method in 8 patients previously found to harbor one mutant allele using the microarray method of screening, led to the identification of a second mutant allele in 6 of them thus raising the complete characterization rate (identification of both mutant alleles) to 70% in this group. Overall, the use of direct sequencing as an initial screening method led to significantly higher complete characterization rate when compared to the microarray (93.1% versus 50%, resp.); therefore, it became the method of choice for *ABCA4* mutation screening by our group. These rates of detection parallel well with the recently published literature [20–22]. For example, in the study by Riveiro-Alvarez et al. [21], the mutation detection rate after complete *ABCA4* sequencing with Sanger sequencing or next generation sequencing (NGS) was 73.6% in arSTGD1 patients.

Most of the patients (42; $n = 59$) (71.1%) were compound heterozygotes. Only six patients were found to be homozygotes (Table 2). A single disease allele was found in 6.7% (4/59) of our cases. No disease allele was detected in 11.8% (7; $n = 59$) of our patients. Possible explanations for this may include erroneous clinical diagnosis, as well as the presence of disease-causing mutations in parts of the gene that were not screened, for example, deep into the introns or other regulatory regions and the presence of disease-causing mutations in other genes. The latter has proved to be the case in two of our ABCA4 negative patients which were found to harbor mutations in CRX and PROM1 genes (unpublished data).

Concurring with earlier studies [10, 23, 24], most *ABCA4* mutations are distributed throughout the entire coding sequence, and no mutational hotspots seem to exist. However, it is of note that 4 mutations lie in introns 29 and 40 (2 in each), 3 in exon 22 and 2 each in exons 1, 4, 6, 13, 14, 23, 35, and 44. In addition, mutations have been detected in half of the exons of the *ABCA4* gene in this cohort; therefore, perhaps initial *ABCA4* screening of Greek patients could include only this set of exons.

Most of the detected mutations were missense mutations (26), 5 were splice defects, 6 were nonsense, and 3 were frameshift mutations (Table 1).

A prevalent set of three mutant alleles composed of c.5714+5G>A representing 16.1% of all screened alleles (19/118), p.Gly1961Glu representing 15.2% (18/118), and p.Leu541Pro either as a single mutation or as a complex allele with the p.Ala1038Val representing 12.7% (15/118) was identified. Notably, of the 48 completely characterized subjects, 13 had two mutated alleles and 24 had one mutated allele from this high incidence set. Therefore, based on the mutation frequencies observed, one would expect that screening for these three mutations only would lead to complete genetic characterization of approximately 22% (13; $n = 59$) or partial genetic characterization of approximately 66.1% (39; $n = 59$) of Greek STGD1 patients providing strong indication of a true *ABCA4*-related retinopathy. Specifically, in our cohort, the most frequent mutation is the intronic splicing mutation IVS40+5G>A, accounting for 16.1% of all screened alleles (19/118). This is considerably higher than the frequency observed in other Europeans (3.9% in Spanish, 4.2% in Italian, and 8.6% in Hungarian patients) [15, 23, 24]. This mutation confers a milder phenotype, and this is especially true when the mutation is in homozygosity (3 patients in our cohort, H1, ATH35A, and ABCA4-44A) with an age of onset at the 4th decade; these patients consist half of the homozygotes in this cohort. The second most frequent mutation is p.Gly1961Glu with a frequency of 15.2% in our cohort of patients. This mutation is one of the most frequently mutated alleles in several populations analyzed. Its frequency ranges from 9% to 9.5% in some European countries or even lower in Spanish and Portuguese patients to 20-21% in Italian, Slovenian, and German patients. Its frequency of 15.2% in our cohort is comparable with the average frequency of 10% for the central European populations. The third most frequent mutation in Greek patients is p.Leu541Pro, alone or as a complex with p.Ala1038Val, with a frequency of 12.7% (15/118). This mutation is traditionally considered to be a German allele and is found in Germanic populations in general with a very low representation in other European populations, for example, 0.7% of the mutated alleles in an Italian cohort [25]. However, in our Greek cohort of patients, this is one of the three prevalent alleles. Although difficult to interpret, this high prevalence of the particular allele among Greek patients may be due to the fact that there has been a strong interaction and tight bonds between Greeks and Germans throughout the years with significant immigration from Greece to Germany starting around 1700. Moreover, it is known that in 1828, 31 Bavarian families came to Greece along with King Otto of Greece (http://www.greece-is.com/

little-bavaria-in-athens/) and were settled in Greece and their Hellenized offspring still living in Greece today. Moreover, it is estimated that between the 1960s and 1970s, 500,000 Greek young people migrated and approximately 30% of them returned to Greece. Considering these facts, a phenomenon of gene flow for this prevalent allele through intermarriage cannot be excluded. A similar hypothesis of gene flow has been used to explain the unusually high incidence of b-globin gene mutations in Germans. It has been hypothesized that mutations in two-thirds of the cases have been introduced from the Mediterranean [26, 27].

Six previously unreported potentially pathogenic mutations, namely, p.Trp12* (exon 1), p.Asn76Thr (exon 3), p.Cys698Arg (exon 14), p.Ser673Argfs*6 (exon 14), c.4352 +4A>C (intron 29), and c.5714+1G>C (intron 40) were detected in this study. Their absence from the ExAC (Exome Aggregation Consortium) database and their in silico analysis for the investigation of their pathogenicity, as mentioned in Results, support their potential pathogenicity. In addition, segregating results in the cases of the c.4352+4A>C and c.5714+1G>C splice variants strengthen their potential pathogenicity. Interestingly, the novel splice mutation c.5714 +1G>C in intron 40 was detected in two apparently unrelated patients, one male patient from the region of the western Greek islands in the Ionian sea and one female patient from the region of the Cyclades islands (Santorini) in the Aegean sea. It was detected in compound heterozygosity in the first patient and in homozygosity in the second patient. Parents of the second patient were found heterozygous for the mutation thus confirming the true homozygous state of the mutation in the patient. Furthermore, this second female patient who comes from the island of Santorini has two-thirds affected male cousins being siblings between them who were found to bear the same homozygous mutation. This family has other affected relatives across different generations once again proving the not so infrequent atypical pattern of inheritance in STGD1 families [28]. The family living in the same village of the island shared the information with us that there are many similarly affected patients in their village. We presume that they all bear the same homozygous mutation due to their common origin and endogamy, and we intend to offer a simple targeted testing to them per their request. It is of note that the paternal origin of the patient from the western Greek islands is from Santorini, and it would be interesting to verify that the c.5714+1G>C is his paternal allele, that is, the same which was detected in the patients from Santorini.

In addition, mutation c.4352+1G>A that was first described by our group in 2009 [18] was detected in two unrelated patients in our cohort in compound heterozygosity with p.Gly2146 (exon 47) (patient ABCA4-5A) or in conjunction with the complex allele p.Leu541Pro/p.Ala1038Val (exons 12/21) (patient ATH44A).

One family (F-F11) presented with an atypical pattern of inheritance of STGD1 with affected members of different age of onset in two successive generations. The male proband (F11A) and his brother (F11B) were diagnosed with presumed STGD1 before school age, whereas their parents were unaffected, and two paternal aunts (F11C and F11J) were diagnosed with the disease in their late twenties. Genotyping of the proband and one of his affected aunts revealed that the proband was homozygous for the p.Leu541Pro/p.Ala1038-Val, whereas his aunt was a compound heterozygote with the p.Gly1961Glu mutation. 13 additional family members were tested for these two mutations as described in Results. In summary, this family segregates two different pathogenic *ABCA4* variants. Based on the different age of onset of the disease in the proband and his other affected siblings and his affected aunts, we assume that the milder phenotype of the two affected aunts is likely due to the p.Gly1961Glu which has been previously associated with a late-onset, milder disease phenotype [28, 29]. Due to the high carrier frequency of disease-causing *ABCA4* alleles in the general population (1 : 20), pseudodominant inheritance in STGD1 has been described [9, 30–32].

All patients of this cohort were referred for genotyping from a network of collaborating ophthalmologists after a clinical diagnosis of presumed Stargardt was put. However, details of the phenotype were not always available thus precluding a systemic genotype-phenotype correlation. Future work towards this direction could provide additional helpful clinical data.

5. Conclusions

In summary, we report here the mutational spectrum of the *ABCA4* gene in a large Greek cohort, with successful identification of both disease-causing alleles at a rate of 81.3% (48/59). In addition, we report the identification of six novel potentially pathogenic mutations thus extending the spectrum of the *ABCA4* gene mutations and of three prevalent alleles which may facilitate the screening of Greek patients with *ABCA4*-related retinopathy. The complete genetic characterization of the patients will improve the accuracy of diagnosis and their counselling and also will assist in more effective patient selection of genetically confirmed participants for current and future clinical trials for *ABCA4*-associated retinal diseases.

Disclosure

This paper was previously presented as a poster in the following link: http://www.ashg.org/2009meeting/abstracts/fulltext/f10084.htm.

Conflicts of Interest

The authors declare that there is no conflict of interest regarding the publication of this paper.

Supplementary Materials

Supplementary Figure 1: family ABCA4-47. Supplementary Figure 2: family ABCA4-27. Supplementary Figure 3: family ABCA4-37. Supplementary Figure 4: family ABCA4-5. Supplementary Figure 5: F-ATH44. Supplementary Figure 6: F-ABCA4-31/33. Supplementary Figure 7: F-ABCA4-31/33. Supplementary Figure 8: F-ATH73. Supplementary Figure 9: F-ATH53. Supplementary Table 1: *ABCA4* PCR primer sequences. Supplementary Table 2: mutations detected in the

ABCA4 gene in a cohort of 59 Greek patients with presumed STGD1. Supplementary Table 3: polymorphic variants of the ABCA4 gene detected in Greek STGD patients. Supplementary Table 4: results of in silico analysis for 2 novel missense variants using the predictive algorithms SIFT, PolyPhen-2, and PROVEAN and for 2 novel splice variants using HSF prediction tool. *(Supplementary Materials)*

References

[1] V. North, R. Gelman, and S. H. Tsang, "Juvenile-onset macular degeneration and allied disorders," *Developments in Ophthalmology*, vol. 53, pp. 44–52, 2014.

[2] K. Zhang, M. Kniazeva, A. Hutchinson, M. Han, M. Dean, and R. Allikmets, "The *ABCR* gene in recessive and dominant Stargardt diseases: a genetic pathway in macular degeneration," *Genomics*, vol. 60, no. 2, pp. 234–237, 1999.

[3] R. Allikmets, "A photoreceptor cell-specific ATP-binding transporter gene (*ABCR*) is mutated in recessive Stargardt macular dystrophy," *Nature Genetics*, vol. 15, no. 3, pp. 236–246, 1997.

[4] L. J. Roberts, C. A. Nossek, L. J. Greenberg, and R. S. Ramesar, "Stargardt macular dystrophy: common *ABCA4* mutations in South Africa–establishment of a rapid genetic test and relating risk to patients," *Molecular Vision*, vol. 18, pp. 280–289, 2012.

[5] B. J. Klevering, A. F. Deutman, A. Maugeri, F. P. M. Cremers, and C. B. Hoyng, "The spectrum of retinal phenotypes caused by mutations in the *ABCA4* gene," *Graefe's Archive for Clinical and Experimental Ophthalmology*, vol. 243, no. 2, pp. 90–100, 2005.

[6] H. Sun, R. S. Molday, and J. Nathans, "Retinal stimulates ATP hydrolysis by purified and reconstituted ABCR, the photoreceptor-specific ATP-binding cassette transporter responsible for Stargardt disease," *The Journal of Biological Chemistry*, vol. 274, no. 12, pp. 8269–8281, 1999.

[7] A. V. Cideciyan, M. Swider, T. S. Aleman et al., "*ABCA4* disease progression and a proposed strategy for gene therapy," *Human Molecular Genetics*, vol. 18, no. 5, pp. 931–941, 2009.

[8] J. Weng, N. L. Mata, S. M. Azarian, R. T. Tzekov, D. G. Birch, and G. H. Travis, "Insights into the function of Rim protein in photoreceptors and etiology of Stargardt's disease from the phenotype in *abcr* knockout mice," *Cell*, vol. 98, no. 1, pp. 13–23, 1999.

[9] R. A. Lewis, N. F. Shroyer, N. Singh et al., "Genotype/phenotype analysis of a photoreceptor-specific ATP-binding cassette transporter gene, *ABCR*, in Stargardt disease," *American Journal of Human Genetics*, vol. 64, no. 2, pp. 422–434, 1999.

[10] A. Rivera, K. White, H. Stöhr et al., "A comprehensive survey of sequence variation in the *ABCA4* (*ABCR*) gene in Stargardt disease and age-related macular degeneration," *American Journal of Human Genetics*, vol. 67, no. 4, pp. 800–813, 2000.

[11] A. R. Webster, E. Héon, A. J. Lotery et al., "An analysis of allelic variation in the *ABCA4* gene," *Investigative Ophthalmology & Visual Science*, vol. 42, no. 6, pp. 1179–1189, 2001.

[12] A. Maugeri, M. A. van Driel, D. J. van de Pol et al., "The 2588G–>C mutation in the *ABCR* gene is a mild frequent founder mutation in the Western European population and allows the classification of *ABCR* mutations in patients with Stargardt disease," *American Journal of Human Genetics*, vol. 64, no. 4, pp. 1024–1035, 1999.

[13] K. Jaakson, J. Zernant, M. Külm et al., "Genotyping microarray (gene chip) for the *ABCR* (*ABCA4*) gene," *Human Mutation*, vol. 22, no. 5, pp. 395–403, 2003.

[14] F. Simonelli, F. Testa, J. Zernant et al., "Genotype-phenotype correlation in Italian families with Stargardt disease," *Ophthalmic Research*, vol. 37, no. 3, pp. 159–167, 2005.

[15] D. Valverde, R. Riveiro-Alvarez, S. Bernal et al., "Microarray-based mutation analysis of the *ABCA4* gene in Spanish patients with Stargardt disease: evidence of a prevalent mutated allele," *Molecular Vision*, vol. 12, pp. 902–908, 2006.

[16] T. A. Braun, R. F. Mullins, A. H. Wagner et al., "Non-exomic and synonymous variants in *ABCA4* are an important cause of Stargardt disease," *Human Molecular Genetics*, vol. 22, no. 25, pp. 5136–5145, 2013.

[17] S. Kamakari, G. Koutsodontis, M. Tsilimbaris, A. Fitsios, and G. Chrousos, "First report of *OPA1* screening in Greek patients with autosomal dominant optic atrophy and identification of a previously undescribed OPA1 mutation," *Molecular Vision*, vol. 20, pp. 691–703, 2014.

[18] S. Kamakari, P. Stamatiou, T. Panagiotoglou, C. Tsika, and M. Tsilimbaris, "Microarray-based mutation analysis of the ABCA4 gene in Greek patients with Stargardt disease: evidence of three mutated alleles," *Investigative Ophthalmology & Visual Science*, vol. 50, no. 13, p. 4118, 2009.

[19] F. Jiang, Z. Pan, K. Xu et al., "Screening of *ABCA4* gene in a Chinese cohort with Stargardt disease or cone-rod dystrophy with a report on 85 novel mutations," *Investigative Ophthalmology & Visual Science*, vol. 57, no. 1, pp. 145–152, 2016.

[20] J. Aguirre-Lamban, R. Riveiro-Alvarez, S. Maia-Lopes et al., "Molecular analysis of the *ABCA4* gene for reliable detection of allelic variations in Spanish patients: identification of 21 novel variants," *The British Journal of Ophthalmology*, vol. 93, no. 5, pp. 614–621, 2009.

[21] R. Riveiro-Alvarez, M. A. Lopez-Martinez, J. Zernant et al., "Outcome of *ABCA4* disease-associated alleles in autosomal recessive retinal dystrophies: retrospective analysis in 420 Spanish families," *Ophthalmology*, vol. 120, no. 11, pp. 2332–2337, 2013.

[22] J. Zernant, Y. A. Xie, C. Ayuso et al., "Analysis of the *ABCA4* genomic locus in Stargardt disease," *Human Molecular Genetics*, vol. 23, no. 25, pp. 6797–6806, 2014.

[23] A. Fumagalli, M. Ferrari, N. Soriani et al., "Mutational scanning of the ABCR gene with double-gradient denaturing-gradient gel electrophoresis (DG-DGGE) in Italian Stargardt disease patients," *Human Genetics*, vol. 109, no. 3, pp. 326–338, 2001.

[24] J. Hargitai, J. Zernant, G. M. Somfai et al., "Correlation of clinical and genetic findings in Hungarian patients with Stargardt disease," *Investigative Ophthalmology & Visual Science*, vol. 46, no. 12, pp. 4402–4408, 2005.

[25] I. Passerini, A. Sodi, B. Giambene, A. Mariottini, U. Menchini, and F. Torricelli, "Novel mutations in of the *ABCR* gene in Italian patients with Stargardt disease," *Eye*, vol. 24, no. 1, pp. 158–164, 2010.

[26] B. Vetter, C. Schwarz, E. Kohne, and A. E. Kulozik, "Beta-thalassaemia in the immigrant and non-immigrant German

populations," *British Journal of Haematology*, vol. 97, no. 2, pp. 266–272, 1997.

[27] E. Kohne and E. Kleihauer, "Hemoglobinopathies: a longitudinal study over four decades," *Deutsches Ärzteblatt International*, vol. 107, no. 5, pp. 65–71, 2010.

[28] T. R. Burke, G. A. Fishman, J. Zernant et al., "Retinal phenotypes in patients homozygous for the G1961E mutation in the *ABCA4* gene," *Investigative Ophthalmology & Visual Science*, vol. 53, no. 8, pp. 4458–4467, 2012.

[29] W. Cella, V. C. Greenstein, J. Zernant-Rajang et al., "G1961E mutant allele in the Stargardt disease gene *ABCA4* causes bull's eye maculopathy," *Experimental Eye Research*, vol. 89, no. 1, pp. 16–24, 2009.

[30] F. P. Cremers, D. J. van de Pol, M. van Driel et al., "Autosomal recessive retinitis pigmentosa and cone-rod dystrophy caused by splice site mutations in the Stargardt's disease gene *ABCR*," *Human Molecular Genetics*, vol. 7, no. 3, pp. 355–362, 1998.

[31] A. N. Yatsenko, N. F. Shroyer, R. A. Lewis, J. R. Lupski et al., "Late-onset Stargardt disease is associated with missense mutations that map outside known functional regions of *ABCR* (*ABCA4*)," *Human Genetics*, vol. 108, no. 4, pp. 346–355, 2001.

[32] W. Lee, Y. Xie, J. Zernant et al., "Complex inheritance of *ABCA4* disease: four mutations in a family with multiple macular phenotypes," *Human Genetics*, vol. 135, no. 1, pp. 9–19, 2016.

[33] S. Gerber, J. M. Rozet, T. J. van de Pol et al., "Complete exon-intron structure of the retina-specific ATP binding transporter gene (*ABCR*) allows the identification of novel mutations underlying Stargardt disease," *Genomics*, vol. 48, no. 1, pp. 139–142, 1998.

[34] T. R. Burke, R. Allikmets, R. T. Smith, P. Gouras, and S. H. Tsang, "Loss of peripapillary sparing in non-group I Stargardt disease," *Experimental Eye Research*, vol. 91, no. 5, pp. 592–600, 2010.

[35] S. Rossi, F. Testa, M. Attanasio et al., "Subretinal fibrosis in Stargardt's disease with fundus flavimaculatus and *ABCA4* gene mutation," *Case Reports in Ophthalmology*, vol. 3, no. 3, pp. 410–417, 2012.

[36] C. E. Briggs, D. Rucinski, P. J. Rosenfeld, T. Hirose, E. L. Berson, and T. P. Dryja, "Mutations in *ABCR* (*ABCA4*) in patients with Stargardt macular degeneration or cone-rod degeneration," *Investigative Ophthalmology & Visual Science*, vol. 42, no. 10, pp. 2229–2236, 2001.

[37] J. M. Rozet, S. Gerber, E. Souied et al., "Spectrum of ABCR gene mutations in autosomal recessive macular dystrophies," *European Journal of Human Genetics*, vol. 6, no. 3, pp. 291–295, 1998.

[38] https://www.ncbi.nlm.nih.gov/clinvar/variation/99132/.

[39] S. Stenirri, I. Fermo, S. Battistella et al., "Denaturing HPLC profiling of the *ABCA4* gene for reliable detection of allelic variations," *Clinical Chemistry*, vol. 50, no. 8, pp. 1336–1343, 2004.

[40] J. Zernant, C. Schubert, K. M. Im et al., "Analysis of the *ABCA4* gene by next-generation sequencing," *Investigative Ophthalmology & Visual Science*, vol. 52, no. 11, pp. 8479–8487, 2011.

[41] P. J. Ernest, C. J. Boon, B. J. Klevering, L. H. Hoefsloot, and C. B. Hoyng, "Outcome of *ABCA4* microarray screening in routine clinical practice," *Molecular Vision*, vol. 15, pp. 841–847, 2009.

[42] T. Eisenberger, C. Neuhaus, A. O. Khan et al., "Increasing the yield in targeted next-generation sequencing by implicating CNV analysis, non-coding exons and the overall variant load: the example of retinal dystrophies," *PLoS One*, vol. 8, no. 11, p. e78496, 2013.

[43] R. Allikmets, N. F. Shroyer, N. Singh et al., "Mutation of the Stargardt disease gene (*ABCR*) in age-related macular degeneration," *Science*, vol. 277, no. 5333, pp. 1805–1807, 1997.

[44] H. L. Schulz, F. Grassmann, U. Kellner et al., "Mutation spectrum of the *?* gene in 335 Stargardt disease patients from a multicenter German cohort-impact of selected deep intronic variants and common SNPs," *Investigative Ophthalmology & Visual Science*, vol. 58, no. 1, pp. 394–403, 2017.

Hindawi
Journal of Ophthalmology
Volume 2018, Article ID 8293452, 6 pages
https://doi.org/10.1155/2018/8293452

Research Article

Evaluation of TGF-Beta 2 and VEGFα Gene Expression Levels in Epiretinal Membranes and Internal Limiting Membranes in the Course of Retinal Detachments, Proliferative Diabetic Retinopathy, Macular Holes, and Idiopathic Epiretinal Membranes

Joanna Stafiej,[1] **Karolina Kaźmierczak**,[1] **Katarzyna Linkowska**,[2] **Paweł Żuchowski**,[3] **Tomasz Grzybowski**,[2] **and Grażyna Malukiewicz**[1]

[1]*Department of Ophthalmology, Faculty of Medicine, Nicolaus Copernicus University in Toruń, Collegium Medicum in Bydgoszcz, Sklodowskiej-Curie 9, 85-094 Bydgoszcz, Poland*
[2]*Department of Molecular and Forensic Genetics, Institute of Forensic Medicine, Faculty of Medicine, Nicolaus Copernicus University in Toruń, Collegium Medicum in Bydgoszcz, Sklodowskiej-Curie 9, 85-094 Bydgoszcz, Poland*
[3]*Clinic of Rheumatology and Connective Tissue Diseases, J. Biziel University Hospital No. 2, Bydgoszcz, Poland*

Correspondence should be addressed to Joanna Stafiej; joanna.stafiej@wp.pl

Received 15 November 2017; Revised 1 February 2018; Accepted 28 February 2018; Published 23 April 2018

Academic Editor: Lev Prasov

Purpose. To evaluate the expression profiles of the VEGFα and TGFβ in the ERMs and ILMs in retinal disorders. *Methods*. In this nonrandomized prospective study, 75 patients (34 females and 41 males) referred to pars plana vitrectomy (PPV) due to different retinal diseases were enrolled to the study. The samples of ERMs and ILMs collected during PPV were immediately put in TRIzol® Reagent (Life Technologies, USA) and stored at −70°C until RNA extraction. Gene expression analysis was done with TaqMan® Gene Expression Assays (Applied Biosystems, USA) following the manufacturer's instructions. *Results*. The gene expression levels of VEGFα as well as of TGFβ2 were significantly higher in ERMs than in ILMs in all studied groups. The level of TGFβ2 expression exhibits a significantly lower values in iERMs as compared with the RRD group ($p = 0.043$). There were differences in TGFβ2 expression in ILM in groups studied: DR versus RRD, $p = 0.003$; DR versus iERM, $p = 0{,}047$; and iERM versus RRD, $p = 0.004$. *Conclusions*. Our results revealed that factors associated with angiogenesis and wound healing processes in eyes with RRD, PDR, iERM, and MH were more upregulated in ERMs than in ILMs. This may indicate that ILM is not responsible for reproliferation and its peeling should be avoided in routine PPV.

1. Introduction

Proliferative vitreoretinopathy (PVR) is a severe retinal detachment (RD) and vitreoretinal surgery complication that can lead to severe vision reduction by tractional retinal detachment. Epiretinal membrane (ERM) is a semitransparent, membranous, pathologic tissue which grows on the internal surface of the retina at the vitreoretinal interface. ERMs can be either idiopathic or secondary to some pathologic conditions, including proliferative diabetic retinopathy, high myopia, uveitis, proliferative vitreoretinopathy, and other retinal degenerative diseases [1, 2]. Reported frequency of ERM falls between 3% to 8.5% after scleral buckling and 6.1% to 12.8% after vitrectomy [3–8].

Due to its structure, the ILM plays a key role in the development of the vitreous–retinal boundary. Composed of a basal membrane of Müller cells, proteoglycans, and type IV collagen fibers, it constitutes the so-called framework for the development of proliferative membranes. Müller cells are responsible for homeostatic and metabolic support of

Table 1: Demographics of patients included in the study groups.

	ERM group	DR group	RD group	Control group
Study population	16 (9 F/7 M)	21 (12 F/9 M)	38 (13 F/25 M)	8 (5 F/3 M)
Age (mean ± SD; min, max)	72 ± 6.53; min 61, max 82, med. 72	60.48 ± 9.06; min 54, max 73, med. 62	63.24 ± 10.54; min 26, max 82, med. 63.5	65.38 ± 15.94; min 30, max 79, med. 68

photoreceptors and neurons. They act as soft, compliant embedding for neurons, protecting them from mechanical trauma, and also release neuroactive signaling molecules that modulate neuronal activity [9]. The ILM peeling in the macula area allows removing all the ERMs and, as a result, all the tractions of the framework and the proliferation environment [10–12]. The majority of surgeons choose to peel the ILM away, but additional ILM peeling for ERM and RD surgery remains controversial. It is believed that ILM peeling during ERM removal may decrease the percentage of eyes experiencing its regrowth [13–15]. Nevertheless, vitreoretinal reproliferations are still among the chief causes behind unsuccessful vitreoretinal surgery. Moreover, ILM peeling has been known to cause mechanical traumatic changes to the retinal nerve fiber layer (RNFL) [16–20].

The molecular formation mechanism of both the primary and secondary ERMs in diabetic and nondiabetic patients is still poorly understood. A number of cytokines are involved in the ERM progression [21–23]. Recent technological advancements in genomics have given researchers new opportunities for identifying global gene expressions in specific tissues [24].

The aim of this prospective study was to analyse whether the gene expression profile of ERMs and ILM occurs in equal measure, which might aid in understanding ILM peeling.

2. Methods

Eighty-three patients (39 F, 44 M, age range: 26–84 years, mean age: 64.4, median: 66, standard deviation (SD): ±10.8), referred to the Department of Ophthalmology of the University Hospital in Bydgoszcz for 23-gauge pars plana vitrectomy (PPV) due to a variety of retinal diseases, were enrolled in the study. Prior to surgery, a detailed ophthalmic examination with OCT assessment was conducted, written informed consent was received from each patient before tissue sample acquisition, and approval for the study was granted by the ethics committee (KB 509/2013).

Three-port PPV with ERM removal and ILM peeling was the surgical technique used in this prospective study (DORC, the Polymed, Poland). Membrane removal and ILM peeling were performed with end-gripping forceps, intending to remove as much as possible of the ERM and remove the ILM from an area around the macula circa 3-4 disc diameter large. The surgeries were performed by two experienced vitreoretinal surgeons (JS and KK).

The patients enrolled in the study were categorized based on the disease they suffered from:

(1) Idiopathic epiretinal membranes (iERMs)

(2) Proliferative diabetic retinopathy (PDR)

(3) Retinal detachment with epiretinal membranes (RD with ERMs)

Table 2: The set of TaqMan Gene Expression Assays used for gene expression analyses.

Gene	Assay ID
GAPDH	Hs03929097_g1
VEGFA	Hs00900055_m1

As a control group, ILM samples collected during PPV performed due to MH from eight patients (5 females, 3 males) were used. Patient demographics are listed in Table 1.

ERM and ILM samples collected during PPV were promptly put in a TRIzol Reagent (Life Technologies, Foster City, CA, USA) and stored at −70°C until RNA extraction. RNA extracts were treated with DNase I using TURBO DNA-free™ Kit (Life Technologies, Foster City, CA, USA). Quantification of total RNA was performed by a DeNovix spectrophotometer (DeNovix, Wilmington, USA). Total RNA (800 ng) was reverse-transcribed using High-Capacity cDNA Reverse Transcription Kit (Life Technologies, Foster City, CA, USA) according to the protocol. Quantitative real-time reverse transcriptase PCR (qRT-PCR) was performed by TaqMan technology using a ViiA™ 7 Real-Time PCR System (Applied Biosystems, Foster City, CA, USA). Gene expression analysis was done with TaqMan Gene Expression Assays (Applied Biosystems, Foster City, CA, USA) following the manufacturer's instructions (Table 2). Negative control consisted of a PCR mix without cDNA. The glyceraldehyde-3-phosphate dehydrogenase (GAPDH) was used as the endogenous control to normalize gene expression levels for relative quantitative analysis through a comparative cycle threshold (ΔCt) method. Finally, the ΔΔCt method was used to compare gene expressions between ERM and ILM from PVR patients.

The data obtained is presented as a mean ± SD and median. For normally and equally distributed data, gene expression levels between the groups were compared using t-test. $p < 0.05$ was considered a statistically significant difference. Statistical analysis was performed using MS Excel 2010.

3. Results

3.1. Epiretinal Membrane. The gene expression levels of VEGFα as well as of TGFβ2 were significantly higher in ERMs than in ILMs ($p = 0.009$ and $p = 0.015$, resp.; mean and SD values are presented in Table 3).

Table 3: Expression levels of VEGFα and TGFβ2 in the ERMs and ILMs in eyes with idiopathic epiretinal membranes (iERMs).

	ERM	ILM	p value
VEGFα (in iERM)			
Mean	4.43	2.55	
Median	4.31	1.87	**0.009**
Standard deviation	1.90	2.34	
TGFβ2 (in iERM)			
Mean	4.16	1.66	
Median	4.66	0.00	**0.015**
Standard deviation	3.36	2.84	

Table 4: Expression levels of VEGFα and of TGFβ2 in the fibrous epiretinal membranes (FERMs) and ILMs in eyes with proliferative diabetic retinopathy (PDR).

	FERM	ILM	p value
VEGFα (in PDR)			
Mean	4.34	2.96	
Median	3.92	3.15	**0.016**
Standard deviation	2.27	1.71	
TGFβ2 (in PDR)			
Mean	5.53	3.23	
Median	5.49	4.65	**0.003**
Standard deviation	2.46	2.69	

Comparison of gene expression of VEGFα and TGFβ2 in ILM in patients who suffered from ERM to gene expression of VEGFα and TGFβ2 in ILM in patients with MH (control group) reveals no statistical differences between these two groups.

3.2. Diabetic Retinopathy. The gene expression levels of VEGFα as well as TGFβ2 were significantly higher in fibrous ERMs compared to ILMs ($p = 0.016$ and $p = 0.003$, resp., mean and SD values are presented in Table 4).

Comparison of gene expression of VEGFα and TGFβ2 in ILM in patients suffered from PDR to gene expression of VEGFα and TGFβ2 in ILM in the control group reveals a statistical difference between these two groups when it comes to TGFβ2 but not VEGFα ($p = 0.007$ and $p = 0.339$, resp., mean and SD values are presented in Table 5).

3.3. Rhegmatogenous Retinal Detachment. The expression levels of VEGFα and TGFβ2 were significantly higher in ERMs than in ILMs ($p = 0.004$ and $p = 0.002$, resp.; mean and SD values are presented in Table 6).

Comparison of gene expression of VEGFα and TGFβ2 in ILM in patients suffering from RD to gene expression of VEGFα and TGFβ2 in ILM in patients from the control group reveals a statistical difference between the two groups when it comes to TGFβ2 but not VEGFα ($p = 0.014$ and $p = 0.45$, resp., mean and SD values are presented in Table 7), resembling the PDR group.

Table 5: Comparison with the control group. Expression levels of VEGFα and of TGFβ2 in the ILMs in the PDR group and control group.

	ILM study group	ILM control group	p value
VEGFα (in PDR)			
Mean	2.96	2.63	
Median	3.15	2.65	0.339
Standard deviation	1.71	2.46	
TGFβ2 (in PDR)			
Mean	3.23	0.64	
Median	4.65	0.00	**0.007**
Standard deviation	2,69	1,92	

Table 6: Expression levels of VEGFα and of TGFβ2 in the ERMs and ILMs in eyes with rhegmatogenous retinal detachment.

	ERM	ILM	p value
VEGFα (in RRD)			
Mean	3.71	2.53	
Median	3.82	2.70	**0.004**
Standard deviation	1.96	1.85	
TGFβ2 (in RRD)			
Mean	5.60	14.92	
Median	5.76	0.00	**0.002**
Standard deviation	2.46	18.74	

Table 7: Comparison with the control group. Expression levels of VEGFα and of TGFβ2 in the ILMs in the RRD group and control group.

	ILM study group	ILM control group	p value
VEGFα (in RRD)			
Mean	2.53	2.63	
Median	2.70	2.65	**0.45**
Standard deviation	1.85	2.46	
TGFβ2 (in RRD)			
Mean	14.92	0.64	
Median	0.00	0.00	**0.014**
Standard deviation	18.74	1.92	

Comparison of gene expression of VEGFα and TGFβ2 in ERMs between groups, depending on diagnosis, reveals no statistical differences between the groups when it comes to VEGFα. The level of TGFβ2 expression exhibits significantly lower values in the iERM group compared to the RRD group ($p = 0.043$).

Similarly, comparison of gene expression of VEGFα and TGFβ2 in ILMs between studied groups produces no

observable statistical differences in term of VEGFα; however, such differences were found between all 3 studied groups when it comes to TGFβ2 (DR versus RRD, $p = 0.003$; DR versus iERM, $p = 0.047$; and iERM versus RRD, $p = 0.004$). The RRD did exhibit the highest level and the iERM the lowest level of TGFβ2.

4. Discussion

Roth and Foos postulated that an idiopathic ERM proliferates as retinal tissue-derived glial cells escape from microdefects in the internal limiting membrane (ILM) that occur during posterior vitreous detachment and migrate to the surface of the retina [25]. Another theory attributes the pathogenesis of an ERM to the growth and fibrous metaplasia of the vitreous cells that remain on the retina surface after posterior vitreous detachment. On the other hand, in the ERM that occur after rhegmatogenous RD, the retinal pigment epithelial cells are thought to migrate to the vitreous cavity through the retinal break and settle on the retinal surface, forming the membrane [26]. None of these theories put forth a reason behind certain patients developing PVR rapidly while others—not at all. The present study characterized the expression profiles of the inflammatory cytokines VEGFα and TGFβ2 in the ERMs and ILMs in retinal disorders such as RRD, DR, and iERM. There might be several important factors that determine cytokine levels either inside the operated eye or the entire body. To overcome this problem, we collected both the ERM and ILM from the same eyes. Various cytokines, including the vascular VEGF, have been identified as playing a role in the pathogenesis of DR [27–29]. VEGF that was first discovered as a vascular permeability factor is specifically a mitogenic cytokine for vascular endothelial cells. Retinal ischemia is the basic stimulus leading to upregulation and increase of VEGF locally and therefore plays a major role in the progression of DR. Increased VEGF interacts with its two tyrosine kinase receptors on the retinal vasculature, resulting in the formation of new vessels and also disruption of the internal blood retinal barrier. The VEGF presence has been reported in iERMs [30, 31]. In previous studies, positive VEGF immunoreactivity of iERMs was found, an unsurprising fact considering that retinal glia have been known to produce VEGF. The question arose why no blood vessels in iERM were present despite the presence of VEGF. One possibility was the existence of other cells in the iERM besides endothelial cells that are targeted by VEGF. It was also plausible that the presence of endothelial growth inhibitory factors, such as TGF-β, may prevent VEGF from exerting its angiogenic activity. Nam et al. investigated the difference in the expression of specific growth factors (including VEGF and TGF β1) between diabetic and nondiabetic ERMs [32]. In our research, there were no statistical differences in VEGFα expression between the study groups either in ERM or ILM. There was a statistical difference ($p = 0.043$) in TGFβ2 expression only between the RD group (mean = 5.60; SD = 2.46) and iERM group (mean = 4.16; SD = 3.36) with regard to ERM. Selim et al. observed that the elevation of VEGF levels was parallel to the severity of DR and to the degree of retinal ischemia, suggesting that the main pathogenic factor causing VEGF elevation and responsible for DR progression in their patients' eyes was retinal hypoxia [33]. Retinal diseases are closely associated with both decreased oxygenation and increased inflammation. It is unknown whether hypoxia-induced VEGF expression in the retina itself evokes inflammation, or whether inflammation is a prerequisite for the development of neovascularization. Interestingly, the majority of the previous studies evaluating the roles of different cytokines and growth factors in the pathogenesis of idiopathic epiretinal membrane were based on the vitreous samples. Few reports are related to expression levels of these factors between ERM and ILM and evaluated them not only in idiopathic epiretinal membranes, but also in fibrotic ones, usually seen in proliferative vitreoretinopathy, such as PDR or advanced RD. To address this issue, we assessed the gene expression levels of VEGFα and TGFβ2 in idiopathic and fibrotic ERMs as well as in ILMs. To the best of our knowledge, this is the first study that compares these parameters in ERMs and ILMs in different diseases. Takahashi et al. showed significant differences in VEGF levels in vitreous body in RRD, MH, PDR, ERM, and RVO ($p < 0.001$) [34]. We found no statistical differences among RRD, PDR, and idiopathic ERM groups comparing VEGFα expression directly in ERMs; however, in RRD, we noticed the lowest expression. The evaluation of VEGFα expression directly in the ILM in RRD, PDR, and idiopathic ERM groups versus MH revealed no statistical differences contrary to Takahashi results. TGFβ2 expressions showed statistical differences between almost all study groups, except one (ERM group versus MH group). Myojin et al. analysed gene expression in the irrigation solution collected during vitrectomy performed due to ERMs and MH and found that the expression levels of TGFβ2 and VEGFα were significantly higher in eyes with iERM versus MH [35]. Nonetheless, we found no differences in gene expression of VEGFα and TGFβ2 in ILM in patients suffering from ERM versus patients with MH. Similarly, there were no statistical differences in expression of VEGFα in ILM between RRD versus MH and DR versus MH groups. Interestingly, at the same time, there was a statistically higher expression of TGFβ2 in ILM between RRD versus MH and DR versus MH groups. As it is well known, the transforming growth factor-β (TGF-β) and fibroblast growth factor (FGF) play crucial cooperative roles in fibrosis. For example, in the pathogenesis of proliferative vitreoretinopathy (PVR), TGFβ plays a pivotal role, promoting transition of retinal pigment epithelial (RPE) cells into myofibroblasts. ERM is thought to be caused by a fibrocellular proliferation of the inner limiting membrane (ILM) and the subsequent vitreoretinal adhesion and traction [36, 37]. TGFβ upregulation was reported in eyes with iERM, PDR, and PVR, and it is associated with intraocular fibrosis [21, 23, 30, 38]. Despite advances in surgical techniques, the percentage of unhealed PVR remains high, producing a failure rate of up to 10% in retinal surgical repairs [39]. In our study, TGF-β expression responsible for fibrosis was significantly higher in ERMs than in ILMs in all studied groups. One of the main targets of genetic studies is to translate evidence and benefits into clinical practice. ILM peeling is a subject of ongoing debate.

Rinaldi et al. found no significant differences between postoperative best-corrected visual acuity or best-corrected visual acuity change in the ILM peeling group compared with the nonpeeling group. There was no significant difference in postoperative central macular thickness and central macular thickness reduction between the two groups [40]. Similarly, Díaz-Valverde et al. noticed that internal limiting membrane peeling does not improve the functional outcome after ERM surgery. The ILM peeling reduces ERM recurrences, but few recurrences are clinically significant [41]. Moreover, a number of researchers noticed that ILM peeling had been considered to cause mechanical retinal damage, including physiological alterations in Müller cells, irregularities of the nerve fiber layer, small paracentral scotomas, loss of Müller cells end-feet within the peeling area, and weakening of the macular glial structure [17, 42–44]. Müller cells react to mechanical and hypoxic stimuli by hypertrophy to resist and protect the neuroretinal layers from traction and to protect photoreceptors from apoptosis [45]. Gao et al. suggested that in some cases of myopic foveoschisis ILM removal resulted in the development of postoperative full-thickness macular holes [46]. Sakimoto et al. found by an image of en face OCT a retinal dimple signs after ILM peeling [47]. There are also results suggesting that ILM peeling may reduce retinal sensitivity and significantly increase the incidence of microscotomas [48]. A meta-analysis of vitrectomy with or without internal limiting membrane peeling for macular hole coexisting with retinal detachment in the highly myopic eyes done by Gao et al. revealed no definite benefit of postoperative visual improvement [49].

5. Conclusions

Our results reveal that VEGFα and TGFβ2 associated with angiogenesis and wound healing processes in eyes with RRD, PDR, and iERM were more upregulated in ERMs than in ILMs. This may indicate that ILM is not responsible for reproliferation and its peeling should be avoided in routine PPV. Further studies are needed to better understand the ILM role in reproliferation and the need of ILM peeling and its consequences.

Conflicts of Interest

The authors declare that they have no conflicts of interest.

References

[1] X. Zhang, G. Barile, S. Chang et al., "Apoptosis and cell proliferation in proliferative retinal disorders: PCNA, Ki-67, caspase-3, and PARP expression," *Current Eye Research*, vol. 30, no. 5, pp. 395–403, 2005.

[2] M. Joshi, S. Agrawal, and J. B. Christoforidis, "Inflammatory mechanisms of idiopathic epiretinal membrane formation," *Mediators of Inflammation*, vol. 2013, 6 pages, 2013.

[3] H. L. Tanenbaum, C. L. Schepens, I. Elzeneiny, and H. M. Freeman, "Macular pucker following retinal detachment surgery," *Archives of Ophthalmology*, vol. 83, no. 3, pp. 286–293, 1970.

[4] S. De Bustros, J. T. Thompson, R. G. Michels, T. A. Rice, and B. M. Glaser, "Vitrectomy for idiopathic epiretinal membranes causing macular pucker," *British Journal of Ophthalmology*, vol. 72, no. 9, pp. 692–695, 1988.

[5] S. De Bustros, T. A. Rice, R. G. Michels, J. T. Thompson, S. Marcus, and B. M. Glaser, "Vitrectomy for macular pucker. Use after treatment of retinal tears or retinal detachment," *Archives of Ophthalmology*, vol. 106, no. 6, pp. 758–760, 1988.

[6] A. Uemura, H. Ideta, H. Nagasaki, H. Morita, and K. Ito, "Macular pucker after retinal detachment surgery," *Ophthalmic Surgery*, vol. 23, no. 2, pp. 116–119, 1992.

[7] M. S. Heo, H. W. Kim, J. E. Lee, S. J. Lee, and I. H. Yun, "The clinical features of macular pucker formation after pars plana vitrectomy for primary rhegmatogenous retinal detachment repair," *Korean Journal of Ophthalmology*, vol. 26, no. 5, pp. 355–361, 2012.

[8] V. Martínez-Castillo, A. Boixadera, L. Distéfano, M. Zapata, and J. García-Arumí, "Epiretinal membrane after pars plana vitrectomy for primary pseudophakic or aphakic rhegmatogenous retinal detachment: incidence and outcomes," *Retina*, vol. 32, no. 7, pp. 1350–1355, 2012.

[9] A. Reichenbach and A. Bringmann, "New functions of Müller cells," *Glia*, vol. 61, no. 5, pp. 651–678, 2013.

[10] D. Ducournau and Y. Ducournau, *A Closer Look at the ILM. A Supplement to Retinal Physician*, 2008.

[11] C. Aras, C. Arici, S. Akar et al., "Peeling of internal limiting membrane during vitrectomy for complicated retinal detachment prevents epimacular membrane formation," *Graefe's Archive for Clinical and Experimental Ophthalmology*, vol. 247, no. 5, pp. 619–623, 2009.

[12] D. Odrobina, M. Bednarski, S. Cisiecki, Z. Michalewska, F. Kuhn, and J. Nawrocki, "Internal limiting membrane peeling as prophylaxis of macular pucker formation in eyes undergoing retinectomy for severe proliferative vitreoretinopathy," *Retina*, vol. 32, no. 2, pp. 226–231, 2012.

[13] D. W. Park, P. U. Dugel, J. Garda et al., "Macular pucker removal with and without internal limiting membrane peeling: pilot study," *Ophthalmology*, vol. 110, no. 1, pp. 62–64, 2003.

[14] A. K. Kwok, T. Y. Lai, W. W. Li, D. C. Woo, and N. R. Chan, "Indocyanine green-assisted internal limiting membrane removal in epiretinal membrane surgery: a clinical and histologic study," *American Journal of Ophthalmology*, vol. 138, no. 2, pp. 194–199, 2004.

[15] H. Shimada, H. Nakashizuka, T. Hattori, R. Mori, Y. Mizutani, and M. Yuzawa, "Double staining with brilliant blue G and double peeling for epiretinal membranes," *Ophthalmology*, vol. 116, no. 7, pp. 1370–1376, 2009.

[16] T. Nakamura, T. Murata, T. Hisatomi et al., "Ultrastructure of the vitreoretinal interface following the removal of the internal limiting membrane using indocyanine green," *Current Eye Research*, vol. 27, no. 6, pp. 395–399, 2003.

[17] S. Wolf, U. Schnurbusch, P. Wiedemann, J. Grosche, A. Reichenbach, and H. Wolburg, "Peeling of the basal membrane in the human retina: ultrastructural effects," *Ophthalmology*, vol. 111, no. 2, pp. 238–243, 2004.

[18] T. Brockmann, C. Steger, M. Westermann et al., "Ultrastructure of the membrana limitans interna after dye-assisted membrane peeling," *Ophthalmologica*, vol. 226, no. 4, pp. 228–233, 2011.

[19] T. Hisatomi, S. Notomi, T. Tachibana et al., "Ultrastructural changes of the vitreoretinal interface during long-term follow-up after removal of the internal limiting membrane," *American Journal of Ophthalmology*, vol. 158, no. 3, pp. 550–556.e1, 2014.

[20] F. Pichi, A. Lembo, M. Morara et al., "Early and late inner retinal changes after inner limiting membrane peeling," *International Ophthalmology*, vol. 34, no. 2, pp. 437–446, 2014.

[21] C. Harada, Y. Mitamura, and T. Harada, "The role of cytokines and trophic factors in epiretinal membranes: involvement of signal transduction in glial cells," *Progress in Retinal and Eye Research*, vol. 25, no. 2, pp. 149–164, 2006.

[22] A. Bringmann and P. Wiedemann, "Involvement of Müller glial cells in epiretinal membrane formation," *Graefe's Archive for Clinical and Experimental Ophthalmology*, vol. 247, no. 7, pp. 865–883, 2009.

[23] L. Iannetti, M. Accorinti, R. Malagola et al., "Role of the intravitreal growth factors in the pathogenesis of idiopathic epiretinal membrane," *Investigative Ophthalmology & Visual Science*, vol. 52, no. 8, pp. 5786–5789, 2011.

[24] G. Wistow, "The NEIBank project for ocular genomics: data-mining gene expression in human and rodent eye tissues," *Progress in Retinal and Eye Research*, vol. 25, no. 1, pp. 43–77, 2006.

[25] A. M. Roth and R. Y. Foos, "Surface wrinkling retinopathy in eyes enucleated at autopsy," *Ophthalmology*, vol. 75, no. 5, pp. 1047–1058, 1971.

[26] K. Y. Nam and J. Y. Kim, "Effect of internal limiting membrane peeling on the development of epiretinal membrane after pars plana vitrectomy for primary rhegmatogenous retinal detachment," *Retina*, vol. 35, no. 5, pp. 880–5, 2015.

[27] Y. Mitamura, C. Harada, and T. Harada, "Role of cytokines and trophic factors in the pathogenesis of diabetic retinopathy," *Current Diabetes Reviews*, vol. 1, no. 1, pp. 73–81, 2005.

[28] N. Shams and T. Ianchulev, "Role of vascular endothelial growth factor in ocular angiogenesis," *Ophthalmology Clinics of North America*, vol. 19, no. 3, pp. 335–344, 2006.

[29] A. P. Adamis, J. W. Miller, M. T. Bernal et al., "Increased vascular endothelial growth factor levels in the vitreous of eyes with proliferative diabetic retinopathy," *American Journal of Ophthalmology*, vol. 118, no. 4, pp. 445–450, 1994.

[30] E. Mandelcorn, Y. Khan, L. Javorska, J. Cohen, D. Howarth, and M. Mandelcorn, "Idiopathic epiretinal membranes: cell type, growth factor expression, and fluorescein angiographic and retinal photographic correlations," *Canadian Journal of Ophthalmology/Journal Canadien d'Ophtalmologie*, vol. 38, no. 6, pp. 457–463, 2003.

[31] Y. S. Chen, S. F. Hackett, C. L. Schoenfeld, M. A. Vinores, S. A. Vinores, and P. A. Campochiaro, "Localisation of vascular endothelial growth factor and its receptors to cells of vascular and avascular epiretinal membranes," *British Journal of Ophthalmology*, vol. 81, no. 10, pp. 919–926, 1997.

[32] D. H. Nam, J. Oh, J. H. Roh, and K. Huh, "Different expression of vascular endothelial growth factor and pigment epithelium-derived factor between diabetic and non-diabetic epiretinal membranes," *Ophthalmologica*, vol. 223, no. 3, pp. 188–191, 2009.

[33] K. M. Selim, D. Sahan, T. Muhittin, C. Osman, and O. Mustafa, "Increased levels of vascular endothelial growth factor in the aqueous humor of patients with diabetic retinopathy," *Indian Journal of Ophthalmology*, vol. 58, no. 5, pp. 375–379, 2010.

[34] S. Takahashi, K. Adachi, Y. Suzuki, A. Maeno, and M. Nakazawa, "Profiles of inflammatory cytokines in the vitreous fluid from patients with rhegmatogenous retinal detachment and their correlations with clinical features," *BioMed Research International*, vol. 2016, Article ID 4256183, 9 pages, 2016.

[35] S. Myojin, T. Yoshimura, S. Yoshida et al., "Gene expression analysis of the irrigation solution samples collected during vitrectomy for idiopathic epiretinal membrane," *PLoS One*, vol. 11, article e0164355, no. 10, 2016.

[36] R. Y. Foos, "Vitreoretinal juncture; epiretinal membranes and vitreous," *Investigative Ophthalmology & Visual Science*, vol. 16, no. 5, pp. 416–422, 1977.

[37] M. B. Bellhorn, A. H. Friedman, G. N. Wise, and P. Henkind, "Ultrastructure and clinicopathologic correlation of idiopathic preretinal macular fibrosis," *American Journal of Ophthalmology*, vol. 79, no. 3, pp. 366–373, 1975.

[38] R. I. Kohno, Y. Hata, S. Kawahara et al., "Possible contribution of hyalocytes to idiopathic epiretinal membrane formation and its contraction," *British Journal of Ophthalmology*, vol. 93, no. 8, pp. 1020–1026, 2009.

[39] A. Nemet, A. Moshiri, G. Yiu, A. Loewenstein, and E. Moisseiev, "A review of innovations in rhegmatogenous retinal detachment surgical techniques," *Journal of Ophthalmology*, vol. 2017, Article ID 4310643, 5 pages, 2017.

[40] M. Rinaldi, R. dell'Omo, F. Morescalchi et al., "ILM peeling in nontractional diabetic macular edema: review and metanalysis," *International Ophthalmology*, pp. 1–6, 2017.

[41] A. Díaz-Valverde and L. Wu, "To peel or not to peel the internal limiting membrane in idiopathic epiretinal membranes," *Retina*, p. 1, 2017.

[42] H. Terasaki, Y. Miyake, R. Nomura et al., "Focal macular ERGs in eyes after removal of macular ILM during macular hole surgery," *Investigative Ophthalmology & Visual Science*, vol. 42, pp. 229–234, 2001.

[43] Y. Ito, H. Terasaki, A. Takahashi, T. Yamakoshi, M. Kondo, and M. Nakamura, "Dissociated optic nerve fiber layer appearance after internal limiting membrane peeling for idiopathic macular holes," *Ophthalmology*, vol. 112, no. 8, pp. 1415–1420, 2005.

[44] C. Haritoglou, C. A. Gass, M. Schaumberger, O. Ehrt, A. Gandorfer, and A. Kampik, "Macular changes after peeling of the internal limiting membrane in macular hole surgery," *American Journal of Ophthalmology*, vol. 132, no. 3, pp. 363–368, 2001.

[45] F. Semeraro, F. Morescalchi, S. Duse, E. Gambicorti, A. Russo, and C. Costagliola, "Current trends about inner limiting membrane peeling in surgery for epiretinal membranes," *Journal of Ophthalmology*, vol. 2015, Article ID 671905, 13 pages, 2015.

[46] X. Gao, Y. Ikuno, S. Fujimoto, and K. Nishida, "Risk factors for development of full-thickness macular holes after pars plana vitrectomy for myopic foveoschisis," *American Journal of Ophthalmology*, vol. 155, no. 6, pp. 1021–1027.e1, 2013.

[47] S. Sakimoto, Y. Ikuno, S. Fujimoto, H. Sakaguchi, and K. Nishida, "Characteristics of the retinal surface after internal limiting membrane peeling in highly myopic eyes," *American Journal of Ophthalmology*, vol. 158, no. 4, pp. 762–768.e1, 2014.

[48] R. Tadayoni, I. Svorenova, A. Erginay, A. Gaudric, and P. Massin, "Decreased retinal sensitivity after internal limiting membrane peeling for macular hole surgery," *British Journal of Ophthalmology*, vol. 96, no. 12, pp. 1513–1516, 2012.

[49] X. Gao, J. Guo, X. Meng, J. Wang, X. Peng, and Y. Ikuno, "A meta-analysis of vitrectomy with or without internal limiting membrane peeling for macular hole retinal detachment in the highly myopic eyes," *BMC Ophthalmology*, vol. 16, no. 1, p. 87, 2016.

Hindawi
Journal of Ophthalmology
Volume 2018, Article ID 5978293, 10 pages
https://doi.org/10.1155/2018/5978293

Research Article

Phenotypic Variation in a Four-Generation Family with Aniridia Carrying a Novel *PAX6* Mutation

Grace M. Wang,[1] Lev Prasov,[1] Hayder Al-Hasani,[1,2] Colin E. R. Marrs,[1] Sahil Tolia,[1] Laurel Wiinikka-Buesser,[1] Julia E. Richards,[1,2] and Brenda L. Bohnsack[1]

[1]*Department of Ophthalmology and Visual Sciences, W.K. Kellogg Eye Center, The University of Michigan, Ann Arbor, MI 48105, USA*
[2]*Department of Epidemiology, The University of Michigan, Ann Arbor, MI 48109, USA*

Correspondence should be addressed to Brenda L. Bohnsack; brendabo@med.umich.edu

Received 11 December 2017; Accepted 5 February 2018; Published 4 April 2018

Academic Editor: Jesús Pintor

Aniridia is a congenital disease that affects almost all eye structures and is primarily caused by loss-of-function mutations in the *PAX6* gene. The degree of vision loss in aniridia varies and is dependent on the extent of foveal, iris, and optic nerve hypoplasia and the presence of glaucoma, cataracts, and corneal opacification. Here, we describe a 4-generation family in which 7 individuals across 2 generations carry a novel disease-causing frameshift mutation (NM_000280.4(PAX6):c.565TC>T) in *PAX6*. This mutation results in an early stop codon in exon 8, which is predicted to cause nonsense-mediated decay of the truncated mRNA and a functionally null *PAX6* allele. Family members with aniridia showed differences in multiple eye phenotypes including iris and optic nerve hypoplasia, congenital and acquired corneal opacification, glaucoma, and strabismus. Visual acuity ranged from 20/100 to less than 20/800. Patients who required surgical intervention for glaucoma or corneal opacification had worse visual outcomes. Our results show that family members carrying a novel *PAX6* frameshift mutation have variable expressivity, leading to different ocular comorbidities and visual outcomes.

1. Introduction

Familial aniridia is a congenital disease caused by autosomal dominant mutations in the *PAX6* gene that disrupt the development and function of almost all eye structures [1, 2]. While aniridia is named for iris hypoplasia, a feature of the trait that is often readily evident without a specialized examination, the main causes of early visual impairment are optic nerve and foveal hypoplasia. Further, many affected individuals suffer progressive vision loss due to glaucoma or limbal stem cell deficiency. The severity of visual impairment and phenotypic expression in affected individuals varies [3–5].

The *PAX6* gene, located on chromosome 11p13, encodes a transcription factor that is vital for ocular development [6, 7]. *PAX6* is expressed in the surface ectoderm and neural ectoderm during early eye development and is essential for the specification and differentiation of the cornea, lens, ciliary body, retina, and optic nerve [8–16]. To date, 221 mutations in *PAX6* have been reported; most are associated with aniridia, though some mutations are associated with other ocular diseases such as coloboma, morning glory disc anomaly, anterior segment dysgenesis, and cataract with late-onset corneal dystrophy (ClinVar: PAX6[gene]) [2–6, 17–37]. Due to its gene-dosage effect, decreased protein function or expression of a single copy of *PAX6* results in characteristic ocular malformations [11, 17, 20, 38]. While aniridia can be sporadic, the mode of inheritance for the familial form is considered autosomal dominant; however, unlike classical autosomal dominance, PAX6 inheritance shows two phenotypes associated with the different genotypic combinations. Specifically, the presence of one defective copy of PAX6 results in ocular malformations, but mutations in both copies of *PAX6* cause ocular phenotypes that are more severe (e.g., anophthalmia) and brain abnormalities that are incompatible with life [6, 39, 40]. Differences in expressivity are seen when comparing one *PAX6* mutation

to another. However, studies have reported that even within families carrying the same mutation, individuals may have different ocular findings [3, 5, 24, 35]. In the current study, we describe the relationships and detailed phenotypes in a 4-generation family in which individuals affected with aniridia carry a novel loss-of-function *PAX6* frameshift mutation. Our findings confirm that significant intrafamily phenotypic variability occurs among individuals carrying the same *PAX6* mutation.

2. Methods

This study was approved by the University of Michigan Institutional Review Board and complied with the US Health Insurance Portability and Accountability Act of 1996 and the Declaration of Helsinki. Informed consent was obtained either from participating individuals or from parents of minor patients. A retrospective chart review was performed on a family that had four generations of individuals affected by aniridia. The following data were collected: age, sex, ocular diagnoses, and history of intraocular surgeries. Visual acuities, anterior segment and fundus examinations, intraocular pressures (IOP), refraction, strabismus examination, and ocular medications were recorded from the last examination. Visual acuity was determined by Snellen or Allen figure optotypes in adults and verbal children. Teller visual acuity cards with conversion to Snellen equivalent were used in preverbal children. Anterior and posterior segment exams were performed using slit lamp biomicroscopy and indirect ophthalmoscopy. IOPs were obtained by Goldmann applanation, Tono-Pen (Reichert, Depew, NY, USA) or iCare (Revenio, Vantaa, Finland) tonometry.

2.1. PAX6 Mutation Screening. Genomic DNA was extracted from buccal epithelial cells obtained by swabs or mouthwash samples of the recruited individuals using the DNeasy kit (Qiagen, Hilden, Germany). Eleven exons of the *PAX6* coding region were amplified from genomic DNA by polymerase chain reaction (PCR) using AmpliTaq Gold polymerase (Applied Biosystems, Foster City, CA, USA). PCR primers and conditions are listed in Table 1. PCR cycling conditions were as follows: denaturation at 94°C for 10 minutes then amplification with 36 cycles of denaturation at 94°C for 30 seconds, annealing at 60°C for 30 seconds, and extension at 72°C for 1 minute, with a final extension at 72°C for 10 minutes. PCR products were verified by the size of amplicons on a 1% agarose gel electrophoresis, diluted, and sequenced via Sanger dideoxynucleotide partial chain termination sequencing on an ABI3730 DNA Analyzer (Applied Biosystems) at the University of Michigan DNA Sequencing Core. All exons were sequenced with the same primers used for amplification, except exon 8 for which the following primer was additionally used: 5′- AGGCTGTCG GGATATAATGC-3′. All variants were compared to high-quality sequence reads in the Exome Aggregation Consortium (ExAC) database. Segregation was confirmed by screening DNA from all available affected and unaffected individuals in the family.

3. Results

Seven related patients affected with familial aniridia were identified and recruited for this study. There were 3 female and 4 male patients and the ages ranged from 2 to 31 years. Based on information obtained by family history, a 4-generation pedigree was constructed, which included a total of 13 affected individuals (Figure 1). The clinical findings for the 7 patients in which genetic analysis was performed are described in Table 2.

3.1. Patient III-5. Patient III-5 is a 29-year-old male with no previous history of glaucoma or ocular surgeries. He has no history of diabetes or other metabolic abnormalities. At the time of his last examination, his best-corrected visual acuity was 20/150 in each eye individually and 20/100 binocularly. IOPs were 23 mmHg in the right eye and 19 mmHg in the left eye. Slit lamp biomicroscopy of both eyes showed mild corneal pannuses, hypoplastic irides with small remnant stumps, and visually insignificant cortical cataracts. Funduscopic examination revealed bilateral foveal hypoplasia and optic nerve hypoplasia. The cup to disc ratio in the right eye was 0.1 and in the left eye was 0.3. The patient had bilateral small amplitude and high-velocity horizontal nystagmus with no relative null point, and he was orthophoric.

3.2. Patient IV-1. Patient IV-1 is the 3-year-old son of patient III-5. He has a body mass index of 23.7 kg/m^2 and to date has no history of diabetes or other metabolic problems. Unlike his father, he was diagnosed with glaucoma at 4 months of age and underwent placement of a Baerveldt101-350 glaucoma drainage device (Abbott Medical Optics, Santa Ana, CA, USA) in his left eye at 6 months of age and in his right eye at 9 months of age. He also underwent bilateral medial rectus recessions for esotropia at 2 years of age. At his last examination, his best-corrected visual acuity was 20/200 in each eye and binocularly. The patient was not on any glaucoma medications, and IOPs were 13 mmHg in the right eye and 14 mmHg in the left eye. Slit lamp examination of each eye showed a superotemporal glaucoma drainage device with an overlying bleb. The tube in each eye was oriented vertically along the temporal zonules and was not touching the cornea or lens. The corneas were clear with minimal pannuses, the irides were hypoplastic with small remnant stumps, and the lenses were clear. Fundoscopic examination showed foveal and optic nerve hypoplasia. The optic nerves had a cup to disc ratio of 0.0 in each eye. Cycloplegic refraction was $+1.00 + 1.00 \times 90$ in the right eye and $+1.00 + 1.00 \times 80$ in the left eye. Like his father, the patient had bilateral small amplitude and high-velocity horizontal nystagmus with no relative null point, and he was orthophoric in all gazes.

3.3. Patient III-8. Patient III-8 is a 31-year-old woman who is a first cousin of patient III-5. She has a history of type 1 diabetes mellitus that was diagnosed at 5 years of age and has been on an insulin pump since 2009. Her last hemoglobin A1C was 7.7% and her current body mass index was 47.8 kg/m^2. She also has a history of hypothyroidism, which is well-controlled on levothyroxine. She underwent cataract

Table 1: PCR primer sequences.

Exon	Forward primer	Chromosomal coordinates*	Reverse primer	Chromosomal coordinates*	Fragment size
4	TTCCAGTACTTTGTTTCAAGCCCC	chr11:31,806,650-31,806,673	AAACTCGGGCGGGCTGTTCTTAAG	chr11:31,806,160-31,806,183	514 bp
5	CCTCTTCACTCTGCTCTCTT	chr11:31,802,874-31,802,893	ATGAAGAGAGGGCGTTGAGA	chr11:31,802,637-31,802,656	258 bp
5a	TGAAAGTATCATCATATTTGTAG	chr11:31,801,999-31,802,021	GGGAAGTGGACAGAAAACCA	chr11:31,801,785-31,801,804	237 bp
6	TGAAAGTATCATCATATTTGTAG	chr11:31,801,999-31,802,021	AGGAGAGAGCATTGGGCTTA	chr11:31,801,507-31,801,526	515 bp
7	CAGGAGACACTACCATTTGG	chr11:31,800,880-31,800,899	CAGGCCTTCAAATGCAGTCTCACC	chr11:31,800,557-31,800,580	343 bp
8	GGGAATGTTTTGGTGAGGCT	chr11:31,794,891-31,794,910	CAAAGGGCCCTGGCTAAATT	chr11:31,794,540-31,794,559	371 bp
9	GTAGTTCTGGCACAATATGG	chr11:31,794,136-31,794,155	GTACTCTGTACAAGCACCTC	chr11:31,793,950-31,793,969	206 bp
10	GTAGACACAGTGCTAACCTG	chr11:31,793,820-31,793,839	CCCGGAGCAAACAGGTTTAA	chr11:31,793,597-31,793,616	243 bp
11	TTAAACCTGTTTGCTCCGGG	chr11:31,793,597-31,793,616	AGTGCGAAAAGCTCTCAAGGGTGC	chr11:31,793,326-31,793,349	291 bp
12	GCTGTGTGATGTGTTCCTCA	chr11:31,790,891-31,790,910	TTTCCCTTTTCAATCCCCATCCCC	chr11:31,790,566-31,790,589	345 bp
13	CATGTCTGTTTCTCAAAGGGA	chr11:31,790,055-31,790,075	CCCCAGTGGTACAATACAGGACAC	chr11:31,789,782-31,789,805	294 bp

*UCSC human genome, hg38 accessed 9/10/2017. In a 25 μL PCR reaction for each coding exon, 0.3 μL of AmpliTaq Gold (Applied Biosystems), with 2 μL of 25 mM MgCl2, 0.2 of 25 mM dinucleotide triphosphate, and 0.5 μL of 25 mM primers were used. For exon 4, we used 5 μL of Q-solution (Qiagen) and changed MgCl2 volume to to 2.5 μL and accounted for this from the water to keep the reaction volume at 25 μL. In all of the amplicons, genomic DNA was denatured at 94°C for 10 minutes then amplified by 36 cycles of 94°C denaturation for 30 seconds, 60°C annealing for 30 seconds, and 72°C extension for 1 minute with final extension of 72°C for 10 minutes.

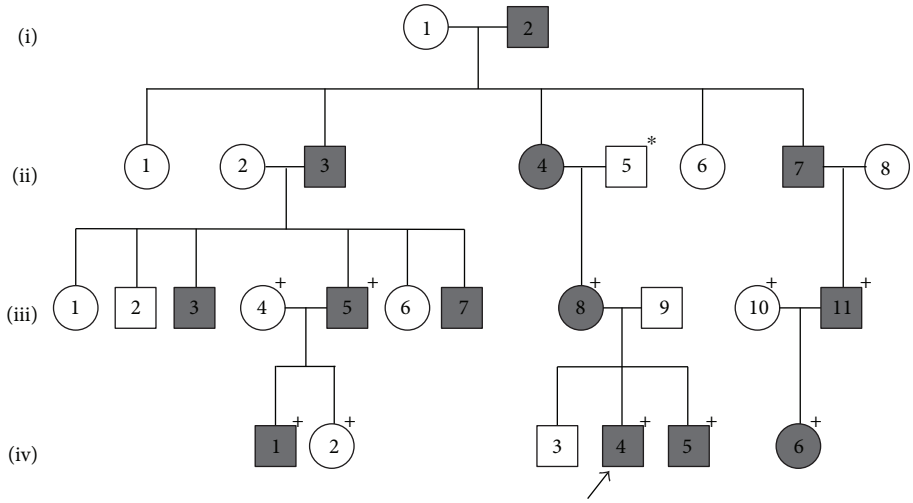

Figure 1: Four-generation family with familial aniridia. Pedigree of a four-generation family in which 13 individuals were affected with familial aniridia (gray circles and gray squares). The plus sign (+) denotes individuals who underwent *PAX6* sequencing and affected individuals with genetic confirmation of the novel frameshift mutation PAX6 p.Ile190SerfsTer17. The arrow indicates the proband. The star (*) indicates a family member with reported aniridia.

extraction with intraocular lens placement in both eyes when she was 15 years old. At 20 years of age, she was diagnosed with glaucoma, which has been managed medically with use of timolol and dorzolamide. She also has a history of a V-pattern exotropia for which she underwent bilateral lateral rectus recessions at 2 years of age and bilateral medial rectus resections and bilateral inferior oblique recessions at 2.5 years of age. She then developed a consecutive esotropia and underwent bilateral medial rectus recessions with inferior transpositions and left inferior oblique anteriorization at 7 years of age. At her last examination, her best-corrected visual acuity was 20/125 in the right eye and 20/200 in the left eye and her IOPs by Goldmann applanation were 14 mmHg in the right eye and 17 mmHg in the left eye. Slit lamp examination showed corneal epithelial irregularities and pannus with neovascularization in both eyes (arrows, Figure 2(a)). The irides were hypoplastic with small remnant stumps (arrowheads, Figure 2(a)). Fundoscopic examination showed foveal hypoplasia. The optic nerves were hypoplastic and had a cup to disc ratio of 0.4 in the right eye and 0.5 in the left eye. Refraction was $-2.25 + 4.00 \times 160$ in the right eye and $-1.50 + 2.50 \times 85$ in the left eye. She had horizontal high-velocity nystagmus of both eyes and a V-pattern exotropia. Per patient and family report, both of her parents had aniridia (II-4 and II-5).

3.4. Patient IV-4. Patient IV-4 is the 10-year-old son of patient III-8 and second cousin of patient IV-1. His last body mass index was 23.8 kg/m^2 and to date has no history of diabetes or other metabolic abnormalities. He was diagnosed with glaucoma at 5 years of age and underwent placement of Baerveldt 101-350 glaucoma drainage devices in both eyes at 6 years of age. He also has a history of a V-pattern esotropia and bilateral medial rectus recessions with half tendon infraplacement. Further, bilateral inferior oblique partial anteriorization was performed at 3 years of age. At his last examination, his best-corrected visual acuity was 20/300 in the right eye, 20/250 in the left eye, and 20/200 binocularly. IOPs were 14 mmHg in the right eye and 17 mmHg in the left eye on timolol and dorzolamide in both eyes. Slit lamp examination showed superotemporal glaucoma drainage devices with overlying blebs. The tubes were in the anterior chamber, oriented vertically along the temporal zonules without corneal or lens touch. Both corneas had 360 degrees of pannus with neovascularization (arrows, Figure 2(b)). In the right eye, the pannus extended into the visual axis and had underlying corneal stromal haze. The irides were hypoplastic with short remnant stumps (arrowheads, Figure 2(b)). There were mild cortical and posterior subcapsular cataracts that were not visually significant. Fundoscopic examination showed optic nerve and foveal hypoplasia. The optic nerves had a cup to disc ratio of 0.8 and 0.6 for the right and left eye, respectively. Cycloplegic refraction was −3.50 in the right eye and −3.00 in the left eye. He had bilateral moderate amplitude and moderate velocity horizontal nystagmus with no null point, and he showed a 50 prism diopter exotropia.

3.5. Patient IV-5. Patient IV-5 is the 3-year-old son of patient III-8, brother of patient IV-4, and second cousin of patient IV-1. He has no history of diabetes or metabolic abnormalities. He was diagnosed with glaucoma at 2 years of age and has been medically managed with timolol and dorzolamide in both eyes. At his last examination, visual acuity by Teller Acuity cards was estimated to be 20/380 in each eye individually and 20/260 binocularly. IOPs were 20 mmHg in the right eye and 15 mmHg in the left eye. Slit lamp examination showed clear corneas without pannuses, and hypoplastic irides were very small remnant stumps. There was a focal cortical cataract in the right eye that was not visually significant. Fundoscopic examination showed foveal hypoplasia in both eyes. The optic nerves had no cupping or evidence of hypoplasia. The patient has a small amplitude, has high-velocity horizontal nystagmus with a null point in left gaze, and has a 45 prism diopter exotropia.

Table 2: Summary of clinical findings.

Patient	VA	Initial anterior segment findings	Initial posterior segment findings	IOP (mmHg) glaucoma meds	Glaucoma diagnosis (Dx) and glaucoma surgeries	Other ocular surgeries
III-5	OD: 20/150 OS: 20/150 OU: 20/100	Corneal pannuses Hypoplastic irides Cortical cataracts	Foveal hypoplasia Optic nerve Hypoplasia	OD: 23 OS: 19 No meds	No glaucoma	OD: none OS: none
IV-1	OD: 20/200 OS: 20/200 OU: 20/200	Corneal pannuses Hypoplastic irides	Foveal hypoplasia Optic nerve Hypoplasia	OD: 13 OS: 14 No meds	Glaucoma Dx @ 0.3 years OD: s/p Baerveldt 101-350 OS: s/p Baerveldt 101-350	Strabismus: s/p bilateral medial rectus recessions
III-8	OD: 20/125 OS: 20/200	Corneal epithelial irregularities and pannus with neovascularization Hypoplastic irides	Foveal hypoplasia Optic Nerve hypoplasia	OD: 14 OS: 17 Timolol Dorzolamide	Glaucoma Dx @ 20 years No glaucoma surgeries	OD: s/p ECCE-IOL OS: s/p ECCE-IOL Strabismus: s/p bilateral lateral rectus Recessions, s/p Bilateral Inferior Oblique Recessions, s/p Bilateral Medial Rectus Recessions with Inferior Transpositions, s/p Left Inferior Oblique Anteriorization
IV-4	OD: 20/300 OS: 20/250 OU: 20/200	Corneal pannus Cortical and posterior subcapsular cataracts	Foveal hypoplasia Optic nerve Hypoplasia	OD: 14 OS: 17 Timolol Dorzolamide	Glaucoma Dx @ 5 years OD: s/p Baerveldt 101-350 OS: s/p Baerveldt 101-350	Strabismus: s/p bilateral medial rectus recessions with half tendon infraplacement, s/p bilateral inferior oblique partial anteriorization
IV-5	OD: 20/380 OS: 20/380 OU: 20/260	Hypoplastic irides Focal cataract OD	Foveal hypoplasia	OD: 20 OS: 15 Timolol Dorzolamide	Glaucoma Dx @ 2 years No glaucoma surgeries	OD: none OS: none
III-11	OD: CF @ 1 ft OS: CF @ 1 ft	Peters anomaly Partial hypoplastic irides	Foveal hypoplasia	OD: 20 OS: 15 Timolol	Glaucoma Dx @ 6 years OD: none OS: s/p trabeculectomy with mitomycin C × 2, s/p cyclophotocoagulation × 2	OD: s/p penetrating keratoplasty OS: s/p ECCE, s/p superficial keratectomy, s/p penetrating keratoplasty
IV-6	OD: 20/150 OS: 20/100	Corneal pannuses Hypoplastic irides Posterior subcapsular cataracts	Foveal hypoplasia	OD: unable OS: unable	No glaucoma	OD: none OS: none

ECCE: extracapsular cataract extraction; IOL: intraocular lens; CF: counting fingers.

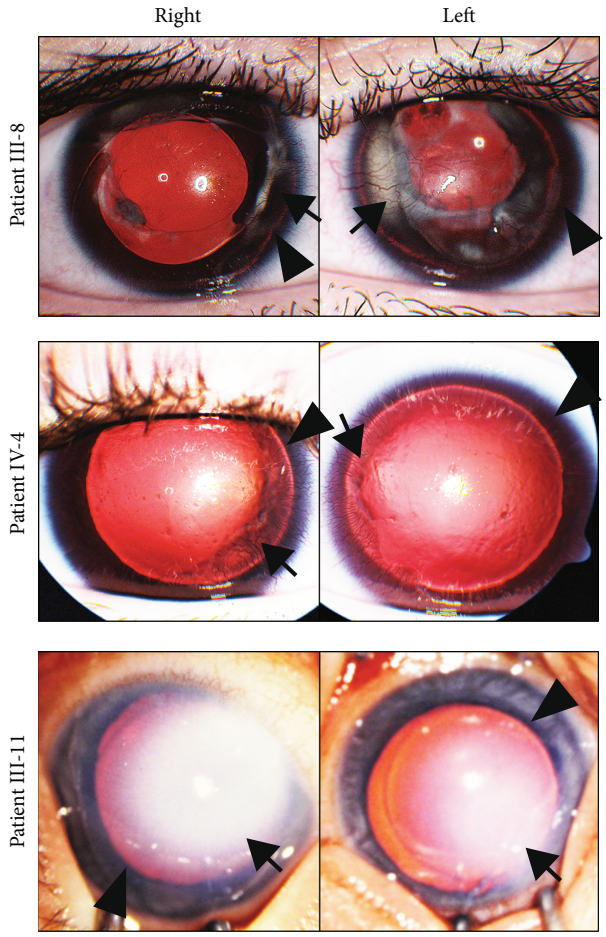

Figure 2: Phenotypic variations in individuals with *PAX6* p.Ile190SerfsTer17. mutation. Anterior segment photographs of the right and left eyes of individuals with the *PAX6* NM_000280.4(PAX6):c.565TC>T frameshift mutation showed phenotypic variation. Patient III-8 (a) at 31 years of age had almost complete iris hypoplasia with small remnant stumps (arrowheads), intraocular lenses, and corneal pannuses with neovascularization (arrows) in both eyes. In the left eye, the corneal pannus was associated with underlying stromal scarring. Patient IV-4 (b) at 5 years of age, prior to placement of glaucoma drainage devices, had corneal pannuses with neovascularization (arrows) and corneal epithelial irregularities in both eyes. Patient IV-4 also had almost complete iris hypoplasia with small remnant stumps (arrowheads) in both eyes. Patient III-11 (c) at 2 months of age, prior to penetrating keratoplasty, had bilateral central corneal opacities consistent with Peters anomaly (arrows) with the opacity of the right eye much denser than the left eye. However, patient III-11 exhibited only partial iris hypoplasia (arrowheads) in both eyes.

His cycloplegic refraction was $-3.50 + 2.00 \times 120$ in the right eye and $-3.50 + 2.00 \times 60$ in the left eye.

3.6. Patient III-11. Patient III-11 is a 29-year-old male who is first cousins with patient III-4 and patient III-8. He has no history of diabetes or metabolic abnormalities. His ocular history is notable for bilateral Peters anomaly and partial iris hypoplasia (Figure 2(c)). At 2 months of age, he underwent penetrating keratoplasty of the right eye, which subsequently became vascularized and was not replaced due to poor visual potential. In the left eye, he underwent extracapsular cataract extraction at 2 years of age. He developed glaucoma of the left eye, which necessitated 2 trabeculectomies with mitomycin C at 6 years of age and 2 treatments of cyclophotocoagulation at 7 years of age. The left cornea underwent a superficial keratectomy for band keratopathy at 9 years of age and then penetrating keratoplasty at 11 years of age. The left corneal graft was complicated by persistent epithelial defects and by 20 years of age, the graft had failed and the patient did not desire repeat penetrating keratoplasty. At his last examination, he was not able to see the 20/800 optotypes and was only able to detect the number of fingers held at 1 foot in front of each eye. IOPs were 20 mmHg in the right eye and 15 mmHg in the left eye on timolol. Slit lamp examination on the right showed a corneal graft with central and inferior conjunctivalization, hypoplastic iris, and white cataract. The left eye had a corneal graft with diffuse stromal thickening, band keratopathy, and 360 degrees of pannus and hypoplastic iris. Neither eye had a view to the fundus.

3.7. Patient IV-6. Patient IV-6 is a 5-year-old daughter of patient III-11 and second cousin to patients IV-1, IV-4, and IV-5 and has no history of diabetes or metabolic abnormalities. Further, she has no history of glaucoma or previous ocular surgeries. At her last examination, her best-corrected visual acuity was 20/150 in the right eye and 20/100 in the left eye. She was unable to tolerate IOP testing, but both eyes were soft by digital palpation. Slit lamp examination of both eyes showed mild corneal pannuses, small remnant iris stumps, and trace visually insignificant posterior subcapsular cataracts. Fundoscopic examination showed foveal hypoplasia and normal optic nerves with cup to disc ratios of 0.2 in both eyes. Cycloplegic refraction was $+0.2\ 5 + 4.25 \times 102$ in the right eye and $+1.25 + 5.00 \times 70$ in the left eye. She had a 9 prism diopter esotropia and horizontal nystagmus of both eyes.

3.8. PAX6 Mutational Analysis. The paired homeobox gene PAX6 gene on chromosome 11p13 comprises two major splice forms, with a total of 14 exons, including 11 coding exons. *PAX6* gene sequencing was performed on all seven patients in this study, and three unaffected family members A novel frameshift mutation from a single nucleotide deletion (NM_000280.4(PAX6):c.565TC>T) was found to perfectly segregate in all seven patients with aniridia and was absent in family members without aniridia (Figure 3). Individual III-8 was found to carry a single *PAX6* mutation presumably inherited from her mother, despite the reported history that both of her parents had aniridia. This frameshift mutation p.Ile190SerfsTer17 in exon 8 of *PAX6* is predicted to cause an early stop codon and a functionally null *PAX6* allele. This mutation was not found in the ClinVar or ExAC databases.

4. Discussion

The ocular phenotypes associated with *PAX6* mutations underscore the essential role of *PAX6* in eye development.

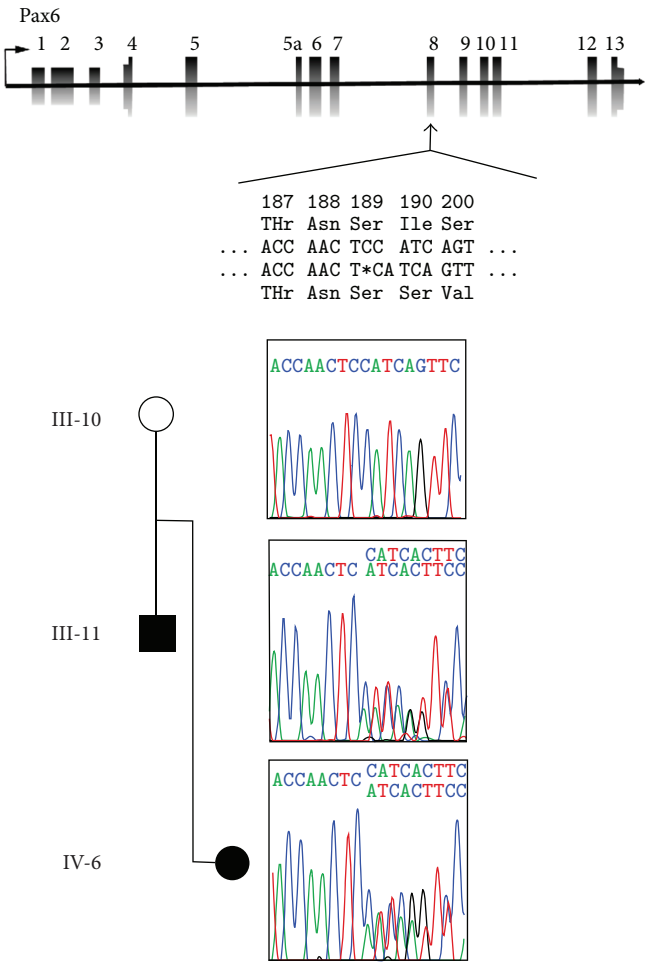

Figure 3: Sequencing confirming *PAX6* frameshift mutation. Schematic of *PAX6* gene shows the location of the NM_000280.4(PAX6):c.565TC>T frameshift mutation and its effect on the coding protein. The Sanger chromatogram traces show transmission of the mutation from father (III-11) to daughter (IV-6) in one branch of the family and absence of the mutation in the unaffected mother (III-10).

The "classic" presentation of aniridia includes iris, optic nerve, and foveal hypoplasia and congenital cataracts with progressive corneal opacification due to limbal stem cell deficiency [1, 20, 41]. In addition, approximately 50% of affected individuals have glaucoma secondary to anterior rotation of the iris root and/or inherent goniotrabeculodysgenesis [26, 32, 38, 42, 43]. However, there is a phenotypic spectrum associated with *PAX6* mutations, which can include some to all of the abovementioned ophthalmic findings as well as congenital corneal opacification (Peters anomaly), anterior segment dysgenesis, and colobomas [4, 6, 17, 20, 25, 32, 34].

PAX6 is a transcription factor, which has 2 DNA-binding domains, a long paired domain, and a homeodomain [44]. Disease-causing mutations span the *PAX6* coding sequence and regulatory regions. Missense mutations are associated with milder phenotypes such as isolated congenital cataracts, anterior segment dysgenesis, and colobomas [2, 6, 27, 32, 34, 45]. In contrast, large deletions and mutations that cause premature stop codons are associated with aniridia. We identified a novel frameshift mutation (NM_000280.4(PAX6):c.565TC>T) from a single nucleotide deletion in exon 8, which encodes the initial homeodomain sequence. It is hypothesized that truncated mutant *PAX6* mRNA is degraded through nonsense-mediated decay prior to translation [42, 43]. Thus, it is predicted to be a complete loss of a function *PAX6* allele, consistent with the aniridia phenotype.

In the current study, we present an example of phenotypic variation in a 4-generation family with aniridia. Of the 7 affected individuals who were genotyped, the visual acuity ranged from 20/100 to worse than 20/800. Within our family, all affected individuals had foveal hypoplasia, which is the main cause of visual impairment. Six of the 7 individuals had almost complete iris hypoplasia. Two individuals had progressive corneal irregularities with significant pannus and corneal neovascularization, due to severe limbal stem cell deficiency. Five individuals were diagnosed with glaucoma between 4 months and 20 years of age, and 3 required surgery to obtain IOP control. Most notably, one individual had bilateral congenital corneal opacifications (Peters anomaly), which resulted in poor vision after failed corneal transplantation in both eyes. These results indicate that the same *PAX6* mutation can yield a wide range of ocular phenotypes and that more severe visual impairment correlated with glaucoma and corneal opacification, requiring surgical intervention.

The phenotypic variation associated with *PAX6* mutations may be due to differences in genetic background that affect the expression of *PAX6* coregulators and downstream targets. *PAX6* encodes a transcription factor that is an early marker of neural epithelium and demarcates specific domains of the developing central nervous system. Within the neural epithelial-derived optic vesicle, animal studies have demonstrated that *Pax6* acts together with additional transcription factors such as *Pax2*, *Six6*, *Gsx2*, *Pax5*, and *Lhx2* to regulate invagination to form the bilayered cup that will become the retina, retinal pigmented epithelium, and iris pigmented epithelium [8, 10, 12, 46]. Further, *Pax6* is specifically expressed in the lens placode through a combination of activation by *Sox2*, *Oct-1*, and *Foxe3* in the surface ectoderm and inhibition by TGFβ and Wnt signaling in the periocular neural crest [47–51]. Together, these signaling pathways stimulate separation of the lens vesicle from the overlying surface ectoderm and neural crest migration into the anterior segment. Minor alterations in expression or function of these additional signaling pathways and coregulators through single nucleotide polymorphism variants may exacerbate or mitigate the effect of a *PAX6* mutation during different processes of eye development.

Transcriptional and epigenetic regulation also alter the function of *PAX6*, which may result in different ocular phenotypes. The *PAX6* locus is complex and is regulated by three promoters. The P0 and P1 promoters drive expression of the *Pax6* transcript and the alternatively spliced *Pax6(5a)* variant, while the internal Pα promotor encodes truncated Pax6 p32 proteins that lack the DNA-binding paired domain [52, 53]. The specific regulation of the Pα promoter and the function of these truncated proteins have yet to be

determined. In addition, the paired domain of *Pax6(5a)* has a different DNA-binding capacity, and this variant primarily plays a role in iris formation [54]. Stochastic events, which may differentially regulate the transcription and activity of *Pax6* and the *Pax6(5a)* variant, may influence phenotype. Further, epigenetic alteration of *PAX6* regulates DNA binding, transcriptional activation, and protein degradation. For example, posttranslational sumoylation of the Pax6 p32 protein by SUMO-1 enhances DNA-binding activity of the homeodomain and increases transcriptional activation of target proteins [55]. In contrast, Trim11, a ubiquitin E3 ligase decreases *PAX6* activity by tagging the protein for degradation by the proteasome [56]. In addition, the DNA-binding activity of the *PAX6* homeobox domain is modified by histone variants such as *H3K4me1*, *H3K27ac*, *H3K4m3*, and *H3K37me3* [57]. Thus, *PAX6* transcription and protein function are regulated at multiple levels, all of which are targets for differential expression and activity in the functional copy of PAX6. These may account for the phenotypic variability in the ocular findings associated with dominantly inherited *PAX6* null mutations.

In addition to its role in ocular development, *PAX6* has been shown to regulate pancreatic islet cell development [58, 59]. The clinical implications of *PAX6* mutations on glucose tolerance are unclear as published studies include few patients and show conflicting results [60, 61]. In our study, only 1 patient had a history of type 1 diabetes, while the remainder of the individuals had no history of glucose intolerance. Additional studies, which include a larger number of individuals with aniridia, are required to better understand whether *PAX6* mutations also have phenotypic variability in regards to glucose regulation.

In the current study, we describe a novel disease-causing frameshift mutation (NM_000280.4(PAX6):c.565TC>T) in *PAX6* in a 4-generation family affected with aniridia. Family members with aniridia showed phenotypic variation and differences in visual outcomes that correlated with surgical intervention for glaucoma or corneal opacification. Further studies which investigate modifications and interactions of *PAX6* are required for better understanding of the phenotypic variations in aniridia.

5. Conclusions

We describe a novel disease-causing frameshift mutation (NM_000280.4(PAX6):c.565TC > T) in *PAX6* which showed phenotypic variation in a 4-generation family. Differences in ocular comorbidities resulted in a range of visual outcomes in affected individuals.

Disclosure

A portion of this manuscript was presented at the 2017 Annual Meeting of the American Association of Pediatric Ophthalmology and Strabismus and published with the meeting abstracts in J AAPOS [62]. The authors alone are responsible for the content and writing of this article.

Conflicts of Interest

The authors report no conflicts of interest.

Acknowledgments

This study is funded in part by Research to Prevent Blindness and a grant from the Public Health Genetics Certificate Program of the University of Michigan School of Public Health.

References

[1] S. C. Brauner, D. S. Walton, and T. C. Chen, "Aniridia," *International Ophthalmology Clinics*, vol. 48, no. 2, pp. 79–85, 2008.

[2] A. Cvekl and P. Callaerts, "Pax6: 25th anniversary and more to learn," *Experimental Eye Research*, vol. 156, pp. 10–21, 2017.

[3] S. K. Dubey, N. Mahalaxmi, P. Vijayalakshmi, and P. Sundaresan, "Mutational analysis and genotype-phenotype correlations in southern Indian patients with sporadic and familial aniridia," *Molecular Vision*, vol. 21, pp. 88–97, 2015.

[4] M. Hingorani, K. A. Williamson, A. T. Moore, and V. van Heyningen, "Detailed ophthalmologic evaluation of 43 individuals with PAX6 mutations," *Investigative Ophthalmology & Visual Science*, vol. 50, no. 6, p. 2581, 2009.

[5] T. Yokoi, S. Nishina, M. Fukami et al., "Genotype-phenotype correlation of PAX6 gene mutations in aniridia," *Human Genome Variation*, vol. 3, no. 1, article 15052, 2016.

[6] T. Glaser, L. Jepeal, J. G. Edwards, S. R. Young, J. Favor, and R. L. Maas, "PAX6 gene dosage effect in a family with congenital cataracts, aniridia, anophthalmia and central nervous system defects," *Nature Genetics*, vol. 7, no. 4, pp. 463–471, 1994.

[7] T. Glaser, D. S. Walton, and R. L. Maas, "Genomic structure, evolutionary conservation and aniridia mutations in the human PAX6 gene," *Nature Genetics*, vol. 2, no. 3, pp. 232–239, 1992.

[8] R. Ashery-Padan, T. Marquardt, X. Zhou, and P. Gruss, "Pax6 activity in the lens primordium is required for lens formation and for correct placement of a single retina in the eye," *Genes & Development*, vol. 14, no. 21, pp. 2701–2711, 2000.

[9] N. Bäumer, T. Marquardt, A. Stoykova, R. Ashery-Padan, K. Chowdhury, and P. Gruss, "Pax6 is required for establishing naso-temporal and dorsal characteristics of the optic vesicle," *Development*, vol. 129, no. 19, pp. 4535–4545, 2002.

[10] M. V. Canto-Soler and R. Adler, "Optic cup and lens development requires Pax6 expression in the early optic vesicle during a narrow time window," *Developmental Biology*, vol. 294, no. 1, pp. 119–132, 2006.

[11] N. Davis, C. Yoffe, S. Raviv et al., "Pax6 dosage requirements in iris and ciliary body differentiation," *Developmental Biology*, vol. 333, no. 1, pp. 132–142, 2009.

[12] J. C. Grindley, D. R. Davidson, and R. E. Hill, "The role of Pax-6 in eye and nasal development," *Development*, vol. 121, no. 5, pp. 1433–1442, 1995.

[13] R. E. Hill, J. Favor, B. L. M. Hogan et al., "Mouse small eye results from mutations in a paired-like homeobox-containing gene," *Nature*, vol. 354, no. 6354, pp. 522–525, 1991.

[14] B. L. Hogan, E. M. Hirst, G. Horsburgh, and C. M. Hetherington, "Small eye (Sey): a mouse model for the analysis of craniofacial abnormalities," *Development*, vol. 103, pp. 115–119, 1988.

[15] M. Kroeber, N. Davis, S. Holzmann et al., "Reduced expression of Pax6 in lens and cornea of mutant mice leads to failure of chamber angle development and juvenile glaucoma," *Human Molecular Genetics*, vol. 19, no. 17, pp. 3332–3342, 2010.

[16] S. Nornes, M. Clarkson, I. Mikkola et al., "Zebrafish contains two Pax6 genes involved in eye development," *Mechanisms of Development*, vol. 77, no. 2, pp. 185–196, 1998.

[17] N. Azuma, Y. Yamaguchi, H. Handa et al., "Mutations of the PAX6 gene detected in patients with a variety of optic-nerve malformations," *The American Journal of Human Genetics*, vol. 72, no. 6, pp. 1565–1570, 2003.

[18] F. Bayrakli, I. Guney, Y. Bayri et al., "A novel heterozygous deletion within the 3′ region of the PAX6 gene causing isolated aniridia in a large family group," *Journal of Clinical Neuroscience*, vol. 16, no. 12, pp. 1610–1614, 2009.

[19] S. Bhatia, H. Bengani, M. Fish et al., "Disruption of autoregulatory feedback by a mutation in a remote, ultraconserved PAX6 enhancer causes aniridia," *The American Journal of Human Genetics*, vol. 93, no. 6, pp. 1126–1134, 2013.

[20] A. Brown, M. McKie, V. van Heyningen, and J. Prosser, "The human PAX6 mutation database," *Nucleic Acids Research*, vol. 26, no. 1, pp. 259–264, 1998.

[21] P. Chen, X. Zang, D. Sun et al., "Mutation analysis of paired box 6 gene in inherited aniridia in northern China," *Molecular Vision*, vol. 19, pp. 1169–1177, 2013.

[22] F. Cheng, W. Song, Y. Kang, S. Yu, and H. Yuan, "A 556 kb deletion in the downstream region of the PAX6 gene causes familial aniridia and other eye anomalies in a Chinese family," *Molecular Vision*, vol. 17, pp. 448–455, 2011.

[23] A. V. D'Elia, L. Pellizzari, D. Fabbro et al., "A deletion 3′ to the PAX6 gene in familial aniridia cases," *Molecular Vision*, vol. 13, pp. 1245–1250, 2007.

[24] I. De Becker, M. Walter, and L.-P. Noel, "Phenotypic variations in patients with a 1630 A>T point mutation in the PAX6 gene," *Canadian Journal of Ophthalmology*, vol. 39, no. 3, pp. 272–278, 2004.

[25] M. Sarfarazi, R. R. McInnes, E. F. Percin et al., "Human microphthalmia associated with mutations in the retinal homeobox gene CHX10," *Nature Genetics*, vol. 25, no. 4, pp. 397–401, 2000.

[26] E. Gramer, C. Reiter, and G. Gramer, "Glaucoma and frequency of ocular and general diseases in 30 patients with aniridia: a clinical study," *European Journal of Ophthalmology*, vol. 22, no. 1, pp. 104–110, 2018.

[27] I. M. Hanson, J. M. Fletcher, T. Jordan et al., "Mutations at the PAX6 locus are found in heterogeneous anterior segment malformations including Peters' anomaly," *Nature Genetics*, vol. 6, no. 2, pp. 168–173, 1994.

[28] Y. Kang, Y. Lin, X. Li et al., "Mutation analysis of PAX6 in inherited and sporadic aniridia from northeastern China," *Molecular Vision*, vol. 18, pp. 1750–1754, 2012.

[29] J. D. Lauderdale, J. S. Wilensky, E. R. Oliver, D. S. Walton, and T. Glaser, "3′ deletions cause aniridia by preventing PAX6 gene expression," *Proceedings of the National Academy of Sciences of the United States of America*, vol. 97, no. 25, pp. 13755–13759, 2000.

[30] Y. Lin, X. Liu, S. Yu et al., "PAX6 analysis of two sporadic patients from southern China with classic aniridia," *Molecular Vision*, vol. 18, pp. 2190–2194, 2012.

[31] S. H. Park, M. S. Kim, H. Chae, Y. Kim, and M. Kim, "Molecular analysis of the PAX6 gene for congenital aniridia in the Korean population: identification of four novel mutations," *Molecular Vision*, vol. 18, pp. 488–494, 2012.

[32] J. Prosser and V. van Heyningen, "PAX6 mutations reviewed," *Human Mutation*, vol. 11, no. 2, pp. 93–108, 1998.

[33] D. O. Robinson, R. J. Howarth, K. A. Williamson, V. van Heyningen, S. J. Beal, and J. A. Crolla, "Genetic analysis of chromosome 11p13 and the PAX6 gene in a series of 125 cases referred with aniridia," *American Journal of Medical Genetics Part A*, vol. 146A, no. 5, pp. 558–569, 2008.

[34] I. Tzoulaki, I. M. S. White, and I. M. Hanson, "PAX6 mutations: genotype-phenotype correlations," *BMC Genetics*, vol. 6, no. 1, p. 27, 2005.

[35] A. Wawrocka, B. Budny, S. Debicki, A. Jamsheer, A. Sowinska, and M. R. Krawczynski, "PAX6 3′ deletion in a family with aniridia," *Ophthalmic Genetics*, vol. 33, no. 1, pp. 44–48, 2011.

[36] N. Weisschuh, B. Wissinger, and E. Gramer, "A splice site mutation in the PAX6 gene which induces exon skipping causes autosomal dominant inherited aniridia," *Molecular Vision*, vol. 18, pp. 751–757, 2012.

[37] X. Zhang, P. Wang, S. Li, X. Xiao, X. Guo, and Q. Zhang, "Mutation spectrum of PAX6 in Chinese patients with aniridia," *Molecular Vision*, vol. 17, pp. 2139–2147, 2011.

[38] H. Kokotas and M. B. Petersen, "Clinical and molecular aspects of aniridia," *Clinical Genetics*, vol. 77, no. 5, pp. 409–420, 2010.

[39] B. Schmidt-Sidor, K. Szymańska, K. Williamson et al., "Malformations of the brain in two fetuses with a compound heterozygosity for two PAX6 mutations," *Folia Neuropathologica*, vol. 47, no. 4, pp. 372–382, 2009.

[40] B. D. Solomon, D. E. Pineda-Alvarez, J. Z. Balog et al., "Compound heterozygosity for mutations inPAX6in a patient with complex brain anomaly, neonatal diabetes mellitus, and microophthalmia," *American Journal of Medical Genetics. Part A*, vol. 149A, no. 11, pp. 2543–2546, 2009.

[41] M. Hingorani, I. Hanson, and V. van Heyningen, "Aniridia," *European Journal of Human Genetics*, vol. 20, no. 10, pp. 1011–1017, 2012.

[42] H. Lee, R. Khan, and M. O'Keefe, "Aniridia: current pathology and management," *Acta Ophthalmologica*, vol. 86, no. 7, pp. 708–715, 2008.

[43] L. B. Nelson, G. L. Spaeth, T. S. Nowinski, C. E. Margo, and L. Jackson, "Aniridia: a review," *Survey of Ophthalmology*, vol. 28, no. 6, pp. 621–642, 1984.

[44] C. C. T. Ton, H. Hirvonen, H. Miwa et al., "Positional cloning and characterization of a paired box- and homeobox-containing gene from the aniridia region," *Cell*, vol. 67, no. 6, pp. 1059–1074, 1991.

[45] I. Hanson, A. Churchill, J. Love et al., "Missense mutations in the most ancient residues of the PAX6 paired domain underlie a spectrum of human congenital eye malformations," *Human Molecular Genetics*, vol. 8, no. 2, pp. 165–172, 1999.

[46] H. M. Reza, Y. Takahashi, and K. Yasuda, "Stage-dependent expression of Pax6 in optic vesicle/cup regulates patterning genes through signaling molecules," *Differentiation*, vol. 75, no. 8, pp. 726–736, 2007.

[47] A. Bhinge, J. Poschmann, S. C. Namboori et al., "MiR-135b is a direct PAX6 target and specifies human neuroectoderm by inhibiting TGF-β/BMP signaling," *The EMBO Journal*, vol. 33, no. 1, pp. 1271–1283, 2014.

[48] A. Blixt, H. Landgren, B. R. Johansson, and P. Carlsson, "Foxe3 is required for morphogenesis and differentiation of the

anterior segment of the eye and is sensitive to Pax6 gene dosage," *Developmental Biology*, vol. 302, no. 1, pp. 218–229, 2007.

[49] T. Grocott, S. Johnson, A. P. Bailey, and A. Streit, "Neural crest cells organize the eye via TGF-β and canonical Wnt signalling," *Nature Communications*, vol. 2, p. 265, 2011.

[50] Y. Kamachi, M. Uchikawa, A. Tanouchi, R. Sekido, and H. Kondoh, "Pax6 and SOX2 form a co-DNA binding partner complex that regulates initiation of lens development," *Genes & Development*, vol. 15, no. 10, pp. 1272–1286, 2001.

[51] Y. Ma, K. Certel, Y. Gao et al., "Functional interactions between drosophila bHLH/PAS, Sox, and POU transcription factors regulate CNS midline expression of the slit gene," *The Journal of Neuroscience*, vol. 20, no. 12, pp. 4596–4605, 2000.

[52] C. Carrière, S. Plaza, J. Caboche et al., "Nuclear localization signals, DNA binding, and transactivation properties of quail Pax-6 (Pax-QNR) isoforms," *Cell Growth & Differentiation*, vol. 6, no. 12, pp. 1531–1540, 1995.

[53] P. X. Xu, X. Zhang, S. Heaney, A. Yoon, A. M. Michelson, and R. L. Maas, "Regulation of Pax6 expression is conserved between mice and flies," *Development*, vol. 126, no. 2, pp. 383–395, 1999.

[54] S. Singh, R. Mishra, N. A. Arango, J. M. Deng, R. R. Behringer, and G. F. Saunders, "Iris hypoplasia in mice that lack the alternatively spliced Pax6(5a) isoform," *Proceedings of the National Academy of Sciences of the United States of America*, vol. 99, no. 10, pp. 6812–6815, 2002.

[55] Q. Yan, L. Gong, M. Deng et al., "Sumoylation activates the transcriptional activity of Pax-6, an important transcription factor for eye and brain development," *Proceedings of the National Academy of Sciences of the United States of America*, vol. 107, no. 49, pp. 21034–21039, 2010.

[56] T. C. Tuoc and A. Stoykova, "Trim11 modulates the function of neurogenic transcription factor Pax6 through ubiquitin-proteosome system," *Genes & Development*, vol. 22, no. 14, pp. 1972–1986, 2008.

[57] J. Sun, S. Rockowitz, Q. Xie, R. Ashery-Padan, D. Zheng, and A. Cvekl, "Identification of in vivo DNA-binding mechanisms of Pax6 and reconstruction of Pax6-dependent gene regulatory networks during forebrain and lens development," *Nucleic Acids Research*, vol. 43, no. 14, pp. 6827–6846, 2015.

[58] M. Sander, A. Neubuser, J. Kalamaras, H. C. Ee, G. R. Martin, and M. S. German, "Genetic analysis reveals that PAX6 is required for normal transcription of pancreatic hormone genes and islet development," *Genes & Development*, vol. 11, no. 13, pp. 1662–1673, 1997.

[59] L. St-Onge, B. Sosa-Pineda, K. Chowdhury, A. Mansouri, and P. Gruss, "Pax6 is required for differentiation of glucagon-producing alpha-cells in mouse pancreas," *Nature*, vol. 387, no. 6631, pp. 406–409, 1997.

[60] T. Yasuda, Y. Kajimoto, Y. Fujitani et al., "PAX6 mutation as a genetic factor common to aniridia and glucose intolerance," *Diabetes*, vol. 51, no. 1, pp. 224–230, 2002.

[61] L. Hergott-Faure, S. Borot, C. Kleinclauss, M. Abitbol, and A. Penfornis, "Pituitary function and glucose tolerance in a family with a PAX6 mutation," *Annales d'endocrinologie*, vol. 73, no. 6, pp. 510–514, 2012.

[62] G. M. Wang, L. Prasov, J. Richards, and B. L. Bohnsack, "Phenotypic variation in a four-generation family with aniridia carrying a novel PAX6 mutation," *Journal of AAPOS*, vol. 21, no. 4, pp. e36–e37, 2017.

Hindawi
Journal of Ophthalmology
Volume 2018, Article ID 5926906, 11 pages
https://doi.org/10.1155/2018/5926906

Review Article

Molecular Genetics of Pigment Dispersion Syndrome and Pigmentary Glaucoma: New Insights into Mechanisms

Adrian A. Lahola-Chomiak and Michael A. Walter

Department of Medical Genetics, Faculty of Medicine, University of Alberta, 8-32 Medical Science Building, Edmonton, AB, Canada

Correspondence should be addressed to Adrian A. Lahola-Chomiak; alaholac@ualberta.ca

Received 15 December 2017; Accepted 22 February 2018; Published 26 March 2018

Academic Editor: Lev Prasov

We explore the ideas and advances surrounding the genetic basis of pigment dispersion syndrome (PDS) and pigmentary glaucoma (PG). As PG is the leading cause of nontraumatic blindness in young adults and current tailored interventions have proven ineffective, a better understanding of the underlying causes of PDS, PG, and their relationship is essential. Despite PDS being a subclinical disease, a large proportion of patients progress to PG with associated vision loss. Decades of research have supported a genetic component both for PDS and conversion to PG. We review the body of evidence supporting a genetic basis in humans and animal models and reevaluate classical mechanisms of PDS/PG considering this new evidence.

1. Introduction

Pigment dispersion syndrome (PDS) is the shedding of pigment from the posterior surface of the iris into the anterior segment following the flow of aqueous humour. This shedding does not independently impair vision in most affected individuals. However, a subset of patients with PDS progresses to pigmentary glaucoma (PG) with high intraocular pressure (IOP) and glaucomatous optic neuropathy. To date, although several population studies have established a relationship between these two disorders, the underlying pathology remains cryptic. A heterogeneous and possibly complex genetic component appears to underlie at least a proportion of PDS/PG cases. Understanding this genetic component can not only provide insight into the underlying pathology of PDS/PG but also form the basis for rationally designed therapeutics for this important cause of blindness worldwide.

2. Pathophysiology

The defining characteristic of PDS is the bilateral shedding of pigment from the posterior iris pigment epithelium (IPE) and the subsequent deposition of this pigment in the anterior segment, first described in 1899 [1]. Pigment lost in this way can be visualized gonioscopicly as iris transillumination defects which describe depigmented zones that abnormally allow light to pass through them [2]. These slit-like depigmented zones tend to be observed radially in the midperipheral iris and, according to ultrasound biomicroscopy studies, patients with PDS often have abnormal iridozonular contacts [3, 4]. As described in more detail below, these abnormal contacts have previously been proposed to be responsible for pigment shedding via a mechanical rubbing model [3]. Iris transillumination defects are observed in approximately 86% of patients with PDS [5]. Liberated pigment is transported into the anterior segment via aqueous humour flow. Aqueous humour convection currents are driven primarily by blinking [6] then deposit this pigment in a vertical stripe on the cornea known as a Krukenberg's spindle [1, 7]. This phenotype is observed in around 90% of PDS patients and does not correlate with differences in corneal thickness or density [8, 9]. Possibly, the most important clinical sign in the pathophysiology of PDS is the observation of dense trabecular meshwork pigmentation [7]. PDS patients tend to have a diffuse and uniformly dense pigmented trabecular meshwork, unlike patients with the phenotypically related

pseudoexfoliation syndrome where punctate deposits of material in the trabecular meshwork are observed [10].

Histologic examination has revealed that pigment granules are phagocytosed by both corneal epithelial cells and trabecular meshwork cells rather than being adsorbed onto their surface [11–14]. Phagocytic stress causes alterations to the trabecular meshwork extracellular matrix structure and adhesion [15, 16] which could explain the trabecular meshwork dysfunction observed in PDS/PG patients [14]. In PDS/PG patients, trabecular meshwork cells die and exhibit localized necrosis [17]. The resultant reduced conventional aqueous humour outflow which is likely the primary mechanism in the conversion from PDS to PG as reduced outflow is an established mechanism for IOP increase and glaucomatous optic neuropathy [17, 18]. Nevertheless, the degree of trabecular meshwork pigmentation does not directly correlate with conversion risk but is however related to the severity of optic neuropathy in PG patients [19, 20]. The lens and iris have been suggested to function together in a ball-valve pressure mechanism, called the reverse pupillary block, maintaining one-way aqueous humour flow [21]. Elevated anterior segment pressure may bend the iris posteriorly, increasing iridozonular contact and as a result exacerbate pigment shedding [22, 23]. However, iris bending cannot be solely due to pressure as a study using ex vivo iris explants showed that iris bowing is a normal feature of iris dilator muscle activity and position [24]. Hyperplastic iris dilator muscles have been observed in several patients with PDS, and this dysfunction may contribute to posterior iris bowing [25–27].

Although currently limited, some evidence has accrued to support the involvement of the retinal pigment epithelium (RPE) in PDS/PG. Patients with PDS have significantly lower Arden ratios than patients with primary open-angle glaucoma (POAG) or ocular hypertension (OHT) which may indicate RPE degeneration [28]. Lattice retinal degeneration occurs in 22–33% of PDS/PG cases which is high, despite the known association between PDS and myopia [29–31]. An estimated 12% of eyes with PDS also experience retinal detachment, occurring in 5.5-6.6% of total PDS cases [22, 31, 32]. Together these data support a more general involvement of pigmented cells in the pathology of PDS/PG, but further characterization of possible RPE dysfunction associated with PDS/PG is necessary.

3. Epidemiology

At a population scale, there are three main questions to answer about PDS and PG. As PDS is the underlying condition, it is important to know how many people are affected as well as details regarding their demographic characteristics. The incidence of PDS has been estimated to be between 1.4 per 100,000 to 4.8 per 100,000[5] in the United States. However, some estimates place prevalence as high as 2.45% in the United States [33]. Screening for PDS however is complicated by its subclinical nature, the fact that pigment dispersion is more easily observed in lightly pigmented eyes and the phenomenon of symptom abatement known as "burn-out" [5, 20]. People affected by PDS may not seek out eye exams since their vision is not impaired, and affected individuals may be asymptomatic for obvious pigmentary defects due to "burn-out," together leading to an underestimation of PDS prevalence. Burn-out typically occurs in older individuals and it is possible some patients who present with glaucomatous optic neuropathy, who are then diagnosed with POAG, may be more accurately described as PG cases with burn-out. PDS is known to affect young myopes which may explain some of the structural iris pathologies associated with the disease [7, 31, 34]. North American studies have established a higher prevalence of PDS in white patients and a lower than expected incidence of PDS in black patients [34–36], but the aforementioned ability to more readily detect aberrantly located pigment in light-coloured eyes might lead to an ascertainment bias.

Conversion from PDS to PG is a highly variable and heterogeneous phenomenon impacted by both genetic and environmental factors. For example, despite the prevalence of PDS being approximately equal in both men and women, more males progress to PG [6, 19, 22, 31] and that conversion occurs about a decade earlier in men than women [6, 21, 31, 34, 37]. PDS patients have an increased family history (4–21%) of glaucoma [5, 31, 38]; however, that percentage increases greatly in patients with PG (26–48%) [5, 34, 39, 40]. Rigorous exercise has been shown to induce pigment dispersion, enhance posterior iris bending, and increase IOP which all contribute to conversion risk [41–44]. IOP is a major risk factor for PDS to PG conversion, with the increase in risk being proportional to the increase in IOP [5, 45]. The actual rate of conversion is highly variable between studies and seems to in part depend on the ethnic background of patients. Conversion rates as high as 35–50% have been reported in US populations [19, 37, 46]. However, in another study which evaluated conversion over time, the conversion rate was estimated at 10% at 5 years and 15% at 15 years [5]. In a Latin American cohort, the conversion rate was observed to be 37.5% at 50 months which is in good agreement with US studies [45]. However, in a Pakistani cohort, the observed conversion rate was only 4% at 15 years which may support ethnicity as a risk factor for conversion [47]. Ultimately, the diversity in conversion rates supports the observation of heterogeneous genetic and environmental risk factors. In the Western world, PG represents 1–1.5% of total glaucoma cases and, due to its early age of onset, is the most common cause of nontraumatic glaucoma in young adults [33, 48] making it an important cause of debilitating blindness.

4. Human Genetics

Current research on the genetic component of PDS/PG supports a genetically heterogeneous and possibly complex inheritance model. Analysis of four 3-generation pedigrees with Irish or mixed Western European ancestry affected by PDS/PG supported an autosomal dominant mode of inheritance given the identification of affected individuals in every generation without a sex bias [49]. Using microsatellite markers, a chromosomal region named *GPDS1* (glaucoma-related pigment dispersion syndrome 1) (OMIM ID 600510) was mapped to the human chromosome 7 (7q35-q36) in a subset of patients. To date, this linkage has not been

replicated by other mapping studies. Additionally, no candidate genes in this region have been successfully associated with PDS/PG. Of several genes in the region, the most promising candidate is likely human endothelial nitric oxide synthase (*NOS3*) as it is known to play a role in maintaining vascular tone and dysfunction and may contribute to structural abnormalities of the iris [50–52]. However, mutations in *NOS3* have not been reported to be associated with PDS/PG to date.

Another region, on chromosome 18, has also been associated with PDS/PG in several studies. Using a single pedigree, significant linkage to the 18q11-q21 region was observed [53] and later analysis of four additional pedigrees not linked to *GPDS1* found significant linkage to the 18q21 region, assuming an autosomal dominant mode of inheritance [54]. Finally, there exists one case study of an Estonian man with PDS harbouring novel deletions on both the nearby 18q22 and 2q22.1 [55]. However, as for the *GPDS1* locus, no genes in these regions have been associated with PDS/PG.

Two candidate genes associated more broadly with other subtypes of glaucoma, myocilin (*MYOC*), and lysyl oxidase homolog 1 (*LOXL1*) have shown limited association with PDS/PG. *MYOC* is well known for its association with several subtypes of glaucoma including juvenile open-angle glaucoma (JOAG) and primary open-angle glaucoma (POAG) [56–58]. Several cases of potentially damaging mutations in *MYOC* in patients with PDS/PG have been observed [59–61], and *MYOC* is expressed in several ocular tissues including the iris which makes it biologically plausible, despite its still cryptic biological function. However, the very small number of *MYOC* variants found associated with PDS/PG suggests that MYOC is either a very infrequent cause of PDS/PG or that this association is spurious. Given the phenotypic similarities between pseudoexfoliation syndrome (PXS) and PDS (deposition of material in the anterior segment), several studies have investigated a possible association between *LOXL1*, a gene strongly associated with PXS [62–66], and PDS/PG. To date, no causal association of PDS/PG and LOXL1 variants has been observed [67, 68] but variants in LOXL1 could act as a modifier of both of disease risk and age of onset [67, 69]. Interestingly, a patient with coexisting [70] PXS and PDS has been described, supporting again the idea that these related disorders are separate clinical and genetic entities.

There may be also some overlap between PDS and the rare recessive disease Knobloch syndrome (OMIM number 267750) caused by mutations in *COL18A1* [71, 72]. Knobloch syndrome is a developmental disorder with ocular abnormalities and severe skull formation defects. Recently, it is has been reported that PDS and PG are a hallmark sign of Knobloch syndrome and that understanding PDS/PG is important for management of Knobloch syndrome [73]. However, given the severity of the other diagnostic symptoms of Knobloch syndrome, variants in *COL18A1* are unlikely to cause a large proportion of PDS/PG cases. Two case reports have associated Marfan syndrome (OMIM number 154700) with PDS/PG and suggested that *FBN1* variants, while not causative for PDS, may contribute to conversion to glaucoma [74, 75]. Although glaucoma generally has been associated with Marfan syndrome [76], there currently exists insufficient evidence to associate PDS/PG directly with Marfan syndrome or variants in *FBN1*.

5. Animal Studies

Whereas human studies have failed to elucidate any gene associated with PDS/PG, animal research has successfully identified several genes associated with similar phenotypes. Undoubtedly, the most significant progress has been made using the DBA/2J mouse glaucoma model which has proven invaluable to both PDS/PG research and understanding of glaucomatous optic neuropathy as a whole [77–81]. DBA/2J mice were observed to sporadically develop iris atrophy, pigment dispersion, increased IOP, and glaucoma-like retinal ganglion cell death [81]. Later, the genes responsible for these sporadic phenotypes were mapped to two main genes: *Tryp1* and *Gpnmb* which accounted for the iris atrophy and pigment dispersion respectively [77]. Iris pigment dispersion and associated atrophy have also been observed in several other mouse models and causative genes together implicate melanosome genes as playing a central role in iris pigment dispersion pathogenesis [77, 82–84].

Melanin synthesis is a tightly regulated process whereby potentially cytotoxic intermediates [85] polymerize onto structural protein fibrils in melanosomes and the specialized pigmented organelle in melanocytes. Several genes involved in melanin synthesis have been implicated in iris pigment dispersion and atrophy in mice studies. *Tyrp1* encodes *tyrosinase-related protein 1*, an important melanosome membrane-bound structural component of the tyrosinase complex that oxidizes 5,6-dihydroxyindole-2-carboxylic acid (DHICA), has catalase activity, and modulates tyrosinase (*Tyr*) function [86–88]. In a screen of coat color variants, the $Tyrp1^{b\text{-}lt}$ (*light* coat) allele (which contains a single missense *Tyrp1* mutation) was associated with iris pigment dispersion in the LT/SvEiJ inbred mouse [82, 89]. The $Tyrp1^{b}$ (*brown* coat) allele has two missense mutations and has been shown to cause iris atrophy in both the DBA/2J and YBR/EiJ inbred mouse strains [77, 84, 90]. Mutation of essential cysteine residues in both $Tryp1^{b\text{-}lt}$ and $Tyrp1^{b}$ alleles causes the release of cytotoxic melanin synthesis intermediates from melanosomes leading ultimately to melanocyte cell death [87, 89]. A spontaneous coat colour variant *nm2798* is caused by the *dopachrome tautomerase* (*Dct*) allele $Dct^{slt\text{-}lt3J}$ and is associated with iris pigment dispersion [82]. Dct is another protein in the tyrosinase complex and also participates in melanin synthesis by converting dopachrome to DHICA [91]. Mutations of *Dct* are likely to cause melanosomal dysfunction and melanocyte toxicity via escape or accumulation of cytotoxic melanin synthesis intermediates [85, 86, 91, 92]. A large-scale genetic analysis of genetic modifiers of the iris transillumination defect in the DBA/2J mouse model identified the *oculocutaneous albinism type 2* (*Oca2*) gene, an important regulator of melanin synthesis through melanosomal pH control [93, 94]. The human homologue *OCA2* also has a direct tie to iris pigmentation, being the causative loci for both its namesake disease, oculocutaneous albinism type 2 (OMIM number 203200) and iris color [94–98].

Several genes important to melanosome function, but not involved in melanin synthesis, have also been implicated in iris pigment dispersion phenotypes. A C-terminally truncated allele of *glycoprotein nonmetastatic melanoma protein b* (*Gpnmb*) allele, $Gpnmb^{r150x}$, was mapped as causing iris pigment dispersion in the DBA/2J strain [77]. Although not directly involved in melanin synthesis, *Gpnmb* is important to melanosome structural integrity and containing the cytotoxic melanin synthesis intermediates [77]. Intriguingly, C-terminal truncation of its homologue *Pmel* (*Si* allele) in mice causes melanosome dysfunction and melanocyte cell death leading to body-wide pigmentary abnormalities but not iris pigment dispersion [99–101]. *Gpnmb* has additional neuronal and immune cell adhesion functions that are important to the pathology of glaucoma in DBA/2J mice [102–104]. Understanding the immune component of $Gpnmb^{r150x}$-mediated iris pigment dispersion may be important to elucidate the known involvement of the immune system in PDS [25, 105]. Similarly, *Lyst* encodes the lysosomal trafficking regulator protein which is important for trafficking components to the early stage 1 melanosomes, and variants can cause Chediak-Higashi syndrome (number 214500) [106]. The $Lyst^{bg\text{-}j}$ allele causes *beige* coat color in the C57BL/6J background. Beige mice exhibit pronounced pigment dispersion and increased melanosome volume with similarities to both PDS and PXS [82, 83]. The underlying molecular mechanism for this phenotype is not yet understood but could be related again to cytotoxic melanin synthesis intermediates. The same large-scale genetic analysis which identified *Oca2* also identified several genes not directly involved in melanin synthesis. The motor protein *Myosin Va* (*Myo5a*) gene, signalling protein *protein kinase C ζ* (*Pkcζ*), and transcription factor *zinc finger and BTB domain-containing protein 20* (*Zbtb20*) were identified as key modifiers of the iris transillumination defect [93]. Both *Myo5a* and *Pkcζ* have a direct tie to pigmentation either through intercellular trafficking of melanosomes [107–109] or through melanocyte dendrite formation [110] (a structure important to intercellular trafficking), respectively. It is not clear how *Zbtb20* may influence this phenotype as the gene remains an understudied transcription factor with ties to the nervous, detoxification, and immune system function thus far, the latter having been already implicated in the DBA/2J mouse model previously [111–113]. Finally, in the *vitiligo* substrain of C57BL/6J mice, a variant in the master pigmented cell transcription factor *Mitf* (*Microphthalmia-associated transcription factor*) [114] caused relatively late onset pigment dispersion and increased eye size, possibly due to increased IOP^{82}. The $Mitf^{mi\text{-}vit}$ allele likely disrupts the regulation of *Tyrp1*, *Dct*, *Gpnmb*, *Lyst*, *Myo5a*, and even *PKCζ* given *Mitf*'s essential role in regulating melanocyte identity and function [115–117].

One additional animal model exists with some relevance to PDS/PG. Canine ocular melanosis (OM) shares some phenotypic similarities with PDS/PG in that the pigment is lost from the posterior of the iris leading to transillumination defects, pigment accumulates aberrantly in the TM, and increased IOP with glaucoma developing in affected canines. However, OM is characterized by a host of other pigmentary anomalies and pathogenic phenotypes including but not limited to iris root thickening, uveal melanocytic neoplasms, large scleral/episcleral pigment plaques, fundus pigmentation, corneal edema, and anterior uveitis [118, 119]. Together, these dramatic anomalies are more reminiscent of cancer than PDS/PG making the applicability of this model to human disease limited. A genetic screen in Cairn terriers assuming an autosomal dominant mode of inheritance ruled out genes implicated in the DBA/2J model as being causative for OM [120].

Together, the body of animal research strongly supports a central role for dysregulation of melanin synthesis, melanosome integrity, and melanocyte health in the pathogenesis of PDS. Although based on the reverse genetic nature of screening coat color (and thus pigmentation) affecting variants for iris pigment dispersion, it is striking that so many different genes acting in similar processes have been associated with this phenotype in mice. In some sense, the animal literature on iris pigment dispersion is in marked contrast with human clinical research that has focused on the structural features of PDS as opposed to the cellular ones. None of the genes implicated in mouse models have yet been associated with PDS/PG in humans. While not discussed in detail in the current review, there is also a broader literature on the progression of IOP, glaucomatous optic neuropathy, axonal transport changes, and other glaucoma-associated phenotypes studied in the DBA/2J mouse model presented in detail within several informative reviews [121–123]. Interestingly, a recent large genetic analysis has revealed that the iris transillumination defect is independent of the increased IOP observed in the DBA/2J model [124]. Instead, this glaucoma-like phenotype seems to be regulated primarily by other genes such as the calcium voltage-gated channel auxiliary subunit alpha2delta1 (*Cacna2d1*) which has broader relevance for POAG [125]. Although glaucoma develops in both the DBA/2J and YBR/EiJ mouse strains, it is important to note that strong evidence suggests glaucomatous optic neuropathy may be linked to underlying neurodegeneration independent of *Tyrp1* alleles [84, 126]. This gap between the iris pigment dispersion phenotype and the glaucomatous phenotypes observed in these mouse models limits their applicability to PG but remains an interesting contrast to the research in humans.

6. Models of PDS/PG

The discordance between structural features being primarily implicated in human PDS and melanocyte death being implicated in animal studies suggests it is essential to reevaluate classical models of PDS/PG. Undoubtedly, the most thoroughly investigated model of PDS/PG is the "*structural model*" in which a structural abnormality of the iris is responsible for excessive iridozonular contact which removes pigmented cells from the IPE via a mechanical rubbing force (Figure 1) [3]. Several lines of evidence support this structural model. Some patients with PDS have demonstrable iris concavity, and most are myopic further supporting some structural component [4, 7, 31, 34]. Abnormal iridozonular contact can be observed in patients with PDS where

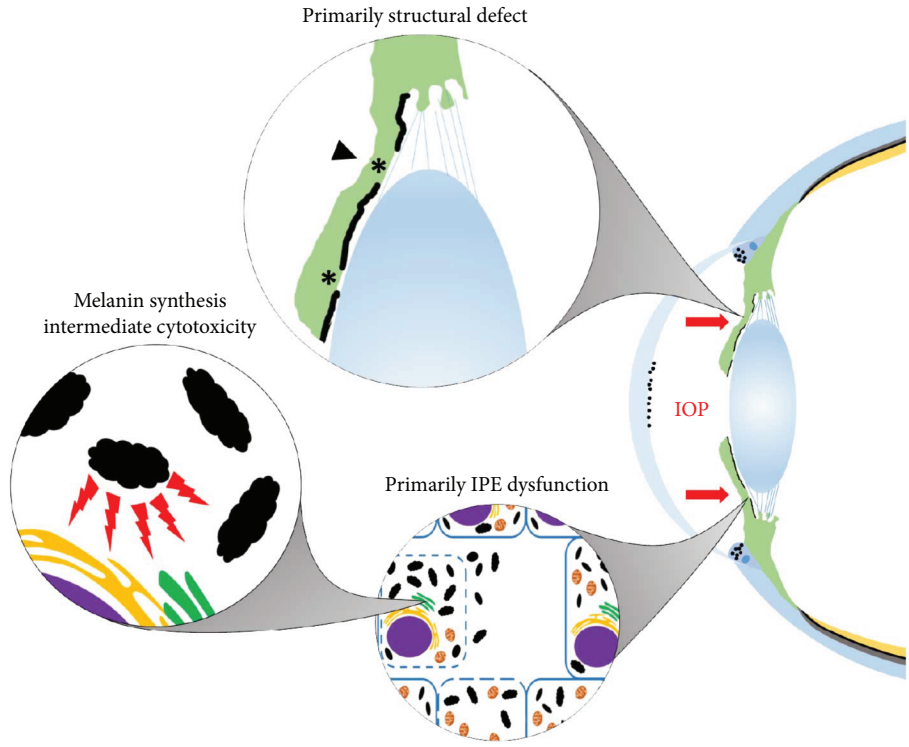

Figure 1: Schematic representation of PDS/PG models. In patients with PDS, pigment liberated from the posterior surface of the iris (green) circulates into the anterior chamber following the flow of aqueous humor where it deposits into the cornea and trabecular meshwork (black dots). High IOP can maintain iris bowing (red arrows) due to the reverse pupillary block in which the lens and iris act together in a ball-valve pressure system which normally acts to maintain unidirectional aqueous humor flow. There are two models of PDS/PG which differ in respect to the origin of pigment dispersion from the ciliary body to the trabecular meshwork. The *structural model* of PDS/PG proposes that posterior iris bowing creates inappropriate iridozonular contacts (black arrowhead, top circle) and that mechanical rubbing between the iris, zonules, and lens is responsible for liberating pigment from the IPE (asterisks, top circle). Although these structural features are well established, it still remains unclear if they predate pigment dispersion as the underlying mechanism. Animal models support IPE dysfunction as the primary driver of this dispersion. In this model, pigmented melanocytes die and/or detach from the IPE (bottom right circle) due to release of cytotoxic melanin synthesis intermediates from dysfunctional melanosomes (bumpy ovals, bottom left circle).

mechanical rubbing may occur [3, 4] correlating well with the midperipheral and radial distribution of iris transillumination defects [2, 22]. Mechanical strain on the eye via rigorous exercise leading to pigment liberation demonstrates the potential mechanical nature of this defect [41–44]. The concept of the reverse pupillary block acting to maintain this abnormal contact and facilitates mechanical rubbing has relevance for both PDS and pseudophakia [3, 23]. However, there are several limitations of this structural model as well. Notable is the lack of evidence supporting laser peripheral iridotomy (LPI) as a beneficial surgical intervention. LPI is designed to flatten the iris and alleviate iris concavity. Given that in a structural paradigm of PDS/PG, such an abnormality would be the source of the abnormal iridozonular contact and thus pigment shedding. However, a Cochrane review of LPI found no clear benefit of LPI in preventing loss of visual field but also rated the studies examining the technique as very low quality [127]. LPI appears to be effective at flattening the iris, thus eliminating the structural insult, but this does not prevent progression to PG [128–130]. Additionally, a paucity of evidence exists surrounding the lifespan progression PDS/PG. Structural abnormalities are associated with PDS, but whether they predate the onset of pigment shedding is unknown. It has previously been proposed that "a gene affecting some aspect of the development of the middle third of the eye early in the third trimester of fetal development may responsible for the structural defect" given the timing of iris development [22]. However, no such gene has been discovered and known anterior segment developmental control genes such as *PAX6* [131], *FOXC1* [132], and *PITX2* [133] are not associated with PDS/PG but are instead causative of other types of glaucoma [134]. It would be highly informative to carefully examine the structure of juvenile eyes, in pedigrees where PDS/PG appears to have a stronger genetic component, to address this shortfall.

An *IPE dysfunction model* of PDS/PG has the possibility to address the shortcomings of the structural model and has several interesting implications. Most notably, IPE dysfunction is best supported by the existing animal literature on iris pigment dispersion, iris atrophy, and pigmentary glaucoma. Consistently, mouse models of these phenotypes have been determined to be caused by genes controlling melanin synthesis, melanosome integrity, and melanocyte health [77, 82]. Although these models are not perfect analogues to PDS/PG, the theoretical model of IPE dysfunction provides a reasonable causal relationship between a genetic

component and the observed clinical features of PDS. IPE dysfunction at the melanocyte level may be mediated by the inappropriate release of cytotoxic melanin synthesis intermediates or impaired response to cellular stresses as pigmentation is inherently a stressful process, and the iris undergoes continuous melanogenesis [85, 92, 135]. Melanocytes impaired in this way may die or detach constituting the liberated pigmented material (Figure 1). It is currently unknown if this material is comprised of melanin granules, melanosomes, or whole cellular debris, but resultant melanocyte cell death in the IPE is well established [11, 13, 25]. A melanocyte focused model has the added benefit of providing a reasonable theoretical basis for the involvement of the RPE in the pathophysiology of PDS/PG given that both structures are pigmented. The differential involvement of the tissues may be a consequence of active melanogenesis in iris melanocytes versus retinal melanocytes which seem to undergo a burst of melanosome biogenesis in development that is then retained for the patient's lifetime [135, 136]. Careful consideration thus should be given to pigmentation and/or melanocyte genes in future investigations into the genetic aetiology of PDS/PG.

7. Conclusion

Recent studies describing the clinical characteristics of PDS and PG and the improved understanding of the role of genes implicated in animal models of PDS/PG are calling into question classical models of the basis of this important causes of blindness. As such, we critically need new research into the fundamental basis of PDS, PG, and the relationship between these two presentations. We believe there are several important questions which researchers could investigate to better understand PDS/PG. Firstly, it would be highly informative to better describe the natural history of PDS/PG in the preclinical phase to better understand the state of the eye proceeding PDS. Large families with high incidence of PDS exist which could be worked with to address whether a structural feature of the iris proceeds PDS and what variability exists in the age of onset. Animal studies have also highlighted a vastly understudied immune component to PDS/PG. Although histologic evidence for immune involvement in PDS existed as early as 1974, human studies have not focused on this component. A better understanding if and how the immune system impacts PDS/PG onset/progression in humans as it does in DBA/2J mice may yield novel insights into the pathology of this disease. Better understanding the nature of pigment loss from the IPE may also be important to ultimately identify the underlying cause of PDS. Although unhealthy/dying melanosomes have been observed histologically, it is unknown if this cell death is the primary mode of pigment loss. As melanosomes are transferred between cells, it is possible that some pigment shedding may be due to inappropriate export of pigmented particles and that melanocyte death is a secondary phenotype. Identifying the composition of the shed pigmented material may assist in determining if shed pigment is comprised purely of melanosomes or also contain additional cell fragments. Finally, as reported conversion rates have varied greatly between ethnic groups, it is possible that these differences in genetic background may be leveraged to identify important haplotypes associated with conversion risk. Large-scale GWAS style genetic analyses may be able to identify these important risk factors and provide novel insight into genetic risks for conversion. However, this will require large-scale cohorts and rigorous phenotyping to undertake successfully. Together, answering these questions with the significant advances in genetic screening technologies and laboratory techniques will yield new insights into the genetic causes of PDS and PG, advancing our understanding of the underlying mechanisms and hopefully leading to new treatment paradigms for this common form of blindness.

Conflicts of Interest

The authors declare that they have no conflicts of interest to disclose.

References

[1] F. Krukenberg, "Beiderseitige angeborene melanose der hornhaut," *Klinische Monatsblätter für Augenheilkunde*, vol. 37, pp. 254–258, 1899.

[2] H. G. Scheie and H. W. Fleischhauer, "Idiopathic atrophy of the epithelial layers of the iris and ciliary body; a clinical study," *A.M.A. Archives of Ophthalmology*, vol. 59, no. 2, pp. 216–228, 1958, -88-91.

[3] D. G. Campbell, "Pigmentary dispersion and glaucoma," *Archives of Ophthalmology*, vol. 97, no. 9, pp. 1667–1672, 1979.

[4] S. D. Potash, C. Tello, J. Liebmann, and R. Ritch, "Ultrasound biomicroscopy in pigment dispersion syndrome," *Ophthalmology*, vol. 101, no. 2, pp. 332–339, 1994.

[5] Y. Siddiqui, R. D. Ten Hulzen, J. D. Cameron, D. O. Hodge, and D. H. Johnson, "What is the risk of developing pigmentary glaucoma from pigment dispersion syndrome?," *American Journal of Ophthalmology*, vol. 135, no. 6, pp. 794–799, 2003.

[6] H. S. Sugar, "Pigmentary glaucoma. A 25-year review," *American Journal of Ophthalmology*, vol. 62, no. 3, pp. 499–507, 1966.

[7] S. HS and B. FA, "Pigmentary glaucoma: a rare clinical entity," *American Journal of Ophthalmology*, vol. 32, no. 1, pp. 90–92, 1949.

[8] W. J. Murrell, Z. Shihab, D. W. Lamberts, and B. Avera, "The corneal endothelium and central corneal thickness in pigmentary dispersion syndrome," *Archives of Ophthalmology*, vol. 104, no. 6, pp. 845-846, 1986.

[9] I. Lehto, P. Ruusuvaara, and K. Setälä, "Corneal endothelium in pigmentary glaucoma and pigment dispersion syndrome," *Acta Ophthalmologica*, vol. 68, no. 6, pp. 703–709, 1990.

[10] A. M. Prince and R. Ritch, "Clinical signs of the Pseudoexfoliation syndrome," *Ophthalmology*, vol. 93, no. 6, pp. 803–807, 1986.

[11] J. Gottanka, D. H. Johnson, F. Grehn, and E. Lutjen-Drecoll, "Histologic findings in pigment dispersion syndrome and pigmentary glaucoma," *Journal of Glaucoma*, vol. 15, no. 2, pp. 142–151, 2006.

[12] T. Iwamoto, R. Witmer, and E. Landolt, "Light and electron microscopy in absolute glaucoma with pigment dispersion

phenomena and contusion angle deformity," *American Journal of Ophthalmology*, vol. 72, no. 2, pp. 420–434, 1971.

[13] C. Kupfer, T. Kuwabara, and M. Kaiser-Kupfer, "The histopathology of pigmentary dispersion syndrome with glaucoma," *American Journal of Ophthalmology*, vol. 80, no. 5, pp. 857–862, 1975.

[14] T. Shimizu, K. Hara, and R. Futa, "Fine structure of trabecular meshwork and iris in pigmentary glaucoma," *Albrecht von Graefes Archiv für Klinische und Experimentelle Ophthalmologie*, vol. 215, no. 3, pp. 171–180, 1981.

[15] Y. Matsumoto and D. H. Johnson, "Trabecular meshwork phagocytosis in glaucomatous eyes," *Ophthalmologica*, vol. 211, no. 3, pp. 147–152, 1997.

[16] H. Naitoh, Y. Suganuma, Y. Ueda et al., "Upregulation of matrix metalloproteinase triggers transdifferentiation of retinal pigmented epithelial cells in *Xenopus laevis*: a link between inflammatory response and regeneration," *Developmental Neurobiology*, vol. 77, no. 9, pp. 1086–1100, 2017.

[17] J. A. Alvarado and C. G. Murphy, "Outflow obstruction in pigmentary and primary open angle glaucoma," *Archives of Ophthalmology*, vol. 110, no. 12, pp. 1769–1778, 1992.

[18] E. Von Hippel, "Zur pathologischen anatomie des glaukom," *Archives of Ophthalmology*, vol. 52, p. 498, 1901.

[19] C. V. Migliazzo, R. N. Shaffer, R. Nykin, and S. Magee, "Long-term analysis of pigmentary dispersion syndrome and piegmentary glaucoma," *Ophthalmology*, vol. 93, no. 12, pp. 1528–1536, 1986.

[20] N. Niyadurupola and D. C. Broadway, "Pigment dispersion syndrome and pigmentary glaucoma–a major review," *Clinical & Experimental Ophthalmology*, vol. 36, no. 9, pp. 868–882, 2008.

[21] D. G. Campbell and R. M. Schertzer, "Pathophysiology of pigment dispersion syndrome and pigmentary glaucoma," *Current Opinion in Ophthalmology*, vol. 6, no. 2, pp. 96–101, 1995.

[22] R. Ritch, "A unification hypothesis of pigment dispersion syndrome," *Transactions of American Ophthalmological Society*, vol. 94, pp. 381–409, 1996, December 2017, http://www.ncbi.nlm.nih.gov/pubmed/8981706.

[23] J. R. Karickhoff, "Pigmentary dispersion syndrome and pigmentary glaucoma: a new mechanism concept, a new treatment, and a new technique," *Ophthalmic Surgery*, vol. 23, no. 4, pp. 269–277, 1992, December 2017, http://www.ncbi.nlm.nih.gov/pubmed/1589198.

[24] R. Amini, J. E. Whitcomb, M. K. Al-Qaisi et al., "The posterior location of the dilator muscle induces anterior iris bowing during dilation, even in the absence of pupillary block," *Investigative Ophthalmology and Visual Science*, vol. 53, no. 3, pp. 1188–1194, 2012.

[25] B. S. Fine, M. Yanoff, and H. G. Scheie, "Pigmentary "glaucoma". A Histologic Study," *Transactions - American Academy of Ophthalmology and Otolaryngology*, vol. 78, no. 2, pp. OP314–OP325, 1974.

[26] W. L. Haynes, W. L. M. Alward, and H. S. Thompson, "Distortion of the pupil in patients with the pigment dispersion syndrome," *Journal of Glaucoma*, vol. 3, no. 4, pp. 329–332, 1994.

[27] W. L. Haynes, H. S. Thompson, R. H. Kardon, and W. L. M. Alward, "Asymmetric pigmentary dispersion syndrome mimicking Horner's syndrome," *American Journal of Ophthalmology*, vol. 112, no. 4, pp. 463-464, 1991.

[28] V. C. Greenstein, W. Seiple, J. Liebmann, and R. Ritch, "Retinal pigment epithelial dysfunction in patients with pigment dispersion syndrome," *Archives of Ophthalmology*, vol. 119, no. 9, pp. 1291–1295, 2001.

[29] P. Weseley, J. Liebmann, J. B. Walsh, and R. Ritch, "Lattice degeneration of the retina and the pigment dispersion syndrome," *American Journal of Ophthalmology*, vol. 114, no. 5, pp. 539–543, 1992.

[30] G. Scuderi, A. Papale, C. Nucci, and L. Cerulli, "Retinal involvement in pigment dispersion syndrome," *International Ophthalmology*, vol. 19, no. 6, pp. 375–378, 1995.

[31] H. G. Scheie and J. D. Cameron, "Pigment dispersion syndrome: a clinical study," *The British Journal of Ophthalmology*, vol. 65, no. 4, pp. 264–269, 1981.

[32] R. Sampaolesi, "Retinal detachment and pigment dispersion syndrome," *Klinische Monatsblätter für Augenheilkunde*, vol. 206, no. 01, pp. 29–32, 1995.

[33] R. Ritch, D. Steinberger, and J. M. Liebmann, "Prevalence of pigment dispersion syndrome in a population undergoing glaucoma screening," *American Journal of Ophthalmology*, vol. 115, no. 6, pp. 707–710, 1993.

[34] S. M. Farrar and M. B. Shields, "Current concepts in pigmentary glaucoma," *Survey of Ophthalmology*, vol. 37, no. 4, pp. 233–252, 1993, Elsevier.

[35] H. C. Semple and S. F. Ball, "Pigmentary glaucoma in the black population," *American Journal of Ophthalmology*, vol. 109, no. 5, pp. 518–522, 1990.

[36] D. K. Roberts, R. E. Meetz, and M. A. Chaglasian, "The inheritance of the pigment dispersion syndrome in Blacks," *Journal of Glaucoma*, vol. 8, no. 4, pp. 250–256, 1999.

[37] C. U. Richter, T. M. Richardson, and W. M. Grant, "Pigmentary dispersion syndrome and pigmentary glaucoma," *Archives of Ophthalmology*, vol. 104, no. 2, pp. 211–215, 1986.

[38] W. E. Gillies, "Pigmentary glaucoma: a clinical review of anterior segment pigment dispersal syndrome," *Australian and New Zealand Journal of Ophthalmology*, vol. 13, no. 4, pp. 325–328, 1985.

[39] E. Gramer, H. Thiele, and R. Ritch, "Family history of glaucoma and risk factors in pigmentary glaucoma. A clinical study," *Klinische Monatsblätter für Augenheilkunde*, vol. 212, no. 6, pp. 454–464, 1998.

[40] G. Gramer, B. H. F. Weber, and E. Gramer, "Results of a patient-directed survey on frequency of family history of glaucoma in 2170 patients," *Investigative Ophthalmology and Visual Science*, vol. 55, no. 1, pp. 259–264, 2014.

[41] D. L. Epstein, W. P. Boger, and W. M. Grant, "Phenylephrine provocative testing in the pigmentary dispersion syndrome," *American Journal of Ophthalmology*, vol. 85, no. 1, pp. 43–50, 1978.

[42] H. I. Schenker, M. H. Luntz, B. Kels, and S. M. Podos, "Exercise-induced increase of intraocular pressure in the pigmentary dispersion syndrome," *American Journal of Ophthalmology*, vol. 89, no. 4, pp. 598–600, 1980.

[43] W. L. Haynes, A. T. Johnson, and W. L. M. Alward, "Effects of jogging exercise on patients with the pigmentary dispersion syndrome and pigmentary glaucoma," *Ophthalmology*, vol. 99, no. 7, pp. 1096–1103, 1992.

[44] P. K. Jensen, O. Nissen, and S. V. Kessing, "Exercise and reversed pupillary block in pigmentary glaucoma," *American Journal of Ophthalmology*, vol. 120, no. 1, pp. 110–112, 1995.

[45] H. F. Gomez Goyeneche, D. P. Hernandez-Mendieta, D. A. Rodriguez, A. I. Sepulveda, and J. D. Toledo, "Pigment dispersion syndrome progression to pigmentary glaucoma in a Latin American population," *Journal of Current Glaucoma Practice with DVD*, vol. 9, no. 3, pp. 69–72, 2015.

[46] S. M. Farrar, M. B. Shields, K. N. Miller, and C. M. Stoup, "Risk factors for the development and severity of glaucoma in the pigment dispersion syndrome," *American Journal of Ophthalmology*, vol. 108, no. 3, pp. 223–229, 1989.

[47] I. A. Shah, S. A. Shah, P. R. Nagdev, S. A. Abbasi, N. A. Abbasi, and S. A. Katpar, "Determination Of association of pigmentary glaucoma with pigment dispersion syndrome," *Journal of Ayub Medical College Abbottabad*, vol. 29, no. 3, pp. 412–414, 2017, November 2017, http://www.ncbi.nlm.nih.gov/pubmed/29076672.

[48] J. W. Yang, D. Sakiyalak, and T. Krupin, "Pigmentary glaucoma," *Journal of Glaucoma*, vol. 10, no. 5, pp. S30–S32, 2001.

[49] J. S. Andersen, A. M. Pralea, E. A. DelBono et al., "A gene responsible for the pigment dispersion syndrome maps to chromosome 7q35-q36," *Archives of Ophthalmology*, vol. 115, no. 3, pp. 384–388, 1997.

[50] L. J. Robinson, S. Weremowicz, C. C. Morton, and T. Michel, "Isolation and chromosomal localization of the human endothelial nitric oxide synthase (NOS3) gene," *Genomics*, vol. 19, no. 2, pp. 350–357, 1994.

[51] S. T. Davidge, P. N. Baker, M. K. McLaughlin, and J. M. Roberts, "Nitric oxide produced by endothelial cells increases production of eicosanoids through activation of prostaglandin H synthase," *Circulation Research*, vol. 77, no. 2, pp. 274–283, 1995.

[52] W. Steudel, F. Ichinose, P. L. Huang et al., "Pulmonary vasoconstriction and hypertension in mice with targeted disruption of the endothelial nitric oxide synthase (NOS 3) gene," *Circulation Research*, vol. 81, no. 1, pp. 34–41, 1997.

[53] J. S. Andersen, R. Parrish, D. Greenfield, E. A. DelBono, J. L. Haines, and J. L. Wiggs, "A second locus for the pigment dispersion syndrome and pigmentary glaucoma maps to 18q11-q21," *American Journal of Human Genetics*, vol. 63, article A279, 1998.

[54] S. H. Wagner, E. DelBono, D. S. Greenfield, R. K. Parrish, J. L. Haines, and J. L. Wiggs, "A second locus for pigment dispersion syndrome maps to chromosome 18q21," *Investigative Ophthalmology & Visual Science*, vol. 46, no. 13, p. 29, 2005.

[55] R. Mikelsaar, H. Molder, O. Bartsch, and M. Punab, "Two novel deletions (array CGH findings) in pigment dispersion syndrome," *Ophthalmic Genetics*, vol. 28, no. 4, pp. 216–219, 2007.

[56] J. H. Fingert, E. Héon, J. M. Liebmann et al., "Analysis of myocilin mutations in 1703 glaucoma patients from five different populations," *Human Molecular Genetics*, vol. 8, no. 5, pp. 899–905, 1999.

[57] E. M. Stone, J. H. Fingert, W. L. Alward et al., "Identification of a gene that causes primary open angle glaucoma," *Science*, vol. 275, no. 5300, pp. 668–670, 1997.

[58] V. C. Sheffield, E. M. Stone, W. L. M. Alward et al., "Genetic linkage of familial open angle glaucoma to chromosome 1q21–q31," *Nature Genetics*, vol. 4, no. 1, pp. 47–50, 1993.

[59] A. L. Vincent, G. Billingsley, Y. Buys et al., "Digenic inheritance of early-onset glaucoma: *CYP1B1*, a potential modifier gene," *American Journal of Human Genetics*, vol. 70, no. 2, pp. 448–460, 2002.

[60] M. Faucher, J.-L. Anctil, M.-A. Rodrigue et al., "Founder *TIGR/myocilin* mutations for glaucoma in the Québec population," *Human Molecular Genetics*, vol. 11, no. 18, pp. 2077–2090, 2002.

[61] W. L. M. Alward, Y. H. Kwon, C. L. Khanna et al., "Variations in the myocilin gene in patients with open-angle glaucoma," *Archives of Ophthalmology*, vol. 120, no. 9, pp. 1189–1197, 2002.

[62] K. Y. C. Lee, S. L. Ho, A. Thalamuthu et al., "Association of *LOXL1* polymorphisms with pseudoexfoliation in the Chinese," *Molecular Vision*, vol. 15, pp. 1120–1126, 2009, December 6, 2017, http://www.ncbi.nlm.nih.gov/pubmed/19503743.

[63] A. W. Hewitt, S. Sharma, K. P. Burdon et al., "Ancestral *LOXL1* variants are associated with pseudoexfoliation in Caucasian Australians but with markedly lower penetrance than in Nordic people," *Human Molecular Genetics*, vol. 17, no. 5, pp. 710–716, 2008.

[64] B. Fan, L. Pasquale, C. L. Grosskreutz et al., "DNA sequence variants in the LOXL1 gene are associated with pseudoexfoliation glaucoma in a U.S. clinic-based population with broad ethnic diversity," *BMC Medical Genetics*, vol. 9, no. 1, p. 5, 2008.

[65] J. A. Aragon-Martin, R. Ritch, J. Liebmann et al., "Evaluation of LOXL1 gene polymorphisms in exfoliation syndrome and exfoliation glaucoma," *Molecular Vision*, vol. 14, pp. 533–541, 2008, December 2017, http://www.ncbi.nlm.nih.gov/pubmed/18385788.

[66] P. Challa and S. Schmidt, "Analysis of LOXL1 polymorphisms in a United States population with pseudoexfoliation glaucoma," *Molecular Vision*, vol. 49, no. 4, pp. 1459–1149, 2008.

[67] C. Wolf, E. Gramer, B. Muïler-Myhsok et al., "Lysyl oxidase-like 1 gene polymorphisms in German patients with normal tension glaucoma, pigmentary glaucoma and exfoliation glaucoma," *Journal of Glaucoma*, vol. 19, no. 2, pp. 136–141, 2010.

[68] K. N. Rao, R. Ritch, S. K. Dorairaj et al., "Exfoliation syndrome and exfoliation glaucoma-associated LOXL1 variations are not involved in pigment dispersion syndrome and pigmentary glaucoma," *Molecular Vision*, vol. 14, pp. 1254–1262, 2008, December 2017, http://www.ncbi.nlm.nih.gov/pubmed/18618003.

[69] E. Giardina, F. Oddone, T. Lepre et al., "Common sequence variants in the LOXL1gene in pigment dispersion syndrome and pigmentary glaucoma," *BMC Ophthalmology*, vol. 14, no. 1, p. 52, 2014.

[70] O. Pokrovskaya and C. O'Brien, "What's in a gene pseudoexfoliation syndrome and pigment dispersion syndrome in the same patient," *Case Reports in Ophthalmology*, vol. 7, no. 1, pp. 54–60, 2016.

[71] A. L. Sertié, V. Sossi, A. A. Camargo, M. Zatz, C. Brahe, and M. R. Passos-Bueno, "Collagen XVIII, containing an endogenous inhibitor of angiogenesis and tumor growth, plays a critical role in the maintenance of retinal structure and in neural tube closure (Knobloch syndrome)," *Human Molecular Genetics*, vol. 9, no. 13, pp. 2051–2058, 2000.

[72] S. Joyce, L. Tee, A. Abid, S. Khaliq, S. Q. Mehdi, and E. R. Maher, "Locus heterogeneity and Knobloch syndrome," *American Journal Medical Genetics Part A*, vol. 152A, no. 11, pp. 2880-2881, 2010.

[73] S. Hull, G. Arno, C. A. Ku et al., "Molecular and clinical findings in patients with Knobloch syndrome," *JAMA Ophthalmology*, vol. 134, no. 7, pp. 753–762, 2016.

[74] J. Kuchtey, T. C. Chang, L. Panagis, and R. W. Kuchtey, "Marfan syndrome caused by a novel *FBN1* mutation with associated pigmentary glaucoma," *American Journal Medical Genetics Part A*, vol. 161, no. 4, pp. 880–883, 2013.

[75] T. Chakravarti and G. Spaeth, "An overlap syndrome of pigment dispersion and pigmentary glaucoma accompanied by Marfan syndrome: case report with literature review," *Journal of Current Glaucoma Practice*, vol. 7, no. 2, pp. 91–95, 2013.

[76] N. J. Izquierdo, E. I. Traboulsi, C. Enger, and I. H. Maumenee, "Glaucoma in the Marfan syndrome," *Transactions of the American Ophthalmological Society*, vol. 90, pp. 111–122, 1992, December 2017, http://www.ncbi.nlm.nih.gov/pubmed/1494814.

[77] M. G. Anderson, R. S. Smith, N. L. Hawes et al., "Mutations in genes encoding melanosomal proteins cause pigmentary glaucoma in DBA/2J mice," *Nature Genetics*, vol. 30, no. 1, pp. 81–85, 2002.

[78] P. A. Williams, G. R. Howell, J. M. Barbay et al., "Retinal ganglion cell dendritic atrophy in DBA/2J glaucoma," *PLoS One*, vol. 8, no. 8, article e72282, 2013.

[79] R. T. Libby, M. G. Anderson, I.-H. Pang et al., "Inherited glaucoma in DBA/2J mice: pertinent disease features for studying the neurodegeneration," *Visual Neuroscience*, vol. 22, no. 5, pp. 637–648, 2005.

[80] G. R. Howell, R. T. Libby, T. C. Jakobs et al., "Axons of retinal ganglion cells are insulted in the optic nerve early in DBA/2J glaucoma," *The Journal of Cell Biology*, vol. 179, no. 7, pp. 1523–1537, 2007.

[81] S. W. John, R. S. Smith, O. V. Savinova et al., "Essential iris atrophy, pigment dispersion, and glaucoma in DBA/2J mice," *Investigative Ophthalmology & Visual Science*, vol. 39, no. 6, pp. 951–962, 1998.

[82] M. G. Anderson, N. L. Hawes, C. M. Trantow, B. Chang, and S. W. M. John, "Iris phenotypes and pigment dispersion caused by genes influencing pigmentation," *Pigment Cell & Melanoma Research*, vol. 21, no. 5, pp. 565–578, 2008.

[83] C. M. Trantow, M. Mao, G. E. Petersen et al., "*Lyst* mutation in mice recapitulates iris defects of human exfoliation syndrome," *Investigative Opthalmology &Visual Science*, vol. 50, no. 3, pp. 1205–1214, 2009.

[84] K. S. Nair, M. Cosma, N. Raghupathy et al., "YBR/EiJ mice: a new model of glaucoma caused by genes on chromosomes 4 and 17," *Disease Models & Mechanisms*, vol. 9, no. 8, pp. 863–871, 2016.

[85] K. Urabe, P. Aroca, K. Tsukamoto et al., "The inherent cytotoxicity of melanin precursors: a revision," *Biochimica et Biophysica Acta (BBA) - Molecular Cell Research*, vol. 1221, no. 3, pp. 272–278, 1994.

[86] C. Olivares, C. Jiménez-Cervantes, J. A. Lozano, F. Solano, and J. C. García-Borrón, "The 5,6-dihydroxyindole-2-carboxylic acid (DHICA) oxidase activity of human tyrosinase," *Biochemical Journal*, vol. 354, no. 1, pp. 131–139, 2001.

[87] T. Kobayashi, G. Imokawa, D. C. Bennett, and V. J. Hearing, "Tyrosinase stabilization by Tyrp1 (the *brown* locus protein)," *The Journal of Biological Chemistry*, vol. 273, no. 48, pp. 31801–31805, 1998.

[88] R. Halaban and G. Moellmann, "Murine and human b locus pigmentation genes encode a glycoprotein (gp75) with catalase activity," *Proceedings of the National Academy of Sciences of the United States of America*, vol. 87, no. 12, pp. 4809–4813, 1990.

[89] R. Johnson and I. J. Jackson, "Light is a dominant mouse mutation resulting in premature cell death," *Nature Genetics*, vol. 1, no. 3, pp. 226–229, 1992.

[90] E. Zdarsky, J. Favor, and I. J. Jackson, "The molecular basis of brown, an old mouse mutation, and of an induced revertant to wild type," *Genetics*, vol. 126, no. 2, pp. 443–449, 1990.

[91] T. Hirobe and H. Abe, "Changes of melanosome morphology associated with the differentiation of epidermal melanocytes in slaty mice," *The Anatomical Record: Advances in Integrative Anatomy and Evolutionary Biology*, vol. 290, no. 8, pp. 981–993, 2007.

[92] G.-E. Costin, J. C. Valencia, K. Wakamatsu et al., "Mutations in dopachrome tautomerase (Dct) affect eumelanin/pheomelanin synthesis, but do not affect intracellular trafficking of the mutant protein," *The Biochemical Journal*, vol. 391, no. 2, pp. 249–259, 2005.

[93] S. Swaminathan, H. Lu, R. W. Williams, L. Lu, and M. M. Jablonski, "Genetic modulation of the iris transillumination defect: a systems genetics analysis using the expanded family of BXD glaucoma strains," *Pigment Cell & Melanoma Research*, vol. 26, no. 4, pp. 487–498, 2013.

[94] I. Yuasa, K. Umetsu, S. Harihara et al., "*OCA2***481Thr*, a hypofunctional allele in pigmentation, is characteristic of northeastern Asian populations," *Journal of Human Genetics*, vol. 52, no. 8, pp. 690–693, 2007.

[95] M. Ramsay, M. A. Colman, G. Stevens et al., "The tyrosinase-positive oculocutaneous albinism locus maps to chromosome 15q11.2-q12," *American Journal of Human Genetics*, vol. 51, no. 4, pp. 879–884, 1992, February 2018, http://www.ncbi.nlm.nih.gov/pubmed/1415228.

[96] R. A. Sturm and T. N. Frudakis, "Eye colour: portals into pigmentation genes and ancestry," *Trends in Genetics*, vol. 20, no. 8, pp. 327–332, 2004.

[97] D. L. Duffy, G. W. Montgomery, W. Chen et al., "A three–single-nucleotide polymorphism haplotype in intron 1 of *OCA2* explains most human eye-color variation," *American Journal of Human Genetics*, vol. 80, no. 2, pp. 241–252, 2007.

[98] P. Sulem, D. F. Gudbjartsson, S. N. Stacey et al., "Genetic determinants of hair, eye and skin pigmentation in Europeans," *Nature Genetics*, vol. 39, no. 12, pp. 1443–1452, 2007.

[99] B. Watt, D. Tenza, M. A. Lemmon et al., "Mutations in or near the transmembrane domain alter PMEL amyloid formation from functional to pathogenic," *PLoS Genetics*, vol. 7, no. 9, article e1002286, 2011.

[100] A. C. Theos, J. F. Berson, S. C. Theos et al., "Dual loss of ER export and endocytic signals with altered melanosome morphology in the *silver* mutation of Pmel17," *Molecular Biology of the Cell*, vol. 17, pp. 3598–3612, 2006.

[101] B. S. Kwon, R. Halaban, S. Ponnazhagan et al., "Mouse *silver*. Mutation is caused by a single base insertion in the putative cytoplasmic domain of Pmel 17," *Nucleic Acids Research*, vol. 23, no. 1, pp. 154–158, 1995.

[102] M. G. Anderson, K. S. Nair, L. A. Amonoo et al., "GpnmbR150X allele must be present in bone marrow derived cells to mediate DBA/2J glaucoma," *BMC Genetics*, vol. 9, no. 1, p. 30, 2008.

[103] J. J. Huang, W. J. Ma, and S. Yokoyama, "Expression and immunolocalization of Gpnmb, a glioma-associated glycoprotein, in normal and inflamed central nervous systems of adult rats," *Brain and Behavior*, vol. 2, no. 2, pp. 85–96, 2012.

[104] K. Nair, J. Barbay, R. S. Smith, S. Masli, and S. W. John, "Determining immune components necessary for progression of pigment dispersing disease to glaucoma in DBA/2J mice," *BMC Genetics*, vol. 15, no. 1, p. 42, 2014.

[105] J.-S. Mo, M. G. Anderson, M. Gregory et al., "By altering ocular immune privilege, bone marrow-derived cells pathogenically contribute to DBA/2J pigmentary glaucoma," *The Journal of Experimental Medicine*, vol. 197, no. 10, pp. 1335–1344, 2003.

[106] S. L. Shiflett, J. Kaplan, and D. M. Ward, "Chediak–Higashi syndrome: a rare disorder of lysosomes and lysosome related organelles," *Pigment Cell & Melanoma Research*, vol. 15, no. 4, pp. 251–257, 2002.

[107] T. N. O'Sullivan, X. S. Wu, R. A. Rachel et al., "*dsu* functions in a MYO5A-independent pathway to suppress the coat color of *dilute* mice," *Proceedings of the National Academy of Sciences of the United States of America*, vol. 101, no. 48, pp. 16831–16836, 2004.

[108] X. Wu, B. Bowers, K. Rao, Q. Wei, and J. A. Hammer, "Visualization of melanosome dynamics within wild-type and dilute melanocytes suggests a paradigm for myosin V function in vivo," *The Journal of Cell Biology*, vol. 143, no. 7, pp. 1899–1918, 1998.

[109] X. Wu, B. Bowers, Q. Wei, B. Kocher, and J. A. Hammer, "Myosin V associates with melanosomes in mouse melanocytes: evidence that myosin V is an organelle motor," *Journal of Cell Science*, vol. 110, pp. 847–859, 1997, February 2018, http://www.ncbi.nlm.nih.gov/pubmed/9133672.

[110] G. A. Scott, M. Arioka, and S. E. Jacobs, "Lysophosphatidylcholine mediates melanocyte dendricity through PKCζ activation," *The Journal of Investigative Dermatology*, vol. 127, no. 3, pp. 668–675, 2007.

[111] F. Mattioli, A. Piton, B. Gérard, A. Superti-Furga, J.-L. Mandel, and S. Unger, "Novel de novo mutations in *ZBTB20* in primrose syndrome with congenital hypothyroidism," *American Journal of Medical Genetics Part A*, vol. 170, no. 6, pp. 1626–1629, 2016.

[112] Z. Xie, H. Zhang, W. Tsai et al., "Zinc finger protein ZBTB20 is a key repressor of alpha-fetoprotein gene transcription in liver," *Proceedings of the National Academy of Sciences*, vol. 105, no. 31, pp. 10859–10864, 2008.

[113] W. Zhang, J. Mi, N. Li et al., "Identification and characterization of DPZF, a novel human BTB/POZ zinc finger protein sharing homology to BCL-6," *Biochemical and Biophysical Research Communications*, vol. 282, no. 4, pp. 1067–1073, 2001.

[114] C. Levy, M. Khaled, and D. E. Fisher, "MITF: master regulator of melanocyte development and melanoma oncogene," *Trends in Molecular Medicine*, vol. 12, no. 9, pp. 406–414, 2006.

[115] M. G. Anderson, R. T. Libby, M. Mao et al., "Genetic context determines susceptibility to intraocular pressure elevation in a mouse pigmentary glaucoma," *BMC Biology*, vol. 4, no. 1, p. 20, 2006.

[116] N. Turque, F. Denhez, P. Martin et al., "Characterization of a new melanocyte-specific gene (QNR-71) expressed in v-myc-transformed quail neuroretina," *The EMBO Journal*, vol. 15, no. 13, pp. 3338–3350, 1996, December 2017, http://www.ncbi.nlm.nih.gov/pubmed/8670835.

[117] I. Aksan and C. R. Goding, "Targeting the Microphthalmia basic helix-loop-helix–leucine zipper transcription factor to a subset of E-box elements in vitro and in vivo," *Molecular and Cellular Biology*, vol. 18, no. 12, pp. 6930–6938, 1998.

[118] S. M. Petersen-Jones, J. Forcier, and A. L. Mentzer, "Ocular melanosis in the cairn terrier: clinical description and investigation of mode of inheritance," *Veterinary Ophthalmology*, vol. 10, Supplement 1, pp. 63–69, 2007.

[119] R. R. O. M. Van De Sandt, M. H. Boevé, F. C. Stades, and M. J. L. Kik, "Abnormal ocular pigment deposition and glaucoma in the dog," *Veterinary Ophthalmology*, vol. 6, no. 4, pp. 273–278, 2003.

[120] P. A. Winkler, J. T. Bartoe, C. R. Quinones, P. J. Venta, and S. M. Petersen-Jones, "Exclusion of eleven candidate genes for ocular melanosis in cairn terriers," *Journal of Negative Results in BioMedicine*, vol. 12, no. 1, 2013.

[121] K. A. Fernandes, J. M. Harder, P. A. Williams et al., "Using genetic mouse models to gain insight into glaucoma: past results and future possibilities," *Experimental Eye Research*, vol. 141, pp. 42–56, 2015.

[122] H. V. Danesh-Meyer, "Neuroprotection in glaucoma: recent and future directions," *Current Opinion in Ophthalmology*, vol. 22, no. 2, pp. 78–86, 2011.

[123] J.-S. Mo, W. Wang, and H. J. Kaplan, "Impact of inflammation on ocular immune privilege," in *Immune Response and the Eye*, vol. 92, pp. 155–165, KARGER, Basel, 2007.

[124] H. Lu, L. Lu, R. W. Williams, and M. M. Jablonski, "Iris transillumination defect and Its gene modulators do not correlate with intraocular pressure in the BXD family of mice," *Molecular Vision*, vol. 22, pp. 224–233, 2016, February 2018, http://www.ncbi.nlm.nih.gov/pubmed/27011731.

[125] S. R. Chintalapudi, D. Maria, X. Di Wang et al., "Systems genetics identifies a role for *Cacna2d1* regulation in elevated intraocular pressure and glaucoma susceptibility," *Nature Communications*, vol. 8, no. 1, p. 1755, 2017.

[126] A. J. Turner, R. Vander Wall, V. Gupta, A. Klistorner, and S. L. Graham, "DBA/2J mouse model for experimental glaucoma: Pitfalls and problems," *Clinical & Experimental Ophthalmology*, vol. 45, no. 9, pp. 911–922, 2017.

[127] M. Michelessi and K. Lindsley, "Peripheral iridotomy for pigmentary glaucoma," in *Cochrane Database of Systematic Reviews*, M. Michelessi, Ed., John Wiley & Sons, Ltd, Chichester, UK, 2016.

[128] V. P. Costa, S. Gandham, M. Smith, and G. L. Spaeth, "The effects of peripheral iridectomy on pigmentary glaucoma," *Arquivos Brasileiros de Oftalmologia*, vol. 57, p. 4, 1994.

[129] V. P. Costa, S. Gandham, G. L. Spaeth et al., "The effect of nd-yag laser iridotomy on pigmentary glaucoma patients-a prospective-study," in *Investigative Ophthalmology & Visual Science*, vol. 35, p. 1852, Lippincott-Raven PUBL, 227 East Washington SQ, Philadelphia, PA , 19106, USA, 1994.

[130] G. T. Georgopoulos, D. S. Papaconstantinou, L. E. Patsea et al., "Laser iridotomy versus low dose pilocarpine treatment in patients with pigmentary glaucoma," in *Investigative Ophthalmology & Visual Science*, vol. 42, pp. S817–S817, Assoc Research Vision Ophthalmology Inc, 9650 Rockville Pike, Bethesda, MD 20814–3998 USA, 2001.

[131] D. C. Baulmann, A. Ohlmann, C. Flügel-Koch, S. Goswami, A. Cvekl, and E. R. Tamm, "Pax6 heterozygous eyes show defects in chamber angle differentiation that are associated with a wide spectrum of other anterior eye segment abnormalities," *Mechanisms of Development*, vol. 118, no. 1-2, pp. 3–17, 2002.

[132] F. B. Berry, M. A. Lines, J. M. Oas et al., "Functional interactions between FOXC1 and PITX2 underlie the sensitivity to FOXC1 gene dose in Axenfeld-Rieger syndrome and anterior segment dysgenesis," *Human Molecular Genetics*, vol. 15, no. 6, pp. 905–919, 2006.

[133] M. Seifi, T. Footz, S. A. M. Taylor, G. M. Elhady, E. M. Abdalla, and M. A. Walter, "Novel PITX2 gene mutations in patients with Axenfeld-Rieger syndrome," *Acta Ophthalmologica*, vol. 94, no. 7, pp. e571–e579, 2016.

[134] D. B. Gould, R. S. Smith, and S. W. M. John, "Anterior segment development relevant to glaucoma," *The International Journal of Developmental Biology*, vol. 48, no. 8-9, pp. 1015–1029, 2004.

[135] N. G. Lindquist, B. S. Larsson, J. Stjernschantz, and B. Sjöquist, "Age-related melanogenesis in the eye of mice, studied by microautoradiography of 3H-methimazole, a specific marker of melanin synthesis," *Experimental Eye Research*, vol. 67, no. 3, pp. 259–264, 1998.

[136] V. S. Lopes, C. Wasmeier, M. C. Seabra, and C. E. Futter, "Melanosome maturation defect in Rab38-deficient retinal pigment epithelium results in instability of immature melanosomes during transient melanogenesis," *Molecular Biology of the Cell*, vol. 18, no. 10, pp. 3914–3927, 2007.

Hindawi
Journal of Ophthalmology
Volume 2018, Article ID 1686297, 8 pages
https://doi.org/10.1155/2018/1686297

Research Article

Association of Optic Neuritis with *CYP4F2* Gene Single Nucleotide Polymorphism and IL-17A Concentration

Mantas Banevicius[1], **Alvita Vilkeviciute**[2], **Brigita Glebauskiene**[1], **Loresa Kriauciuniene**[1,2] **and Rasa Liutkeviciene**[1,2]

[1]*Department of Ophthalmology, Medical Academy, Lithuanian University of Health Sciences, Eiveniu 2, LT-50161 Kaunas, Lithuania*
[2]*Neuroscience Institute, Medical Academy, Lithuanian University of Health Sciences, Eiveniu 2, LT-50161 Kaunas, Lithuania*

Correspondence should be addressed to Mantas Banevicius; baneviciusmantas@gmail.com

Received 8 August 2017; Revised 30 November 2017; Accepted 18 January 2018; Published 15 March 2018

Academic Editor: Stephen T. Armenti

Background. The aetiology and pathophysiology of optic neuritis (ON) is not absolutely clear but genetic and inflammatory factors may be also involved in its development. The aim of the present study was to determine the influence of single nucleotide polymorphism (SNP) of *CYP4F2* (rs1558139) and serum levels of IL-17A on ON development. *Materials and Methods*. Forty patients with ON and 164 control subjects were evaluated. Patients were divided by gender, also ON patients were divided into two subgroups: ON with and without multiple sclerosis (MS). *CYP4F2* rs1558139 was genotyped using real-time PCR. Serum IL-17A levels were measured using ELISA IL-17A kits. *Results*. We found that A/A genotype of *CYP4F2* rs1558139 was statistically significantly more frequent in men with ON and MS than in women: 57.1% versus 0%, $p = 0.009$. Also, allele A was statistically significantly more frequent in men with ON and MS than in women: 71.4% versus 37.5%, $p = 0.044$. Serum levels of IL-17A were higher in ON group than in control group: (median, IQR): 20.55 pg/ml, 30.66 pg/ml versus 8.97 pg/ml, 6.24 pg/ml, $p < 0.001$. *Conclusion*. The higher IL-17A levels were found to be associated with ON, while allele A at rs1558139 was associated only with ON with MS in male patients.

1. Introduction

Optic neuritis (ON) represents demyelinating inflammation of the optic nerve, which slows or blocks the transmission of signals to and from the brain. Many genetic heterogeneous conditions may cause ON. A gradual recovery of visual acuity over time is a characteristic of typical ON, which is characterized by painful, usually monocular visual loss with decreased visual acuity, defects of the visual field and colour vision [1]. The most common cause is acute demyelinating ON, which is associated with multiple sclerosis (MS) as its first symptom [2]. MS is most often diagnosed in young adults and women are affected more than men by a ratio of 2 : 1 [2, 3]. ON is also more frequent in young adults aged 18–45 [1] and the ratio of female preponderance is approximately 3 : 1 [3]. ON is associated with the loss of axons, nerve impulse blockade, or ganglion cell death [4]. Disruption of nerve impulses by the inflammatory process leads to type IV delayed hypersensitivity reaction. When activated peripheral T lymphocytes release cytokines and other inflammatory mediators that can move through the blood-brain barrier and cause decomposition of myelin, nerve cell death, and axonal degeneration [5]. Disruption of the blood-brain barrier leads to T lymphocytes and inflammatory mediators accessing the central nervous system and indicates beginning of optic neuritis [6–8]. The causes of ON are not known. It is believed that the ON is caused by genetic and environmental factors [9]. Typical ON is often associated with multiple sclerosis (MS), causing

axon loss [2]. Atypical ON maybe caused by bacterial, fungal, or viral infections and other inflammatory and autoimmune diseases [10]. Genetic and inflammatory factors may also take part in ON development. It is known that *CYP4F2* gene is found in neurons and glial cells, where the enzyme encoded by this gene metabolises arachidonic acid, helping to maintain the structure of cell membranes in the hippocampus [11] and protecting the brain against oxidative stress [12]. This gene also activates enzymes involved in the growth and regeneration of neurons [13]. Impaired arachidonic acid metabolism is associated with ON, MS, Alzheimer's disease, and bipolar disorder [14]. *CYP4F2*-encoded enzyme reduces arachidonic acid metabolites as well as a number of prostaglandins, which are involved in various inflammatory processes. Also this enzyme is involved in drug metabolism and the synthesis of cholesterol, steroids, fatty acids, and other lipids [15]. It has been shown that this gene single nucleotide polymorphism (SNP) is associated with the development of hypertension [16], cerebral infarction [17], myocardial infarction [18–21], and metabolic syndrome [22]. Also, it has been found that SNP plays a role in the processes of anticoagulant drug metabolism [23, 24].

Another inflammatory factor, associated with neuroinflammatory diseases, is interleukin - 17A (IL-17A). IL - 17A directly affects neurons, but it can also have an effect on the nerves through the signals to the satellite and immune cells. In the central nervous system, IL-17A is associated with a wide range of neuropathological disorders (MS, epilepsy episodes of ischemic brain disorders). IL-17A, acting on spinal nerve roots and the spinal cord, contributes to neuropathic and inflammatory pain promotion through pain receptors. Also, IL-17A is very important to damaged sympathetic axons which innervate the cornea regeneration and growth. In a number of chronic noninfectious diseases involving inflammatory response, the elevated IL-17A concentrations are found [25]. The aim of our research was to find the association of IL-17A and *CYP4F2* rs1558139 gene polymorphism with optic neuritis.

2. Materials and Methods

The permission (number BEC-LSMU (ER-19)) to undertake the study was obtained from Kaunas Regional Biomedical Research Ethics Committee. The study was conducted in the Department of Ophthalmology of the Hospital of Lithuanian University of Health Sciences and Neuroscience Institute, Lithuanian University of Health Sciences. Study participants comprised of 40 subjects with a diagnosis of optic neuritis and 164 persons from the control group. All patients with an attack of ON who were admitted to the Hospital of Lithuanian University of Health Sciences Ophthalmology department between the 1st of January 2012 and the 1st of February 2015 were included in our study. The inclusion criteria for subjects with optic neuritis were as follows: (1) patients with the first attack of an acute ON episode; (2) participation consent; (3) neurologist consultation; and (4) conducted neurological examination for MS (MS diagnosis was established according to the widely accepted and revised McDonald criteria (2005)). The exclusion criteria for subjects were as follows: (1) other diseases of the optic nerve and (2) systemic illnesses (diabetes mellitus, oncological diseases, systemic tissue disorders, chronic infectious diseases, and conditions after organ or tissue transplantation). The inclusion criteria for healthy patients were (1) no ophthalmological eye disorders found on detailed ophthalmological evaluation; (2) detailed general clinical examination of the patients; and (3) participation consent. The exclusion criteria for healthy patients were (1) Any eye disorders and (2) Any general therapeutic disorders. The reference group was made of healthy subjects, who were admitted to the Hospital of Lithuanian University of Health Sciences Ophthalmology Department for preventive ophthalmological evaluation, considering the patient's age and gender in the optic neuritis group. Therefore, the medians of the patient age of the control group and the optic neuritis group did not differ statistically significant ($p < 0.05$). Demographic data of the study subjects are presented in Table 1.

Table 1: Demographic characteristics of patients with optic neuritis (ON) and control group subjects.

Characteristics	ON group ($n = 40$)	Control group ($n = 164$)	p value
Gender			
Females, n (%)	27 (67.5)	132 (80.5)	0.618
Males, n (%)	13 (32.5)	32 (19.5)	
Age, year (min/max/median)	18/57/35	19/65/44	0.735
ON patients without MS*	19	—	—
Females	13	—	—
Males	6	—	—
ON patients with MS	21	—	—
Females	14	—	—
Males	7	—	—

*MS: multiple sclerosis.

2.1. SNP Selection. According to literature data, rs2108622 is a mostly often studied CYP variant. CYP rs1558139 variant (NM_001082.4:c.919-446C>T) was already evaluated in patients with ischemic stroke. In our study, this SNP was selected according to a Chinese scientist group study [19]. There are 225 SNPs for the human *CYP4F2* gene listed in the National Center for Biotechnology Information SNP database Build 126 (http://www.ncbi.nlm.nih.gov/SNP). Authors screened the data for the Tag SNPs on the International HapMap Project website (http://www.hapmap.org/index.html.ja), using a cutoff level of $r^2 \geq 0.5$, and for the minor allele frequency, we used a cutoff level of ≥0.1. According to the above criterion, we selected rs1558139 for this gene as well, and found out that

(1) our genotyped SNP rs1558139 was in very low linkage disequilibrium with rs2108622 which was reported to be linked to ischemic stroke ($r^2 = 0.009$);

(2) additionally, the SNP Function Prediction tool developed by Xu and Taylor [26] and available online at

the SNPinfo Web Server (https://snpinfo.niehs.nih.gov/) reported that the intron variant rs1558139 have regulatory potential function;

(3) on the other hand, there still exist a limitation of papers with functional annotation of associations of SNPs and optic neuritis.

2.2. DNA Extraction and Genotyping. The DNA extraction and analysis of the gene polymorphism of *CYP4F2* (G1347A; rs1558139) was carried out in the Laboratory of Ophthalmology, Neuroscience Institute of LUHS. DNA was extracted from 200 μL venous blood (white blood cells) using a DNA purification kit based on the magnetic beads method (MagJET Genomic DNA Kit, Thermo Scientific) according to the manufacturer's recommendations. The genotyping of *CYP4F2* (G1347A; rs1558139 was carried out using the real-time polymerase chain reaction (PCR) method. Single nucleotide polymorphisms were determined using TaqMan® Drug Metabolism assays (Thermo Scientific). The genotyping was performed using a Rotor-Gene Q real-time PCR quantification system (Qiagen, USA). The real-time PCR reagents (2X TaqMan Universal Master Mix, TaqMan Drug Metabolism assay, and nuclease-free water) were stored at −20°C and thawed at room temperature. Then reagents were centrifuged (10,000 rpm) and stored in an ice tub. The appropriate real-time PCR mixture of *CYP4F2* (G1347A) was prepared for determining single nucleotide polymorphism. The PCR reaction mixture (9 μL) was poured into each of the 72 wells of the Rotor-Disc, and then 1 μL of matrix DNA of the samples (~10 ng) and 1 μL of negative control (−K) were added. The Allelic Discrimination program was used during the real-time PCR. The assay was continued following the manual provided by the manufacturer (http://www.qiagen.com, Allelic Discrimination). After the Allelic Discrimination program was completed, the genotyping results were obtained. The program determined the individual genotypes according to the fluorescence intensity rate of the different detectors (VIC and FAM).

2.3. Assessment of Serum Interleukin-17A Levels. Serum levels of IL-17A were evaluated using an ELISA kit ("Thermo Fisher Scientific Human IL17A ELISA Kit") designed to measure human IL-17A in serum.

2.4. Statistical Analysis. Statistical analysis was performed using the SPSS/W 20.0 software (Statistical Package for the Social Sciences for Windows Inc., Chicago, Illinois, USA). The data are presented as absolute numbers with percentages in brackets, average values, and standard deviations (SD). Hardy–Weinberg analysis was performed to compare the observed and expected frequencies of rs1558139 genotypes using the χ^2 test in all groups. The distribution of the rs1558139 SNP genotypes in the ON and control groups was compared using the χ^2 test or the Fisher's exact test. Binomial logistic regression analysis was performed to estimate the impact of genotypes on AMD development. Odds ratios and 95% confidence intervals are presented. The selection of the best genetic model was based on the Akaike information criterion (AIC); therefore, the best genetic models were those with the lowest AIC values. R studio version 3.4.1 (RStudio Team (2017). RStudio: Integrated Development for R. RStudio Inc., Boston, MA, URL http://www.rstudio.com/) was used for IL-17A concentration analysis. The D'Agostino-Pearson test was used to check the data for normal distribution. The nonparametric data were presented as median and interquartile range (IQR; 25th to 75th percentile).The Mann–Whitney test was used for comparison between these data. When the distribution of the data was parametric, the unpaired Student's *t*-test was used and the results were presented as mean and standard deviation (SD). Differences were considered statistically significant for all tests when $p < 0.05$.

3. Results

There were two groups in our study. The first included 40 ON patients: 13 men (32.5%) and 27 women (67.5%) and the median age was 35. The control group consisted of 164 healthy persons: 32 men (19.5%) and 132 (80.5%) women with a median age of 44. Demographic characteristics are shown in Table 1.

3.1. Analysis of Association of CYP4F2 rs1558139 with Optic Neuritis. Rs1558139 genotype distribution for both studied groups was at Hardy–Weinberg equilibrium ($p > 0.05$). Analysis of *CYP4F2* rs1558139 genotype and allele distribution between ON patients and healthy controls did not reveal any statistically significant differences (Table 2).

Binomial logistic regression analysis was performed. However, it did not show any statistically significant differences (Table 3).

The detailed analysis was performed to analyze genotype distribution by gender, but it did not show any differences either. For the further analysis, there were two new groups of ON patients formed: the ON patients without MS and the ON patients with MS. *CYP4F2* rs1558139 genotype distributions only showed differences when the analysis was performed by gender. Rs1558139 A/A genotype was statistically significantly more frequent in men than in women: 57.1% versus 0%, respectively, $p = 0.009$ (Table 4). Also, allele A was statistically significantly more frequent in men than in women: 71.4% versus 37.5%, respectively, $p = 0.044$ (Table 4).

Binomial logistic regression was performed, but it did not reveal any statistically significant differences.

3.2. IL-17A Concentration Measurements. IL-17A was detected in serum samples from all patients and healthy controls. According to the D'Agostino-Pearson test, IL-17A values in serum did not follow the normal distribution and the result was expressed by median and interquartile range (IQR). IL-17A serum concentration was significantly higher in ON patients than in healthy controls (median, IQR: 20.55 pg/ml, 30.66 pg/ml versus 8.97 pg/ml, 6.24 pg/ml, respectively, $p < 0.001$) (Figure 1).

3.3. IL-17A Concentration in ON Patients with and without Multiple Sclerosis. Further analysis was performed to evaluate differences of IL-17A level between ON patients with and

Table 2: Frequency of *CYP4F2* rs1558139 genotypes and alleles in patients with optic neuritis (ON) and in control group.

Gene	Genotype/allele	Frequency (%) Control group n (%) $n = 164$	p HWE	Frequency (%) ON group n (%) $n = 40$	p HWE	p value
CYP4F2 rs1558139	Genotype					
	G/G	50 (30.5)	0.481	14 (35)	0.616	$\chi^2 = 0.331$
	G/A	77 (47)		18 (45)		$p = 0.848$
	A/A	37 (22.5)		8 (20)		
	Total	164 (100)		40 (100)		
	Allele					
	G	177 (54.0)		46 (57.5)		$p = 0.569$
	A	151 (46.0)		34 (42.5)		

ON: optic neuritis; p value: significance level (alpha = 0.05); p value HWE: significance level (alpha = 0.05) by Hardy–Weinberg equilibrium.

Table 3: *CYP4F2* rs1558139 binomial logistic regression analysis in patients with optic neuritis (ON) and in control group.

Model	Genotype	OR (CI 95%)	p value	AIC
Codominant	G/A	0.835 (0.381–1.828)	0.652	207.599
	A/A	0.722 (0.294–2.031)	0.600	
Dominant	G/A + A/A	0.815 (0.393–1.690)	0.582	205.963
Recessive	A/A	0.858 (0.364–2.022)	0.726	205.802
Overdominant	G/A	0.924 (0.462–1.851)	0.824	205.877
Additive	A allele	0.873 (0.540–1.411)	0.580	205.619

ON: optic neuritis; OR: odd ratio; CI: confidence interval; p value: significance level (alpha = 0.05); AIC: Akaike information criterion.

without MS. According to the D'Agostino-Pearson test, IL-17A values in serum followed the normal distribution and the result was expressed by mean standard deviation (SD). Student's t-test showed that IL-17A concentration in studied groups was normally spread ($p < 0.05$), therefore comparing the concentration of IL-17A between these two groups, the unpaired Student's t-test was used. Comparing concentration of cytokine IL-17A in blood serum of ON patients with or without MS, statistically significant differences were not found (average (SD): 26.19 (21.55) pg/ml versus 30.21 (19.96) pg/ml, respectively, $p = 0.544$) (Figure 2).

3.4. Analysis of Association between Serum IL-17A Levels and Genotypes of CYP4F2 rs1558139. We compared IL-17A levels in serum between all genotype groups of ON patients as well. IL-17A concentration in the three genotype groups (GG, GA, and AA) was normally distributed ($p > 0.05$). The one-way ANOVA analysis did not reveal any differences between IL-17A concentration by genotypes (average (SD): 21.35 (16.13) pg/ml versus 36.20 (22.35) pg/ml versus 18.33 (17.65) pg/ml, respectively, $p = 0.603$) (Figure 3).

4. Discussion

Our study showed that *CYP4F2* gene rs1558139 polymorphism did not reveal any differences in the distribution of G/G, G/A, and A/A genotypes between groups (35.0% versus 45.0% versus 20.0% in patients with optic neuritis, 30.5% versus 47.0% versus 22.5% in control group, resp.). However, the group of patients with optic neuritis without MS had statistically significant differences between genders ($p < 0.05$). Rs1558139 A/A genotype was statistically significantly more frequent in males than females: 57.1% versus 0%, $p = 0.009$, but it must be repeated with a larger sample of the study for the reliability of the results. Patients with acute demyelinating ON are young adults, usually without any other health problems. Female preponderance in observed, with a ratio of approximately 3 : 1. ON is seen more commonly in Caucasians and quite rarely in black populations. Incidence of ON is eight times higher in white northern Europeans than blacks and Asians [27]. Animal experiments have revealed that the expression of a number of CYP (cytochrome P450 enzymes) is sex dependent [28, 29]. Cytochrome P450 (CYP) enzymes are also involved in estrogen metabolism and many are regulated by estrogens. These genes may thus be of relevance to gender-specific differences in lung cancer risk, particularly in early-onset lung cancer, where a high proportion of women is observed [30].We also hypothesised that one of the SNPs in *CYP4F2* (rs1558139) is important in pathogenetic mechanisms of optic neuritis in females. On the other hand, sex dependence in human was found in few other studies: Fava et al. [20] found that V433M mutation in CYP4F2 gene was associated with cerebral infarction in male patients and the study [31] based on Japanese population found that G allele at rs2108622 was more frequent in male patients than in the controls. Haplotype analysis revealed that TCG haplotypes composed by rs3093135-rs1558139-rs2108622 is a risk factor for cerebral infarction in males [18].

An inflammation is one of the key players in pathogenesis of optic neuritis [10]. The data on CYP activity during inflammation process is scare and inconsistent. Haberfeld reported that inflammation suppresses CYP activity [32], but Gilroy et al. stated that levels of CYP 450 enzyme-

Table 4: Frequency of *CYP4F2* rs1558139 genotypes and alleles in the groups of optic neuritis (ON) patients with and without MS by gender.

Gene	Genotype/allele	Frequency (%)					
		ON without MS group *n* (%)		*P* value	ON with MS group *n* (%)		*P* value
		Women *n* = 12	Men *n* = 7		Women *n* = 15	Men *n* = 6	
CYP4F2 rs1558139	Genotype						
	G/G	3 (27)	1 (14.3)	1.000	6 (32.1)	4 (66.7)	0.362
	G/A	9 (75)	2 (28.6)	0.074	5 (53.6)	2 (33.3)	1.000
	A/A	0 (0)	4 (57.1)	0.009	4 (14.3)	0 (0)	0.281
	Total	12 (100)	7 (100)		15 (100)	6 (100)	
	Allele						
	G	15 (62.5)	4 (28.6)	0.044	17 (56.7)	10 (83.33)	0.158
	A	9 (37.5)	10 (71.4)		13 (43.3)	2 (16.67)	

ON: optic neuritis; MS: multiple sclerosis: *p* value: significance level (alpha = 0.05).

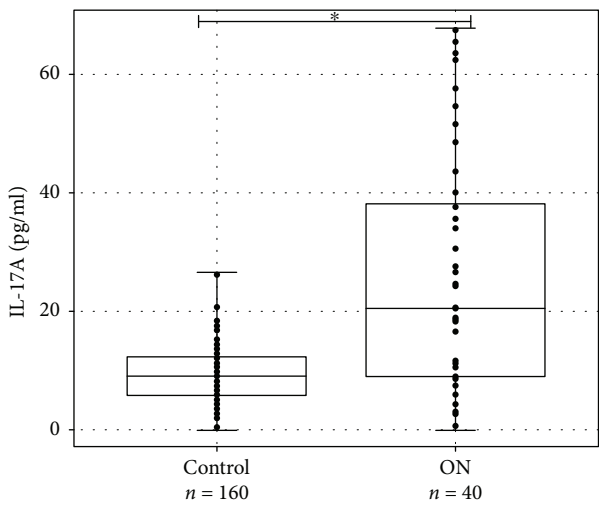

Figure 1: IL-17A concentration (pg/ml) in serum of ON patients and healthy controls. IL-17A levels (pg/ml) in serum of ON patient versus healthy controls are presented as *box*-and-*whisker plots* with the median and IQR and individual dots. Mann–Whitney *U* test was used to assess the differences of IL-17A concentration between ON patients and control groups. $^{*}p < 0.001$.

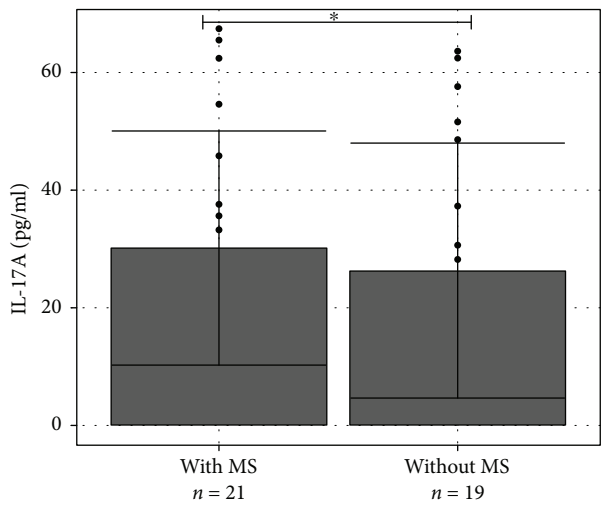

Figure 2: IL-17A concentration (pg/ml) in serum of ON patients with and without MS. IL-17A levels (pg/ml) in serum of ON patients with and without MS are presented as *bar plots* with the mean and SD and individual dots. Student's *t*-test was used to assess the differences of IL-17A concentration among ON without MS and ON with MS groups. $^{*}p = 0.544$.

derived oxylipins are elevated as the expression of *CYP4F2*, *CYP4F3*, and *CYP4A* family enzymes is increased during inflammation [33]. We have not found similar studies investigating *CYP4F2* gene polymorphisms in patients with optic neuritis. Fu and coauthors found that *CYP4F2* rs1558139 polymorphism in combination with other polymorphisms of this gene, which form haplotypes, are related to cardiac and cerebral vascular diseases [18]. In 2015, Lan et al. showed that four polymorphisms (rs7528684, rs945635, rs3761959, and rs2282284) in FCRL3 gene can increase the risk for neuromyelitis optica (NMO) [34]. FCRL3_3 (rs7528684) polymorphism, widely studied in earlier studies, showed that this polymorphism is a characteristic of many autoimmune diseases [35–37]. Recently it was found that rs703842 and rs10876994 in *CYP27B1* gene that encodes a vitamin D metabolising protein are related to neurological demyelinating diseases in a Chinese population. Statistically significant differences were found between genotype distributions of rs703842 ($p = 0.013$) and rs10876994 ($p = 0.001$) polymorphisms comparing patients with their control group [38]. Several studies determined that rs1016140 in *CD58* gene was associated with reduced T cell activity [39, 40]. It was found that the G allele at rs1016140 was associated with an increased risk of CNS diseases. It is believed that an increase in T cell activity depends on the G allele and may result in higher CNS inflammation frequency, which in turn facilitates access of aquaporin 4 (AQP4), a water carrier membrane antibody, into the CNS and ultimately leads to the spread of optic neuritis. Further studies are needed to confirm the role of rs1016140 [41].

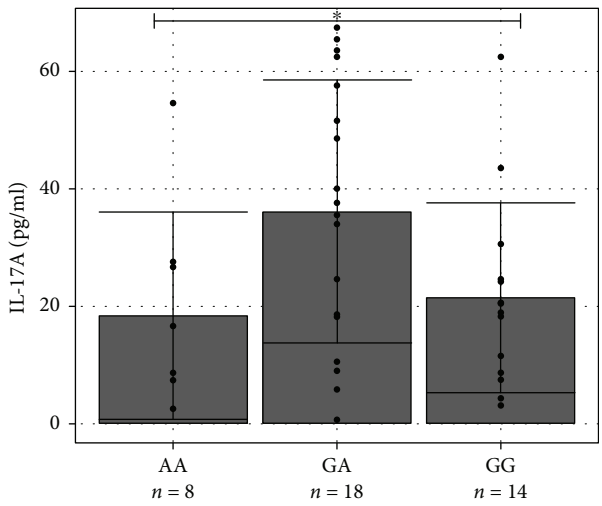

Figure 3: IL-17A concentration (pg/ml) in serum of different genotype groups. IL-17A levels (pg/ml) in serum of ON patients by genotype are presented as *bar plots* with the mean and SD and individual dots. *One-way ANOVA test* was used to assess the differences of IL-17A concentration between groups of ON patients with and without MS. $^{*}p = 0.603$.

Interleukin-17A (IL-17A) participates in the pathogenesis of several immune and inflammatory diseases and upregulates expression of numerous inflammation-related genes [42]. Our research revealed that IL-17A concentration in blood serum was statistically significantly higher for patients with ON in comparison with control group (median, IQR): 18.33 (7.41–37.6) pg/ml versus 8.19 (5.85–11.31) pg/ml, $p < 0.001$), but IL-17A concentration in blood serum of patients with ON with or without MS was not statistically significantly different (average (SD): 27.76 (24.13) pg/ml versus 31.57 (21.89) pg/ml, respectively; $p = 0.641$). There are no studies analysing association of IL-17A concentration with ON, but we think that cytokines are very important for the development of optic neuritis.

Pathogenic mechanisms of inflammatory Th17 cells, releasing a large amount of interleukin-17 (IL-17) and IL-23 and other cytokines are already widely studied [43]. TGF-β cytokine is also adopted in the framework of the differentiation of T cells associated with MS and NMO [44, 45]. Another study with mice autoimmune encephalomyelitis models showed that Th17, IL-6, and IL-17 concentration increases may be associated with autoimmune disorders of central nervous system (CNS). In the experimental study of mice models, a strong relationship was found between IL-17 and Th17 cells [46, 47]. In particular, it showed that sharp differences in IL-17 concentration increase in a mouse model of autoimmune encephalomyelitis [48]. IL-17A association with optic neuritis was also proved in experimental model by Knier et al. [49].

NMO is associated with astrocytic water channel aquaporin-4 (AQP4) antibodies, which is believed to contribute to the pathogenesis of optic nerve inflammation and causes toxic reactions and immune cell infiltration. It is believed that AQP4 antibodies may be considered a reliable marker in distinguishing NMO from MS. AQP4 antibody concentrations appear to be strongly correlated with IL-6 and IL-8 concentrations [48]. In addition, IL-17 and IL-23 levels are elevated in patients with NMO, compared with controls [50].

4.1. Strengths and Limitations. This is the first study to examine the relationship of *CYP4F2* rs1558139 and IL-17A levels with ON and MS. For the first time, *CYP4F2* rs1558139 AA genotype was associated with ON in males with MS, and for the first time, the higher IL-17A levels were determined to be associated with ON. On the other hand, because of a large number of SNPs, it is required to make replication studies in the future, particularly with bigger sample size, to confirm the association between SNPs and ON development.

5. Conclusions

We revealed *CYP4F2* rs1558139 AA genotype association with ON and MS in male. According to statistical analysis, the higher IL-17A levels were determined to be associated with inflammation processes while ON. These findings suggest new biological markers for the diagnostics of ON, but further studies with a larger number of patients, however, are necessary in order to better understand of ON development.

Abbreviations

ON: Optic neuritis
CYP: Cytochrome P450 enzyme
IL: Interleukin
MS: Multiple sclerosis
SNP: Single nucleotide polymorphism
IQR: Interquartile range
SD: Standard deviation
HWE: Hardy–Weinberg equilibrium
NMO: Neuromyelitis optica
FCRL3: Fc receptor-like 3 gene
CNS: Central nerve system
AQP4: Aquaporin 4 protein
TGF-β: Transforming growth factor beta
Th: T helper.

Consent

Consent to publish has been obtained from the participant.

Conflicts of Interest

The authors declare no conflict of interests. None of the authors has any proprietary interests or conflicts of interest related to this submission.

Authors' Contributions

Mantas Banevicius collected all patients and their data included in our study. Rasa Liutkeviciene, Alvita Vilkeviciute, and Brigita Glebauskiene were responsible for the

study concept and design. Alvita Vilkeviciute and Rasa Liutkeviciene made a statistical analysis of the data. Loresa Kriauciuniene and Rasa Liutkeviciene were responsible for the drafting of the manuscript. All authors read, revised, and approved the final manuscript.

References

[1] M. Rodriguez, A. Siva, S. A. Cross, P. C. O'Brien, and L. T. Kurland, "Optic neuritis: a population-based study in Olrnsted County, Minnesota," *Neurology*, vol. 45, no. 2, pp. 244–250, 1995.

[2] A. Ascherio and K. L. Munger, "Environmental risk factors for multiple sclerosis. Part II: noninfectious factors," *Annals of Neurology*, vol. 61, no. 6, pp. 504–513, 2007.

[3] Y. P. Jin, J. de Pedro-Cuesta, M. Söderström, and H. Link, "Incidence of optic neuritis in Stockholm, Sweden, 1990–1995: II. Time and space patterns," *Archives of Neurology*, vol. 56, no. 8, pp. 975–980, 1999.

[4] N. Cikes, D. Bosnic, and M. Sentic, "Non-MS autoimmune demyelination," *Clinical Neurology and Neurosurgery*, vol. 110, no. 9, pp. 905–912, 2008.

[5] K. Ruprecht, E. Klinker, T. Dintelmann, P. Rieckmann, and R. Gold, "Plasma exchange for severe optic neuritis: treatment of 10 patients," *Neurology*, vol. 63, no. 6, pp. 1081–1083, 2004.

[6] B. K. McDonald, O. C. Cockerell, J. W. Sander, and S. D. Shorvon, "The incidence and lifetime prevalence of neurological disorders in a prospective community-based study in the UK," *Brain*, vol. 123, no. 4, pp. 665–676, 2000.

[7] Y. P. Jin, J. de Pedro-Cuesta, M. Söderström, L. Stawiarz, and H. Link, "Incidence of optic neuritis in Stockholm, Sweden 1990–1995: I. Age, sex, birth and ethnic-group related patterns," *Journal of the Neurological Sciences*, vol. 159, no. 1, pp. 107–114, 1998.

[8] Optic Neuritis Study Group, "The clinical profile of optic neuritis. Experience of the Optic Neuritis Treatment Trial," *Archives of Ophthalmology*, vol. 109, no. 12, pp. 1673–1678, 1991.

[9] A. Ascherio and K. L. Munger, "Environmental risk factors for multiple sclerosis. Part I: the role of infection," *Annals of Neurology*, vol. 61, no. 4, pp. 288–299, 2007.

[10] E. Voss, P. Raab, C. Trebst, and M. Stangel, "Clinical approach to optic neuritis: pitfalls, red flags and differential diagnosis," *Therapeutic Advances in Neurological Disorders*, vol. 4, no. 2, pp. 123–134, 2011.

[11] T. Fukaya, T. Gondaira, Y. Kashiyae et al., "Arachidonic acid preserves hippocampal neuron membrane fluidity in senescent rats," *Neurobiology of Aging*, vol. 28, no. 8, pp. 1179–1186, 2007.

[12] Z. J. Wang, C. L. Liang, G. M. Li, C. Y. Yu, and M. Yin, "Neuroprotective effects of arachidonic acid against oxidative stress on rat hippocampal slices," *Chemico-Biological Interactions*, vol. 163, no. 3, pp. 207–217, 2006.

[13] F. Darios and B. Davletov, "Omega-3 and omega-6 fatty acids stimulate cell membrane expansion by acting on syntaxin 3," *Nature*, vol. 440, no. 7085, pp. 813–817, 2006.

[14] S. I. Rapoport, "Arachidonic acid and the brain," *The Journal of Nutrition*, vol. 138, no. 12, pp. 2515–2520, 2008.

[15] D. W. Nebert, K. Wikvall, and W. L. Miller, "Human cytochromes P450 in health and disease," *Philosophical Transactions of the Royal Society B: Biological Sciences*, vol. 368, no. 1612, article 20120431, 2013.

[16] C. R. Curley, A. J. Monsuur, M. C. Wapenaar, J. D. Rioux, and C. Wijmenga, "A functional candidate screen for coeliac disease genes," *European Journal of Human Genetics*, vol. 14, no. 11, pp. 1215–1222, 2006.

[17] F. Fan, Y. Ge, W. Lv et al., "Molecular mechanisms and cell signaling of 20-hydroxyeicosatetraenoic acid in vascular pathophysiology," *Frontiers in Bioscience*, vol. 21, no. 7, pp. 1427–1463, 2016.

[18] Z. Fu, T. Nakayama, N. Sato et al., "A haplotype of the *CYP4F2* gene is associated with cerebral infarction in Japanese men," *American Journal of Hypertension*, vol. 21, no. 11, pp. 1216–1223, 2008.

[19] H. Q. Yan, Y. Yuan, P. Zhang, Z. Huang, L. Chang, and Y. K. Gui, "*CYP4F2* gene single nucleotide polymorphism is associated with ischemic stroke," *Genetics and Molecular Research*, vol. 14, no. 1, pp. 659–664, 2015.

[20] C. Fava, M. Montagnana, P. Almgren et al., "The V433M variant of the *CYP4F2* is associated with ischemic stroke in male Swedes beyond its effect on blood pressure," *Hypertension*, vol. 52, no. 2, pp. 373–380, 2008.

[21] S. Deng, G. Zhu, F. Liu et al., "CYP4F2 gene V433M polymorphism is associated with ischemic stroke in the male Northern Chinese Han population," *Progress in Neuro-Psychopharmacology & Biological Psychiatry*, vol. 34, no. 4, pp. 664–668, 2010.

[22] S. Tabur, S. Oztuzcu, E. Oguz et al., "*CYP* gene expressions in obesity-associated metabolic syndrome," *Obesity Research & Clinical Practice*, vol. 10, no. 6, pp. 719–723, 2016.

[23] S. S. Rathore, S. K. Agarwal, S. Pande, S. K. Singh, T. Mittal, and B. Mittal, "CYP4F2 1347 G> A & GGCX 12970 C> G polymorphisms: frequency in north Indians & their effect on dosing of acenocoumarol oral anticoagulant," *The Indian Journal of Medical Research*, vol. 139, no. 4, pp. 572–578, 2014.

[24] F. Takeuchi, R. McGinnis, S. Bourgeois et al., "A genome-wide association study confirms *VKORC1*, *CYP2C9*, and *CYP4F2* as principal genetic determinants of warfarin dose," *PLoS Genetics*, vol. 5, no. 3, article e1000433, 2009.

[25] M. H. Kang, M. K. Kim, H. J. Lee, H. I. Lee, W. R. Wee, and J. H. Lee, "Interleukin-17 in various ocular surface inflammatory diseases," *Journal of Korean Medical Science*, vol. 26, no. 7, pp. 938–944, 2011.

[26] X. Zongli and J. A. Taylor, "SNPinfo: integrating GWAS and candidate gene information into functional SNP selection for genetic association studies," *Nucleic Acids Research*, vol. 37, Supplement 2, pp. W600–W605, 2009.

[27] H. Hoorbakht and F. Bagherkashi, "Optic neuritis, its differential diagnosis and management," *The Open Ophthalmology Journal*, vol. 6, no. 1, pp. 65–72, 2012.

[28] D. J. Waxman, P. A. Ram, N. A. Pampori, and B. H. Shapiro, "Growth hormone regulation of male-specific rat liver P450s 2A2 and 3A2: induction by intermittent growth hormone pulses in male but not female rats rendered growth hormone deficient by neonatal monosodium glutamate," *Molecular Pharmacology*, vol. 48, no. 5, pp. 790–797, 1995.

[29] D. N. Muller, C. Schmidt, E. Barbosa-Sicard et al., "Mouse Cyp4a isoforms: enzymatic properties, gender- and strain-specific expression, and role in renal 20-hydroxyeicosatetraenoic acid formation," *Biochemical Journal*, vol. 403, no. 1, pp. 109–118, 2007.

[30] M. N. Timofeeva, S. Kropp, W. Sauter et al., "CYP450 polymorphisms as risk factors for early-onset lung cancer: gender-specific differences," *Carcinogenesis*, vol. 30, no. 7, pp. 1161–1169, 2009.

[31] K. Nakamura, K. Obayashi, T. Araki et al., "*CYP4F2* gene polymorphism as a contributor to warfarin maintenance dose in Japanese subjects," *Journal of Clinical Pharmacy and Therapeutics*, vol. 37, no. 4, pp. 481–485, 2012.

[32] H. Haberfeld, Ed., *Austria-Codex (in German)*, Österreichischer Apothekerverlag, Vienna, 2015.

[33] D. W. Gilroy, M. L. Edin, R. P. H. De Maeyer et al., "CYP450-derived oxylipins mediate inflammatory resolution," *Proceedings of the National Academy of Sciences of the United States of America*, vol. 113, no. 23, pp. E3240–E3249, 2016.

[34] W. Lan, S. Fang, H. Zhang, D. T. Wang, and J. Wu, "The Fc receptor-like 3 polymorphisms (rs7528684, rs945635, rs3761959 and rs2282284) and the risk of neuromyelitis optica in a Chinese population," *Medicine*, vol. 94, no. 38, article e1320, 2015.

[35] S. Eyre, J. Bowes, C. Potter, J. Worthington, and A. Barton, "Association of the FCRL3 gene with rheumatoid arthritis: a further example of population specificity?," *Arthritis Research & Therapy*, vol. 8, no. 4, article R117, 2006.

[36] A. B. Begovich, M. Chang, and S. J. Schrodi, "Meta-analysis evidence of a differential risk of the *FCRL3* −169T→C polymorphism in white and East Asian rheumatoid arthritis patients," *Arthritis & Rheumatism*, vol. 56, no. 9, pp. 3168–3171, 2007.

[37] S. Duchatelet, S. Caillat-Zucman, D. Dubois-Laforgue, H. Blanc, J. Timsit, and C. Julier, "FCRL3-169CT functional polymorphism in type 1 diabetes and autoimmunity traits," *Biomedicine & Pharmacotherapy*, vol. 62, no. 3, pp. 153–157, 2008.

[38] J. C. Zhuang, Z. Y. Huang, G. X. Zhao, H. Yu, Z. X. Li, and Z. Y. Wu, "Variants of CYP27B1 are associated with both multiple sclerosis and neuromyelitis optica patients in Han Chinese population," *Gene*, vol. 557, no. 2, pp. 236–239, 2015.

[39] B. J. Hennig, K. Fielding, J. Broxholme et al., "Host genetic factors and vaccine-induced immunity to hepatitis B virus infection," *PLoS One*, vol. 3, no. 3, article e1898, 2008.

[40] K. K. Ryckman, K. Fielding, A. V. Hill et al., "Host genetic factors and vaccine-induced immunity to HBV infection: haplotype analysis," *PLoS One*, vol. 5, no. 8, article e12273, 2010.

[41] J. Y. Kim, J. S. Bae, H. J. Kim, and H. D. Shin, "CD58 polymorphisms associated with the risk of neuromyelitis optica in a Korean population," *BMC Neurology*, vol. 14, no. 1, p. 57, 2014.

[42] H. F. McFarland and R. Martin, "Multiple sclerosis: a complicated picture of autoimmunity," *Nature Immunology*, vol. 8, no. 9, pp. 913–919, 2007.

[43] B. W. Kirkham, A. Kavanaugh, and K. Reich, "Interleukin-17A: a unique pathway in immune-mediated diseases: psoriasis, psoriatic arthritis and rheumatoid arthritis," *Immunology*, vol. 141, no. 2, pp. 133–142, 2014.

[44] F. Sellebjerg, M. Christiansen, J. Jensen, and J. L. Frederiksen, "Immunological effects of oral high-dose methylprednisolone in acute optic neuritis and multiple sclerosis," *European Journal of Neurology*, vol. 7, no. 3, pp. 281–289, 2000.

[45] V. Navikas and H. Link, "Review: cytokines and the pathogenesis of multiple sclerosis," *Journal of Neuroscience Research*, vol. 45, no. 4, pp. 322–333, 1996.

[46] D. M. Wingerchuk, V. A. Lennon, C. F. Lucchinetti, S. J. Pittock, and B. G. Weinshenker, "The spectrum of neuromyelitis optica," *The Lancet Neurology*, vol. 6, no. 9, pp. 805–815, 2007.

[47] L. A. Tesmer, S. K. Lundy, S. Sarkar, and D. A. Fox, "Th17 cells in human disease," *Immunological Reviews*, vol. 223, no. 1, pp. 87–113, 2008.

[48] L. Sun, H. Weng, and Z. Li, "Elevation of AQP4 and selective cytokines in experimental autoimmune encephalitis mice provides some potential biomarkers in optic neuritis and demyelinating diseases," *International Journal of Clinical and Experimental Pathology*, vol. 8, no. 12, pp. 15749–15758, 2015.

[49] B. Knier, V. Rothhammer, S. Heink et al., "Neutralizing IL-17 protects the optic nerve from autoimmune pathology and prevents retinal nerve fiber layer atrophy during experimental autoimmune encephalomyelitis," *Journal of Autoimmunity*, vol. 56, pp. 34–44, 2015.

[50] Y. Li, H. Wang, Y. Long, Z. Lu, and X. Hu, "Increased memory Th17 cells in patients with neuromyelitis optica and multiple sclerosis," *Journal of Neuroimmunology*, vol. 234, no. 1-2, pp. 155–160, 2011.

Hindawi
Journal of Ophthalmology
Volume 2018, Article ID 1030184, 7 pages
https://doi.org/10.1155/2018/1030184

Research Article

Phenotypic Progression of Stargardt Disease in a Large Consanguineous Tunisian Family Harboring New *ABCA4* Mutations

Yousra Falfoul,[1,2] **Imen Habibi**,[3] **Ahmed Turki**,[2] **Ahmed Chebil**,[1,2] **Asma Hassairi**,[1,2] **Daniel F. Schorderet**,[3,4] **and Leila El Matri**[1,2]

[1]*Hedi Rais Institute of Ophthalmology (Department B), Tunis, Tunisia*
[2]*Oculogenetic Laboratory LR14SP01, Tunis, Tunisia*
[3]*Institute for Research in Ophthalmology (IRO), Sion, Switzerland*
[4]*Department of Ophthalmology, University of Lausanne and Faculty of Life Sciences, Ecole Polytechnique Fédérale of Lausanne, Lausanne, Switzerland*

Correspondence should be addressed to Yousra Falfoul; yosra.falfoul@yahoo.fr

Received 9 September 2017; Revised 29 December 2017; Accepted 1 February 2018; Published 15 March 2018

Academic Editor: Robert B. Hufnagel

To assess the progression of Stargardt (STGD) disease over nine years in two branches of a large consanguineous Tunisian family. Initially, different phenotypes were observed with clinical intra- and interfamilial variations. At presentation, four different retinal phenotypes were observed. In phenotype 1, bull's eye maculopathy and slight alteration of photopic responses in full-field electroretinography were observed in the youngest child. In phenotype 2, macular atrophy and yellow white were observed in two brothers. In phenotype 3, diffuse macular, peripapillary, and peripheral RPE atrophy and hyperfluorescent dots were observed in two sisters. In phenotype 4, Stargardt disease-fundus flavimaculatus phenotype was observed in two cousins with later age of onset. After a progression of 9 years, all seven patients displayed the same phenotype 3 with advanced stage STGD and diffuse atrophy. WES and MLPA identified two *ABCA4* mutations M1: c.[(?_4635)_(5714+?)dup; (?_6148)_(6479_+?) del] and M2: c.[2041C>T], p.[R681*]. In one branch, the three affected patients had M1/M1 causal mutations and in the other branch the two affected patients had M1/M2 causal mutations. After 9-year follow-up, all patients showed the same phenotypic evolution, confirming the progressive nature of the disease. Genetic variations in the two branches made no difference to similar end-stage disease.

1. Introduction

The ATP-binding cassette transporter ABCA4, also known as ABCR, is a member of the ATP-binding cassette transporter gene subfamily A [1]. ABCA4 is found in the outer segment disk membrane photoreceptor cells [2] and also marginally present in the brain [3].

ABCA4 is important in the visual cycle, as a retinoid transporter of the toxic all-trans retinal out of the disc for recycling by the retinal pigment epithelium (RPE) [4]. Without this function, an accumulation of toxic all-trans-retinal derivatives in rods and cones may cause an apoptosis of the supporting retinal pigment epithelium cells and, ultimately, degeneration of photoreceptors [5, 6].

Mutations in ABCA4 gene are known to cause Stargardt disease (STGD) which is the most frequent macular dystrophy [7] and typically presents with central macular atrophy and yellow-white dots at the posterior pole, primarily at the level of the RPE. Additional diseases were also linked to mutations in *ABCA4* including fundus flavimaculatus,

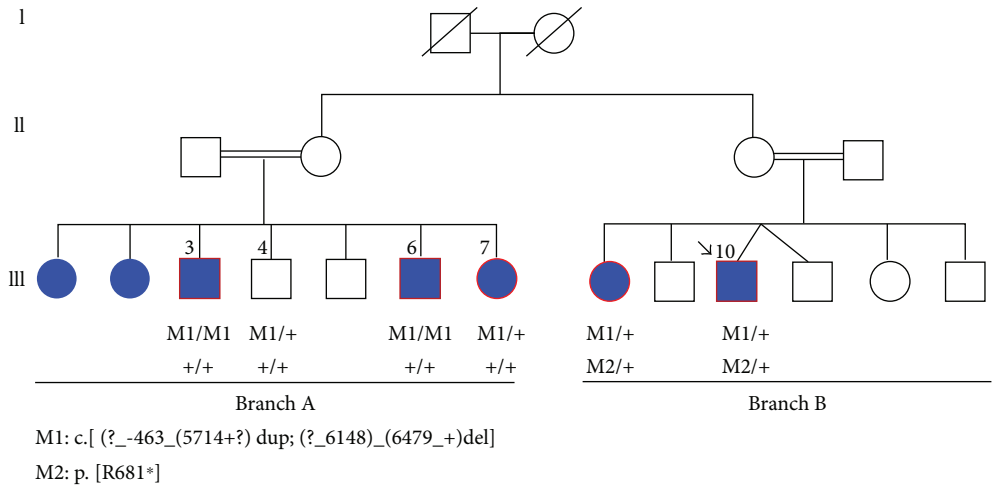

Figure 1: Pedigree structure of the family and segregation analysis of ABCA4 mutations.

cone-rod dystrophy (CRD), and retinitis pigmentosa [8–11] or variants considered as a risk factor for age-related macular degeneration [12, 13].

The present study reports the molecular origin and clinical evolution in a large Tunisian family with remarkable variations in STGD and CRD phenotypes. This family was initially published in 2013 [14]. We now present a 9-year follow-up, showing progressive disease in all patients with evolution to a similar phenotype of diffuse macular, peripapillary, and peripheral RPE atrophy and hyperfluorescent dots.

2. Patients and Methods

2.1. Patients' Recruitment. We followed a large multiplex family originating from Southern Tunisia (Gafsa) whose initial presentation was published previously [12]. Twelve subjects from two branches (A and B) with autosomal recessive STGD disease were enrolled between March 2005 and January 2014. Written informed consent was obtained from each study participant. Analyses were done in accordance with local guidelines, and regulation study was approved by the Local Ethics Committee of the Hedi Rais Institute.

In accordance with the Helsinki Declaration, clinical examination was performed in 7 patients, biological material was obtained from 11 members, and family genealogical data were gathered (Figure 1).

2.2. Clinical Investigation. A detailed clinical examination including visual acuity, fundus photography, fluorescein angiography, and electroretinography (full-field ERG) were performed for all subjects. The initial data were compared to those at follow-up.

Patients were classified into four phenotypes:

(i) Phenotype 1: bull's eye maculopathy, slightly altered photopic responses on full-field ERG

(ii) Phenotype 2: macular atrophy and yellow-white dots, altered photopic responses on full-field ERG

(iii) Phenotype 3: diffuse macular, peripapillary, and peripheral RPE atrophy and hyperfluorescent dots, altered photopic and scotopic responses on full-field ERG.

(iv) Phenotype 4: Stargardt disease-fundus flavimaculatus (STGD-FFM) with central atrophy, yellow-white dots, hyperfluorescent atrophic spots, and silent choroid, altered photopic responses on full-field ERG (this phenotype appeared similar to phenotype II but was considered a separate nosology due to older age of onset)

2.3. Molecular Analysis. Peripheral blood of all subjects was collected for genomic DNA isolation from leukocytes using the "salting out" standard method. A DNA sample of the index patient was subjected to WES. WES was performed using the Roche NimbleGen version 2 paired-end sample preparation kit and Illumina HiSeq2000 at a mean coverage ×31. Sequence reads were aligned to the human genome reference sequence (build hg19), and variants were identified and annotated using the NextGene software package v.2.3.5. (Softgenetics, State College, PA). To determine the regions of homozygosity from the WES data, we used an in-house developed Excel macro.

2.4. In Silico Analysis. All variants were first filtered against several public databases for the minor allele frequency (MAF) < 1%. dbSNP served as a reference to exclude any known frequent variants. We only focused on nonsynonymous variants, variants in splicing sites, and frame-shift coding insertions or deletions. The pathogenicity index for the identified missense mutations was calculated in silico using Sorting Intolerant from Tolerant (SIFT) (http://sift.bii.a-star.edu.sg/) and Polymorphism Phenotyping V2 (PolyPhen-2) (http://genetics.bwh.harvard.edu/pph2/). The PhyloP score and Grantham distances were also recorded to check the nucleotide conservation and change in amino acid physiochemical properties.

2.5. Mutation Validation. Variants were confirmed by Sanger sequencing, and segregation analysis was done in the family. The following primers designed to amplify exon 14 of *ABCA4* were used: ABCA4-14F: 5′-TCAACAAACATTTA TTCTGCCTCT-3′ and *ABCA4*-14R: 5′-AGCTTCTCCAG ATGGTCACG-3′. PCR was realized in a total reaction mixture of 20 μl, containing 20 ng of genomic DNA, 10 pmol of each primer (Eurogentec, Liège, Belgium), and 10 μl of FastStart PCR Master Mix (Roche, Basel, Switzerland). The DNA was denatured at 95°C for 1 minute, prior to 35 cycles of amplification of 1 min at 94°C, 1 min at 58°C, 1 min at 72°C, and the final extension step at 72°C for 10 min using a GeneAmp 9700 thermal cycler (Applied Biosystems, Carlsbad, California, USA). The amplified fragment was sequenced using a BigDye terminator sequencing kit (Perkin Elmer). Sequenced samples were purified using Performa®V3 96-well short plate, according to manufacturer's instructions, loaded in a 3100 XL ABI sequencer (Applied Biosystems) and analyzed using ABI Prisms Navigator Software.

2.6. MLPA. We performed multiplex ligation-dependent probe amplification (MLPA) on all family members to confirm a large deletion, suspected through lack of PCR amplification in cousins.

The following 2 kits were used: SALSA P151-B1 and P152-B2 kits where both contained probes for all exons of the *ABCA4* gene. MLPA analysis was performed according to manufacturer's instructions (MRC, Holland, Amsterdam, The Netherlands), and data analysis was carried out by GeneMapper software. The MLPA test was performed twice for confirmation of abnormal changes.

3. Results

3.1. Clinical Data. At the 9-year follow-up control, all 7 patients displayed disease progression with advanced stage STGD and diffuse RPE atrophy.

In branch A, 5 patients displayed STGD with initially 3 different phenotypes [14]. Patient III7, who originally presented with phenotype 1, developed after 9 years a large central area of pronounced chorioretinal atrophy in both eyes, with yellow-white dots distributed at the posterior pole and midperiphery. The peripapillary area was normal. Visual acuity fell from 20/200 to 20/400. Full-field ERG showed both altered photopic and scotopic responses. Patients III3 and III6 with STGD-FFM phenotype 2, associating macular atrophy, yellow-white dots, hyperfluorescent atrophic spots, and silent choroid, developed diffuse macular, peripapillary, and RPE atrophy extending beyond the vascular arcades. The yellow-white dots in the midperiphery regressed to be replaced by numerous atrophic dots. Full-field ERG showed both altered photopic and scotopic responses. Primary STGD phenotype 3 III1 and III2 patients with diffuse macular, peripapillary, and peripheral RPE atrophy and hyperfluorescent dots progressed to severe CRD, with extensive areas of atrophy, pigment clumping, and migration throughout the posterior pole involving the peripheral retina. Hyperfluorescent atrophic dots progressed with hypofluorescent spots beyond the vascular arcades.

In branch B, 2 patients III8 and III10 presented initial phenotype 4 STGD (Stargardt fundus flavimaculatus, later age of onset) with central atrophy, yellow-white dots, macular atrophy, hyperfluorescent atrophic spots, and silent choroid. After 9-year progression of the disease, both presented CRD with diffuse macular, peripapillary, and peripheral RPE atrophy, regression of the yellow-white dots, and hyperfluorescent dots. Full-field ERG showed severe altered photopic and scotopic responses.

Phenotype progression of the disease is illustrated in Figure 2.

Clinical results at baseline and follow-up are summarized in Table 1.

3.2. Genetic Findings. Homozygosity mapping and Sanger sequencing of retinal dystrophy-associated genes did not reveal any mutation in this consanguineous family.

WES revealed a previously identified nonsense mutation c.[2041C>T]; p.[R681*] found in exon 14, but in heterozygous form in the proband, which did not segregate with the phenotype in the family. The affected sister carried this heterozygous mutation while the three affected cousins were wild type for this variant.

Multiplex ligation-dependent probe amplification was used to search for a potential deletion in the index patient carrying the heterozygous nonsense mutation. This analysis showed a new complex rearrangement in *ABCA4*: a heterozygous deletion of exon 45 to 47 and heterozygous duplication of exon 32 to 40. This rearrangement was also observed in his sister. The index patient was thus a compound heterozygous: c.[2041C>T], p.[R681*]; c.[(?_-4635)_(5714+?)dup; (?_6148)_(6479_+?) del].

The three affected cousins with no previously detected mutation were then tested by MLPA, identifying the similar complex rearrangement in a homozygous state.

4. Discussion

The aim of the current study was to provide a comprehensive genetic and clinical profile of ABCA4-associated diseases in a consanguineous Tunisian family. In the index patient of branch A, we identified a new genomic rearrangement c.[(?_-4635)_(5714+?)dup; (?_6148)_(6479_+?) del] in *ABCA4*. This rearrangement was present in a homozygous state in the two affected brothers. To date, large genomic rearrangements account for a minor portion of STGD disease alleles. The first one was described by Yatsenko et al. [15]. In our cohort, this is the first large genomic rearrangement identified in Tunisian STGD patients.

It is likely that skipping of exons 45–47 and the duplication of exons 32–40 affect the three-dimensional structure and thereby the function of the protein. Theoretically, these mutations could cause a shift in the reading frame, resulting in a premature termination codon at the NBD2 domain and the absence of C-terminal segment that is crucial for the proper folding of ABCA4 into its native form. Alternatively, nonsense-mediated mRNA

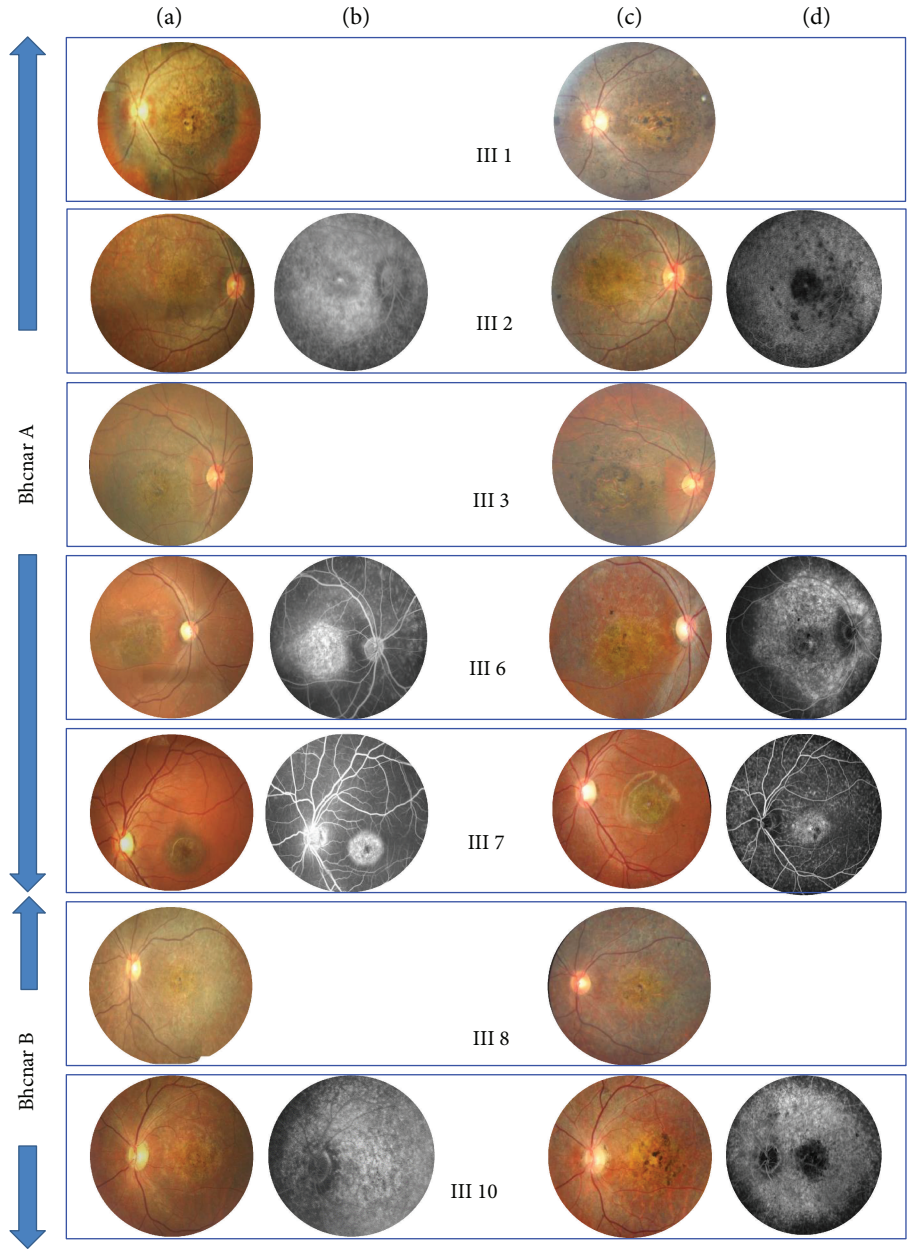

Figure 2: (a, b) Primary phenotype. (c, d) Final phenotype after 9-year progression of the disease.

decay could inhibit protein production and generate a severe loss of function. A malfunctioning ABCA4 cannot remove N-retinylidene-phosphatidylethanolamine from photoreceptors. As a result, N-retinylidene-PE combines with another substance to produce lipofuscin, which builds up in retinal cells. The buildup of lipofuscin is toxic and causes progressive vision loss in subjects with STGD macular degeneration.

However, in branch B of the family, the two cousins were heterozygous for this large rearrangement and carry a heterozygous nonsense mutation p.[R681*]. This mutation is localized in the transmembrane segment and was described previously by two groups [16, 17]. More than 640 mutations in *ABCA4* have been found in different forms of STGD. It is unclear, however, how mutations in *ABCA4* can cause different ocular disorders. A recent study evaluated the severity of specific ABCA4 alleles and showed that variants localized in the transmembrane segment must produce a sufficient amount of functional ABCA4, but induce deterioration of peripheral retinal function with time [18].

The identification of these two new alleles c.[(?_4635)_(5714+?)dup; (?_6148)_(6479_+?) del] and c.[2041C>T], [(?_4635)_(5714+?)dup; (?_6148)_(6479_+?) del] in a Tunisian family confirms the potential complex variations in *ABCA4*. The segregation analysis was important to confirm the molecular diagnosis. Our analysis could explain the clinical data with different phenotypes and age of onset

Table 1: Clinical results at baseline and follow-up: visual acuity, fundus appearance, and full-field ERG responses.

Family	Code sex	Age of onset	Primary visual acuity	Fundus and FA at baseline	Primary full-field ERG	Baseline diagnosis	Final visual acuity	Fundus and FA at last follow-up	Final full-field ERG	Last follow-up diagnosis
Family A	III1F	6	<20/400	Diffuse macular, peripapillary, and peripheral RPE atrophy; hyperfluorescent dots	Altered photopic and scotopic responses	Stargardt dystrophy "phenotype III"	Light perception	Extensive areas of atrophy, pigment clumping, and migration throughout the posterior pole, to the peripheral retina; hyperfluorescent atrophic dots progression with hypofluorescent spots beyond the vascular arcades	Altered photopic and scotopic responses	Severe Stargardt dystrophy "phenotype III"
	III2F	6	<20/400	Diffuse macular, peripapillary, and peripheral RPE atrophy; hyperfluorescent dots	Altered photopic and scotopic responses	Stargardt dystrophy "phenotype III"	Light perception	Extensive areas of atrophy, pigment clumping, and migration throughout the posterior pole, to the peripheral retina	Altered photopic and scotopic responses	Severe Stargardt dystrophy "phenotype III"
	III3M	6	20/330	Macular atrophy; white-yellow flecks; hyperfluorescent atrophic spots; silent choroid	Altered photopic responses	Stargardt fundus flavimaculatus "phenotype II"	Hand movement	Diffuse macular, peripapillary, and RPE atrophy extending beyond the vascular arcades	Altered photopic and scotopic responses	Stargardt dystrophy "phenotype III"
	III6M	6	20/400	Central atrophy with white-yellow flecks; macular atrophy; hyperfluorescent atrophic spots; silent choroid	Altered photopic responses	Stargardt fundus flavimaculatus "phenotype II"	Light perception	Diffuse macular, peripapillary, and RPE atrophy extending beyond the vascular arcades; regression of the white-yellow flecks in the midperiphery replaced by numerous atrophic dots	Altered photopic and scotopic responses	Stargardt dystrophy "phenotype III"
	III7F	5	20/200	Bull's eye maculopathy; temporal peripapillary atrophy; silent choroid; fibroglial scar	Slightly altered photopic responses	Stargardt maculopathy "phenotype I"	20/400	Central atrophy with white-yellow flecks; macular atrophy; hyperfluorescent atrophic spots; silent choroid	Altered photopic and scotopic responses	Stargardt fundus flavimaculatus "phenotype III"
Family B	III8F	10	20/500	Central atrophy with white-yellow flecks; hyperfluorescent atrophic spots; silent choroid	Altered photopic responses	Stargardt fundus flavimaculatus	Light perception	Diffuse macular, peripapillary, and peripheral RPE atrophy; regression of the white-yellow flecks hyperfluorescent dots	Altered photopic and scotopic responses	Stargardt dystrophy "phenotype III"
	III10M	12	20/400	Central atrophy with white-yellow flecks; macular atrophy hyperfluorescent atrophic spots; silent choroid	Altered photopic responses	Stargardt fundus flavimaculatus	Light perception	Diffuse macular, peripapillary, and peripheral RPE atrophy; regression of the white-yellow flecks hyperfluorescent dots	Altered photopic and scotopic responses	Stargardt dystrophy "phenotype III"

[14]. Regarding phenotype and severity of visual symptoms, the family showed Stargardt disease at various stages of progression. After a 9-year follow-up, all patients confirmed the progressive nature of the disease. Progressive retinal degeneration, including development/resorption of flecks, atrophy enlargement, and deterioration of retinal function, has been reported in STGD [19, 20].

In patient III7 who initially presented phenotype 1, the loss of visual acuity was accompanied by appearance of yellow-white lesions at the level of RPE, which are referred to as fundus flecks. In full-field ERG, we also found a progression to scotopic and photopic response alterations. Patients with phenotypes 2 and 3 demonstrated atrophic-appearing lesions within the macula and peripheral retina as previously reported with a final severe CRD phenotype as shown in full-field ERG responses [19]. Patients from branch B with primary phenotype STGD-FFM characterized by a later age of onset and a better primary visual acuity progressed also into severe phenotype 3 with severe macular and peripheral atrophy.

In terms of retinal function, STGD has been classified into three full-field ERG groups: group I with normal rod and cone responses; group II with relative loss of photopic function; and group III with both altered photopic and scotopic functions [11]. ERG findings in our two branches with primary different ERG responses from preserved photoreceptor response to both photopic and scotopic altered responses and a final severely altered ERG responses highlighted the assumption of different stages of progression course of the disease from macular dystrophy to CRD in ABCA4 mutations.

It has been demonstrated that genetic variability influenced the primary severity of the condition and that age of onset correlated with the amount of ABCR activity in photoreceptors [21, 22]. In addition, it was recognized that STGD-FFM had an older age of onset as observed in our patients and had slower progression and thus better prognosis [23]. However, in our two STGD-FFM patients, progression was towards severe diffuse macular, peripapillary, and peripheral RPE atrophy and regression of the yellow-white dots joining severe phenotype 3 shown in branch A, irrespective of the haplotype variability. This would suggest that the primary phenotype observed corresponds to a stage of progression of the disease in both branches and that genotypic difference between M1/M1 versus M1/M2 will influence age of onset, degree of progression, and rapidity of development of the final phenotype less severe in branch B.

In conclusion, the observed progression of disease supports the hypothesis that all phenotypes described at an initial stage of disease are variable stages of a single progressive disease, depending on age in family A and on various haplotype combinations in family B.

We report two genetically different abnormalities in a STGD consanguineous family. The mechanism by which the large homozygous rearrangement, or the compound heterozygous mutations, leads to the same phenotype after 9 years of follow-up is not fully understood. Further biochemical and functional studies should provide deeper insights into the pathogenesis of STGD.

Conflicts of Interest

The authors declare no conflict of interest.

Authors' Contributions

Daniel F. Schorderet and Imen Habibi identified the mutation. Yousra Falfoul, Ahmed Chebil, Ahmed Turki, Asma Hassairi, and Leila El Matri referred patients and clinical data. Yousra Falfoul, Imen Habibi, and Daniel F. Schorderet wrote the paper. Yousra Falfoul and Imen Habibi prepared the figures. Daniel F. Schorderet and Leila El Matri designed the experiments. All authors reviewed and approved the manuscript. Yousra Falfoul and Imen Habibi contributed equally in the paper.

Acknowledgments

The authors acknowledge all the participating family members and are thankful for their cooperation in this study. The authors thank the family members for their invaluable participation and cooperation. The authors acknowledge the help provided by colleagues who referred patients to them. The authors also thank Susan E. Houghton for editing the manuscript. This work was supported by the Institute for Research in Ophthalmology (IRO).

References

[1] M. Illing, L. L. Molday, and R. S. Molday, "The 220-kDa rim protein of retinal rod outer segments is a member of the ABC transporter superfamily," *Journal of Biological Chemistry*, vol. 272, no. 15, pp. 10303–10310, 1997.

[2] M. Dean and T. Annilo, "Evolution of the ATP-binding cassette (ABC) transporter superfamily in vertebrates," *Annual Review of Genomics and Human Genetics*, vol. 6, no. 1, pp. 123–142, 2005.

[3] J. Bhongsatiern, S. Ohtsuki, M. Tachikawa, S. Hori, and T. Terasaki, "Retinal-specific ATP-binding cassette transporter (ABCR/ABCA4) is expressed at the choroid plexus in rat brain," *Journal of Neurochemistry*, vol. 92, no. 5, pp. 1277–1280, 2005.

[4] R. Allikmets, N. Singh, H. Sun et al., "A photoreceptor cell-specific ATP-binding transporter gene (*ABCR*) is mutated in recessive Starqardt macular dystrophy," *Nature Genetics*, vol. 15, no. 3, pp. 236–246, 1997.

[5] J. Weng, N. L. Mata, S. M. Azarian, R. T. Tzekov, D. G. Birch, and G. H. Travis, "Insights into the function of Rim protein in photoreceptors and etiology of Stargardt's disease from the phenotype in *abcr* knockout mice," *Cell*, vol. 98, no. 1, pp. 13–23, 1999.

[6] N. L. Mata, J. Weng, and G. H. Travis, "Biosynthesis of a major lipofuscin fluorophore in mice and humans with *ABCR*-mediated retinal and macular degeneration," *Proceedings of the National Academy of Sciences of the United States of America*, vol. 97, no. 13, pp. 7154–7159, 2000.

[7] B. Bocquet, A. Lacroux, M. O. Surget et al., "Relative frequencies of inherited retinal dystrophies and optic neuropathies in Southern France: assessment of 21-year data management," *Ophthalmic Epidemiology*, vol. 20, no. 1, pp. 13–25, 2013.

[8] A. Maugeri, B. J. Klevering, K. Rohrschneider et al., "Mutations in the *ABCA4* (*ABCR*) gene are the major cause of autosomal recessive cone-rod dystrophy," *The American Journal of Human Genetics*, vol. 67, no. 4, pp. 960–966, 2000.

[9] M. Michaelides, A. J. Hardcastle, D. M. Hunt, and A. T. Moore, "Progressive cone and cone-rod dystrophies: phenotypes and underlying molecular genetic basis," *Survey of Ophthalmology*, vol. 51, no. 3, pp. 232–258, 2006.

[10] C. P. Hamel, "Cone rod dystrophies," *Orphanet Journal of Rare Diseases*, vol. 2, no. 1, p. 7, 2007.

[11] N. Lois, G. E. Holder, C. Bunce, F. W. Fitzke, and A. C. Bird, "Phenotypic subtypes of stargardt macular dystrophy-fundus flavimaculatus," *Archives of Ophthalmology*, vol. 119, no. 3, pp. 359–369, 2001.

[12] R. Allikmets, N. F. Shroyer, N. Singh et al., "Mutation of the Stargardt disease gene (*ABCR*) in age-related macular degeneration," *Science*, vol. 277, no. 5333, pp. 1805–1807, 1997.

[13] R. Allikmets and International ABCR Screening Consortium, "Further evidence for an association of *ABCR* alleles with age-related macular degeneration," *The American Journal of Human Genetics*, vol. 67, no. 2, pp. 487–491, 2000.

[14] L. El Matri, F. Ouechtati, A. Chebil, L. Largueche, and S. Abdelhak, "Clinical polymorphism of Stargardt disease in a large consanguineous Tunisian family; implications for nosology," *Journal of Ophthalmic & Vision Research*, vol. 8, no. 4, pp. 341–350, 2013.

[15] A. N. Yatsenko, N. F. Shroyer, R. A. Lewis, and J. R. Lupski, "An *ABCA4* genomic deletion in patients with Stargardt disease," *Human Mutation*, vol. 21, no. 6, pp. 636–644, 2003.

[16] A. Maugeri, M. A. Van Driel, D. J. R. van de Pol et al., "The 2588G→C mutation in the *ABCR* gene is a mild frequent founder mutation in the Western European population and allows the classification of *ABCR* mutations in patients with Stargardt disease," *American Journal of Human Genetics*, vol. 64, no. 4, pp. 1024–1035, 1999.

[17] M. Bertelsen, J. Zernant, M. Larsen, M. Duno, R. Allikmets, and T. Rosenberg, "Generalized choriocapillaris dystrophy, a distinct phenotype in the spectrum of *ABCA4*-associated retinopathies," *Investigative Ophthalmology & Visual Science*, vol. 55, no. 4, pp. 2766–2776, 2014.

[18] A. Fakin, A. G. Robson, J. (P. W.) Chiang et al., "The effect on retinal structure and function of 15 specific *ABCA4* mutations: a detailed examination of 82 hemizygous patients," *Investigative Ophthalmology & Visual Science*, vol. 57, no. 14, pp. 5963–5973, 2016.

[19] K. Fujinami, N. Lois, A. E. Davidson et al., "A longitudinal study of Stargardt disease: clinical and electrophysiologic assessment, progression, and genotype correlations," *American Journal of Ophthalmology*, vol. 155, no. 6, pp. 1075–1088.e13, 2013.

[20] R. A. Lewis, N. F. Shroyer, N. Singh et al., "Genotype/phenotype analysis of a photoreceptor-specific ATP-binding cassette transporter gene, *ABCR*, in Stargardt disease," *The American Journal of Human Genetics*, vol. 64, no. 2, pp. 422–434, 1999.

[21] J. D. Armstrong, D. Meyer, S. Xu, and J. L. Elfervig, "Long-term follow-up of Stargardt's disease and fundus flavimaculatus," *Ophthalmology*, vol. 105, no. 3, pp. 448–457, 1998.

[22] K. Fuginami, N. Lois, R. Mukherjee et al., "A longitudinal study of stargardt disease: quantitative assessment of fundus autofluorescence, progression, and genotype correlations," *Investigative Ophthalmology & Visual Science*, vol. 54, no. 13, pp. 8181–8190, 2013.

[23] A. N. Yatsenko, N. F. Shroyer, R. Lewis, and J. Lupski, "Late-onset Stargardt disease is associated with missense mutations that map outside known functional regions of *ABCR* (*ABCA4*)," *Human Genetics*, vol. 108, no. 4, pp. 346–355, 2001.

Hindawi
Journal of Ophthalmology
Volume 2018, Article ID 9171536, 10 pages
https://doi.org/10.1155/2018/9171536

Research Article

DNA Methylation Status of the Interspersed Repetitive Sequences for LINE-1, Alu, HERV-E, and HERV-K in Trabeculectomy Specimens from Glaucoma Eyes

Sunee Chansangpetch,[1] **Sasiprapa Prombhul**,[2] **Visanee Tantisevi**,[1] **Pimpayao Sodsai**,[2] **Anita Manassakorn**,[1] **Nattiya Hirankarn**,[2] **and Shan C. Lin**[3]

[1]*Department of Ophthalmology, Faculty of Medicine, Chulalongkorn University and King Chulalongkorn Memorial Hospital, Thai Red Cross Society, Bangkok, Thailand*
[2]*Center of Excellence in Immunology and Immune-Mediated Diseases, Department of Microbiology, Faculty of Medicine, Chulalongkorn University, Bangkok, Thailand*
[3]*Department of Ophthalmology, University of California - San Francisco, San Francisco, CA, USA*

Correspondence should be addressed to Sunee Chansangpetch; sunee.ch@chula.ac.th

Received 15 September 2017; Accepted 6 December 2017; Published 31 January 2018

Academic Editor: Lev Prasov

Background/Aims. Epigenetic mechanisms via DNA methylation may be related to glaucoma pathogenesis. This study aimed to determine the global DNA methylation level of the trabeculectomy specimens among patients with different types of glaucoma and normal subjects. *Methods*. Trabeculectomy sections from 16 primary open-angle glaucoma (POAG), 12 primary angle-closure glaucoma (PACG), 16 secondary glaucoma patients, and 10 normal controls were assessed for DNA methylation using combined-bisulfite restriction analysis. The percentage of global methylation level of the interspersed repetitive sequences for LINE-1, Alu, HERV-E, and HERV-K were compared between the 4 groups. *Results*. There were no significant differences in the methylation for LINE-1 and HERV-E between patients and normal controls. For the Alu marker, the methylation was significantly lower in all types of glaucoma patients compared to controls (POAG 52.19% versus control 52.83%, $p = 0.021$; PACG 51.50% versus control, $p = 0.005$; secondary glaucoma 51.95% versus control, $p = 0.014$), whereas the methylation level of HERV-K was statistically higher in POAG patients compared to controls (POAG 49.22% versus control 48.09%, $p = 0.017$). *Conclusions*. The trabeculectomy sections had relative DNA hypomethylation of Alu in all glaucoma subtypes and relative DNA hypermethylation of HERV-K in POAG patients. These methylation changes may lead to the fibrotic phenotype in the trabecular meshwork.

1. Introduction

Epigenetics include the chemical reactions that control the genome activities at certain time points and locations within the DNA [1]. These reactions produce a chemical mark on the DNA that can serve as an additional system to control whether the gene will become functional or silent, without modifying the DNA's base sequences. Major epigenetic mechanisms that have been identified are DNA methylation, chromatin remodeling, deployment of noncoding DNA, and histone modification [2–5].

Several studies in complex multifactorial diseases have reported that elucidating the epigenetic mechanisms have helped clarify the understanding of their etiology and disease progression [2]. Stress, diet, behavior, toxins, and other factors can also activate the processes at the epigenomic level [5]. These epigenetic factors may partly explain the clinical variations seen among various multifactorial diseases such

as different onset, severity, and progression, beyond simple genetic determination [6]. One of the major processes in epigenetic modification is DNA methylation. Once the heritable methylation patterns in the DNA are disrupted, the chromatin structure and gene expression can be altered and subsequently result in the creation of an aberrant gene expression. Furthermore, there can be pronounced differences in overall and specific methylation levels between different tissue types as well as between normal cells and pathological cells of the same tissue [4, 7]. These tissue-specific characteristics suggest a potential use of methylation changes as a clinical biomarker indicative for disease.

Glaucoma is a progressive optic neuropathy, which is characterized by typical optic disc changes and associated visual function loss [8]. Elevated intraocular pressure (IOP) is the most significant risk factor and is usually a result of impaired aqueous outflow facility due to trabecular meshwork (TM) dysfunction [9]. Glaucoma-associated genes have been discovered but only a small fraction of glaucoma cases are associated with mutations in these genes. The clinical manifestation of onset and severity of glaucoma vary from person to person and even between eyes of the same patient in most cases. It is possible that epigenetic mechanisms that control gene expression may interact with and be related to glaucoma pathogenesis and progression.

At present, there is limited data on epigenetics and glaucoma. A genome-wide methylation analysis conducted in cultured human TM showed that dexamethasone may induce DNA methylation change at some gene promotors [10]. In another study, there was a significant difference in DNA methylation in peripheral mononuclear cells from patients with primary open-angle glaucoma (POAG) compared to the normal controls [11]. These studies suggest that changes in DNA methylation may have a role in glaucoma pathogenesis. However, certain epigenetic mechanisms may be characteristic for specific tissues [12]. Trabeculectomy section or scleral tissue that contains TM may be a better candidate for the epigenetic study, but to the best of our knowledge, there are no studies that have described methylation in excised ocular tissue.

Dysregulation of the DNA methylation processes can occur either as locally, in the promotors of genes, or globally. The total methylcytosine level can be assessed by chromatographic methods to determine the global methylated levels. But there are some limitations to directly quantitate the global outcome so Weisenberger et al. [13] proposed to measure the methylation at interspersed repetitive sequences (IRSs) instead to reflect the global methylcytosine content. Thus, for this study, we assessed the global methylcytosine content by investigating the IRSs of the CpG-rich regions which exist throughout the genome and comprise approximately 45% of the human genome. Our study focused on the 4 major IRSs: long interspersed nuclear elements-1 (LINE-1), Alu element, human endogenous retrovirus-E (HERV-E), and human endogenous retrovirus-K (HERV-K). In brief, there are two major groups of IRSs based on its location: the DNA transposon (2.8% of human genome) and retrotransposon (42.2% of human genome). Long interspersed nuclear elements or LINEs and short interspersed nuclear elements such as ALU are classified as retrotransposon without long terminal repeats (LTR), while human endogenous retrovirus or HERV is a retrotransposon with LTR retroelements [14].

Taken together, our study aimed to investigate the DNA methylation levels for LINE-1, Alu, HERV-E, and HERV-K in scleral tissue from trabeculectomy sections of glaucoma patients and control.

2. Materials and Methods

The study followed the tenets of the Declaration of Helsinki and was approved by the Institutional Review Board of the Faculty of Medicine, Chulalongkorn University, Bangkok, Thailand. Informed consent was obtained from each subject before enrollment.

2.1. Subjects. Forty-four patients scheduled for trabeculectomy operation were recruited. Glaucoma diagnosis was based on International Society of Geographical and Epidemiological Ophthalmology (ISGEO) guidelines [15]:

(1) In category 1, a visual field defect is consistent with glaucomatous optic neuropathy and either a vertical cup-to-disc ratio (C/D) of at least 0.7 (97.5th percentile) or C/D asymmetry between the right and left eyes of at least 0.2 (97.5th percentile).

(2) In category 2, visual field results are not definitive or are unattainable due to patient inability to perform an adequate quality test, and optic disc has C/D of at least 0.9 (99.5th percentile) or C/D asymmetry between the right and left eyes of at least 0.3 (99.5th percentile).

(3) In category 3, visual field testing and optic disc examination are not possible in the subject; visual acuity is less than 20/400 (for any ophthalmic pathology) and IOP exceeds the 21 mmHg (99.5th percentile for the population).

Inclusion criteria for all patients included (1) age greater than 18 years, (2) uncontrolled IOP on maximally tolerated medications and/or poor compliance with medical therapy, and (3) structural and/or functional deterioration. All glaucoma subjects were classified into the following: (1) POAG—defined as glaucoma patients with open anterior chamber angle by gonioscopy; (2) primary angle-closure glaucoma (PACG)—defined as glaucoma patients with more than 180 degrees iridotrabecular contact or presence of peripheral anterior synechiae by gonioscopy; and (3) secondary glaucoma—defined as glaucoma with an identifiable cause of increased IOP resulting in glaucomatous optic nerve damage. Patients with mixed mechanisms of glaucoma (e.g., POAG with superimposed secondary glaucoma), had other ocular pathology (except for cataract and primary diseases accounting for secondary glaucoma), or had any ocular surgery 6 months prior to the study and patients who were unable to give consent were excluded. Secondary glaucoma patients who had the family history of glaucoma or had any glaucoma suspect sign in the fellow eye were also excluded.

All the diagnostic and glaucoma subtype classifications were performed by glaucoma specialists (VT, AM, and SC).

The study was conducted from September to October 2014 at the Ophthalmology Department, King Chulalongkorn Memorial Hospital. Among the 44 recruited patients, 16 had POAG, 12 had PACG, and 16 had secondary glaucoma.

2.2. Control Group. Ocular tissue from normal controls were obtained from collaborative partners: the Department of Microbiology, Faculty of Medicine, Chulalongkorn University, and the Department of Forensic Medicine, Police General Hospital, with informed consent from authorized representatives. Subjects included those who had no history of glaucoma according to available medical records and interviews from relatives. To ensure the integrity of specimen quality for optimal measurement of methylation status (which has been shown to be preserved within 48–72 hours postmortem [16, 17]), we collected ten scleral/trabecular tissues from subjects within 24 hours of expiration. The tissue collection procedure was similar to what was done in the glaucoma group, which is described below.

2.3. Specimen Collection. The tissue was collected from the sclerostomy during the performance of a standard trabeculectomy, where a section of half-thickness scleral tissue containing TM is cut (block-shaped) to make a connection between the anterior chamber and the subconjunctival space. These trabeculectomy sections, which were approximately 1 mm in width and 1 mm in length, were immediately transported in liquid nitrogen to the laboratory unit for DNA extraction processing and global methylation analysis.

2.4. DNA Preparation for Combined-Bisulfite Restriction Analysis (COBRA). DNA from samples was isolated using QIAamp DNA Micro Kit (QIAGEN, Valencia, CA, USA). DNA quantification was measured by using a NanoDrop 2000c Spectrophotometer (Thermo Fisher Scientific, Waltham, MA, USA). Since the sclera is a fibrillar collagen-type tissue with minimal DNA content, our study used 20 μL of DNA elutes in the bisulfite conversion experiment using EZ DNA Methylation-Gold Kit (Zymo Research, Orange, CA, USA), according to the manufacturer's recommended protocol. One to two microliters of bisulfite-converted DNA were used as a template for the COBRA PCR as a quantitative method to study the DNA methylation of each repetitive sequence. Bisulfite-treated DNA from HeLa, Daudi, and Jurkat have been used as positive controls for each PCR reaction. Specific primers for repetitive sequence markers (i.e., LINE-1, Alu, HERV-E, and HERV-K) were selected and mixed into the PCR reactions. Protocols for COBRA PCR and band measurements have been previously described [14, 18–20]. Polyacrylamide gel electrophoresis revealed banding patterns after restriction enzyme digestion. This COBRA PCR technique is a standard combined-bisulfite method for detecting the methylation of the CpG loci by using a specific set of conserved primers for each repetitive sequence.

2.5. Methylation Analyses of Each Repetitive Marker. Percentage of global methylation level has been determined to demonstrate an overall methylation level for each target. Formulas and equations for methylation calculations have been previously described [14]. Results from methylation profiles for LINE-1 and Alu markers are categorized into 4 groups according to the prevalence of methylated/unmethylated CpG occurrence at each specific position: % $^{m}C^{m}C$, % $^{m}C^{u}C$, % $^{u}C^{m}C$, and % $^{u}C^{u}C$.

For LINE-1, numbers of CpG dinucleotides of each motif were normalized and the measured band intensity were divided according to the sizes to generate parameters as follows: %92 bp/92 = A, %60 bp/56 = B, %50 bp/48 = C, %42 bp/40 = D, %32 bp/28 = E, and $[(D+E)-(B+C)]/2 = F$. Percentage of global methylation was calculated by the following formula: $[(A+2C+F)\times 100]/(2A+2B+2C+2F)$ = % global methylation. Percentage of hypermethylation pattern (% $^{m}C^{m}C$) at both CpG motifs was calculated by $[(C/2)\times 100]/[(C/2)+A+B+F]$ = % $^{m}C^{m}C$. Percentages of partial methylation of $^{m}C^{u}C$ and $^{u}C^{m}C$ were calculated by $(A\times 100)/[(C/2)+A+B+F]$ = % $^{m}C^{u}C$ and $(F\times 100)/[(C/2)+A+B+F]$ = % $^{u}C^{m}C$, respectively. Percentage of hypomethylation (% $^{u}C^{u}C$) was calculated by $(B\times 100)/[(C/2)+A+B+F]$ = % $^{u}C^{u}C$.

For the Alu marker, we generated parameters to be used for normalization and calculation of the methylation level of each motif as follows: %133 bp/133 = A, %58 bp/58 = B, %75 bp/75 = C, %90 bp/90 = D, %43 bp/43 = E, and $[(E+B)-(C+D)]/2 = F$.

Methylation profiles for the Alu marker have been measured and calculated by the following formulas: global methylation level (% ^{m}C) = $[100\times(2F+D+C)]/(2A+2C+2D+2F)$, hypermethylation pattern (% $^{m}C^{m}C$) = $(100\times F)/(A+C+D+F)$, partial methylation (% $^{m}C^{u}C$) = $(100\times D)/(A+C+D+F)$, partial methylation (% $^{u}C^{m}C$) = $(100\times C)/(A+C+D+F)$, and hypomethylation (% $^{u}C^{u}C$) = $(100\times A)/(A+C+D+F)$. As for the HERV methylation levels, the summation of the methylated motifs was calculated by using either the percentage of the band intensity measurement of the digested fragments of HERV-E or HERV-K.

Methylation bands for LINE-1, Alu, HERV-E, and HERV-K from normal control samples are shown in Figures 1–3, respectively.

2.6. Statistical Analyses. Wilcoxon rank-sum test (two-tailed) was used to compare the methylated levels between groups. p value < 0.05 was considered statistically significant. All analyses were performed utilizing Stata 13.0 (StataCorp, College Station, TX).

3. Results

3.1. Patient Characteristics. The demographic and clinical characteristics of the glaucoma patients and control subjects are shown in Table 1. All subjects were of Thai ethnicity. Most of the glaucoma patients had only trabeculectomy done. Combination of cataract surgery and trabeculectomy was performed in six, eight, and one patient from POAG, PACG, and secondary glaucoma groups, respectively. The diagnoses of primary eye condition in secondary neovascular glaucoma groups included proliferative diabetic retinopathy

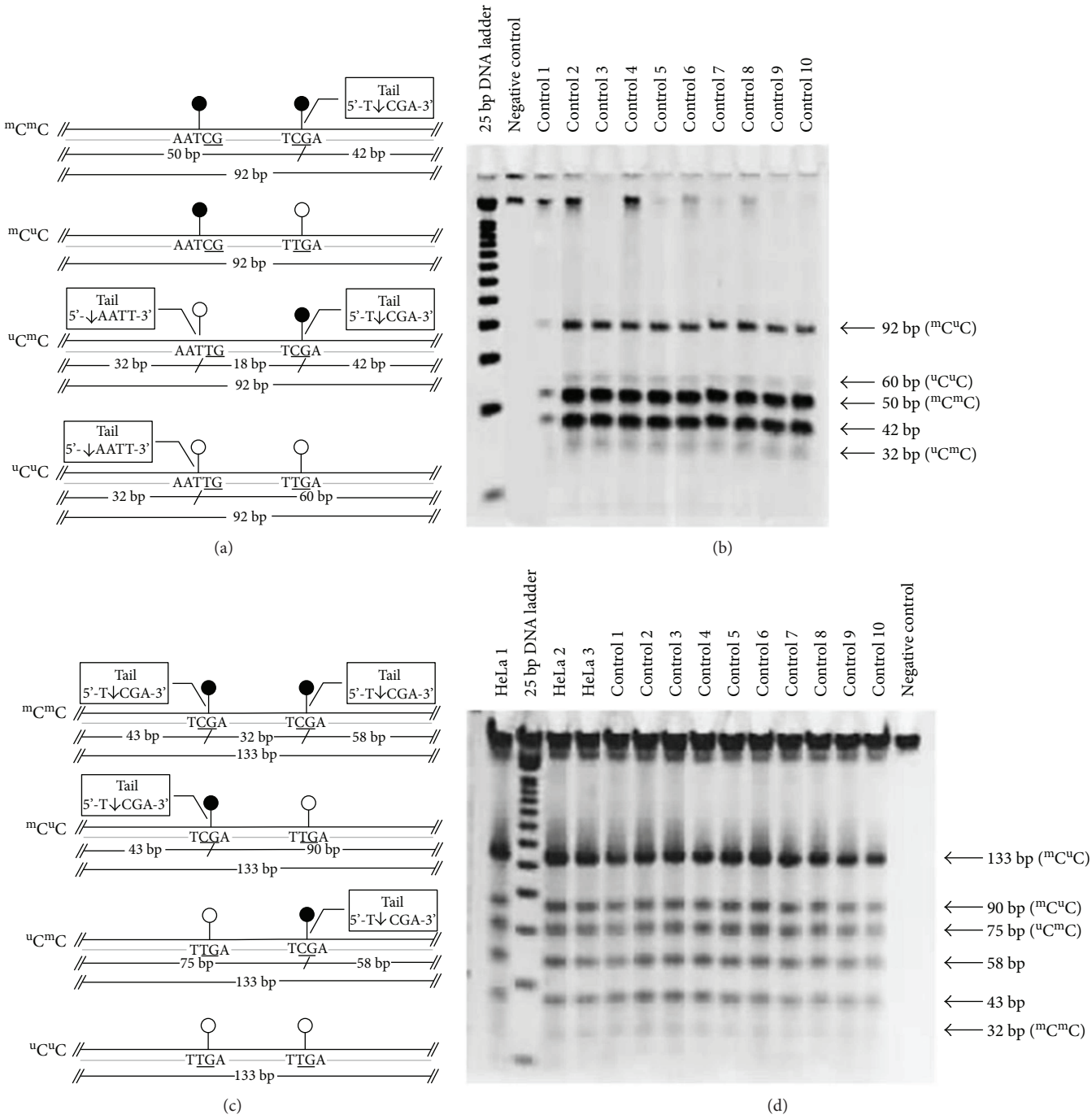

Figure 1: Combined-bisulfite restriction analysis (COBRA) for LINE-1 (a, b) and Alu (c, d) methylation patterns. The diagrams (a, c) demonstrate the following four patterns of methylated CpGs (from top to bottom): hypermethylation ($^{m}C^{m}C$), hypomethylation ($^{u}C^{u}C$), and two forms of partial methylation ($^{m}C^{u}C$ and $^{u}C^{m}C$). Polyacrylamide gel electrophoresis (b, d) shows the locations for the bands for each pattern of methylated CpGs. Quantitative DNA ladder was used to assess the size of the bands. The representative gels of cell line and normal control samples are shown. Water is used as a negative control.

and central retinal vein occlusion (7 cases), uveitis (4 cases), trauma (3 cases), postcorneal surgery (1 case), and ICE syndrome (1 case). Three POAG cases and 3 PACG cases reported to have family history of glaucoma. However, it should be noted that only the results with clear patterns in the gel electrophoresis as shown in Figures 1–3 were included in the analysis. Therefore, the number of samples analyzed in Tables 2–5 are not always equal.

3.2. LINE-1 Methylation Analysis. The averages of the methylation percentages are shown in Table 2. There were no statistical significant differences in the overall methylation

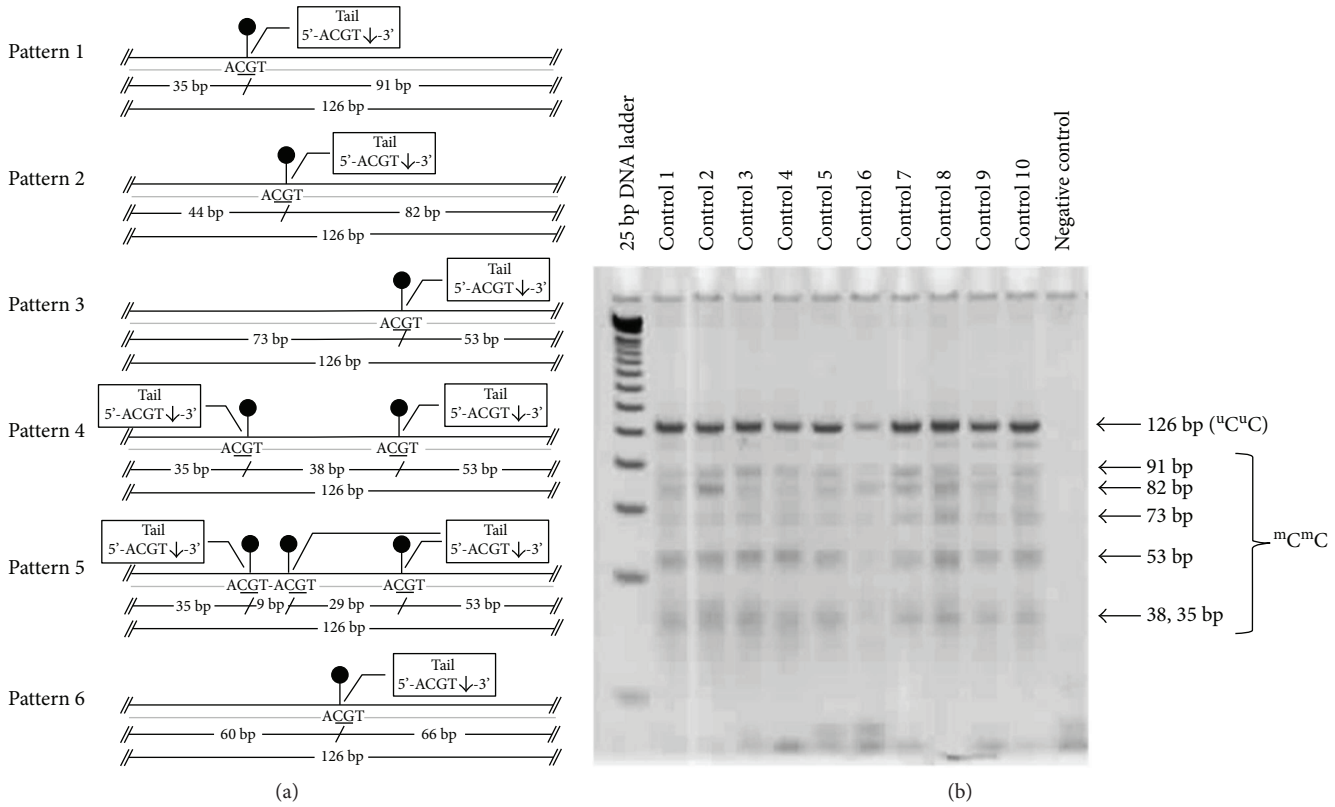

FIGURE 2: Combined-bisulfite restriction analysis (COBRA) for HERV-E methylation patterns. The diagrams (a) demonstrate six patterns of hypermethylation ($^{m}C^{m}C$). Polyacrylamide gel electrophoresis (b) shows the locations for the bands for each pattern of methylated CpGs. Quantitative DNA ladder was used to assess the size of the bands. The representative gels of cell line and normal control samples are shown. Water is used as a negative control.

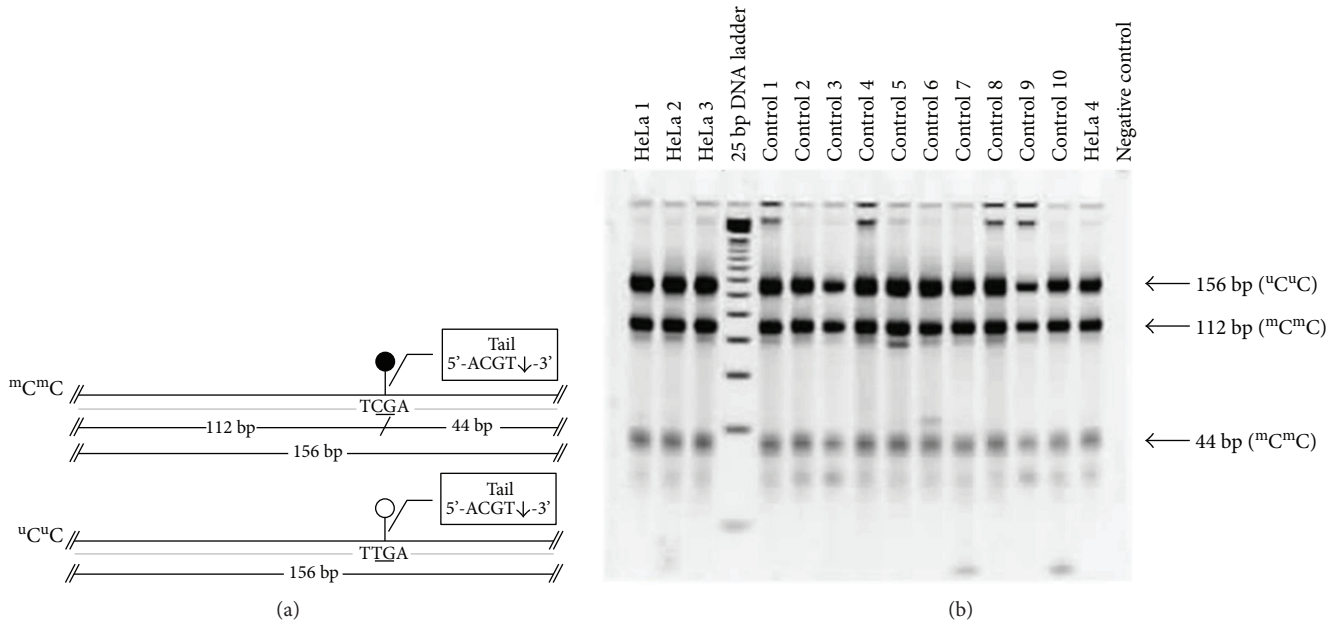

FIGURE 3: Combined-bisulfite restriction analysis (COBRA) for HERV-K methylation patterns. The diagrams (a) demonstrate the following two patterns of methylated CpGs (from top to bottom): hypermethylation ($^{m}C^{m}C$) and hypomethylation ($^{u}C^{u}C$). Polyacrylamide gel electrophoresis (b) shows the locations for the bands for each pattern of methylated CpGs. Quantitative DNA ladder was used to assess the size of the bands. The representative gels of cell line and normal control samples are shown. Water is used as a negative control.

Table 1: Demographic and clinical characteristics of the subjects.

	Normal control	POAG	PACG	Secondary glaucoma
N	10	16	12	16
Age				
Mean (SD)	40 (20.8)	69 (8.1)	65 (10.0)	53 (15.0)
Gender, male				
N (%)	5 (50.0)	11 (64.7)	2 (15.4)	9 (56.3)
Laterality, right				
N (%)	5 (50.0)	9 (52.9)	7 (58.3)	8 (50.0)
Duration (month)				
Median (IQR)	—	36.0 (24.0, 84.0)	12 (7.0, 132.0)	2.5 (1.75, 9.75)
Vertical C : D ratio				
Median (IQR)	—	0.9 (0.8, 0.9)	0.8 (0.8, 0.9)	0.8 (0.7, 0.9)
IOP (mmHg)				
Mean (SD)	—	20 (8.1)	21.6 (9.8)	33.3 (13.0)
VA (decimal)				
Median (IQR)	—	0.677 (0.200, 1.000)	0.500 (0.100, 0.700)	0.015 (0.001, 0.400)
Number of medication				
Median (IQR)	—	4.0 (3.75, 4.0)	4.0 (4.0, 4.3)	4.0 (4.0, 5.0)
Visual field MD				
Median (IQR)	—	−11.31 (−16.98, −9.43)	−10.62 (−14.85, −4.50)	NA
Visual field PSD				
Median (IQR)	—	7.75 (3.31, 8.21)	7.59 (1.98, 9.22)	NA

POAG = primary open-angle glaucoma; PACG = primary angle-closure glaucoma; C : D = optic cup to optic disc ratio; VA = visual acuity; MD = mean deviation; PSD = pattern standard deviation; NA = not applicable due to poor visual acuity.

Table 2: LINE-1 methylation levels in glaucoma eyes and control eyes.

	N	% ^{m}C	% $^{m}C^{m}C$	% $^{m}C^{u}C$	% $^{u}C^{m}C$	% $^{u}C^{u}C$
Normal control	10	50.8810 ± 3.4356	18.2732 ± 2.5257	23.2248 ± 2.1280	24.1912 ± 0.4800	34.3107 ± 3.6554
POAG	16	49.8650 ± 3.0136	17.4822 ± 2.5099	23.7864 ± 1.8280	23.5895 ± 0.8576	35.1419 ± 2.5862
PACG	12	49.8900 ± 1.8009	17.9876 ± 2.2382	22.2586 ± 2.9002	23.5921 ± 0.4616	36.1617 ± 0.7060
Secondary glaucoma	14	49.3133 ± 1.5371	17.2674 ± 1.8776	23.0947 ± 2.4025	23.5456 ± 0.3893	36.0923 ± 0.6032

All values are presented as mean ± standard deviation. % ^{m}C = percentage of LINE-1 methylation; % $^{m}C^{m}C$ = percentage of LINE-1 hypermethylated loci number; % $^{m}C^{u}C$, % $^{u}C^{m}C$ = percentage of LINE-1 partially methylated loci; % $^{u}C^{u}C$ = percentage of LINE-1 hypomethylated loci number.

Table 3: Alu methylation levels in glaucoma eyes and control eyes.

	N	% ^{m}C	% $^{m}C^{m}C$	% $^{m}C^{u}C$	% $^{u}C^{m}C$	% $^{u}C^{u}C$
Normal control	10	52.8278 ± 0.5926	25.1117 ± 1.2948	27.5755 ± 2.2979	27.8567 ± 2.4824	19.4560 ± 0.1800
POAG	16	52.1945 ± 0.6916	24.0020 ± 1.5875	27.5126 ± 2.2014	28.8725 ± 0.4600	19.6130 ± 0.3089
PACG	12	51.4995 ± 1.3884	22.6191 ± 2.7542	28.8866 ± 2.7807	28.8743 ± 0.3395	19.6201 ± 0.2302
Secondary glaucoma	16	51.9548 ± 0.9712	23.5236 ± 1.9268	27.9738 ± 2.0784	28.8885 ± 0.4241	19.6140 ± 0.2888

All values are presented as mean ± standard deviation. % ^{m}C = percentage of Alu methylation; % $^{m}C^{m}C$ = percentage of Alu hypermethylated loci number; % $^{m}C^{u}C$, % $^{u}C^{m}C$ = percentage of Alu partially methylated loci; % $^{u}C^{u}C$ = percentage of Alu hypomethylated loci number.

among the glaucoma patients and the normal controls or among the patients with different types of glaucoma (Figure 4(a)).

3.3. Alu Methylation Analysis. The average level of Alu methylation is shown in Table 3. The overall methylation was significantly lower in the tissues of the patients with all types of glaucoma compared to the controls: POAG (52.19%) compared to controls (52.83%), $p = 0.021$; PACG (51.50%) compared to controls, $p = 0.005$; and secondary glaucoma (51.95%) compared to controls, $p = 0.014$ (Figure 4(b)).

Table 4: HERV-E methylation levels in glaucoma eyes and control eyes.

	N	% ^{m}C	% ^{u}C
Normal control	10	76.4320 ± 0.5745	23.5680 ± 0.5745
POAG	12	76.6092 ± 0.3342	23.3908 ± 0.3342
PACG	10	76.4990 ± 0.4257	23.5010 ± 0.4257
Secondary glaucoma	13	75.9462 ± 1.0527	24.0538 ± 1.0527

All values are presented as mean ± standard deviation. % ^{m}C = percentage of HERV-E methylation; % ^{u}C = percentage of HERV-E nonmethylation.

Table 5: HERV-K methylation levels in glaucoma eyes and control eyes.

	N	% ^{m}C	% ^{u}C
Normal control	10	48.0928 ± 0.1242	51.9072 ± 0.1242
POAG	16	49.2227 ± 1.1984	50.7773 ± 1.1984
PACG	12	48.9118 ± 1.1630	51.0882 ± 1.1630
Secondary glaucoma	16	48.4693 ± 1.2119	51.5307 ± 1.2119

All values are presented as mean ± standard deviation. % ^{m}C = percentage of HERV-K methylation; % ^{u}C = percentage of HERV-K nonmethylation.

3.4. HERV-E Methylation Analysis. The level of HERV-E methylation is shown in Table 4. The overall methylation in the tissue was not statistically different among glaucoma patients compared to the controls. However, there was significantly lower methylation in patients from the secondary glaucoma group (75.95%) when compared to the POAG (76.61%) and PACG (76.50%) groups ($p = 0.036$ and $p = 0.043$, resp.) (Figure 4(c)).

3.5. HERV-K Methylation Analysis. The level of HERV-K methylation is shown in Table 5. The overall methylation in the tissue specimens was statistically higher for the POAG (49.22%) patients compared to the controls (48.09%) ($p = 0.017$) (Figure 4(d)).

4. Discussion

This study is the first epigenetic study conducted using ocular tissues from glaucoma patients. We demonstrated that the global methylation levels for Alu were significantly lower in POAG, PACG, and secondary glaucoma groups compared to the controls. Hypomethylation of HERV-E was also observed in the secondary glaucoma group. On the other hand, the methylation levels for HERV-K were significantly higher in the POAG group compared to controls.

The characteristic of high IOP found in most types of glaucoma is thought to be due to increased resistance in the trabecular outflow pathway. Gottanka et al. found that trabecular sheath plaques inside TM are significantly higher in patients with glaucomatous problems compared to patients with normal eyes [21]. The plaque materials were composed of fine fibrils and other components of the extracellular matrix that adhered to the sheaths of the TM fibers [22, 23]. Also, Sihota et al. [24] demonstrated the excessive fibrillary structure in the extracellular matrix in PACG patients, affecting the narrow TM beams. The area with such changes was away from the peripheral anterior synechiae. This finding may explain why after a successful angle widening in some PACG patients resulted in unsatisfactory reduction of the IOP.

There is evidence indicating that TGF-β2, a profibrotic cytokine, played a role in the changes of the extracellular matrix of the trabecular outflow pathway. TGF-β2 levels were documented to be higher in aqueous humor in nearly half of the patients with POAG [25]. In vitro, this cytokine can stimulate trabecular cells to increase the synthesis of various extracellular matrix components and tissue transglutaminase enzyme, which cross-links proteins to complexes not degradable by metalloproteinases [26]. The enzyme metalloproteinases are also inhibited by plasminogen activator inhibitor, which can be upregulated by TGF-β2 [23, 27]. Moreover, the eyes treated with TGF-β2 can result in substantially decreased outflow facility [28].

Aside from that, there is evidence suggesting the role of epigenetic regulation of the TGF-β pathway [29, 30]. The TGF-β signaling pathway has been shown to be suppressed by the methylation process. Treating cells with DNA methyltransferase (DNMT), the enzyme that is responsible for the transfer of methyl groups to the DNA can inhibit the TGF-β pathway activity [29]. In addition, the methylation also affects the level of thrombospondin-1 (TSP1), which is known to regulate the TGF-β pathway [31]. It is possible that changes in the methylation level may affect the TGF-β signaling pathways as well as the regulation of TSP1 level, subsequently increasing the production of extracellular matrix to form plaques in the TM.

Hypoxia has been shown to induce epigenetic changes in other fibrotic diseases as well as being implicated in the pathogenesis of glaucoma. Tezel and Wax [32] found that hypoxia-inducible factor 1α and its related hypoxia-induced proteins (i.e., vascular endothelial growth factor) level was increased in the retina and optic nerve head of glaucoma patients [33]. Decreased ocular blood flow [34], disturbed ocular autoregulation [35], and increased IOP or IOP fluctuation [33] may potentially cause intraocular hypoxia. Many reports suggested the role of hypoxia in inducing changes at the epigenetic level. Recently, McDonnell et al. [36] studied the hypoxic response in human lamina cribrosa cells and found that hypoxia significantly increased expression of DNMT and the levels of global DNA methylation when compared to the normoxic lamina cribrosa cells.

However, it is not clear why methylation change was observed only with certain subtypes of IRSs. There is a lot of evidence indicating that DNA methylation of the IRSs, particularly LINE-1 and Alu, are biomarkers for environmental exposures such as air pollution, metal exposure, and alcohol consumption [37]. The association between methylation and the exposures may vary between the markers for IRSs. Previous studies showed that there was an increase in the expression of Alu RNAs in response to cellular stress [38]. Alu RNA-induced cytotoxicity was also proposed to be implicated in age-related macular degeneration via inducing proinflammatory cytokine cascade [39]. On the other hand, an increased expression of HERV protein was

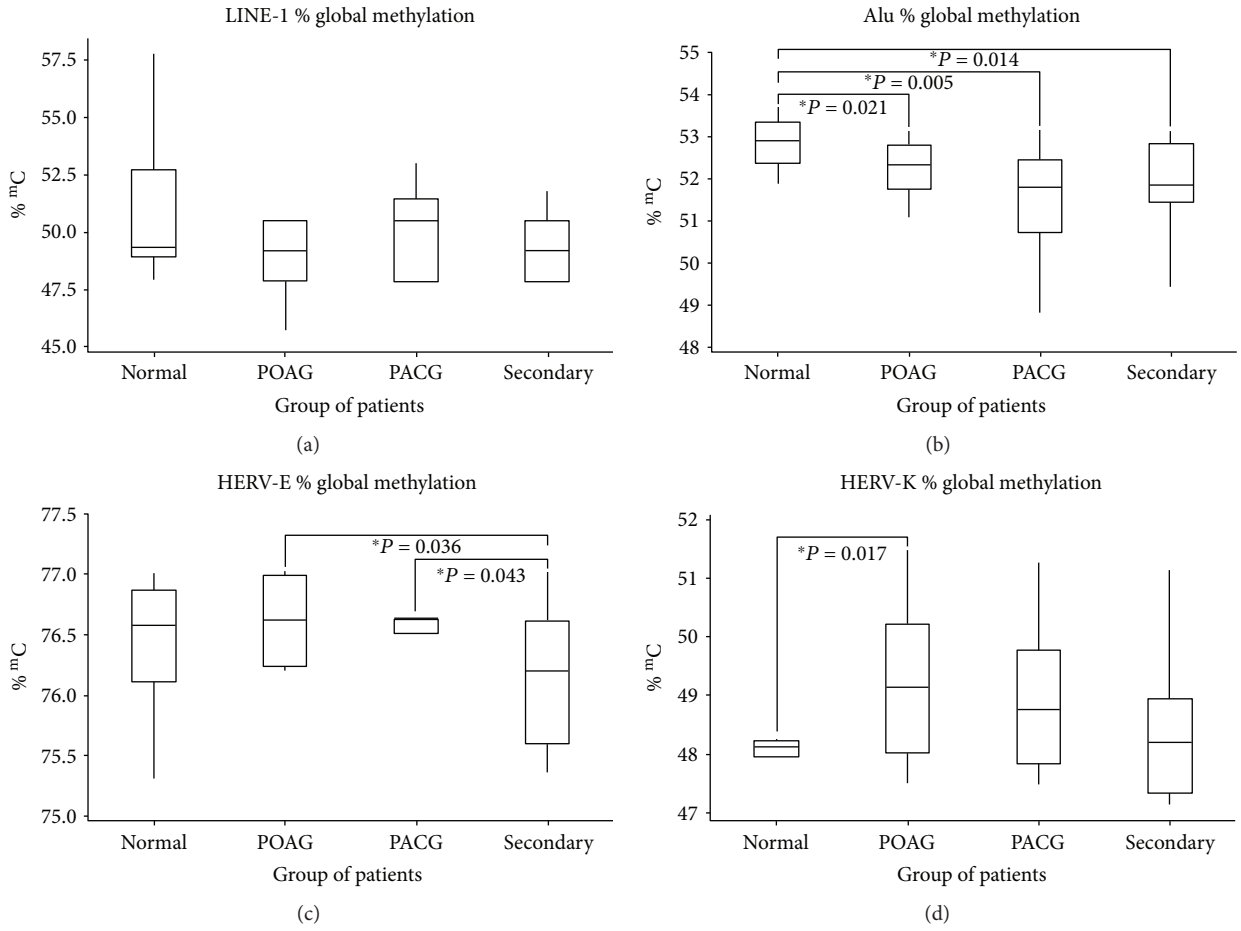

Figure 4: Box plots showing methylation percentage: (a) LINE-1 methylation analysis, (b) Alu methylation analysis, (c) HERV-E methylation analysis, and (d) HERV-K methylation analysis. POAG = primary open-angle glaucoma; PACG = primary angle-closure glaucoma; secondary = secondary glaucoma; % ^{m}C = percentage of methylation. * represents a significant difference at $p < 0.05$ by Wilcoxon rank-sum test.

documented in many studies that were associated with cytokines, hypoxia, microorganisms, steroid hormones, and even the environment [40–43].

In contrast to the Alu results in which the methylation change was found in all 3 glaucoma groups, the DNA hypermethylation for HERV-K was detected only in patients with POAG. This makes sense because POAG is known to have a very strong genetic predisposition [44, 45]. The HERV-K marker may be more specific to epigenetic modulation of genetic susceptible persons, whereas we speculate that the Alu marker is more susceptible to oxidative stress and hypoxic condition. However, this hypothesis needs to be confirmed by investigating how hypomethylation at Alu and hypermethylation at HERV-K may relate to the pathogenesis of glaucoma and to what extent these modulating factors contribute to such changes. Additional studies on the downstream effects of the expressions of Alu, HERV-K, and gene-specific methylation, are needed.

Our studies have some limitations. First, the tissues in this study were collected from patients who fulfilled the criteria for trabeculectomy. Consequently, the results cannot be generalized to the milder form of glaucoma and the methylation changes that may not be representative of the stage of the disease. Second, because it is unethical to obtain scleral/trabecular tissue from normal subjects, we collected the tissue from postmortem eyes. Hence, a detailed ocular examination by the authors was not possible. The inclusion criteria were thus based on having no history of glaucoma which might not totally exclude the existence of glaucomatous changes in this group. Third, the ages of the control samples were within a wide range with an overall lower average age compared to the glaucoma groups. The difference in age potentially affect the comparison of the methylation levels of Alu and HERV-K. A study from Jintaridth et al. found that both Alu and HERV-K methylation levels had an inverse correlation with age [46]. Our high methylation level of normal control compared to glaucoma groups in Alu could be a result of the age effect. Nevertheless, the hypermethylation in HERV-K despite the older age POAG subjects compared to the controls may represent the true difference of methylation level in this marker. It should be noted that the study from Jintaridth et al. was conducted in peripheral blood mononuclear cells and not the ocular tissue. Given that available control eyes were usually obtained from individuals who had an unnatural cause of death such as accident or trauma, they tended to be younger. This limited our ability

to perform age-matching in our study. Lastly, since this is an exploratory study, each group contained small numbers of subjects which limited our ability to build multivariable models with various covariates due to low statistical power and overfitting concerns. Future studies with large numbers of subjects and age-matching design are warranted to confirm these potential associations with incorporation of potential confounders into a statistical model.

In conclusion, trabeculectomy sections from POAG, PACG, and secondary glaucoma patients had DNA hypomethylation at Alu, and DNA hypermethylation was detected at HERV-K for POAG patients. These methylation changes may lead to TM transformation and dysfunction. Our findings also suggest that epigenetic modulation may be a potential mechanism of glaucoma pathogenesis.

Disclosure

The abstract of this article was presented as a poster at the 7th World Glaucoma Congress, Helsinki, Finland, June 2017.

Conflicts of Interest

The authors declare that there is no conflict of interest regarding the publication of this paper.

Acknowledgments

This study was supported by the Grant for International Research Integration, Chula Research Scholar, Ratchadaphiseksomphot Endowment Fund, and the Ratchadaphiseksomphot Fund, Faculty of Medicine, Chulalongkorn University. Also, support was from Research to Prevent Blindness Unrestricted Grant and the NIH-NEI EY002162 Core Grant for Vision Research. The mentioned funding did not lead to any conflict of interests regarding the publication of this manuscript. The authors would like to thank their glaucoma colleagues, Dr. Paneeya Tapaneeyangkul, Dr. Rath Itthipanichpong, Dr. Tanate Chira-Adisai, Dr. Yuyaporn Tangseepha, and Dr. Sithichoke Nakaphongse for their kind assistance in providing the study with the sample tissues. The authors would also like to thank Professor Apiwat Mutirangura and Dr. Nakarin Kitkumthorn for providing the authors guidance on the use of the COBRA protocol.

References

[1] R. R. Kanherkar, N. Bhatia-Dey, and A. B. Csoka, "Epigenetics across the human lifespan," *Frontiers in Cell and Developmental Biology*, vol. 2, p. 49, 2014.

[2] B. S. Shastry, "Emerging concept of genetic and epigenetic contribution to the manifestation of glaucoma," in *Glaucoma - Basic and Clinical Aspects*, S. Rumelt, Ed., pp. 57–74, InTechOpen, Rijeka, Croatia, 2013.

[3] J. Tuo, L. Wei, and N. Hu, "Genetic/epigenetic modulation, ocular diseases, and therapeutic prospective," *Journal of Ophthalmology*, vol. 2013, Article ID 980608, 2 pages, 2013.

[4] T. Phillips, "The role of methylation in gene expression," *Nature Education*, vol. 1, no. 1, p. 116, 2008.

[5] M. M. Liu, C. C. Chan, and J. Tuo, "Epigenetics in ocular diseases," *Current Genomics*, vol. 14, no. 3, pp. 166–172, 2013.

[6] R. W. Nickells and S. L. Merbs, "The potential role of epigenetics in ocular diseases," *Archives of Ophthalmology*, vol. 130, no. 4, pp. 508-509, 2012.

[7] C. Stirzaker, D. S. Millar, C. L. Paul et al., "Extensive DNA methylation spanning the *Rb* promoter in retinoblastoma tumors," *Cancer Research*, vol. 57, no. 11, pp. 2229–2237, 1997.

[8] R. J. Casson, G. Chidlow, J. P. Wood, J. G. Crowston, and I. Goldberg, "Definition of glaucoma: clinical and experimental concepts," *Clinical & Experimental Ophthalmology*, vol. 40, no. 4, pp. 341–349, 2012.

[9] B. E. Prum Jr., L. F. Rosenberg, S. J. Gedde et al., "Primary open-angle glaucoma preferred practice pattern® guidelines," *Ophthalmology*, vol. 123, no. 1, pp. 41–111, 2016.

[10] A. Matsuda, Y. Asada, K. Takakuwa, J. Sugita, A. Murakami, and N. Ebihara, "DNA methylation analysis of human trabecular meshwork cells during dexamethasone stimulation," *Investigative Ophthalmology & Visual Science*, vol. 56, no. 6, pp. 3801–3809, 2015.

[11] A. G. M. Junemann, B. Lenz, U. Reulbach, U. Schlotzer-Schrehardt, R. Rejdak, and S. Bleich, "Genomic (epigenetic) DNA methylation in patients with open-angle glaucoma," *Investigative Ophthalmology & Visual Science*, vol. 55, no. 13, p. 3809, 2014.

[12] B. C. Christensen, E. A. Houseman, J. J. Godleski et al., "Epigenetic profiles distinguish pleural mesothelioma from normal pleura and predict lung asbestos burden and clinical outcome," *Cancer Research*, vol. 69, no. 1, pp. 227–234, 2009.

[13] D. J. Weisenberger, M. Campan, T. I. Long et al., "Analysis of repetitive element DNA methylation by MethyLight," *Nucleic Acids Research*, vol. 33, no. 21, pp. 6823–6836, 2005.

[14] P. Sukapan, P. Promnarate, Y. Avihingsanon, A. Mutirangura, and N. Hirankarn, "Types of DNA methylation status of the interspersed repetitive sequences for LINE-1, Alu, HERV-E and HERV-K in the neutrophils from systemic lupus erythematosus patients and healthy controls," *Journal of Human Genetics*, vol. 59, no. 4, pp. 178–188, 2014.

[15] P. J. Foster, R. Buhrmann, H. A. Quigley, and G. J. Johnson, "The definition and classification of glaucoma in prevalence surveys," *British Journal of Ophthalmology*, vol. 86, no. 2, pp. 238–242, 2002.

[16] M. Rhein, L. Hagemeier, M. Klintschar, M. Muschler, S. Bleich, and H. Frieling, "DNA methylation results depend on DNA integrity-role of post mortem interval," *Frontiers in Genetics*, vol. 18, no. 6, p. 182, 2015.

[17] M. Barrachina and I. Ferrer, "DNA methylation of Alzheimer disease and tauopathy-related genes in postmortem brain," *Journal of Neuropathology & Experimental Neurology*, vol. 68, no. 8, pp. 880–891, 2009.

[18] J. Nakkuntod, P. Sukkapan, Y. Avihingsanon, A. Mutirangura, and N. Hirankarn, "DNA methylation of human endogenous retrovirus in systemic lupus erythematosus," *Journal of Human Genetics*, vol. 58, no. 5, pp. 241–249, 2013.

[19] T. Pobsook, K. Subbalekha, P. Sannikorn, and A. Mutirangura, "Improved measurement of LINE-1 sequence methylation for cancer detection," *Clinica Chimica Acta*, vol. 412, no. 3-4, pp. 314–321, 2011.

[20] P. Sirivanichsuntorn, S. Keelawat, K. Danuthai, A. Mutirangura, K. Subbalekha, and N. Kitkumthorn, "LINE-1 and Alu

hypomethylation in mucoepidermoid carcinoma," *BMC Clinical Pathology*, vol. 13, no. 1, article 10, 2013.

[21] J. Gottanka, D. H. Johnson, P. Martus, and E. Lutjen-Drecoll, "Severity of optic nerve damage in eyes with POAG is correlated with changes in the trabecular meshwork," *Journal of Glaucoma*, vol. 6, no. 2, pp. 123–132, 1997.

[22] E. Lutjen-Drecoll, R. Futa, and J. W. Rohen, "Ultrahistochemical studies on tangential sections of the trabecular meshwork in normal and glaucomatous eyes," *Investigative Ophthalmology & Visual Science*, vol. 21, no. 4, pp. 563–573, 1981.

[23] O. Y. Tektas and E. Lutjen-Drecoll, "Structural changes of the trabecular meshwork in different kinds of glaucoma," *Experimental Eye Research*, vol. 88, no. 4, pp. 769–775, 2009.

[24] R. Sihota, N. C. Lakshmaiah, K. B. Walia, S. Sharma, J. Pailoor, and H. C. Agarwal, "The trabecular meshwork in acute and chronic angle closure glaucoma," *Indian Journal of Ophthalmology*, vol. 49, no. 4, pp. 255–259, 2001.

[25] G. Picht, U. Welge-Luessen, F. Grehn, and E. Lutjen-Drecoll, "Transforming growth factor β2 levels in the aqueous humor in different types of glaucoma and the relation to filtering bleb development," *Graefe's Archive for Clinical and Experimental Ophthalmology*, vol. 239, no. 3, pp. 199–207, 2001.

[26] U. Welge-Lussen, C. A. May, M. Eichhorn, H. Bloemendal, and E. Lutjen-Drecoll, "αB-crystallin in the trabecular meshwork is inducible by transforming growth factor-β," *Investigative Ophthalmology & Visual Science*, vol. 40, no. 10, pp. 2235–2241, 1999.

[27] R. Fuchshofer, U. Welge-Lussen, and E. Lutjen-Drecoll, "The effect of TGF-β2 on human trabecular meshwork extracellular proteolytic system," *Experimental Eye Research*, vol. 77, no. 6, pp. 757–765, 2003.

[28] J. Gottanka, D. Chan, M. Eichhorn, E. Lutjen-Drecoll, and C. R. Ethier, "Effects of TGF-β2 in perfused human eyes," *Investigative Ophthalmology & Visual Science*, vol. 45, no. 1, pp. 153–158, 2004.

[29] N. Matsumura, Z. Huang, S. Mori et al., "Epigenetic suppression of the TGF-beta pathway revealed by transcriptome profiling in ovarian cancer," *Genome Research*, vol. 21, no. 1, pp. 74–82, 2011.

[30] Q. Zhou, L. Yang, Y. Wang et al., "TGFβ mediated transition of corneal fibroblasts from a proinflammatory state to a profibrotic state through modulation of histone acetylation," *Journal of Cellular Physiology*, vol. 224, no. 1, pp. 135–143, 2010.

[31] A. Rojas, S. Meherem, Y. H. Kim et al., "The aberrant methylation of *TSP1* suppresses TGF-β1 activation in colorectal cancer," *International Journal of Cancer*, vol. 123, no. 1, pp. 14–21, 2008.

[32] G. Tezel and M. B. Wax, "Hypoxia-inducible factor 1α in the glaucomatous retina and optic nerve head," *Archives of Ophthalmology*, vol. 122, no. 9, pp. 1348–1356, 2004.

[33] J. Flammer, K. Konieczka, and A. J. Flammer, "The role of ocular blood flow in the pathogenesis of glaucomaotus damage," *US Ophthalmic Review*, vol. 04, no. 02, pp. 84–87, 2011.

[34] M. C. Leske, "Ocular perfusion pressure and glaucoma: clinical trial and epidemiologic findings," *Current Opinion in Ophthalmology*, vol. 20, no. 2, pp. 73–78, 2009.

[35] J. Flammer, I. O. Haefliger, S. Orgul, and T. Resink, "Vascular dysregulation: a principal risk factor for glaucomatous damage?," *Journal of Glaucoma*, vol. 8, no. 3, pp. 212–219, 1999.

[36] F. McDonnell, A. F. Clark, C. J. O'Brien, and D. M. Wallace, "The role of hypoxia in inducing aberrant epigenetic and fibrotic states in glaucoma," *Investigative Ophthalmology & Visual Science*, vol. 55, no. 13, p. 5716, 2014.

[37] H. H. Nelson, C. J. Marsit, and K. T. Kelsey, "Global methylation in exposure biology and translational medical science," *Environmental Health Perspectives*, vol. 119, no. 11, pp. 1528–1533, 2011.

[38] M. A. Batzer and P. L. Deininger, "Alu repeats and human genomic diversity," *Nature Reviews Genetics*, vol. 3, no. 5, pp. 370–379, 2002.

[39] V. Tarallo, Y. Hirano, B. D. Gelfand et al., "DICER1 loss and *Alu* RNA induce age-related macular degeneration via the NLRP3 inflammasome and MyD88," *Cell*, vol. 149, no. 4, pp. 847–859, 2012.

[40] E. Balada, J. Ordi-Ros, and M. Vilardell-Tarres, "Molecular mechanisms mediated by human endogenous retroviruses (HERVs) in autoimmunity," *Reviews in Medical Virology*, vol. 19, no. 5, pp. 273–286, 2009.

[41] D. Bessis, J. P. Moles, N. Basset-Seguin, A. Tesniere, C. Arpin, and J. J. Guilhou, "Differential expression of a human endogenous retrovirus E transmembrane envelope glycoprotein in normal, psoriatic and atopic dermatitis human skin," *British Journal of Dermatology*, vol. 151, no. 4, pp. 737–745, 2004.

[42] I. Knerr, E. Beinder, and W. Rascher, "Syncytin, a novel human endogenous retroviral gene in human placenta: evidence for its dysregulation in preeclampsia and HELLP syndrome," *American Journal of Obstetrics and Gynecology*, vol. 186, no. 2, pp. 210–213, 2002.

[43] S. Mi, X. Lee, X. Li et al., "Syncytin is a captive retroviral envelope protein involved in human placental morphogenesis," *Nature*, vol. 403, no. 6771, pp. 785–789, 2000.

[44] B. S. Shastry, "Genetic susceptibility to primary angle closure glaucoma (PACG)," *Discovery Medicine*, vol. 15, no. 80, pp. 17–22, 2013.

[45] J. H. Fingert, "Primary open-angle glaucoma genes," *Eye*, vol. 25, no. 5, pp. 587–595, 2011.

[46] P. Jintaridth and A. Mutirangura, "Distinctive patterns of age-dependent hypomethylation in interspersed repetitive sequences," *Physiological Genomics*, vol. 41, no. 2, pp. 194–200, 2010.